# Biomechanical Constraints on Molar Emergence in Primates

by

Halszka Glowacka

A Dissertation Presented in Partial Fulfillment
of the Requirements for the Degree
Doctor of Philosophy

Approved July 2017 by the
Graduate Supervisory Committee:

Gary T. Schwartz, Chair
William H. Kimbel
Kaye E. Reed
Barth W. Wright

ARIZONA STATE UNIVERSITY

August 2017

ABSTRACT

Across primates, molar-emergence age is strongly correlated to life-history variables, such as age-at-first-reproduction and longevity. This relationship allows for the reconstruction of life-history parameters in fossil primates. The mechanism responsible for modulating molar-emergence age is unknown, however. This dissertation uses a biomechanical model that accurately predicts the position of molars in adults to determine whether molar emergence is constrained by chewing biomechanics throughout ontogeny. A key aspect of chewing system configuration in adults is the position of molars: the distal-most molar is constrained to avoid tensile forces at the temporomandibular joint (TMJ). Using three-dimensional data from growth samples of 1258 skulls, representing 21 primate species, this research tested the hypothesis that the location and timing of molar emergence is constrained to avoid high and potentially dangerous tensile forces at the TMJ throughout growth. Results indicate that molars emerge in a predictable position to safeguard the TMJ during chewing. Factors related to the size of the buffer zone, a safety feature that creates greater stability at the TMJ during biting, account for a large portion of both ontogenetic and interspecific variation in the position of emergence. Furthermore, the rate at which space is made available in the jaws and the duration of jaw growth both determine the timing of molar emergence. Overall, this dissertation provides a mechanical and developmental model for explaining temporal and spatial variation in molar emergence and a framework for understanding how variation in the timing of molar emergence has evolved among primates. The findings suggest that life history is related to ages at molar emergence through its influence on the rate and duration of jaw growth. This dissertation provides support for the functionally

integrated nature of craniofacial growth and has implications for the study of primate life history evolution and masticatory morphology in the fossil record.

# DEDICATION

To my grandparents, Drs. Halina and Andrzej Gałuszka, who cultivated my curiosity in the natural world.

ACKNOWLEDGMENTS

This research would not have been possible without the support of several funding agencies. Thank you to the National Science Foundation, the Leakey Foundation, the Wenner-Gren Foundation, the James F. Nacey Fellowship, Sigma Xi, the Institute of Human Origins, the Elizabeth H. Harmon Research Endowment, the Donald C. Johanson Paleoanthropological Research Endowment, Arizona State University Graduate and Professional Student Association, and the School of Human Evolution and Social Change for financial support.

Thank you to all curators and staff of the skeletal collections that I visited during data collection.

I would like to thank my committee (Gary Schwartz, Bill Kimbel, Kaye Reed, and Barth Wright) for their support throughout this process, their feedback, and patience.

To my mentors throughout graduate school, Gary Schwartz, Bill Kimbel, and Shannon McFarlin. Thank you for teaching me how to be a careful scientist, for your kindness and unwavering support. Gary, thank you for being such a supportive adviser, your encouragement in all aspects of life has been wonderful. Bill, you have taught me many skills, but most importantly, perspective. Your friendship and mentorship throughout the years has meant the world to me. Shannon, thank you for giving me the opportunity to work with you on such great research. You have taught me how to be a good collaborator and that humility and kindness go a long way.

To my Master's adviser, David Begun with whom I took my first biological anthropology class. Thank you for your enthusiasm and passion for the subject, it was infectious.

To my graduate school friends (in no particular order), Terry Ritzman, Laura Stroik, Kathleen Paul, Ellis Locke, Andy Seidel, Hallie Edmonds, Genevieve Housman, John Rowan, Neysa Grider-Potter, Maria Nieves Colón, Jon Paige, Robyn Merchant, Irene Smail, Susanne Daly, and many more, thank you for being my sounding boards, my reasons to take breaks, and my support system. I could not have done this without you.

To Kathy Pitirri, your friendship throughout the years has been an important constant in my life. Thank you for always being up for an adventure. I cannot wait to sit on the stoop with you and yell at kids when we are old. To Vivek Venkataraman, you have helped me become a better scientist and person, thank you for your unwavering support.

Finally, I would like to thank my family: my mom, Jagna Glowacka; sister, Zuzi Valente; and grandmother, Halina Gałuszka, who have been my cheerleaders. Thank you for encouraging me to pursue my passion and supporting me through that pursuit. I am lucky to have such strong female role models in my life.

TABLE OF CONTENTS

Page

CHAPTER Page

CHAPTER Page

LIST OF TABLES

Table Page

Table Page

LIST OF FIGURES

Figure Page

Figure Page

Figure Page

# LIST OF EQUATIONS

Equation Page

Equation Page

# CHAPTER 1

## INTRODUCTION

It has long been recognized that one of the unique aspects of human biology is our relatively slow life history (Schultz 1960b). A species' life history is the schedule of its allocation of energetic resources to growth, maintenance, and reproduction. Life history can be described by a series of variables, such as gestation length, weaning age, age-at-first-reproduction, litter size, and inter-birth interval, among many others ( Harvey and Clutton-Brock 1985; Stearns 1992; Charnov 1993). Together, these variables describe how a species apportions energy to maximize individual fitness. Overall, humans reach reproductive maturity later, have longer periods of nutritionally independent growth between weaning and maturity, and have longer maximum lifespans than other apes (Hawkes 2006; Robson, van Schaik, and Hawkes 2006). But not all aspects of human life history are slower than those of other great apes. Strikingly, humans have shorter inter-birth intervals and wean relatively early, both in absolute time and relative to body and brain size (Wood 1990; Galdikas and Wood 1990; Kennedy 2005; Robson, van Schaik, and Hawkes 2006; Humphrey 2010). Early weaning in humans is associated with faster reproductive rates ( Lee 1996; Blurton Jones, Hawkes, and O'Connell 1999) and an extended period of cognitive development (Bogin 1999; Kennedy 2005), both facilitated by cooperative breeding and the presence of post-menopausal females, older males, and siblings, who aid in child rearing (Hawkes et al. 1998; Peccei 2001; Robson, van Schaik, and Hawkes 2006; Madrigal and Meléndez-Obando 2008).

One of the more interesting questions in paleoanthropology is when the modern human pattern of life history emerged in our evolutionary history. This human pattern of

life history is associated with a slew of other human-like traits, such as cooperative breeding, the evolution of childhood (i.e., the extended period of growth in humans that provides the time required for complex cognitive development (Bogin 1999; Kennedy 2005)), and menopause (Hawkes et al. 1998), to name a few. Knowing when the earliest appearance of a modern humanlike life history occurred thus allows inferences to be made regarding these other aspects of fossil human biology.

A species' schedule of allocation of energetic resources to growth, maintenance, and reproduction does not fossilize, but skeletal proxies for life history can be used to reconstruct its evolution in the hominin[1] lineage. Evidence for growth (increase in size) and development (progress towards maturity) in fossil hominins can be found by studying their fossilized skeletal remains. In order to understand patterns of skeletal growth in fossil hominins, they must first be understood in extant taxa (Schultz 1924; Wood 1996). The approach to reconstructing life history in the fossil record has been to identify how skeletal growth covaries with life history among extant taxa (Smith 1989; Kelley and Schwartz 2010), and then, once such patterns are identified, to use them to retrodict in extinct relatives life-history profiles—the particular scheduling of important developmental milestones of hominins (e.g., Smith and Tompkins 1995; Kelley and Schwartz 2012; Schwartz 2012).

[1] The following taxonomic terminology is used here: Hominoidea (hominoids) = Hylobatidae (hylobatids) + Hominidae (hominids); Hominidae = Ponginae (pongines) + Homininae (hominines); Ponginae (pongines) =*Pongo* (orangutan); Homininae= African apes (*Pan* + *Gorilla*) + Hominini (hominins); Hominini= humans and closest relatives after the divergence from *Pan*.

The fossil record preserves skeletons of both adult and subadult individuals, from which growth patterns (e.g., rates of growth, ages at growth cessation, growth-related shape changes) can be inferred, but the taphonomic bias towards preserving large bones (Behrensmeyer, Western, and Dechant Boaz 1979; Behrensmeyer 1981) means that juvenile skeletal elements are less likely to be preserved in the fossil record. Consequently, juvenile fossilized remains are rare relative to adult remains. Although burials have increased the chances of juvenile and infant bone preservation (e.g., Rak, Kimbel, and Hovers 1994), this practice has only been identified in Neandertals and modern humans (but see Dirks et al. 2015, for an argument for burial practices in *Homo naledi,* ca. 250-350 ka). Among older hominin species, only a handful of specimens preserve both skull and postcranial remains (e.g., *Homo erectus*, KNM-WT 15000 (Brown et al. 1985); *Australopithecus sediba*, MH-1 (Berger et al. 2010); *A. afarensis*, DIK-1-1 (Alemseged et al. 2006)). A recent discovery of at least 18 individuals attributed to the species *Homo naledi* (Berger et al. 2015; Hawks et al. 2017), several of which are subadults, augments this sample substantially.

In contrast to bone, teeth are readily fossilized at all stages of development because enamel and dentine are highly mineralized tissues even before the process of fossilization begins (Robinson et al. 1995). Teeth can be used to determine the age-at-death of individuals who died while the dentition was still forming (e.g., Boyde 1964; Beynon, Dean, and Reid 1991a, b; Dean and Beynon 1991a; Dirks 1998; Kelley and Smith 2003; Dean 2006; Schwartz et al. 2006; Smith et al. 2007a; Kelley and Schwartz 2010; Smith 2016). Ageing methods for modern human skeletons have been developed based on collections of known-age skeletons (e.g., Scheuer and Black 2000). Although

recent efforts are producing primate skeletal collections of know-age individuals (e.g., McFarlin et al. 2009), only a handful of such collections currently exist for most non-human primates. Therefore, the information preserved by the microstructure of primate teeth provides the most reliable ageing method (Boyde 1963, 1990).

## Molar Emergence and Life History

Predicated on the work of Schultz (1935, 1960a), Sacher (1959, 1975), and Harvey and Clutton-Brock (1985), B. Holly Smith (Smith 1989) showed that the absolute timing of molar emergence in primates is a critical indicator of life history. She demonstrated that ages at molar emergence correlate strongly with brain size and body size, and also many key life-history variables: gestation length, age-at-weaning, inter-birth interval, age-at-sexual-maturity, age-at-first-breeding, and lifespan (Smith 1989, 1991b, 1992; Smith, Crummett, and Brandt 1994). The emergence of the first permanent molar (M1) is a particularly good predictor of life-history variables among primates; the strongest correlations with M1 emergence were found with both brain size and age-at-weaning. Smith (1989, 1992) argued that the link between brain size, age-at-weaning, and M1 emergence exists because adult brain size is attained around the time of weaning, which is also the time when the M1 emerges in most primates (because the weanling must have the proper dental "equipment" to process an adult diet). She argued further that M1 emergence may be pleiotropically tied to brain growth. While it is true that smaller-brained primates tend to wean their offspring earlier and have more precocial dental development (Smith, Crummett, and Brandt 1994; Godfrey et al. 2001), the M1 does not always emerge at or near the age-at-weaning, especially among strepsirrhines (Godfrey et

al. 2001b, 2003). Therefore, the reason for the strong association between M1 emergence and adult brain size might be indirectly related to weaning, but the mechanism for such a relationship remain unknown.

Life-history variables are all strongly correlated with one another (Smith 1989). This strong relationship is likely why M1 emergence is strongly correlated to all life-history variables, and not just weaning age. Similarly, M3 emergence is a skeletal marker of adulthood and thus the onset of reproduction ( Smith 1989; Smith and Tompkins 1995). The strong interspecific link between molar-emergence ages and life history is indisputable. This aspect of skeletal development has, thus far, proven to be the most reliable predictor of life-history variables for extant primates. Not only does it predict the uniquely slow life history of modern humans (except for the unusually early weaning age in humans (Kennedy 2005; Humphrey 2010)), but it also predicts the fast life history of many lemurs and small-bodied monkeys. Furthermore, the relationships demonstrated by Smith (1989) still hold even when shared phylogenetic history is incorporated into the analysis ( Smith 2013).

The mechanism underlying the relationship between age-at-M1-emergence and life history remains unknown. Two unanswered questions stand in the way of a more complete understanding of the timing of molar emergence in primates: (1) What factors influence variation in ages at M1 emergence among primates? and (2) Why is age at M1 emergence so closely associated with fundamental aspects of a species' life history? This dissertation provides a mechanical and developmental model for explaining temporal and spatial variation in molar-emergence ages among primates and a framework for understanding how variation in the timing of molar emergence evolves among primates.

*Intraspecific Variation in Molar Emergence, a Cautionary Tale?*

Few data exist on intraspecific variation in M1 emergence, and it is unclear whether variation in M1-emergence age coincides with variation in weaning age. Machanda et al. (2015a) reported substantial variation in tooth-emergence ages within populations of wild Kanyawara and captive chimpanzees, much of which is only weakly associated with life-history variables that have been reported as being strongly associated with emergence ages at an interspecific level (e.g., inter-birth interval and age-at-first-reproduction). Similarly, in a study of wild chimpanzees from Kanyawara, the timing of M1 emergence was compared to the onset and duration of weaning behavior to determine if these variables were strongly associated across individuals (Smith et al. 2013). It was found that chimpanzees continued to nurse long past the emergence of their M1s, but they began consuming the same percentage of fibrous foods as adults even before M1 emergence (Smith et al. 2013).

Based on the results of their studies, Smith et al. (2013) and Machanda et al. (2015a) warned against using molar-emergence age to reconstruct life history in the fossil record because the association between the two is not strong at the intraspecific level. This conclusion may be premature, however. The small number of individuals studied ($n$ = 6 between the Smith et al. (2013) and Machanda et al. (2015a) studies) may not represent a random sample of the Kanyawara chimpanzee population. Furthermore, dental development is part of overall somatic development, and so molar-emergence ages at the individual level should, at least to some extent, depend on individual somatic growth rates. Variation in molar emergence is to be expected within a population, as is variation in somatic growth rates. Furthermore, weaning age is variable within primate

populations. Smith et al. (2013) report weaning age as the age of last nipple contact, yet it is unclear when nutritional transfer between infant and mother ceases, as this may occur much earlier than last nipple contact (Lee 1996; Cameron 1998). The process of weaning is largely controlled by the mother, and its variability depends on many factors, including maternal condition, parity, age, and local ecology (Lee 1996). Social factors may also play an important role in weaning age. In olive and yellow baboons, for example, female rank influences weaning age, with lower ranking mothers weaning their infants at significantly younger ages than high ranking mothers (Altmann and Alberts 2003; Johnson 2003). Given the variability in both M1 emergence and weaning age and the small sample size of Smith et al.'s (2013) study (n=5), their finding is perhaps unsurprising. As such, dismissing the strong interspecific association between age-at-weaning and M1 emergence may not be warranted at present. Further studies replicating Smith et al.'s (2013) study with larger sample sizes and in more primate populations would help resolve this issue. As the sample size increases, however, it should begin to represent the population means, which should be similar given the strong interspecific association between age-at-M1-emergence and weaning age. The predictive power of this strong interspecific association, should not be discarded based on current evidence. The Smith et al. (2013) and Machanda et al. (2015a) studies highlight the fact that little is known regarding the process that modulates molar emergence and therefore how variation in emergence age can arise both within and between populations. The process modulating molar emergence should be investigated in order to confidently use this skeletal proxy to reconstruct fossil life history.

*Fossil Primate M1 Emergence and Life-History Reconstructions*

The timing of molar emergence is one of the most accurate clues to the life history of extinct taxa. Determining the age at molar emergence can be accomplished by using the microstructures of dental tissues to establish the age-at-death of an individual that died during molar eruption.

An age-at-M1-emergence of ~1.45 years for *Anapithecus hernyaki,* is not unexpected for a catarrhine of its size, and indicates that a somewhat prolonged life history existed in stem catarrhines (Nargolwalla et al. 2005). Similarly, apelike ages at M1 emergence were found in the middle Miocene hominoid *Afropithecus turkanensis* (Kelley 1997; Kelley and Smith 2003) and the late Miocene hominid *Sivapithecus parvada* (Kelley 1997), suggesting that a prolongation in life history is a hominoid synapomorphy (Kelley 1997, 2002).

The role of M1 emergence in the reconstruction of hominin life history is contentious. Robson and Wood (2008) noted that among extant hominids there is poor correspondence between ages at M1 emergence and various life-history variables, suggesting that M1 emergence is not a robust predictor of life history for fossil hominins. Some of the data sources used by Robson and Wood were anecdotal and M1 emergence data and life-history data were often drawn from different populations (Kelley and Schwartz 2010, 2012), and different species in some cases (e.g., molar emergence data for *Gorilla gorilla*, but life history data for *G. beringei*). Robson and Wood (2008) did not perform any statistical analyses of the correspondence between molar-emergence age and life history, making their conclusions difficult to evaluate (Kelley and Schwartz 2012). An analysis of the correlation between M1-emergence ages and life-history

variables among hominoids using only wild-shot ape individuals, with life-history data from corresponding populations, yielded a strong relationship between M1-emergence age and life-history variables (Kelley and Schwartz 2010).

Estimates of ages at M1 emergence for australopiths (*Australopithecus* and *Paranthropus*) based on information preserved by the incremental nature of dental hard tissue deposition has yielded a range of 2.7-3.9 years (Dean et al. 1993; Kelley and Schwartz 2012). Although this range overlaps with the range of M1-emergence ages known for wild-shot apes (2.5-4.6 y: Kelley and Schwartz 2012; Smith et al. 2013; Machanda et al. 2015a), it falls at the lower end of the extant ape range. This result may indicate that australopiths had a somewhat accelerated life history relative to the extant great apes, which would be surprising given the absolutely and relatively larger brain sizes of australopiths compared to the extant great apes (Kimbel and Villmoare 2016). This conclusion does not consider M1-emergence age of mountain gorillas, which have an accelerated life history compared to western lowland gorillas (Breuer et al. 2009; Stoinski et al. 2013). If age-at-M1-emergence is correspondingly earlier than that reported for other great apes, then australopiths may have had a life-history that was more similar to mountain gorillas than to any other great ape (Kelley and Schwartz 2012).

*Paranthropus* presents an interesting test case for how age-at-M1-emergence can help to inform other aspect of an extinct species' biology. Ages-at-M1-emergence have been estimated for two *Paranthropus* species using several methods. These include (1) the relationship between cranial capacity and molar emergence and (2) incremental lines in dental tissues to establish age-at-death of an individual that died around M1 emergence. The reported age-at-M1-emergence for *P. robustus* ranges between 2.9 and

3.9 years (Bromage and Dean 1985; Beynon and Dean 1988; Conroy and Vannier 1991; Dean et al. 1993; Kelley and Schwartz 2012), while that for *P. boisei* ranges between 2.7 and 3.3 years (Dean 1987; Beynon and Dean 1988; Kelley and Schwartz 2012). The *P. boisei* M1 emergence estimates are generally younger than those for *P. robustus*, suggesting a faster life history for *P. boisei*. These data fit well with the dietary reconstructions for the two taxa. The finding that *P. boisei* bears a strong C4 signature has led to the suggestion that this hominin consumed a highly specialized diet of grasses and/or sedges (Cerling et al. 2011; Ungar and Sponheimer 2011). Dietary reconstructions for *P. robustus*, on the other hand, indicate a mixed C3-C4 diet that changed seasonally and interannually (Sponheimer et al. 2006) and consisted of hard and brittle foods (Scott et al. 2005), such as fruit and seeds (Lee-Thorp, van der Merwe, and Brain 1994). Primates that consume low quality, non-frugivorous diets generally have faster life histories than closely related primates that consume higher quality, frugivorous diets (Harvey, Martin, and Clutton-Brock 1987; Godfrey et al. 2001b; Dirks 2003; Leigh 2004; see section on diet in "Proposed Influences on Molar Emergence" below). Although there is still much debate regarding the diets of early hominins, the dietary reconstructions described above align with the expectations of the earlier ages at M1 emergence reported for *P. boisei* and point to a faster life history for this species.

Modern humans grow slower than any other hominid but a short inter-birth interval coupled with accelerated weaning and cooperative care allows for fast reproductive rates, which in turn, allows mothers to have several offspring that overlap in life-history stages. The energetic burden of multiple offspring is offset by the aid of fathers, older relatives (i.e., older offspring and grandparents), as well as nonkin members

of the community (Hawkes 2006). It is of particular interest to paleoanthropologists to reconstruct how and when human life history first evolved, and whether it evolved as a package or in a more piecemeal manner.

Reconstruction of australopith life history via ages at M1 emergence has helped to clarify the fact that early hominins had life-history profiles that were more similar to those of the great apes than to those of modern humans (Bromage and Dean 1985; Dean 1987; Beynon and Dean 1988). Studies of M1 emergence have also helped shed light on the evolution of life history in our own genus. The earliest species of the genus *Homo* for which M1 emergence data are available is *H. erectus* (KNM-WT 15000, 1.55 Ma). At ~4.5 y (Dean et al. 2001), its M1-emergence age falls just above those reported for the great apes and below the range reported for modern humans (4.7-7.0 y: Liversidge 2003). The relatively young age-at-M1-emergence for *H. erectus* (compared to modern humans) suggests that the extended period of growth present in modern humans was not yet a part of the life-history profile of extinct hominin species. Similarly, evidence suggests that M1 emergence in the sister taxon to modern humans, *H. neanderthalensis*, occurred at the lower end of the distribution of M1 emergence in modern humans (Smith et al. 2010b) indicating that a modern humanlike life history had still not evolved before the split between Neanderthals and modern humans (but see Austin et al. (2013) for isotopic evidence of early weaning in Neanderthals). This idea is supported by the work of Ramirez Rozzi and Bermudez de Castro (2004) who showed that the rate of dental development was faster in Neandertals than in modern humans, but not by the work of Macchiarelli et al. (2006) who reported an M1-emergence age at the top range of human

variation (~6.7 years) for one Neandertal specimen. The question of whether Neandertals grew at the same, faster, or slower rate than modern humans remains unresolved.

## Proposed Influences on Molar Emergence

Molar emergence is but one part of dental development, which itself is a component of overall somatic growth. As such, factors known to influence somatic growth rates, such as diet and body/brain size, have generally been invoked to explain variation in molar emergence schedules among primates.

Life-history theory posits that adult body mass is influenced by mortality rates and that selection optimizes adult body mass and the age of its attainment to maximize fitness (Stearns 1992; Charnov 1993; Charnov and Berrigan 1993). Large-bodied animals tend to grow at slower rates than small-bodied animals (Taylor 1965; Western 1979) and should thus exhibit later molar-emergence ages. Indeed, in primates there is a strong positive correlation between molar-emergence age and adult body mass (Smith 1989). Many primate species exhibit a decoupling of somatic growth rates, ages at molar emergence, and adult body mass, however (e.g., Schwartz et al. 2002; Dirks 2003; Dirks and Bowman 2007). For example, among strepsirrhines, *Propithecus verreauxi* and *Eulemur fulvus* possess similar adult body masses yet differ dramatically in rates of dental and somatic development. At birth, *P. verreauxi* is far more dentally precocious than *E. fulvus* (Schwartz et al. 2002; Godfrey et al. 2004), yet a comparison of somatic growth rates indicates that *E. fulvus* grows at a faster rate than *P. verreauxi* (Godfrey et al. 2004). Similarly, adaptive (grade) shifts in life history between hominoids and cercopithecoids are reflected in slower rates of dental development and emergence in

hominoids than in similar-sized cercopithecoids (Dirks and Bowman 2007). These examples illustrate that body mass alone cannot explain variation in dental development and molar emergence schedules among primates.

Adult brain size is also positively related to molar-emergence age (Smith 1989, 1991b; Smith, Crummett, and Brandt 1994; Godfrey et al. 2001b, 2003). This relationship may exist because adult brain size is attained at around the time of weaning (Smith 1989, 1992; Martin 1983) and weanlings might require their M1s to process an adult diet (Smith 1989). Yet, while it is true that smaller-brained primates tend to wean their offspring earlier and have more precocious dental development (Smith, Crummett, and Brandt 1994; Godfrey et al. 2001), the M1 does not always emerge at or near the time of weaning (Godfrey et al. 2001; Godfrey et al. 2003; Smith et al. 2013). As a result, the biological basis of the strong relationship among brain size, age-at-weaning, and age-at-M1-emergence remains unclear.

The idea that diet influences molar emergence schedules stems from the ecological-risk-aversion hypothesis, which posits that populations experiencing high food competition should exhibit slow somatic growth rates to reduce the risk of death due to starvation (Janson and van Schaik 1993). Species that feed on high-quality resources (e.g., frugivores), for which food competition is high, should exhibit slow somatic growth and, as a result, late ages at molar emergence. This prediction is borne out in several anthropoid species (e.g., *Gorilla gorilla*, which includes more fruit in its diet than *G. beringei,* has later ages at M1 emergence than *G. beringei* (Watts 1984; Rogers et al. 2004; Masi 2007; Kelley and Schwartz 2010; Vakiener et al. 2016)). There are several exceptions to this rule among primates, however (e.g., Godfrey et al. 2004; Bolter 2011;

Borries et al. 2011). Bolter (2011) investigated skeletal growth between two cercopithecids (the folivorous *Trachypithecus cristatus* and the omnivorous *Cercopithecus aethiops*) and found that, skeletally, *C. aethiops* grew faster than *T. cristatus*. These results are contradictory to the predictions of the ecological-risk-aversion hypothesis and suggest that dietary category alone is insufficient to explain growth variation in many primate taxa. Further work has undermined the idea that feeding competition is low in folivores (Koenig 2000; Snaith and Chapman 2007; Robbins 2008) and indicated that leaf availability can be highly seasonal (Koenig et al. 1997; Harris, Chapman, and Monfort 2010). These findings suggest that the folivore-frugivore dichotomy may be too simplistic to tease apart the effects of diet (food abundance, food quality, and resulting competition) on growth and development. This is further illustrated by a comparison two strepssirhine taxa. The highly folivorous species of Indriidae grow and mature more slowly than similar-sized frugivorous species of Lemuridae (Godfrey et al. 2004). In contrast to somatic growth, dental development in indriids is faster than in lemurids (Godfrey et al. 2004). These results indicate that the mechanisms coordinating dental growth and somatic growth are not similarly influenced by diet.

It has been suggested that available space in the jaws influences the initiation of molar formation (Bradley 1961; Osborn 1978; Dean and Beynon 1991b; Tompkins 1996). According to this view, variation in molar-emergence ages could simply be a function of the age at which molars initiate development. This hypothesis was tested by Boughner and Dean (2004), who found little support for the role of space in regulating or constraining the timing of molar development, and thus molar emergence. Their study focused on the degree of temporal overlap between the completion of one molar crown

(e.g., M1), and the initiation of crown formation in a subsequent molar (e.g., M2). Comparative dental developmental research shows that cercopithecoid monkeys do not exhibit any temporal overlap in molar formation (e.g., Swindler and Gavin 1962; Swindler 1985; Dirks et al. 2002; Dirks and Bowman 2007), whereas apes exhibit some temporal overlap in molar formation, especially between M1 and M2 (Anemone, Watts, and Swindler 1991; Beynon, Dean, and Reid 1991a; Dirks 1998; Dirks and Bowman 2007). Thus, Boughner and Dean (2004) expected cercopithecoids to be more constrained (relative to hominoids) by available space in the jaw. They compared the amount of space available in the jaw at the same relative times in *Pan* and *Papio*. At no time during molar development was the space between adjacent molars different between these two taxa, indicating that spatial availability in the jaws does not constrain dental development. While Boughner and Dean (2004) determined that space is not a limiting factor in molar initiation and growth, they did not test whether space constrains the position and timing of molar emergence. The position of tooth initiation and crown growth can differ from the position of tooth emergence. Mandibular molars, for example, initiate and grow much of their crown within the root of the mandibular ramus, but emerge from within the mandibular corpus. The spatial relationship between the tooth crown and alveolar bone changes throughout a tooth's ontogeny and it is therefore possible that the space required to initiate and grow a tooth may be independent from the space required for tooth emergence.

Despite considerable attention, not one of the several research streams discussed above has adequately explained what governs variation in molar emergence times across primates. In the end, most primate paleobiologists (including paleoanthropologists)

continue to retrodict aspects of life history based on significant correlations between the timing of tooth emergence and life-history variables, without a clear understanding of the mechanism that produces this relationship.

## Growth and Functional Integration of the Masticatory System

Growth is a general term applied to the incremental changes in size (i.e., mass) and morphology that occur throughout the development of the individual. Bones of the skull grow in concert with one another as well as with numerous organs and spaces. The interaction between parts of the growing face can be understood through the use of Melvin Moss's "functional matrices theory" (Moss and Young 1960; Moss and Salentijn 1969a, b; Moss 1997a, b, c, d) or Donald Enlow's "counterpart principle" (Enlow et al. 1969; Enlow and Hans 1996).

Functional matrices theory (FMT) posits that the head is a collection of functional matrices, made up of soft tissues and the spaces that they occupy. The bone that contains a functional matrix is called its skeletal capsule and together they make up a functional cranial component. Such functional cranial components include aspects of the head involved in vision, olfaction, the central nervous system, and mastication, to name a few. According to the FMT, the size, shape, and position of soft tissues that make up a functional matrix, which is enclosed or supported by a skeletal capsule, determines the size, shape, and position of the skeletal capsule. Therefore, changes in skeletal morphology during growth are driven by changes in the growth of soft tissues that are part of the same functional matrix and, accordingly, the morphology and position of bones relative to one another during growth is determined entirely by their functional

matrices. The idea that bone growth is not genetically determined has been challenged. A more recent evaluation of the FMT by Moss allows for more genetic control of bone growth (Moss 1997a, b, c, d) and elaborates on the notion that each functional matrix influences the growth of adjacent functional matrices, as most parts of the skull contribute to more than one functional matrix. For example, the floor of the nasal cavity (composed of the maxillae and palatine bones) is also the roof of the oral cavity. Similarly, the floor of the anterior cranial fossa is also the roof of the orbits. The FMT remains heuristically useful especially if distinction is made between primary interactions (between a functional matrix and its skeletal capsule) and secondary interactions (between a functional matrix and other skeletal capsules that it might influence) (McCarthy 2004; Lieberman 2011).

The counterpart principle (Enlow et al. 1969; Enlow and Hans 1996) was an amendment to the work of Moss, and suggested that the growth and development of different parts of the skull influence the growth and development of structural counterparts, thus maintaining a structural equilibrium (Enlow and Moyers 1971). One example of such counterparts is the mandibular and maxillary arches, which must maintain similar growth so as to maintain functional occlusion of the teeth throughout growth. Similarly, the mandibular corpus can be divided into different counterparts that grow in conjunction with one another. Although structures superior to the inferior alveolar nerve canal (i.e., alveolar bone) differ in the pattern of bone remodeling to those inferior to the alveolar nerve canal (e.g., in humans the superior unit is externally resorptive while the inferior unit is externally depository: Duterloo and Enlow 1970), these two counterparts grow together in order to maintain functionality (Enlow and Hans

1996).

The FMT and the counterpart principle state that growth of the craniofacial skeleton results from the complex interactions among their different components. Both are therefore useful and complementary frameworks for describing the growth of the skull because both focus on how growth and development relates to function and both recognize the relevance of biomechanical factors in the ultimate determination of morphology (Daegling 2010). That the masticatory apparatus as a whole can be considered a functional cranial component has been supported by several workers (Pucciarelli, Dressino, and Niveiro 1990; Kiliaridis 1995). Most researchers, however, describe the alveolar bone, mandibular corpus, and ramus as parts of separate functional cranial components (Enlow and Hans 1996; Klingenberg, Mebus, and Auffray 2003; Sardi and Ramirez Rozzi 2005), and these parts interact during development to produce a functional system during growth (Klingenberg, Mebus, and Auffray 2003).

The interactions among different parts of the masticatory apparatus are influenced by intrinsic factors (i.e., hormones and genes) and extrinsic stimuli (i.e., soft tissue growth, dental development, biomechanical forces of mastication) (Moss and Young 1960; Enlow and Hans 1996; Moss 1997a, b, c, d; Lieberman, McBratney, and Krovitz 2002; Lieberman 2011). The mandible and maxilla, for example, are functionally integrated due to the demands of functional occlusion (Lieberman 2011) and the role of mastication is important in stimulating growth of the jaws and proper maxillary and mandibular integration (Lieberman et al. 2004).

In her original publication reporting the relationship between molar emergence and life history, B. Holly Smith noted that molar emergence should be completely

integrated into the growth of the skull (Smith 1989). This follows from the idea that the components of an integrated masticatory system must grow together in order to stay functional during development. Smith's insight generated the idea that molar emergence schedules are related to the biomechanics of the masticatory system (Spencer and Schwartz 2008; Schwartz 2012). Molars function with the jaws and chewing muscles to break down food. Developmental coordination among these parts of the chewing system is critical for food ingestion throughout life. In adult primates, the configuration of the chewing system constrains the position of molars to avoid damage to the temporomandibular joint (TMJ) during chewing (e.g., Spencer 1999) and so it is logical to assume that the same biomechanical constraint operating in adults also operates at all stages of ontogeny.

## Biomechanical Constraints on Molar Position

Research on jaw biomechanics and kinematics has been used to understand feeding adaptations of extant (e.g., Bramble 1978; Smith 1978; Hylander 1985a; Spencer 1995; Daegling and Hylander 2000; Ravosa et al. 2000; Williams et al. 2002; Daegling 2004; Wright 2005; Ross et al. 2007, 2012; Hylander et al. 2011; Perry, Hartstone-Rose, and Logan 2011; McGraw and Daegling 2012) and fossil primates (e.g., Du Brul 1976; Demes and Creel 1988; Daegling and Grine 1991; Spencer and Demes 1993; Antón 1996; Wood and Lieberman 2001; Rak and Hylander 2008; Strait et al. 2012). Since the 1970s, the Constrained Lever Model (CLM) has been used to show that in order to prevent injury at the jaw joint during chewing, the position of teeth in the jaws is constrained (Greaves 1978, 1982, 1983, 1988; Spencer and Demes 1993; Spencer 1995,

1999). More recently, Spencer and Schwartz (2008) and Schwartz (2012) suggested the existence of similar constraints on the position of molar emergence.

The CLM was developed as a way of understanding variation in overall masticatory system configuration and the relative position of different tooth types, in particular (Greaves 1978, 1982, 1983). The model hinges on the assumption that the morphology of the masticatory system is constrained so that the TMJ is not loaded in a way that regularly or forcefully pulls the mandibular condyle away from the articular eminence. Such distractive forces are avoided by changing the activity of the masticatory muscles at different bite points and by limitations on the configuration that the masticatory components might assume through evolution (Spencer 1999). Both of these expectations have been tested; Spencer (1998) showed that during maximum bite force production on different bite points, masticatory muscles change their activation in a manner consistent with the expectations of the model. Furthermore, Spencer (1999) and Perry, Hartstone-Rose, and Logan (2011) reported that the position of molars in adult primates is also consistent with the expectations of the model. The CLM has been used to compare masticatory configurations among mammals (e.g., Spencer and Demes 1993; Spencer 1995, 1999), to investigate how bite forces change along the dental arcade in taxa with different masticatory configurations (Greaves 1988; Spencer and Demes 1993; Lucas 2012), and to explain diet-driven morphological differences among extant and fossil primates (Wright 2005; Koyabu and Endo 2009; Strait et al. 2009; Smith et al. 2015; Ledogar et al. 2016b). Most important for the purposes of this dissertation, the CLM predicts where molars should be located within the jaws if distraction of the TMJ is to be avoided (Spencer 1995, 1999). To understand how the CLM may modulate the

position and timing of molar emergence across primates, it is first necessary to explore the biomechanical boundaries of the CLM that are requisite for evaluating masticatory configuration, namely, the anteroposterior (AP) and mediolateral (ML) positions of the jaw-adductor muscle resultant relative to the triangle of support.

*Constrained Lever Model Description and Predictions for Molar Position*

Forces applied to the mandible by the masticatory adductor muscles are resisted at three points: the bite point, the working-side TMJ, and the balancing-side TMJ (Gysi 1921; Walker 1976; Greaves 1978; Smith 1978; Hylander 1985b; Spencer 1998). These three points make up the corners of the *triangle of support*, a theoretical area through which the masticatory adductor muscle resultant vector must pass to ensure TMJ stability (Fig. 1A; Greaves 1978, 1982, 1983, 1988). The key parameter for rendering an intact CLM is the position of the adductor muscles' resultant, in both the AP and ML dimensions relative to the three principle resistance points of the triangle of support.

When the working-side and balancing-side adductor muscles are equally active, the resultant lies on the midsagittal plane (Fig. 1A). During anterior biting, when the triangle of support is large and can easily encompass the resultant, the working-side and balancing-side TMJs can resist most of the load. As the bite point moves posteriorly along the postcanine row, however, the triangle of support gets increasingly smaller and, ultimately, a midline muscle resultant will fall outside of the triangle of support (Fig. 1B; Spencer 1995, 1999), loading the TMJ in tension and causing TMJ distraction. To avoid loading the TMJ in tension during posterior molar biting, the muscle resultant migrates laterally away from the midline and towards the working side, a movement enabled by

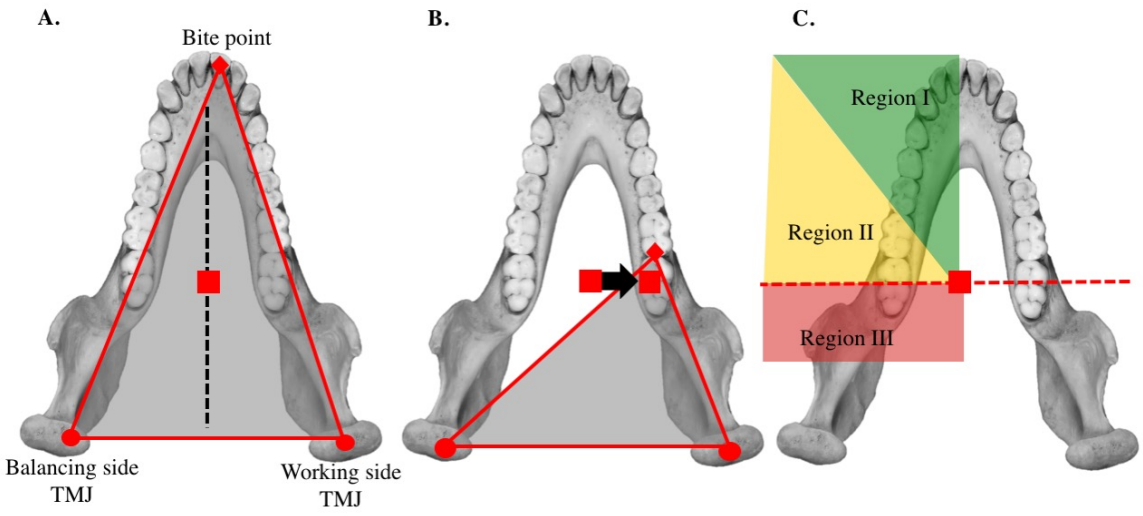


Figure 1. Occlusal view of mandible showing (A) the triangle of support with the muscle resultant (red square) falling within it. The triangle of support is bounded by the working-side and balancing-side TMJs and the bite (red diamond). When biting in anterior bite points, the resultant falls within the midline (black sashed line) because both balancing- and working-side adductor muscles are used with equal force. (B) As the bite point moves posteriorly, the triangle of support gets smaller and the muscle resultant must shift laterally towards the working side from its midline position in order to stay within the triangle of support. This lateral movement is achieved by reducing the balancing-side adductor force. (C) The spatial relationship among the resultant and working-side TMJ in conjunction with the midline sagittal plane are used to define three regions of the mandible: Regions I and II are separated by an oblique line passing though the working-side TMJ and the resultant's intersection with the triangle of support; Regions II and III are separated by a transverse (dashed) line passing thought the muscle resultant. See text for the biomechanical definitions of Regions I, II, and III. Bite points are only located in Regions I and II (i.e., anterior to the resultant), but never in Region III as they would distract the TMJ at the working-side TMJ.

reducing balancing-side muscle force (Fig. 1B; Greaves 1978). Based on the AP position at which the resultant crosses the triangle of support and its ML movements, the mandible has been divided into three regions (Fig. 1C). Region I contains bite points at which the muscle resultant can stay in the midline. Region II contains bite points that cause the resultant to shift laterally in order to stay within the triangle of support. Regions I and II contain teeth because biting in these regions will not result in TMJ distraction.

On the other hand, biting in Region III, in which the muscle resultant fails to pass within the triangle of support, would distract the TMJ. Thus, teeth should only be positioned anterior to the muscle resultant and within Regions I and II. Importantly, the boundary between Region II and Region III is determined by the AP position of the resultant. This boundary represents the most posterior possible position of bite points that will not cause distractive forces to the TMJ.

The CLM was developed using the artiodactyl masticatory system (Greaves 1978), with the assumption that the TMJ is positioned at the level of the occlusal plane, as is the case for many artiodactyls. This general configuration results in the muscle resultant vector being aligned perpendicular to the occlusal plane (Greaves 1978). A TMJ positioned at the level of the occlusal plane produces a triangle of support that falls along the occlusal plane. Recall that the distal boundary of Region II occurs where the muscle resultant vector crosses the triangle of support. In artiodactyls and many other mammals that have TMJs at the level of the occlusal plane (e.g., many carnivores, rodents, strepsirrhines), the point at which the muscle resultant crosses the triangle support is the same as the point at which the resultant vector crosses the occlusal plane (i.e., points 1 and 2 in Fig. 2A are coincident in space). In anthropoid primates, however, the TMJ is raised above the occlusal plane, which yields a triangle of support that is inclined to the occlusal plane (Fig. 2B). In such a configuration, unless the muscle resultant vector is perpendicular to the occlusal plane, the AP position at which the vector crosses the triangle of support will differ from the position that it crosses the occlusal plane (i.e., points 1 and 2 in Fig. 2B are not coincident in space). This affects the distribution of Region II. Primates tend to have anteriorly inclined muscle resultant vectors (Perry,

Hartstone-Rose, and Logan 2011). An anteriorly inclined resultant vector will cross the triangle of support at a more anterior location (point 2 in Fig. 2B) than the point at which it crosses the occlusal plane (point 1 in Fig. 2B), resulting in a more anteriorly positioned boundary between Region II and Region III.

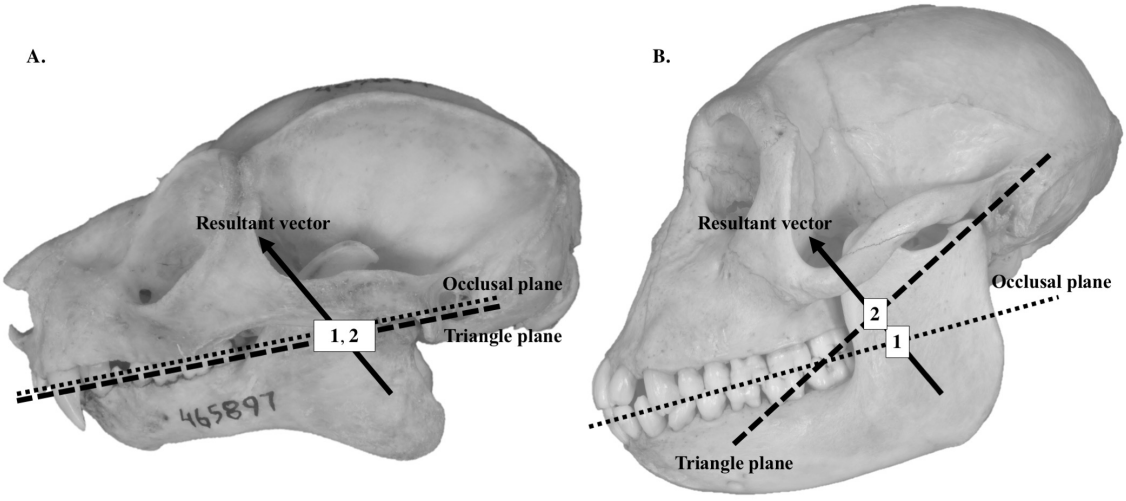


Figure 2. Lateral views of lemur (A) and macaque (B) skulls illustrating the effects of moving the TMJ above the occlusal plane and inclining the muscle resultant force vector. A TMJ at the occlusal plane (as in A) produces a triangle of support that falls along the occlusal plane. In this scenario, the point at which a resultant vector crosses the occlusal plane (Point 1) will coincide with the point at which that vector crosses the plane of the triangle of support (Point 2), even if the vector is inclined anteriorly. When the TMJ is raised above the occlusal plane (B) the plane of the triangle of support becomes inclined to the occlusal plane. If the muscle resultant vector is inclined anteriorly then at any bite point, the vector will cross the occlusal plane more posteriorly (Point 1) than it does the plane of the triangle of support (Point 2). Skulls not to scale. Figure modified from Spencer (1999).

## Introduction to Hypothesis

The utility of the CLM in describing the configuration of the masticatory system in infant and juvenile primates has not been explored systematically across primates, though it would seem logical that the same biomechanical constraint operating in adults must also operate at all stages throughout ontogeny. Indeed, in modern humans, chimpanzees, and papionin primates, molars emerge at a constant position, anterior to the TMJ (Spencer and Schwartz 2008; Schwartz 2012; Singleton 2015), a finding consistent with the expectations of the CLM.

This dissertation explores molar emergence as part of a masticatory system that is coordinated in its growth and provides an explicit causal model explaining variation in the emergence time of molars across primates. Extending the CLM into ontogeny suggests that molars should always emerge anterior to the muscle resultant. The availability of space anterior to the muscle resultant should be a constraint on *where* molars emerge. The rate at which this space is made available should, therefore, determine *when* molars emerge (i.e., the schedule of molar emergence).

The subsequent three chapters of this dissertation test the hypothesis that the location and timing of molar emergence is constrained to avoid TMJ distraction throughout ontogeny. The hypothesis is tested from three perspectives. Chapter 2 investigates the position of molar emergence and considers whether molars emerge directly anterior to the point at which the muscle resultant intersects the triangle of support, as per the original formulation of the CLM by Greaves (1978), or whether molars emerge significantly anterior to this point, which would be consistent with the finding that the last molar is positioned significantly anterior to the muscle resultant in

adult primates (Spencer 1995, 1999; Perry, Hartstone-Rose, and Logan 2011). Chapter 3 considers potential factors that influence ontogenetic and interspecific variation in the position of molar emergence and determines whether the position of emerging molars is influenced by factors related to the size of the buffer zone, a safety factor that creates greater stability at the TMJ during biting. Specifically, Chapter 3 investigates four factors that may contribute to ontogenetic and interspecific variation in the distance between the muscle resultant's intersection with the triangle of support and the position of emerging molars: food material properties, skull size, jaw gape, and the length of the next emerging molar. Finally, Chapter 4 investigates whether the rate at which space is made available in the jaw (anterior to the point at which the muscle resultant intersects the triangle of support) and the duration of jaw growth determine the timing of molar emergence. Overall, this dissertation is aimed at providing a mechanical and developmental model for explaining temporal and spatial variation in molar-emergence ages among primates.

CHAPTER 2

# BIOMECHANICAL CONSTRAINTS ON THE POSITION OF MOLAR EMERGENCE IN PRIMATES


## Abstract

Molar-emergence age serves as a skeletal proxy for life history in the fossil record. Knowledge of how variation in molar-emergence age arises and why it is closely associated with life history is lacking, however. Understanding the mechanism that produces variation in molar-emergence age is critical to evaluating why molar emergence tracks life history. Molars are part of an integrated system in which they function to comminute food. Developmental coordination among parts of this system is critical for proper food ingestion throughout life. In adult primates, the biomechanics of masticatory system configuration constrain where molars can be situated to avoid damage to the temporomandibular joint (TMJ) during chewing. This research tested the hypothesis that the location of molar emergence is constrained to avoid damage to the TMJ throughout ontogeny. Two predictions were tested: that molars emerge directly anterior to the adductor resultant and that molars emerge significantly anterior to the adductor resultant. 3D coordinate data were collected from cross-sectional ontogenetic samples of primate skulls (n = 21 species, 1258 specimens). The position of the resultant was estimated using two methods: (1) the average position of the three adductor muscle lines of action (MLAs) and (2) the most anterior MLA. Results indicate that molars emerge significantly anterior to the resultant throughout ontogeny; however, when the most anterior MLA is used to approximate the position of the resultant, the last molar is posterior to the MLA in later ontogenetic stages and adults of some taxa. This latter result contradicts previous

findings for adult primates and possible reasons for this are discussed. Overall, the study supports the idea that molar emergence is constrained by the biomechanics of mastication, especially early in ontogeny.

## Introduction

The age at which the permanent first molar (M1) emerges into the oral cavity is strongly correlated with life-history variables across primates (Smith 1989; Smith, Crummett, and Brandt 1994; Kelley and Schwartz 2010), and has been used to reconstruct the life history of fossil primates (e.g., Kelley 1997; Kelley and Smith 2003; Zihlman et al. 2004; Kelley and Schwartz 2012). The underlying mechanism driving this strong correlation remains unknown. Molar emergence should be completely integrated into the growth of the skull and part of an integrated masticatory system (Smith 1989; Spencer and Schwartz 2008). This study therefore examines molar emergence in the context of masticatory ontogeny.

The adult masticatory system of mammals is configured to avoid distraction of the temporomandibular joint (TMJ) (i.e., when the mandibular condyle is pulled away from the articular eminence) during biting and chewing (Greaves 1978, 1982, 1983, 1991, 2000; Spencer and Demes 1993; Spencer 1995, 1999; Thompson et al. 2003; Perry, Hartstone-Rose, and Logan 2011). According to the Constrained Lever Model (CLM), three points of resistance occur during unilateral biting (one at each TMJ and one at the bite point), and define the edges of the triangle of support. During unilateral biting, the adductor muscle resultant vector must pass through the triangle of support. If the resultant passes outside of the triangle of support, the bite point and balancing-side TMJ

experience rotation while the working-side TMJ experiences tension (i.e., TMJ distraction, Greaves 1978; Spencer 1999). Given this limitation, a key aspect of masticatory system configuration is the position of molars along the maxillary and mandibular arches in relation to the adductor muscle resultant vector. As per the CLM, the distal-most molar's position is constrained so that it is located anterior to the point at which the jaw adductor muscle resultant crosses the triangle of support because biting posterior to this point produces distractive forces at the working-side TMJ (Greaves 1978; Spencer 1999). Molars should, therefore, always be positioned along the mandibular and maxillary arches such that TMJ distraction is mitigated during mastication. The original CLM, as described by Greaves (1978, 1982, 1983, 1988), predicts that the distal-most molar lies immediately anterior to the muscle resultant (Greaves 1978). Several studies have found, however, that the molar's position is more anterior than predicted by the original CLM (Spencer 1999; Perry, Hartstone-Rose, and Logan 2011; Lucas, 2012). Extending the CLM model into ontogeny will require a test of these two scenarios.

Extending the CLM to ontogenetic stages suggests that molars should emerge anterior to the muscle resultant. The availability of space between the muscle resultant and the distal-most tooth present in the tooth row should be a constraint on where molars emerge. Most tests of the CLM in primates have been performed on adult primates and the utility of the CLM in describing the configuration of the masticatory system in infant and juvenile primates has not been explored systematically across primates, though it would seem logical that the same biomechanical constraint operating in adults should also operate at all stages throughout ontogeny. Indeed, in humans, chimpanzees, and

papionins, molars emerge at a constant distance to the TMJ (Spencer and Schwartz 2008; Schwartz 2012; Singleton, 2015), a finding consistent with the expectations of the CLM. Therefore, despite there being substantial variation in craniofacial configuration among these taxa, there appears to be a common constraint on the position of molar emergence that operates during ontogeny.

## Hypothesis

This research tests the hypothesis that the location of molar emergence is constrained to avoid TMJ distraction throughout ontogeny. Based on the CLM and previous research on adult primates, the hypothesis has two predictions. Prediction 1 states that as primates grow, molars emerge directly anterior to the point at which the muscle resultant intersects the triangle of support. This prediction tests the assumption of the CLM made by Greaves (1978), who stated that the last molar is situated directly anterior to the muscle resultant. Prediction 2, on the other hand, states that across primates, molars emerge significantly anterior to the point at which the muscle resultant intersects the triangle of support. This prediction is consistent with the finding that the last molar is positioned significantly anterior to the muscle resultant in adult primates (Spencer 1995, 1999; Perry, Hartstone-Rose, and Logan 2011).

## Material and Methods

### *Data Collection*

Following the methods of Spencer (1995) and Lucas (2012), data were collected on the spatial configuration of the masticatory system throughout primate ontogeny by digitizing 32 homologous landmarks (Table 1, Figure 3) characterizing overall skull size and masticatory configuration, including the position of teeth and the origins and insertions of the masticatory muscles. The data were obtained using a Microscribe G3X digitizer (Immersion Corp., San Jose, CA). To collect landmark data, primate crania were positioned on a ring, secured with dental wax. The ring was supported by a ring stand. The crania were inverted, with the basicranium positioned superior to the neurocranium. Landmarks were first collected from the inferior and lateral aspects of the cranium (landmarks 1-12) and the occlusal portions of maxillary teeth (landmarks 13-22). Mandibular landmarks (landmarks 23-32) were collected after the mandible was articulated with the cranium so that maxillary and mandibular teeth were in occlusion. Because infant and juvenile primates do not possess a full complement of adult teeth, the number of landmarks varied depending on the molar emergence category (see below) of each skull.

### *Sample*

The data were collected from cross-sectional ontogenetic samples of primate skulls representing 21 species across the primate order (see Table 2 for species list and sample sizes). The sample was aimed at capturing a wide range of taxonomic and morphological variation and species were selected based on the richness of skeletal

Table 1. List of landmarks collected for study.

| Landmark # | Landmark description |
|---|---|
| 1 | Left center of articular eminence |
| 2 | Left inferior edge of zygomatic arch at the zygomaticotemporal suture |
| 3 | Left inferior edge of zygomatic arch at the anterior-most point of origin of the superficial masseter |
| 4 | Left intersection of temporal line and frontozygomatic suture |
| 5 | Left pterion |
| 6 | Left center of medial surface of lateral pterygoid plate |
| 7 | Right center of medial surface of lateral pterygoid plate |
| 8 | Right pterion |
| 9 | Right intersection of temporal line and frontozygomatic suture |
| 10 | Right inferior edge of zygomatic arch at the anterior-most point of origin of the superficial masseter |
| 11 | Right inferior edge of zygomatic arch at the zygomaticotemporal suture |
| 12 | Right center of articular eminence |
| 13 | Left center of trigon basin of $M^3$ |
| 14 | Left center of trigon basin of $M^2$ |
| 15 | Left center of trigon basin of $M^1$ |
| 16 | Left center of trigon basin of $P^4/dp^4$ |
| 17 | Left center of trigon basin of $P^3/dp^3$ |
| 18 | Right center of trigon basin of $P^3/dp^3$ |
| 19 | Right center of trigon basin of $P^4/dp^4$ |
| 20 | Right center of trigon basin of $M^1$ |
| 21 | Right center of trigon basin of $M^2$ |
| 22 | Right center of trigon basin of $M^3$ |
| 23 | Left coronion |
| 24 | Left centroid of insertion of superficial masseter on lateral ramus |
| 25 | Left centroid of insertion of medial pterygoid on medial angle of mandible |
| 26 | Right centroid of insertion of medial pterygoid on medial angle of mandible |
| 27 | Right centroid of insertion of superficial masseter on lateral ramus |
| 28 | Right coronion |
| 29 | Left distal to $P_4/dp_4$ alveolar border |
| 30 | Left distal to $M_1$ alveolar border |
| 31 | Left distal to $M_2$ alveolar border |
| 32 | Left distal to $M_3$ alveolar border |

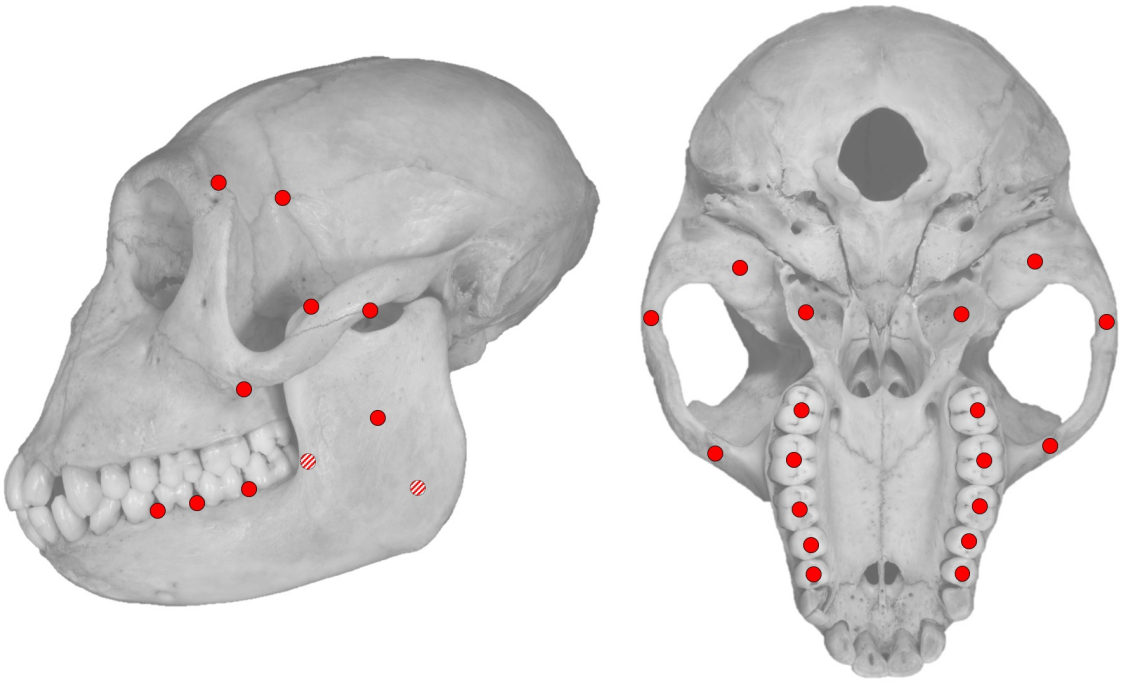

Figure 3. Lateral (left) and inferior (right) views of an adult female macaque skull illustrating the landmarks used in this study. Circles filled in with a solid color indicate landmarks that are on the surface, while circles with lines indicate landmarks that are obstructed from view.

ontogenetic samples available for study worldwide. Although every effort was made to maintain taxonomic diversity and equal sample sizes, the samples for catarrhine species tend to be larger due to the greater availability of ontogenetic material while the sample sizes for strepsirrhine species are smaller due to the relative paucity of ontogenetic skeletal material.

Table 2. List of species examined in this study, including sample sizes listed according to molar emergence category.

| Taxon | Sample size for molar emergence category | | | | Institution |
|---|---|---|---|---|---|
| | dp4 | M1 | M2 | M3 | |
| **Platyrrhini** | | | | | |
| *Alouatta palliata* | 10 | 10 | 10 | 20 | 1 |
| *Ateles geoffroyi* | 7 | 10 | 10 | 20 | 1,2,3 |
| *Cebus (Sapajus) apella* | 10 | 10 | 6 | 30 | 1,4 |
| *Saimiri sciureus* | 4 | 9 | 10 | 19 | 1,4 |
| **Cercopithecidae** | | | | | |
| *Colobus angolensis* | 10 | 9 | 10 | 19 | 2,5 |
| *Colobus polykomos* | 3 | 5 | 8 | 20 | 1,3,4 |
| *Procolobus verus* | - | 6 | 7 | 19 | 5 |
| *Macaca mulatta* | 28 | 33 | 31 | 58 | 1,6 |
| *Macaca fascicularis* | 10 | 10 | 8 | 16 | 1,2,3,4 |
| *Papio anubis* | 10 | 10 | 10 | 28 | 5,7 |
| *Papio cynocephalus* | 12 | 10 | 17 | 34 | 1,3,5,7 |
| **Hominidae** | | | | | |
| *Gorilla beringei* | 16 | 14 | 9 | 57 | 1,5, 8 |
| *Gorilla gorilla* | 7 | 10 | 5 | 29 | 1,2,3,4,5 |
| *Homo sapiens* | 25 | 22 | 31 | 50 | 1,9 |
| *Pan paniscus* | 10 | 10 | 12 | 21 | 5 |
| *Pan troglodytes* | 16 | 21 | 21 | 69 | 1,5,10,11 |
| *Pongo pygmaeus* | 9 | 11 | 12 | 19 | 1,2,3,4 |
| **Strepsirrhini** | | | | | |
| *Eulemur mongoz* | - | 2 | - | 13 | 1,2,4 |
| *Lemur catta* | 3 | - | 5 | 18 | 1,2,3,4 |
| *Perodicticus potto* | 2 | 8 | 8 | 20 | 1,2, 3,4 |
| *Otolemur monteiri* | 3 | 3 | - | 31 | 2,5 |

(1) National Museum of Natural History, Washington, DC; (2) American Museum of Natural History, New York, NY; (3) Museum of Comparative Zoology, Harvard University, Cambridge, MA; (4) Vienna Museum of Natural History Museum, Vienna, Austria; (5) Royal Museum for Central Africa, Tervuren, Belgium; (6) Caribbean Primate Research Center, Laboratory of Primate Morphology and Genetics at the University of Puerto Rico, Puerto Rico; (7) Amboseli Baboon Research Project, Skeletal Collection, National Museums Kenya; Nairobi, Kenya; (8) Mountain Gorilla Skeletal Project, Musanze, Rwanda; (9) Spencer Atkinson Collection, University of the Pacific School of Dentistry, San Francisco, CA; (10) Max Planck Institute, Leipzig, Germany; (11) Department of Anthropology, University of Minnesota, Minneapolis, MN.

*Masticatory System Measurements*

The coordinate data were used to calculate the following two parameters: (1) the distance between the TMJ and the point at which each of the adductor muscles' line of action (MLA) intersects the triangle of support, projected onto the occlusal plane ($d_{TMJ\_MLA\_Occlusal}$), and (2) the distance between the TMJ and the last molar, projected onto the occlusal plane ($d_{TMJ\_Molar\_Occlusal}$) (described in further detail below). All landmark data were analyzed using customized code written in R 3.0.2 (R Core Team 2013) by HG.

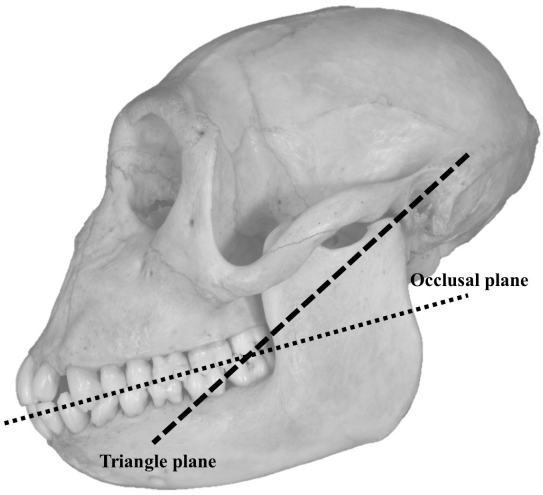


Figure 4. Lateral view of adult female macaque skull illustrating the occlusal plane and the plane of the triangle of support (i.e., the triangle plane).

Because the TMJ is raised above the occlusal plane in many primate species, the triangle of support is inclined to the occlusal plane. This, along with an anteriorly inclined muscle resultant, found in most primates (Perry, Hartstone-Rose, and Logan 2011), yields an intersection point between the resultant and the triangle of support that is more anterior than the intersection between the resultant and the occlusal plane (see

Chapter 1, Fig. 2). To accommodate the influence of a raised TMJ on the intersection of the resultant vector and the triangle of support, this study investigated the anteroposterior position at which the resultant vector crosses the triangle of support, which was then projected onto the occlusal plane and compared to the position of the last molar in that same occlusal plane. Landmark data were used to determine the points at which MLAs of the masseter muscle, the anterior temporalis muscle, and the medial pterygoid muscle cross the triangle of support.

Table 3. Landmarks used to establish planes.

| Plane | Molar emergence category | Landmarks |
|---|---|---|
| Triangle of support plane | M3 emerged | Left: 1, 12, 13, Right: 1, 12, 22 |
| | M2 emerged | Left: 1, 12, 14, Right: 1, 12, 21 |
| | M1 emerged | Left: 1, 12, 15, Right: 1, 12, 20 |
| | dp4 emerged | Left: 1, 12, 16, Right: 1, 12, 19 |
| Occlusal plane | M3 emerged | Left: 13, 22, 17, Right: 13, 22, 18 |
| | M2 emerged | Left: 14, 21, 17, Right: 14, 21, 18 |
| | M1 emerged | Left: 15, 20, 17, Right: 15, 20, 18 |
| | dp4 emerged | Left: 16, 19, 17, Right: 16, 19, 18 |

Two planes were defined for the purposes of data collection. The plane of the triangle of support (from here on referred to as the *triangle plane*, Fig. 4)) was defined using three points: two points for the centers of the right and left articular eminences and the trigon basin of the last molar (Table 3). The occlusal plane (Fig. 4) was defined using the trigon basin of the right and left last two molars and the P3/dp3 (Table 3). A plane is defined by any three points that lie in that plane. For a hypothetical plane that contains the points *P1*(*x1,y1,z1*), *P2*(*x2,y2,z2*), and *P3*(*x3,y3,z3*), two vectors can be defined as:

*Equation 1:* $\overrightarrow{P1P2} = (x2, y2, z2) - (x1, y1, z1) = Ax, Ay, Az$

*Equation 2:* $\overrightarrow{P1P3} = (x3, y3, z3) - (x1, y1, z1) = Bx, By, Bz$

The cross product of these two vectors will be a vector that is orthogonal to the hypothetical plane:

*Equation 3*: $\overrightarrow{P1P2} \times \overrightarrow{P1P3} = \begin{vmatrix} \vec{\imath} & \vec{\jmath} & \vec{k} \\ Ax & Ay & Az \\ Bx & By & Bz \end{vmatrix} = i(AyBz - AzBy) + j(AzBx - AxBz) +$

$$k(AxBy - AyBx)$$

If $(AyBz - AzBy)$ is represented by $E$,

if $(AzBx - AxBz)$ is represented by $F$,

if $(AxBy - AyBx)$ is represented by $G$,

then,

*Equation 4:* $\overrightarrow{P1P2} \times \overrightarrow{P1P3} = Ei + Fj + Gk$

The scalar equation of the plane is therefore:

*Equation 5:* $Ex + Fy + Gz + D = 0$

where D is a constant, found by plugging a point into the equation that is in the plane (*P1*[*x1,x2,x3*]):

Equation 6: $E(x - x1) + F(y - y1) + G(z - z1) + D = 0$

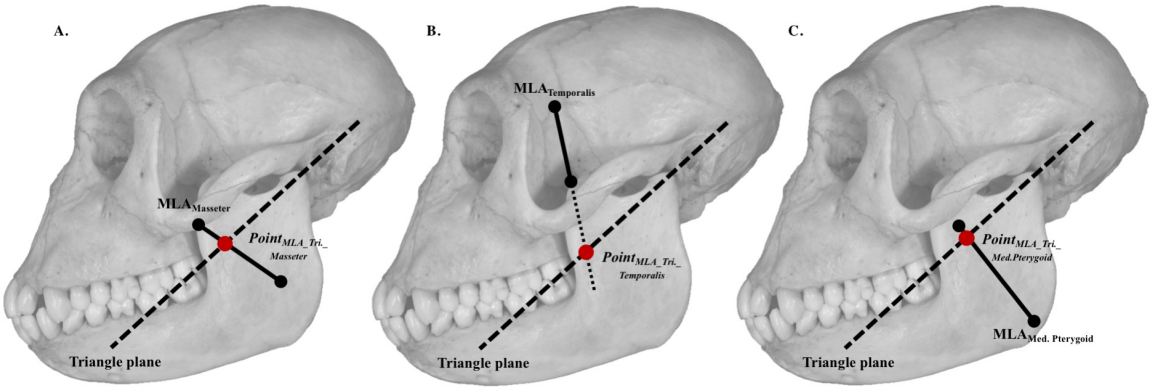


Figure 5. Lateral views of adult female macaque skulls illustrating the points of intersection between each of the MLAs and the triangle plane for (A) the masseter muscle ($Point_{MLA\_Tri\_Masseter}$), (B) the anterior temporalis muscle ($Point_{MLA\_Tri\_Temporalis}$), and (C) the medial pterygoid muscle ($Point_{MLA\_Tri\_Med.\ Pterygoid}$). In each case, the point of intersection is shown by the red dot.

Once the planes were established, the points of intersection between each of the MLAs and the triangle plane were determined ($Point_{MLA\_Tri}$, Fig. 5). To do this, the equation of the plane (Equation 5) and the equation of the MLAs, which are lines, are needed. The equation of a line in the form:

$$\textit{Equation 7: } r = r_0 + vt$$

can be decomposed into

$$\textit{Equation 8: } x = x_0 + v_x t$$

$$\textit{Equation 9: } y = y_0 + v_y t$$

$$\textit{Equation 10: } z = z_0 + v_z t$$

Equations 8, 9, and 10 were used in the triangle plane equation (Equation 5) to solve for *t.* The values of *t* were then plugged back into equations 8, 9, and 10 to determine the x-, y-,

and z-coordinates of the intersection of an MLA and the triangle plane ($Point_{MLA\_Tri}$). Next, the distance from $Point_{MLA\_Tri}$ and the occlusal plane ($d_{MLA\_Occlusal}$, Fig. 4) was measured using Equation 11.

$$Equation\ 11:\ d_{MLA\_Occlusal} = \frac{\left|Ex_{MLA\_Tri} + Fy_{MLA\_Tri} + Gz_{MLA\_Tri} + D\right|}{\sqrt{E^2 + F^2 + G^2}}$$

Where, E, F, G, and D are components from equation 5, in this case for the occlusal plane. Similarly, the distance from the TMJ to the occlusal plane ($d_{TMJ\_Occlusal}$, Fig. 6) was measured using Equation 12.

$$Equation\ 12:\ d_{TMJ_{Occlusal}} = \frac{\left|Ex_{TMJ} + Fy_{TMJ} + Gz_{TMJ} + D\right|}{\sqrt{E^2 + F^2 + G^2}}$$

The Euclidean distance between the TMJ and $Point_{MLA\_Tri}$ ($d_{TMJ\_MLA}$, Fig. 6) was then measured using Equation 13.

$$Equation\ 13:\ d_{TMJ\_MLA} =$$

$$\sqrt{(x_{MLA\_Tri} - x_{TMJ})^2 + (y_{MLA\_Tri} - y_{TMJ})^2 + (z_{MLA\_Tri} - z_{TMJ})^2}$$

$D_{TMJ\_MLA}$ represents the hypotenuse of a right triangle (Fig. 6), the opposite distance of which was determined using Equation 14.

$$Equation\ 14:\ d_{Opposite\_TMJ} = d_{TMJ\_Occlusal} - d_{MLA\_Occlusal}$$

The distance from the TMJ to the intersection of the MLA with the triangle plane, projected onto the occlusal plane ($d_{TMJ\_MLA\_Occlusal}$, Fig. 6) is therefore defined as:

$$Equation\ 15:\ d_{TMJ\_MLA\_Occlusal} = \sqrt{\left|{d_{Opposite\_TMJ}}^2 - {d_{TMJ\_MLA}}^2\right|}$$

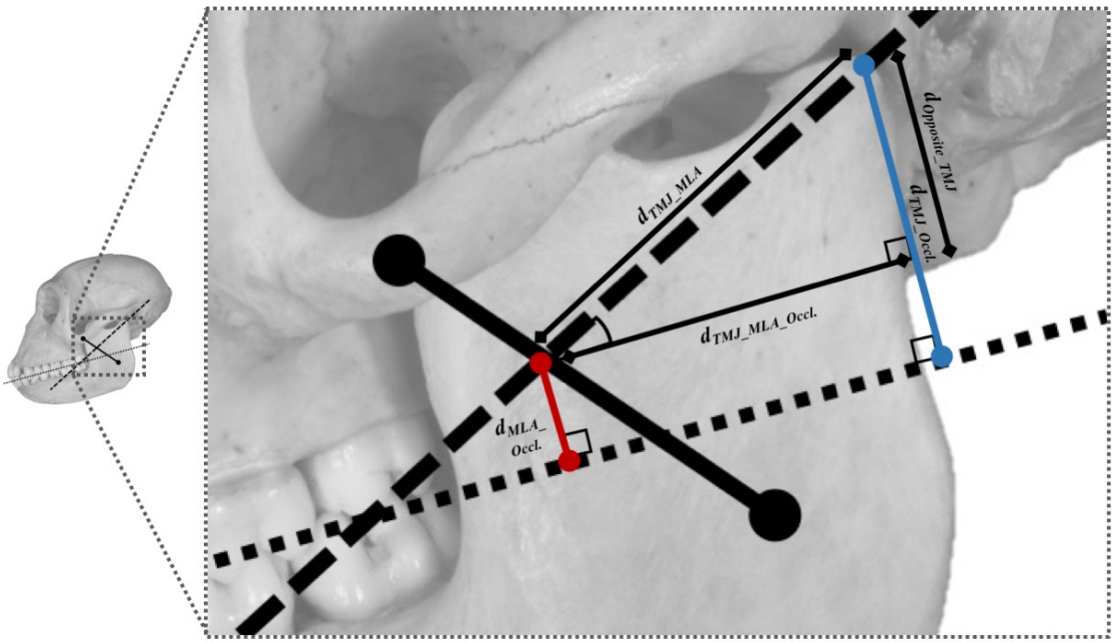


Figure 6. Lateral view of adult female macaque skull showing measurements used to determine the distance between the TMJ and the MLA, projected onto the occlusal plane. Image shows the occlusal plane (short-dashed black line), the triangle plane (long-dashed black line), and an MLA (thick solid black line). Red line represents the projected distance between the MLA's intersection with the triangle plane to the occlusal plane ($d_{MLA\_Occlusal}$) and the blue line represents the distance between the TMJ and the occlusal plane ($d_{TMJ\_Occlusal}$). Enlarged portion of the skull illustrates variables that were measured to determine the distance between the TMJ and the MLA, projected onto the occlusal plane ($d_{TMJ\_MLA\_Occlusal}$). See text for definitions of other variables and details of their calculations.

Finally, it was necessary to determine the distance from the TMJ to the last emerged molar, projected onto the occlusal plane. The point on the alveolar margin, just distal to the last mandibular molar was projected onto the occlusal plane using Equation 16.

Equation 16: $d_{Molar_{Occlusal}} = \frac{|Ex_{Molar}+Fy_{Molar}+Gz_{Molar}+D|}{\sqrt{E^2+F^2+G^2}}$

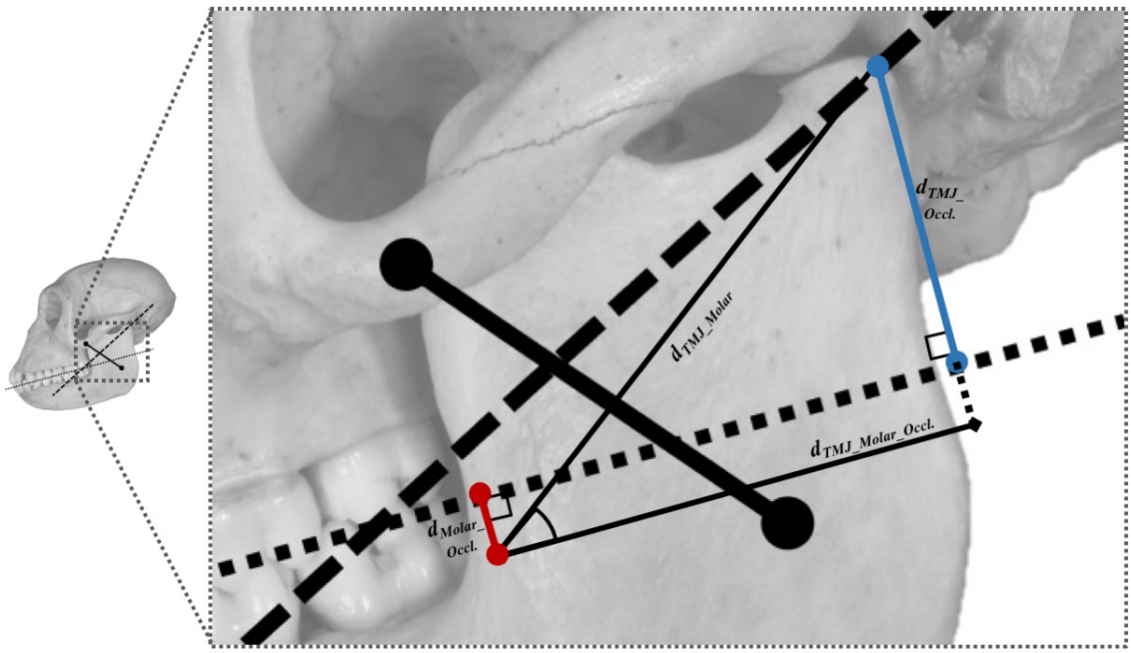


Figure 7. Lateral view of adult female macaque skull showing measurements used to determine the distance between the TMJ and the last molar, projected onto the occlusal plane. Image shows the occlusal plane (short-dashed black line), the triangle plane (long-dashed black line), and an MLA (thick solid black line). Red line represents the projected distance between the last molar and the occlusal plane ($d_{Molar\_Occlusal}$) and the blue line represents the distance between the TMJ and the occlusal plane ($d_{TMJ\_Occlusal}$). Enlarged portion of the skull illustrates variables that were measured to determine the distance between the TMJ and the last molar, projected onto the occlusal plane ($d_{TMJ\_Molar\_Occlusal}$). See text for definitions of other variables and details of their calculations.

The distance from the TMJ to the occlusal plane ($d_{TMJ\_Occlusal}$) was previously determined. The Euclidean distance between the TMJ and the point distal to the last molar ($d_{TMJ\_Molar}$, Fig. 5) was measured using Equation 17.

*Equation 17:* $d_{TMJ\_Molar} = \sqrt{(x_{TMJ} + x_{Molar})^2 + (y_{TMJ} + y_{Molar})^2 + (z_{TMJ} + z_{Molar})^2}$

The sum of the distances $d_{TMJ\_Occlusal}$ and $d_{Molar\_Occlusal}$ formed the hypotenuse of a right triangle (Fig. 7). The opposite of this right triangle was equal to $d_{TMJ\_Occlusal}$ (Fig. 7) and

so the distance from the TMJ to the last erupted molar, projected onto the occlusal plane ($d_{TMJ\_Molar\_Occlusal}$, Fig. 7), is calculated using Equation 18.

$$\textit{Equation 18: } d_{TMJ\_Molar\_Occlusal} = \sqrt{\left|{d_{TMJ\_Occlusal}}^2 - {d_{TMJ\_Molar}}^2\right|}$$

The variable *Resultant-Molar* (Fig. 8) represents the distance between the resultant and the last molar, along the occlusal plane. *Resultant-Molar* was calculated by taking the difference between $d_{TMJ\_Molar\_Occlusal}$ and $d_{TMJ\_MLA\_Occlusal}$, using the formula:

$$\textit{Equation 19: } Resultant - Molar = d_{TMJ\_Molar\_Occlusal} - d_{TMJ\_MLA\_Occlusal}$$

*Resultant-Molar* was calculated using two different methods of estimating the position of the resultant (see below).

Finally, the variable *MLA-Molar* was calculated. This variable is similar to *Resultant-Molar* but represents the distance between a specific MLA and the last molar, rather than the resultant and the last molar, along the occlusal plane. *MLA-Molar* was calculated by taking the difference between $d_{TMJ\_Molar\_Occlusal}$ and $d_{TMJ\_MLA\_Occlusal}$, using the formula:

$$\textit{Equation 20: } MLA - Molar = d_{TMJ\_Molar\_Occlusal} - d_{TMJ\_MLA\_Occlusal}$$

but only using data for specific MLAs (e.g., only the masseter).

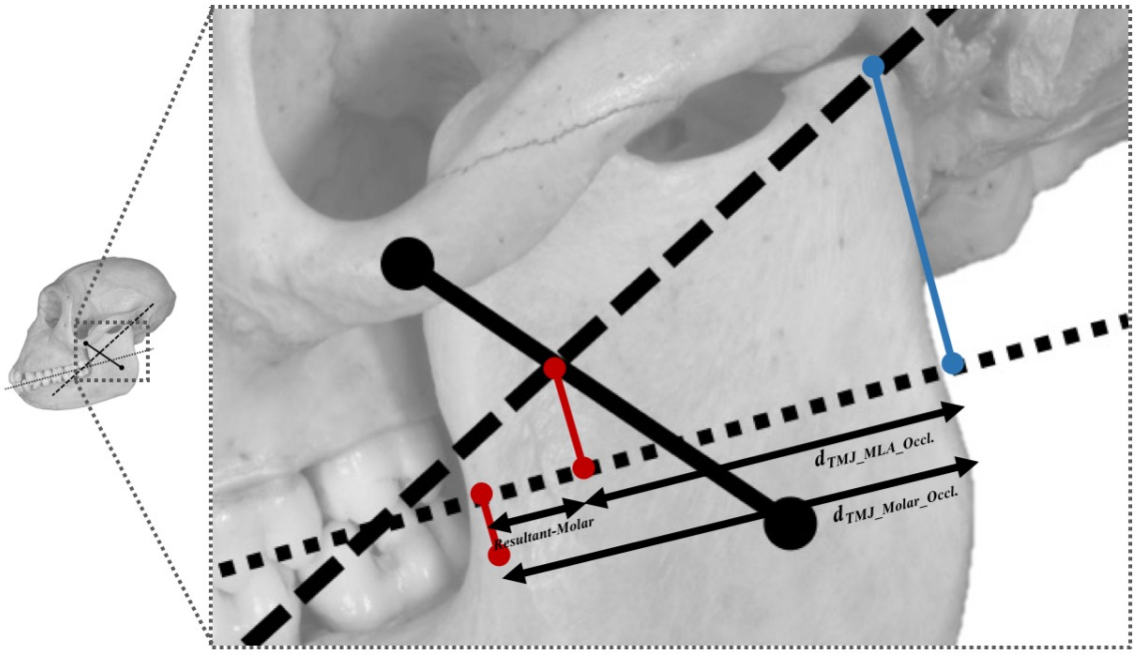


Figure 8. Lateral view of adult female macaque skull showing measurements used to measure the distance between the resultant and the last molar. Image shows the occlusal plane (short-dashed black line), the triangle plane (long-dashed black line), and an MLA (thick solid black line). Red and blue lines as in Figs. 6 and 7. Enlarged portion of the skull illustrates variables that were used to measure the distance between the resultant and the last molar (*Resultant-Molar*). See text for definitions of other variables and details of their calculations.

Several landmarks were used for the attachment points of the temporalis and masseter muscles. Two landmarks were used to estimate masseter origin (landmarks 2 and 3 on the left side and landmarks 10 and 11 on the right side, Table 1) and one to estimate masseter insertion (landmark 24 on the left side and 27 on the right side, Table 1). The anterior temporalis muscle fibers run vertically and act in jaw adduction. This portion of the temporalis muscle is continuous with the posterior temporalis, which has muscle fibers that are positioned more horizontally and act in retrusion of the mandible. The anterior temporalis was defined here as that portion of the temporalis muscle that originates lateral and distal to the orbit and in the pterion region. Two landmarks were

used to estimate anterior temporalis origin (landmarks 4 and 5 on the left side and landmarks 8 and 9 on the right side, Table 1) and one landmark for its insertion (landmark 23 on the left side and landmark 28 on the right side, Table 1). These multiple landmarks were used to capture variation in the attachment sites of these muscles and the effect that this variation has on estimating the resultant. Only one landmark was used to represent the origin (landmark 6 on the right side and landmark 7 on the left side, Table 1) and insertion (landmark 25 on the right side and landmark 26 on the left side, Table 1) of the medial pterygoid muscle.

The position of the muscle resultant vector was estimated using skeletal landmarks. This was done in two ways. The first was by calculating the average $d_{TMJ\_MLA\_Occlusal}$ value for each of the three adductor muscles' MLAs using all combinations of landmarks as described above, and then calculating the average $d_{TMJ\_MLA\_Occlusal}$ of these three to yield an overall mean $d_{TMJ\_MLA\_Occlusal}$ value. This assumes that each muscle contributes equal force during isometric maximum bite force production, the implications of which are addressed in the "Discussion" section below.

The second method used to estimate resultant position was more conservative. The position of the muscle resultant vector can be bracketed by examining the position of its component forces (i.e., the three adductor muscles). Because the resultant of the three vectors is a combination of the positions, orientations, and magnitudes of the three adductor vectors, it has to cross the triangle plane at a point that is bracketed by the MLA points of intersection (Spencer 1999). Therefore, the MLA that crosses the triangle plane at the most anterior position can represent the most anterior point that the resultant can cross the triangle plane. For each specimen, it was determined which MLA crossed the

triangle plane at the most anterior position (i.e., the greatest value for $d_{TMJ\_MLA\_Occlusal}$) and this value was used to represent the most anterior position of the resultant.

The above two methods were used to determine the variables *Resultant$_{Mean}$-Molar* and *Resultant$_{Max}$-Molar*, which represented *Resultant-Molar* (described above as the distance between the resultant and the last molar, and herein used to refer to *Resultant$_{Mean}$-Molar* and *Resultant$_{Max}$-Molar* together) calculated using the first (i.e., mean MLA) and second (i.e., max MLA) method to estimate the position of the resultant, respectively.

*Analyses*

For each species, specimens were divided into four molar emergence categories: (1) dp4 emerged, (2) M1 emerged, (3) M2 emerged, and (4) M3 emerged. A molar was scored as emerged if its occlusal surface was in the occlusal plane.

To determine the position of molar emergence relative to the resultant, the length *Resultant-Molar (*i.e., the distance from the resultant to the last molar, along the occlusal plane, see Fig. 8) was used. A positive *Resultant-Molar* value indicated that the last molar lies anterior to the resultant, zero indicated that the last molar is positioned at the resultant, and a negative *Resultant-Molar* value indicated that the last molar is posterior to the resultant.

Species-samples and developmental categories were analyzed separately. A power analysis on pilot data, with a significance level of 0.05 and power of 0.8, determined that a sample of size of at least seven individuals was needed to detect a significant difference in the position of the muscle resultant in relation to the last molar.

Tests were not performed on samples that contained less than seven individuals. To test both predictions, the length of *Resultant-Molar* was compared to zero. The first prediction stated that molars emerge directly anterior to the point at which the muscle resultant intersects the triangle of support. To test this, *Resultant-Molar* was compared to zero using two-sided one sample *t*-tests. *Resultant-Molar* was not expected to differ significantly from zero. The second prediction stated that molars emerge significantly anterior to the point at which the muscle resultant intersects the triangle of support. To test this *Resultant-Molar* was compared to zero using one-sided two sample *t*-tests. According to this prediction *Resultant-Molar* was expected to be significantly greater than zero. Analyses were performed for both methods of determining resultant position (i.e., using $Resultant_{Mean}$-*Molar* and $Resultant_{Max}$-*Molar*). Due to the high number of *t*-tests performed, a Bonferroni correction was used to ensure that any significant results were not due to chance. A total of 264 *t*-tests were performed, resulting in an adjusted alpha value of 0.000189.

Previous research on the biomechanical constraints on molar emergence identified that the distance between the TMJ and the last molar remains constant in humans and chimpanzees throughout ontogeny (Spencer and Schwartz 2008; Schwartz, 2012) and increases only late in ontogeny for some papionins (Singleton 2015). The current research attempted to replicate these results by determining whether there are intraspecific differences (among molar emergence categories) within species in $d_{TMJ\_Molar\_Occlusal}$ using one-way analyses of variance (ANOVAs) with Tukey's post-hoc tests for significant results.

In previous analyses (Spencer and Schwartz 2008; Schwartz 2012; Singleton 2015), the distance between the TMJ and the last molar was used as a surrogate for the distance between the resultant and the last molar. In addition to duplicating the analyses of these researchers, the research here also tested whether there are ontogenetic changes (among molar emergence categories) in the distance between the last molar and the resultant (i.e., *Resultant-Molar*) using one-way analyses of variance (ANOVAs) with Tukey's post-hoc tests for significant results.

## Results

The distal-most molar was anterior to the masseter MLA in all specimens with erupted dp4s (n = 195) and M1s (n = 223), and all but one specimen with erupted M2s (n = 230) (Figure 9). For individuals with erupted M3s (n = 610), the M3 was anterior to the masseter MLA in all cercopithecoids and strepsirrhines, but not in all specimens of some hominids (*G. beringei*, *G. gorilla*, *P. pygmaeus*, and *H. sapiens*) and platyrrhines (*A. palliata*) (Fig. 9).

The distal-most molar was anterior to the anterior temporalis MLA in all but one specimen with erupted dp4s (one *M. mulatta* specimen) and in all specimens with erupted M1s (Fig. 10). For individuals with erupted M2s, all cercopithecoids, strepsirrhines, and platyrrhines possessed M2s that were anterior to anterior temporalis MLA. Similarly, most hominid specimens with M2s emerged, with the exception of one *P. pygmaeus* and four *H. sapiens* individuals, had distal-most molars that were anterior to anterior temporalis MLAs (Fig. 8). All cercopithecoid and most platyrrhine, and strepsirrhine

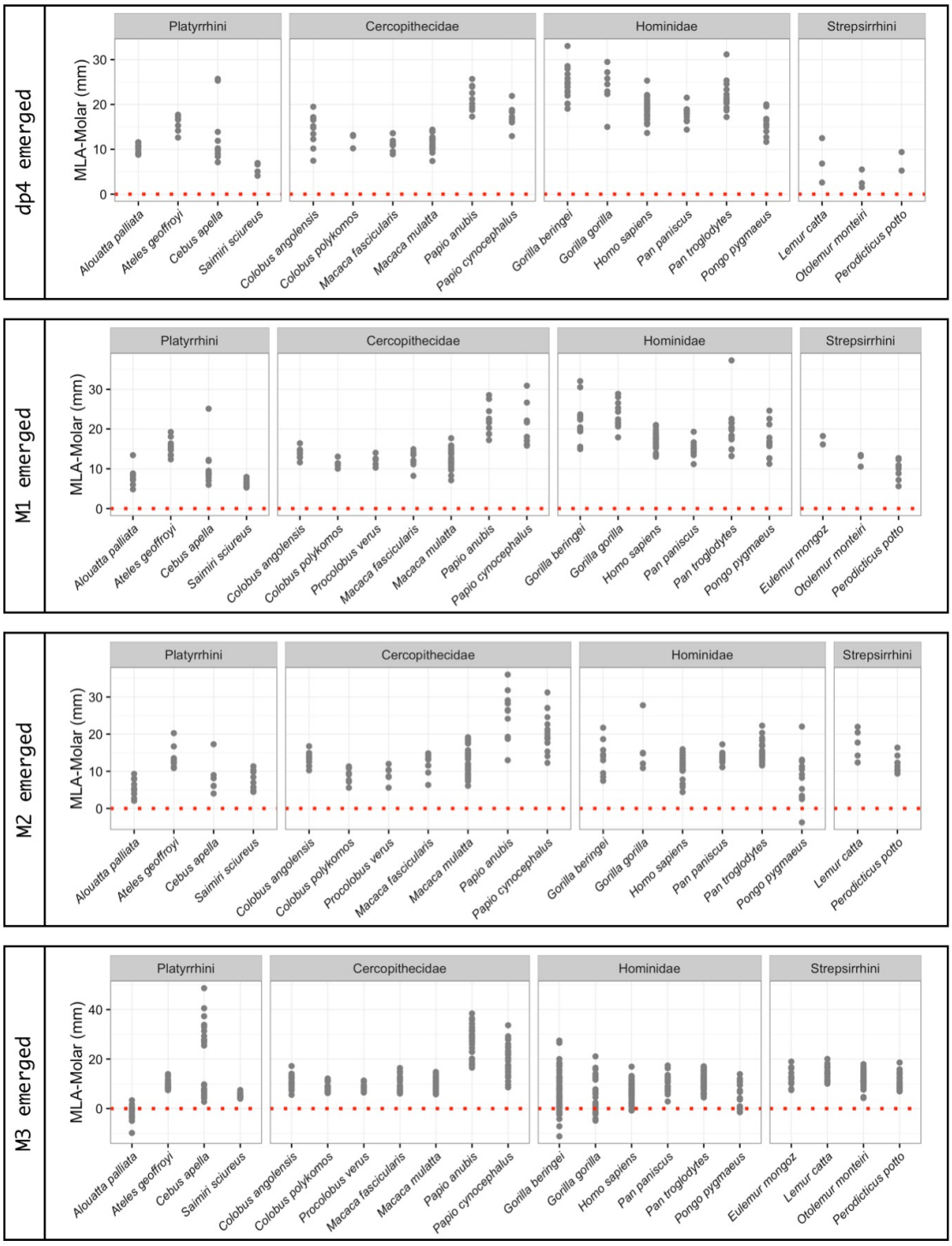


Figure 9. Distance between the MLA and the last molar, projected onto the occlusal plane (*MLA-Molar*) for the **masseter muscle** for each molar emergence category. Red dashed line represents the position that the MLA crosses the triangle of support, projected onto the occlusal plane. Positive *MLA-Molar* values indicate that the last molar is anterior to the MLA and negative values indicate that the last molar is posterior to the MLA.

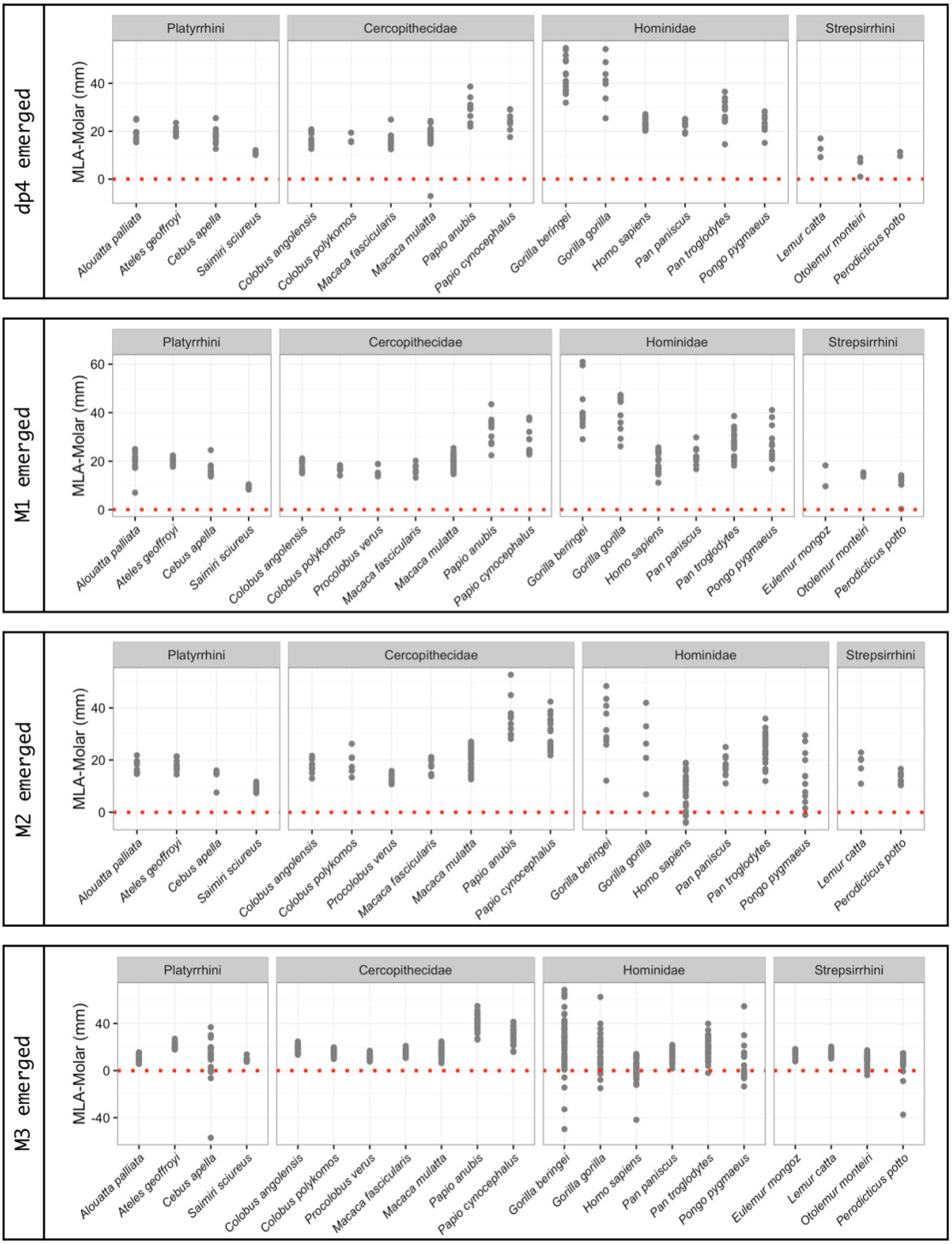


Figure 10. Distance between the MLA and the last molar, projected onto the occlusal plane (*MLA-Molar*) for the **anterior temporalis muscle** for each molar emergence category. Red dashed line represents the position that the MLA crosses the triangle of support, projected onto the occlusal plane. Positive *MLA-Molar* values indicate that the last molar is anterior to the MLA and negative values indicate that the last molar is posterior to the MLA.

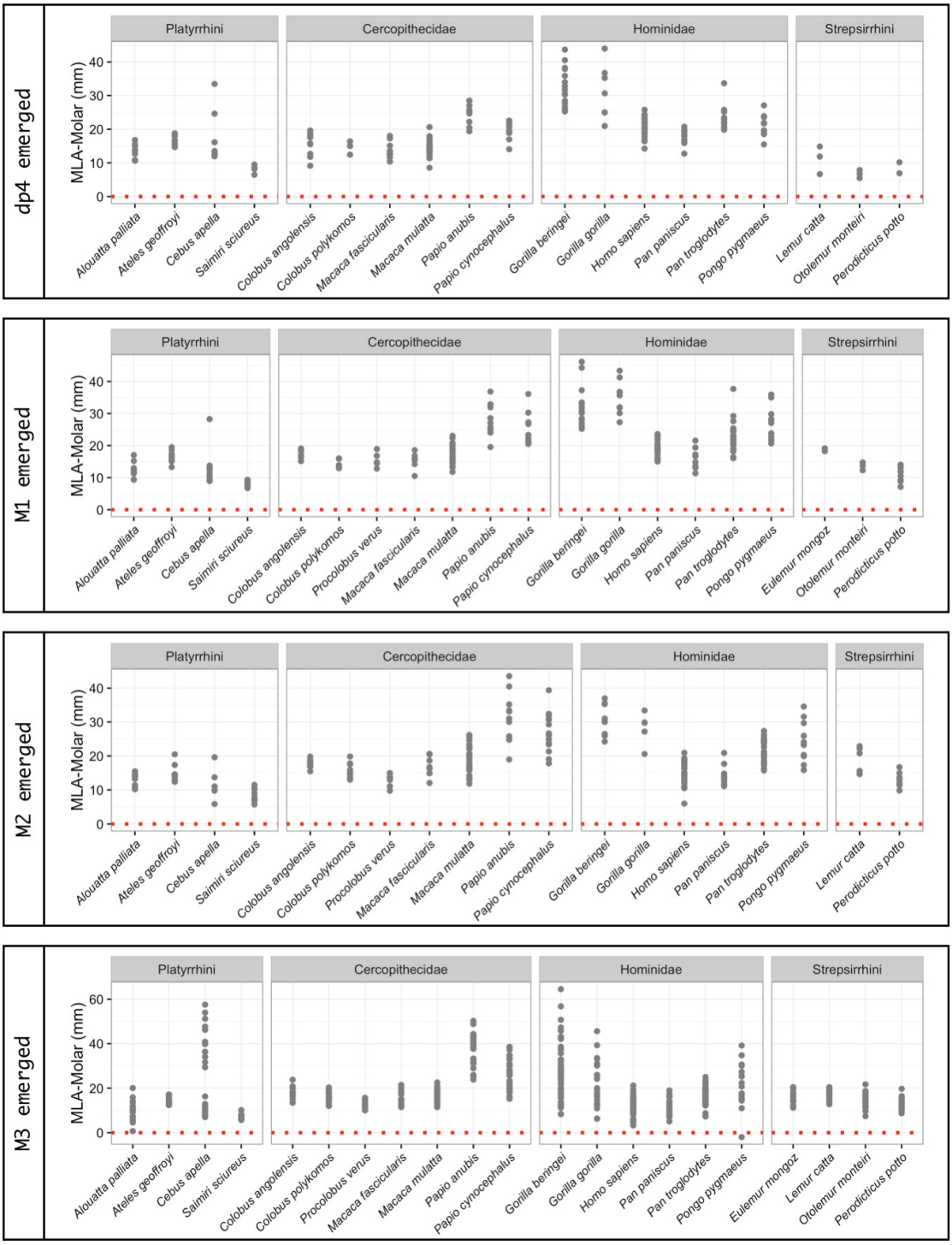


Figure 11. Distance between the MLA and the last molar, projected onto the occlusal plane (*MLA-Molar*) for the **medial pterygoid muscle** for each molar emergence category. Red dashed line represents the position that the MLA crosses the triangle of support, projected onto the occlusal plane. Positive *MLA-Molar* values indicate that the last molar is anterior to the MLA and negative values indicate that the last molar is posterior to the MLA.

individuals with M3s emerged possessed M3s that were anterior to anterior temporalis MLAs. The exceptions among platyrrhines were three specimens of *C. apella* and the exceptions among strepsirrhines were two specimens of *O. monteiri* and three specimens of *P. potto* (Fig. 10). Among hominids, several species (*G. beringei*, *G. gorilla*, *H. sapiens*, *P. troglodytes*, and *P. pygmaeus*) have at least one specimen with an M3 that was posterior to the anterior temporalis MLA (Fig. 10).

All specimens in all molar emergence categories, except for one *P. pygmaeus* individual with M3s emerged, had distal-most molars that were anterior to medial pterygoid MLAs (Fig. 11).

Results of *t*-tests comparing $Resultant_{Mean}$-*Molar* to zero indicate that, for all species and developmental categories, $Resultant_{Mean}$-*Molar* was both significantly different from and greater than zero (Fig. 12, SM 1). All mean, maximum and minimum $Resultant_{Mean}$-*Molar* values for each species and molar emergence category were positive, except for two minimum $Resultant_{Mean}$-*Molar* values (SM 1). These two values are based on two individuals that have average $Resultant_{Mean}$-*Molar* estimates just below zero. These two individuals are both adults (molar emergence category: M3 emerged) and represent one specimen of *H. sapiens*, and one specimen of *C. apella* (Fig. 12). Beyond these exceptions, all other specimens, regardless of species designation and molar emergence category, possessed $Resultant_{Mean}$-*Molar* estimates that were greater than zero (Fig. 12).

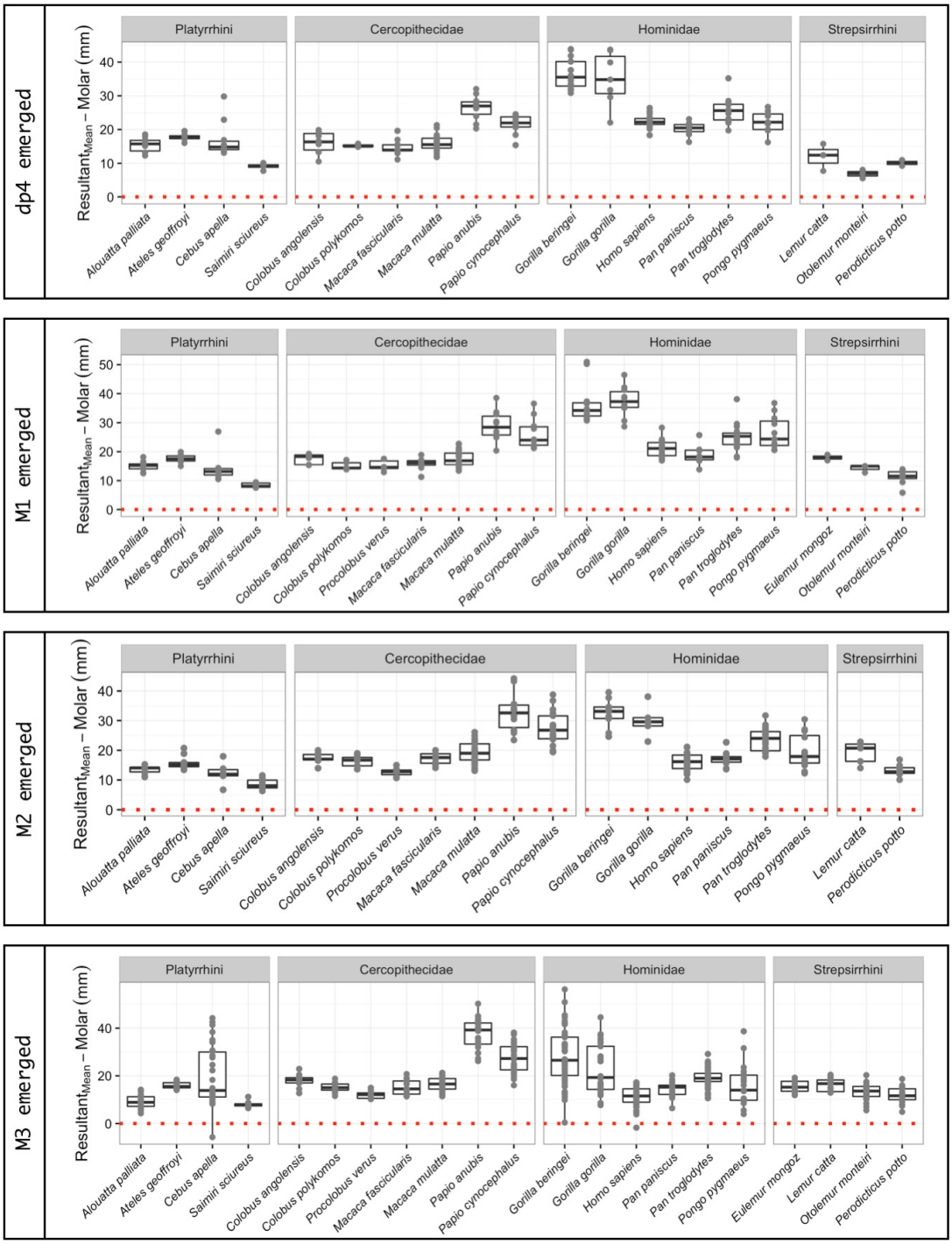


Figure 12. Boxplots of the distance between the resultant and the last molar, projected onto the occlusal plane (*Resultant$_{Mean}$-Molar*) using the first method of determining resultant position (average MLA; see text for details). Red dashed line represents the position that the resultant crosses the triangle of support, projected onto the occlusal plane. Positive *Resultant$_{Mean}$-Molar* values indicate that the last molar is anterior to the resultant and negative values indicate that the last molar is posterior to the resultant.

The second method for determining the position of the resultant (i.e., the position of the most anterior MLA) indicates that the masseter and temporalis crossed the triangle of support at more anterior positions than the medial pterygoid in almost all cases (Fig. 13). In cercopithecoids, platyrrhines, and strepsirrhines, the masseter tended to cross the triangle of support more anteriorly than the other MLAs, in specimen with dp4s emerged. This was also true in hominids, except for in *P. troglodytes*, for which the most anterior MLA was a mix of masseter and temporalis (Fig. 13), and in *P. paniscus*, where the medial pterygoid tended to cross the triangle of support most anteriorly (Fig. 13). These general patterns tended hold for individuals with M1s emerged (Fig. 13). For specimens with M2s emerged, the masseter continued to cross the triangle of support at the most anterior point in platyrrhines, cercopithecoids, and most strepsirrhines. In hominids with M2s emerged, the masseter crossed the triangle of support more anteriorly in *G. beringei*, *G. gorilla*, and *P. troglodytes*, the temporalis tended to cross more anteriorly in *P. pygmaeus* and *H. sapiens*, while the medial pterygoid tended to cross the triangle most anteriorly in *P. paniscus* (Fig. 13), with some variation within species. At M3 emergence, most cercopithecoid and platyrrhine specimens, with the exception of a few *C. apella* specimens had masseter muscles that crossed the triangle of support most anteriorly. Among most hominids and strepsirrhines, the masseter and temporalis muscles both crossed the triangle of support at the most anterior point at similar frequencies, with the exception of *P. paniscus* specimens which were a combination of individuals that had the masseter, temporalis, and medial pterygoid crossing the triangle most anteriorly (Fig. 13).

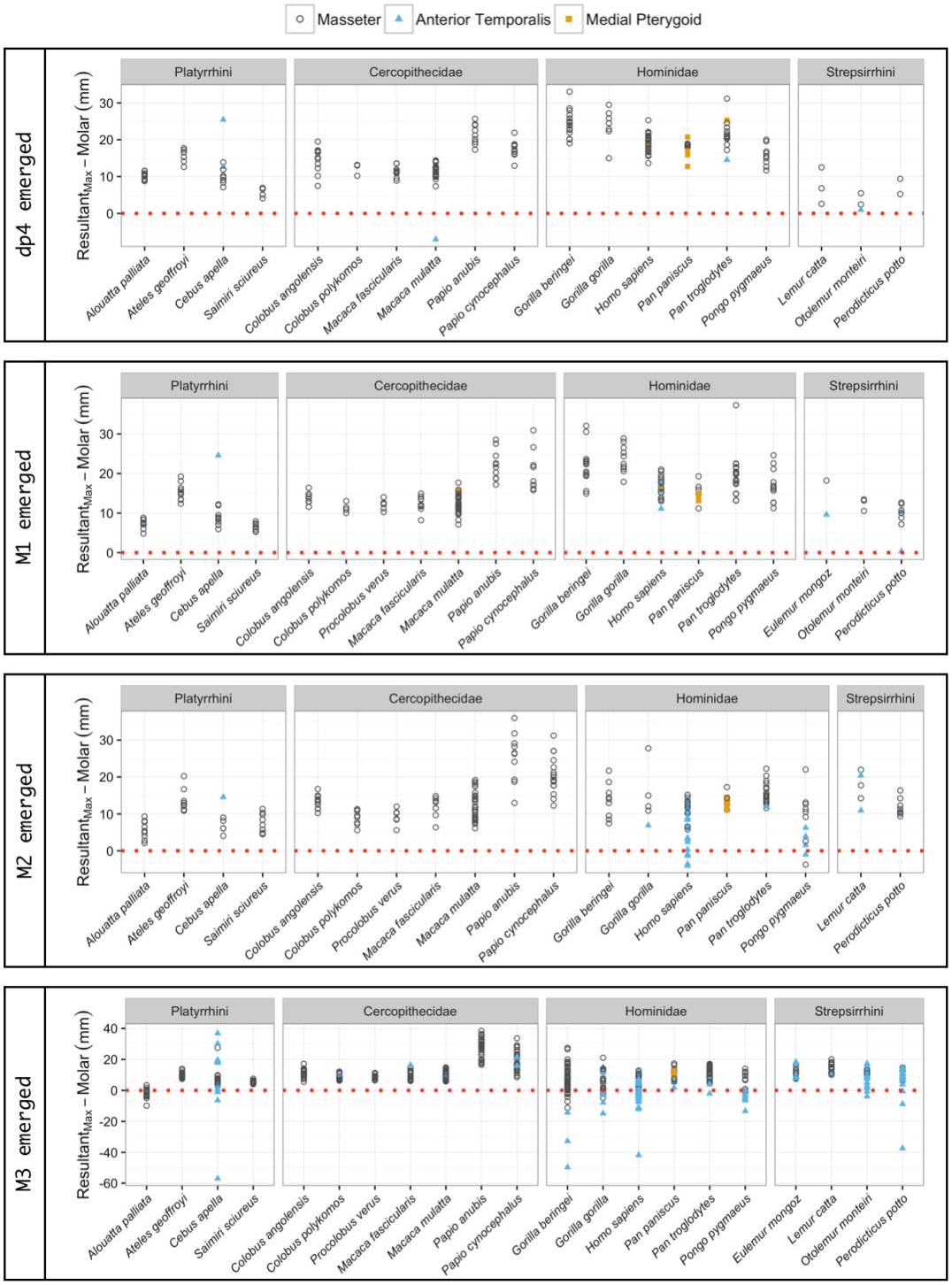


Figure 13. Distance between the resultant and the last molar, projected onto the occlusal plane (*Resultant$_{Max}$-Molar*) using the second method of determining resultant position (most anterior MLA; see text for details). Color and shape indicate the MLA that represents the resultant (i.e., the most anterior MLA). Red dashed line represents the position that the resultant crosses the triangle of support, projected onto the occlusal plane.

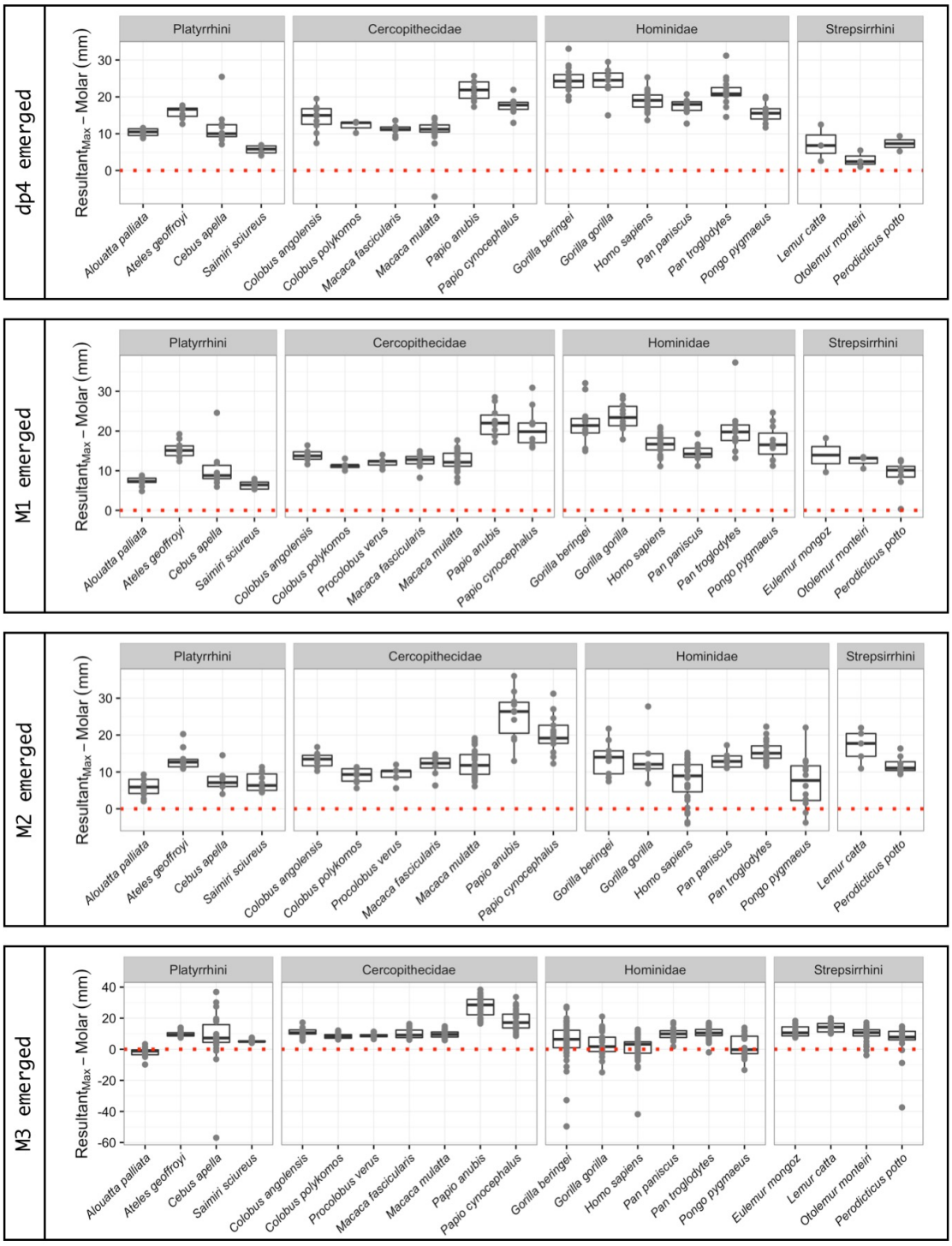


Figure 14. Boxplots of the distance between the resultant and the last molar, projected onto the occlusal plane (*Resultant$_{Max}$-Molar*) using the second method of determining resultant position (most anterior MLA; see text for details). Red dashed line represents the position that the resultant crosses the triangle of support, projected onto the occlusal plane. Positive *Resultant$_{Max}$-Molar* values indicate that the last molar is anterior to the resultant and negative values indicate that the last molar is posterior to the resultant.

Results of *t*-tests comparing $Resultant_{Max}$-*Molar* to zero indicated that for all species and all dp4 and most M1 and M2 molar emergence categories, $Resultant_{Max}$-*Molar* was both significantly different from and greater than zero indicating that these teeth tend to emerge significantly anterior to the most anterior MLA (i.e., the most anterior estimate of the resultant) (Fig. 14, SM 2). Within the M1 emerged category, one *P. potto* $Resultant_{Max}$-*Molar* value was close to zero, which appears to be driving the result that *P. potto* $Resultant_{Max}$-*Molar* values do not differ significantly from zero (Fig. 14, SM 2). Within the M2 emerged category, *P. pygmaeus* had a similar distribution of $Resultant_{Max}$-*Molar* values to *H. sapiens*, that possessed values significantly different and greater than zero. The values for *P. pygmaeus*, on the other hand, did not differ significantly from zero and were not significantly greater than zero. This difference may be driven by the fact that for *H. sapiens*, there was a greater concentration of data points with more positive values. Finally, within the M3 emerged category, there were several non-significant results: *A. palliata, C. apella, G. beringei, G. gorilla, H. sapiens, P. potto,* and *P. pygmaeus,* exhibited $Resultant_{Max}$-*Molar* values that were not significantly different from zero and not significantly greater than zero (Fig. 14, SM 2).

Results of ANOVAs comparing the distance between the TMJ and the last molar ($d_{TMJ\_Molar\_Occlusal}$) among molar emergence categories indicated that throughout ontogeny, significant differences exist in $d_{TMJ\_Molar\_Occlusal}$ among most species (Table 4). The species that did not exhibit significant differences throughout ontogeny are: *A. palliata*, *E. mongoz*, *G. gorilla*, *L. catta*, and *P. verus*. Based on the mean values for each molar emergence category, the general pattern among species was that the distance between the TMJ and the last molar increases throughout ontogeny. Post-hoc Tukey's

tests indicated that significant differences were manifested throughout all the emergence categories measured here, although variation exists among taxa (Table 4).

Table 4. Mean $d_{TMJ\_Molar\_Occlusal}$ values for molar emergence categories and results of ANOVAs comparing $d_{TMJ\_Molar\_Occlusal}$ within species.

| | Mean for molar emergence category | | | | | | |
|---|---|---|---|---|---|---|---|
| **Taxon** | **dp4** | **M1** | **M2** | **M3** | ***F*-statistic** | ***p*-value** | **Significant Tukey comparison** |
| **Platyrrhini** | | | | | | | |
| *Alouatta palliata* | 25.77 | 27.35 | 28.90 | 29.10 | 2.43 | 0.077 | - |
| *Ateles geoffroyi* | 23.07 | 24.43 | 23.67 | 30.03 | 37.93 | **<0.001** | dp4-M3; M1-M3; M2-M3 |
| *Cebus apella* | 25.60 | 21.95 | 21.90 | 35.29 | 4.45 | **0.007** | M1-M3 |
| *Saimiri sciureus* | 14.30 | 13.44 | 12.09 | 14.63 | 9.94 | **<0.001** | dp4-M2; M2-M3 |
| **Cercopithecidae** | | | | | | | |
| *Colobus angolensis* | 21.34 | 26.78 | 29.24 | 33.61 | 34.22 | **<0.001** | dp4-M1; dp4-M2; dp4-M3; M1-M3; M2-M3 |
| *Colobus polykomos* | 23.25 | 24.92 | 29.87 | 32.59 | 21.68 | **<0.001** | dp4-M2; dp4-M3; M1-M2; M1-M3 |
| *Procolobus verus* | - | 23.92 | 22.86 | 24.38 | 1.01 | 0.377 | - |
| *Macaca fascicularis* | 22.88 | 25.84 | 30.37 | 29.47 | 10.49 | **<0.001** | dp4-M2; dp4-M3; M1-M2 |
| *Macaca mulatta* | 26.55 | 30.53 | 35.40 | 34.47 | 31.77 | **<0.001** | dp4-M1; dp4-M2; dp4-M3; M1-M2; M1-M3 |
| *Papio anubis* | 39.05 | 43.86 | 50.03 | 62.14 | 30.09 | **<0.001** | dp4-M2; dp4-M3; M1-M3; M2-M3 |
| *Papio cynocephalus* | 32.32 | 40.56 | 45.41 | 48.53 | 14.09 | **<0.001** | dp4-M2; dp4-M3; M1-M3 |
| **Hominidae** | | | | | | | |
| *Gorilla beringei* | 57.84 | 62.56 | 64.89 | 68.15 | 3.91 | **0.011** | dp4-M3 |
| *Gorilla gorilla* | 55.53 | 67.05 | 65.85 | 63.18 | 1.66 | 0.189 | - |
| *Homo sapiens* | 41.86 | 46.19 | 46.95 | 45.35 | 7.70 | **<0.001** | dp4-M1; dp4-M2; dp4-M3 |
| *Pan paniscus* | 35.11 | 37.04 | 41.35 | 42.86 | 12.66 | **<0.001** | dp4-M2; dp4-M3; M1-M2; M1-M3 |
| *Pan troglodytes* | 40.77 | 47.20 | 52.03 | 51.24 | 24.78 | **<0.001** | dp4-M1; dp4-M2; dp4-M3; M1-M2; M1-M3 |
| *Pongo pygmaeus* | 41.91 | 53.12 | 55.04 | 60.00 | 9.01 | **<0.001** | dp4-M2; dp4-M3 |
| **Strepsirrhini** | | | | | | | |
| *Eulemur mongoz* | - | 22.51 | - | 22.12 | 0.04 | 0.843 | - |
| *Lemur catta* | 18.51 | - | 23.69 | 21.41 | 2.94 | 0.073 | - |
| *Otolemur monteiri* | 12.86 | 19.06 | - | 20.40 | 12.97 | **<0.001** | dp4-M1; dp4-M3 |
| *Perodicticus potto* | 15.04 | 16.14 | 16.19 | 18.44 | 6.35 | **0.002** | M1-M3; M2-M3 |

Where ANOVAs indicated significant differences within species, results of significant pairwise Tukey comparisons are listed. Significant ANOVA results indicated in bold.

Table 5. Mean *Resultant$_{Mean}$-Molar* values for molar emergence categories and results of ANOVAs comparing *Resultant$_{Mean}$-Molar* within species.

| | Mean for molar emergence category | | | | | | |
|---|---|---|---|---|---|---|---|
| **Taxon** | **dp4** | **M1** | **M2** | **M3** | ***F*-statistic** | ***p*-value** | **Significant Tukey comparison** |
| **Platyrrhini** | | | | | | | |
| *Alouatta palliata* | 15.48 | 15.01 | 13.54 | 9.34 | 23.09 | **<0.001** | dp4-M3; M1-M3; M2-M3 |
| *Ateles geoffroyi* | 17.73 | 17.68 | 15.78 | 15.94 | 4.61 | **0.007** | M1-M3 |
| *Cebus apella* | 16.95 | 14.14 | 12.30 | 19.83 | 1.49 | 0.228 | - |
| *Saimiri sciureus* | 9.09 | 8.36 | 8.61 | 7.94 | 1.46 | 0.242 | - |
| **Cercopithecidae** | | | | | | | |
| *Colobus angolensis* | 16.15 | 17.57 | 17.40 | 18.05 | 1.62 | 0.199 | - |
| *Colobus polykomos* | 15.22 | 15.12 | 16.40 | 15.24 | 0.96 | 0.426 | - |
| *Procolobus verus* | - | 15.21 | 12.69 | 12.05 | 8.92 | **0.001** | M1-M2; M1-M3 |
| *Macaca fascicularis* | 14.67 | 15.87 | 17.22 | 15.20 | 1.70 | 0.183 | - |
| *Macaca mulatta* | 15.90 | 17.61 | 19.06 | 16.60 | 7.46 | **<0.001** | dp4-M2; M2-M3 |
| *Papio anubis* | 26.46 | 28.89 | 32.91 | 37.71 | 11.84 | **<0.001** | dp4-M3; M1-M3 |
| *Papio cynocephalus* | 21.67 | 26.17 | 27.47 | 27.49 | 3.62 | **0.017** | dp4-M2; dp4-M3 |
| **Hominidae** | | | | | | | |
| *Gorilla beringei* | 36.47 | 36.17 | 32.37 | 27.59 | 5.86 | **0.001** | dp4-M3; M1-M3 |
| *Gorilla gorilla* | 35.04 | 37.34 | 29.96 | 22.60 | 8.42 | **<0.001** | dp4-M3; M1-M3 |
| *Homo sapiens* | 22.49 | 21.06 | 16.13 | 11.38 | 82.91 | **<0.001** | dp4-M2; dp4-M3; M1-M2; M1-M3; M2-M3 |
| *Pan paniscus* | 20.23 | 18.93 | 17.10 | 14.53 | 11.04 | **<0.001** | dp4-M3; M1-M3 |
| *Pan troglodytes* | 25.46 | 25.02 | 23.60 | 19.26 | 22.62 | **<0.001** | dp4-M3; M1-M3; M2-M3 |
| *Pongo pygmaeus* | 22.29 | 26.47 | 19.70 | 16.00 | 5.74 | **0.002** | M1-M3 |
| **Strepsirrhini** | | | | | | | |
| *Eulemur mongoz* | - | 17.98 | - | 15.47 | 1.89 | 0.193 | - |
| *Lemur catta* | 11.95 | - | 19.19 | 16.28 | 5.38 | **0.012** | dp4-M2 |
| *Otolemur monteiri* | 6.82 | 14.27 | - | 13.24 | 6.72 | **0.003** | dp4-M1; dp4-M3 |
| *Perodicticus potto* | 10.10 | 11.23 | 13.20 | 11.91 | 0.93 | 0.439 | - |

Where ANOVAs indicated significant differences within species, results of significant pairwise Tukey comparisons are listed. Significant ANOVA results indicated in bold.

Table 6. Mean *Resultant$_{Max}$-Molar* values for molar emergence categories and results of ANOVAs comparing *Resultant$_{Max}$-Molar* within species.

| | Mean for molar emergence category | | | | | | |
|---|---|---|---|---|---|---|---|
| **Taxon** | **dp4** | **M1** | **M2** | **M3** | ***F*-statistic** | ***p*-value** | **Significant Tukey comparison** |
| **Platyrrhini** | | | | | | | |
| *Alouatta palliata* | 10.36 | 7.27 | 5.88 | -1.89 | 84.09 | **<0.001** | dp4-M1; dp4-M2; dp4-M3; M1-M3; M2-M3 |
| *Ateles geoffroyi* | 15.75 | 15.37 | 13.40 | 9.74 | 23.09 | **<0.001** | dp4-M3; M1-M3; M2-M3 |
| *Cebus apella* | 11.81 | 10.52 | 7.98 | 8.06 | 0.31 | 0.820 | - |
| *Saimiri sciureus* | 5.67 | 6.36 | 7.23 | 5.18 | 4.43 | **0.009** | M2-M3 |
| **Cercopithecidae** | | | | | | | |
| *Colobus angolensis* | 14.34 | 13.80 | 13.28 | 10.99 | 4.86 | **0.005** | dp4-M3; M1-M3 |
| *Colobus polykomos* | 12.12 | 11.34 | 9.03 | 8.64 | 5.72 | **0.003** | dp4-M3; M1-M3 |
| *Procolobus verus* | - | 12.13 | 9.38 | 8.93 | 9.90 | **0.001** | M1-M2; M1-M3 |
| *Macaca fascicularis* | 11.31 | 12.47 | 11.85 | 10.13 | 1.89 | 0.147 | - |
| *Macaca mulatta* | 10.77 | 12.57 | 12.33 | 9.58 | 9.62 | **<0.001** | M1-M3; M2-M3 |
| *Papio anubis* | 21.72 | 22.20 | 25.30 | 27.36 | 3.56 | **0.020** | dp4-M3 |
| *Papio cynocephalus* | 17.54 | 20.71 | 20.41 | 18.70 | 1.09 | 0.358 | - |
| **Hominidae** | | | | | | | |
| *Gorilla beringei* | 24.46 | 21.91 | 13.66 | 5.30 | 21.75 | **<0.001** | dp4-M3; M1-M3 |
| *Gorilla gorilla* | 23.88 | 23.69 | 14.51 | 3.70 | 31.56 | **<0.001** | dp4-M3; M1-M3; M2-M3 |
| *Homo sapiens* | 18.90 | 16.58 | 7.76 | 1.07 | 57.62 | **<0.001** | dp4-M2; dp4-M3; M1-M2; M1-M3; M2-M3 |
| *Pan paniscus* | 17.45 | 14.62 | 13.07 | 9.72 | 18.10 | **<0.001** | dp4-M2; dp4-M3; M1-M3; M2-M3 |
| *Pan troglodytes* | 21.42 | 19.66 | 15.66 | 10.53 | 59.99 | **<0.001** | dp4-M2; dp4-M3; M1-M2; M1-M3; M2-M3 |
| *Pongo pygmaeus* | 15.74 | 17.07 | 7.37 | 1.69 | 18.86 | **<0.001** | dp4-M2; dp4-M3; M1-M2; M1-M3 |
| **Strepsirrhini** | | | | | | | |
| *Eulemur mongoz* | - | 13.92 | - | 11.57 | 0.61 | 0.451 | - |
| *Lemur catta* | 7.30 | - | 17.04 | 14.07 | 7.12 | **0.004** | dp4-M2; dp4-M3 |
| *Otolemur monteiri* | 2.98 | 12.38 | - | 9.47 | 3.53 | **0.041** | dp4-M1 |
| *Perodicticus potto* | 7.31 | 9.04 | 11.88 | 5.69 | 0.99 | 0.409 | - |

Where ANOVAs indicated significant differences within species, results of significant pairwise Tukey comparisons are listed. Significant ANOVA results indicated in bold.

Results of ANOVAs comparing *Resultant-Molar* among molar emergence categories indicated that throughout ontogeny, significant differences exist in the distance between the resultant and the last molar (*$Resultant_{Mean}$-Molar*: Table 5 and *$Resultant_{Max}$-Molar*: Table 6) among most species. The species that did not exhibit significant differences throughout ontogeny in *$Resultant_{Mean}$-Molar* are*: C. apella, S. sciureus, C. angolensis, C. polykomos, M. fascicularis, E. mongoz*, and *P. potto* (Table 5). Similarly, the species that did not exhibit significant differences throughout ontogeny in *$Resultant_{Max}$-Molar* are*: C. apella, M. fascicularis, P. cynocephalus, E. mongoz*, and *P. potto* (Table 6). For the species that exhibited significant differences throughout ontogeny in the distance between the resultant and the last molar, the general pattern among species is that this distance decreases throughout ontogeny (Tables 5 and 6). There were several exceptions to this pattern, however, especially among strepsirrhines and papionins, which tended to exhibit the opposite pattern (Tables 5 and 6). Post-hoc Tukey's tests indicated that significant differences were manifested throughout all the emergence categories measured here, although variation existed among taxa, and differences occurred most frequently between the dp4 and M3 emergence categories (Tables 5 and 6).

## Discussion

This study examined the position of molar emergence in relation to the position of the adductor muscle resultant. The CLM predicts that the last molar should be positioned anterior to the resultant so that biting on this molar will not produce distractive forces at the TMJ (Greaves 1978, 1982, 1983, 1988; Spencer and Demes 1993; Spencer 1995, 1999). Following this model, this chapter determined if molars emerge anterior to the

resultant to maintain an intact masticatory system throughout ontogeny. Two specific predictions were tested: (1) molars emerge directly anterior to the resultant (following the predictions of the original formulation of the CLM (Greaves 1978)) and (2) molars emerge significantly anterior to the resultant (based on findings in adult primates (Spencer 1995, 1999; Perry, Hartstone-Rose, and Logan 2011; Lucas, 2012)). The first prediction was not supported by this research; in almost all cases, the last molar was not positioned directly anterior to the resultant. Results indicate that when the assumption is made that all muscles contribute equally to maximum bite force then the second prediction is supported in almost all cases. In this case, molars emerge in a position that is significantly anterior to the resultant. When the assumption is made that the most anterior MLA represents the most anterior position of the resultant then the second prediction is partially supported, especially at earlier points in ontogeny.

Previous research on adult primates has shown that molars are positioned significantly anterior to the resultant (Spencer 1995, 1998; Perry, Hartstone-Rose, and Logan 2011; Lucas 2012). This previous research calculated the position of the resultant in a variety of ways. Spencer (1995, 1998) reported the positions at which MLAs crossed the occlusal plane in adult primates, all of which were posterior to the last molar. Like the second method used in this chapter to determine the position of the resultant, Spencer's (1995, 1998) method was intended to approximate the most anterior possible position of the resultant. It differs from the methodology employed here, however, because it does not account for the fact that most primates possess TMJs that are raised above the occlusal plane, which results in triangles of support that are inclined to the occlusal plane. Measuring the position at which an MLA crosses the occlusal plane will therefore

underestimate the position at which the resultant crosses the triangle of support (assuming an anteriorly inclined resultant, which has been shown for primates by Perry, Hartstone-Rose, and Logan (2011)). This is the likely reason for the discrepancy between the results of Spencer (1995, 1998) and those reported here (discussed further below).

Lucas (2012) estimated the position of the resultant in a similar way as the first method used here, by averaging the position of the three adductor MLAs, and reported that in adult primates, the last molar is positioned anterior to the resultant. Similar to the studies of Spencer (1995, 1998), however, Lucas (2012) calculated the position that the resultant crossed the occlusal plane and not where it crossed the triangle of support.

The assumption made by Lucas (2012), and the first method used to determine resultant position in this study, that all adductor muscles contribute equally to maximum bite force is not realistic. Data on muscle physiological cross-sectional area (PCSA) are necessary to determine the maximum magnitude of each of the adductor muscles, and thus each muscle's relative contribution to maximum bite force. Research by Perry, Hartstone-Rose, and Logan (2011) is, currently, the only study to have used data on muscle anatomy in addition to skeletal anatomy to calculate the position of the jaw adductor resultant in adult primates. Data on PCSA were used to determine the magnitude of force that each muscle can produce and then vector addition was used to determine the position of the resultant (Perry, Hartstone-Rose, and Logan 2011). This method is superior to the previous two because information on the anatomy of the adductor muscles allows for a more accurate determination of the positon of the resultant during maximum force production. Like the previous research described above, however, the study by Perry, Hartstone-Rose, and Logan (2011) only considered the position of the

resultant as it crossed the occlusal plane rather than the triangle of support, potentially underestimating the anterior position of the resultant. Despite this limitation, the Perry, Hartstone-Rose, and Logan (2011) study confirmed that estimating the position of the resultant by including information on muscle anatomy in addition to skeletal anatomy, yields a similar result to estimating the position of the resultant using skeletal anatomy alone.

Data on PCSA are available for adult individuals from several of the species examined in this study (Table 7). Most studies report PCSA values for the masseter and temporalis muscles, while comparable data for the medial pterygoid are only available for two strepsirrhine and two macaque species (Table 7; Antón 2000; Perry, Hartstone-Rose, and Logan 2011). Available data indicate that the medial pterygoid is the muscle with the smallest PCSA, suggesting that it contributes the smallest magnitude to bite force and thus has the least influence on the position of the resultant. Its contribution is not insignificant, however. Although smaller, the medial pterygoid is often similar in PCSA to the masseter. The muscle's line of action is also similar to that of the masseter and thus the two muscles together, contribute force in a similar direction. Due to the paucity of data on the medial pterygoid, it is impossible to draw conclusions regarding its relative size in other taxa. Information in Table 7 suggests that in most taxa, the temporalis muscle has a larger PCSA than the masseter muscle and can therefore contribute a greater magnitude to maximum bite force. The position of the resultant in most taxa should therefore be most strongly influenced by the temporalis muscle. There are a few caveats to this statement, however. The available PCSA data for the temporalis represent the

Table 7. Adductor muscle physiological cross-sectional area (PCSA) data (cm2).

| Species | Superficial masseter m. | Temporalis m. | Med. pterygoid m. | Source |
|---|---|---|---|---|
| *Alouatta palliata* | 6.55 | 5.1 | - | Taylor et al. (2015) |
| *Ateles geoffroyi* | 2.02 | 3.18 | - | Taylor et al. (2015) |
| *Cebus apella* | 5.54 | 10.2 | - | Taylor et al. (2015) |
| *Gorilla gorilla* | 31.94 | 47.24 | - | Taylor and Vinyard (2013) |
| *Homo sapiens* | 4.96 | 10.39 | - | van Eijden et al. (1997) as reported in Taylor and Vinyard (2013) |
| *Lemur catta* | 1.56 | 2.67* | 1.18 | Perry et al. (2011) |
| *Macaca mulatta* | 3.36 | - | 2.12 | Antón (1999, 2000) as reported in Ross et al. (2005) |
| *Macaca fascicularis* | 1.56 | - | 1.45 | Antón (1999, 2000) as reported in Ross et al. (2005) |
| *Macaca fascicularis* | 4.42** | 12.18** | | Terhune et al. (2015) |
| *Macaca* | 5.07 | 12.26 | - | Vinyard and Taylor (2010) |
| *Pan paniscus* | 12.79 | - | - | Taylor and Vinyard (2013) |
| *Pan troglodytes* | 16.78 | 19.95 | - | Taylor and Vinyard (2013) |
| *Papiob anubis* | 23.87 | 21.91 | - | Vinyard and Taylor (2010) |
| *Perodicticus potto* | 0.81 | 1.52* | 0.71 | Perry et al. (2011) |
| *Pongo* | 14.88 | - | - | Taylor and Vinyard (2013) |
| *Saimiri sciureus* | 0.8 | 2.41 | - | Taylor et al. (2015) |

*Sum of superficial and deep temporalis.

**Average of reported male and female PCSA.

PCSA of the entire muscle. It is known, however, that anterior temporalis muscle fibers contribute to jaw adduction, while posterior muscle fibers act in jaw retraction (e.g., Hylander et al. 2005). The only available data on the PCSA of the anterior temporalis suggest that it is smaller than the PCSA of the masseter, at least in one species of macaque (*M. fuscata*, Anton 1993). It is unknown whether this is the case in other macaques or other species of primates, but if true, then the masseter would influence the position of the resultant most strongly. A further complication is that all available data are for adult specimens. Cachel's (1984) report that the masticatory muscles grow isometrically was based on very small sample sizes (often one specimen per species) and on an interspecific scale. Richer intraspecific ontogenetic data are necessary to confirm

this assertion, but given the shape changes in the bony masticatory apparatus that occur during growth (e.g., Krogman 1931a, b; Corner and Richtsmeier 1991, 1992, 1993; Richtsmeier et al. 1993; Cobb and O'Higgins 2004; Strand Vioarsdóttir and Cobb 2004; Ackermann 2005; Hens 2005; Leigh 2006a; Martinez-Maza, Rosas, and Nieto-Díaz 2013; Singleton 2015), isometric growth seems unlikely.

A further caveat is that PCSA data only provide information on maximum muscular effort and do not speak to how many motor units (i.e., collections of muscle fibers innervated by one motor neuron's axonal terminals) are recruited (i.e., how much of the muscle is used) during submaximal biting (Spencer 1998), or the timing of muscle activation (i.e., whether all adductors are active at the same time). The CLM predicts that the resultant moves mediolaterally to accommodate a shifting size of the triangle of support as the bite point changes. Because the model assumes maximum bite force, the resultant is static in the anteroposterior direction. The resultant is not static in the anteroposterior direction during submaximum bite force production, although single muscles can produce forces of variable position through heterogeneous activity (Herring, Grimm, and Grimm 1979; Tonndorf, Sasaki, and Hannam 1989; Blanksma and van Eijden 1990; Blanksma, van Eijden, and Weijs 1992) and many combinations of muscle activity are adequate for the generation of a bite force with a given magnitude (Koolstra et al. 1988; van Eijden et al. 1988, 1990, 1991). The anteroposterior position of the resultant can therefore change if only some of the adductors are recruited to produce bite force or if some muscles are recruited to a greater degree than others (Spencer 1999).

The second method of calculating resultant position was aimed at capturing variation in resultant position by determining the most anterior possible position of the

resultant (i.e., the position of the most anterior MLA), which would only occur if the muscle with the MLA that crosses the triangle of support at the most anterior position is the only muscle active during biting. This is a "worst-case scenario" in terms of the most anterior possible migration of the resultant. The results of this method indicate that earlier in ontogeny (during dp4 and M1 emergence), molars emerge anterior to even the most anterior MLA. Later in ontogeny and in adulthood, however, the most anterior MLA is positioned anterior to the last molar in some species, especially in gorillas, humans, and orangutans as well as some platyrrhines and strepsirrhines.

The finding that in the adults of some species the last molar is not positioned anterior to the most anterior MLA differs from the results of Spencer (1995, 1999), who showed that the last molar is positioned anterior to even the most anterior MLA. As discussed above, however, Spencer calculated the point at which the MLAs crossed the occlusal plane rather than where they crossed the triangle of support, potentially underestimating the distance between the MLA and the last molar. If the TMJs are situated near the occlusal plane, then the angle between the triangle of support and the occlusal plane is close to zero. As the height of the TMS above the occlusal plane increases, so should the angle between the triangle and the plane, all other things being equal. Conversely, as the distance from the last molar to the TMJ along the occlusal plane increases, the angle between the plane and the triangle of support should decrease. Unlike previous research, which showed that the distance between the TMJ and the last molar does not change throughout most of ontogeny (Spencer and Schwartz 2008; Schwartz 2012; Singleton 2015), the results of this study indicate that this distance increases significantly thorough all of ontogeny in most taxa (Table 4). Similarly, in most of the

sample used in this study, the angle between the triangle of support and the occlusal plane also increases during ontogeny, with the smallest angles appearing in the youngest molar emergence category (dp4 emerged) and the greatest angles in the oldest emergence category (M3 emerged) (Table 8). Because in most primate species included in this study the distance between the TMJ and the last molar increases during ontogeny, the growth in height of the TMJ above the occlusal plane must occur at a faster rate than the increase in length between the TMJ and the last molar in order for the angle between the triangle of support and the occlusal plane to increase during ontogeny. The exception to this occurs in all of the strepsirrhine species, which exhibit the highest angles between the triangle of support and the occlusal plane early in ontogeny followed by a decrease in this angle throughout growth (Table 8). In these taxa, the distance between the TMJ and the last molar does not increase throughout growth or does so only very slightly (Table 4). The height of the TMJ above the occlusal plane must also not increase throughout growth in these taxa in order for the angle between the TMJ and the triangle of support to remain constant with age.

The species that did not possess posterior-most molars that are significantly anterior to the most anterior MLA as adults (i.e., those that did not follow the expected pattern) are: *A. palliata, C. apella, G. beringei, G. gorilla, H. sapiens, P. potto,* and *P. pygmaeus.* With the exception of *P. potto*, these are also the species with some of the most obtuse angles between the occlusal plane and the triangle of support as adults (Table 8). This supports the idea that the difference between the results of this study and previously reported results (Spencer 1995, 1999; Perry, Hartstone-Rose, and Logan 2011; Lucas 2012) is due to the fact that previous studies measured the point at which the

resultant crossed the occlusal plane and not the triangle of support.

Table 8. Average angle (degrees) between the occlusal plane and the triangle plane for all molar emergence categories and species examined.

| | dp4 emerged | | M1 emerged | | M2 emerged | | M3 emerged | |
|---|---|---|---|---|---|---|---|---|
| **Taxon** | **Mean** | **SD** | **Mean** | **SD** | **Mean** | **SD** | **Mean** | **SD** |
| **Platyrrhini** | | | | | | | | |
| *Alouatta palliata* | 20.14 | 4.01 | 29.59 | 3.52 | 28.76 | 6.91 | 39.99 | 3.85 |
| *Ateles geoffroyi* | 6.40 | 5.83 | 6.80 | 3.29 | 8.04 | 4.45 | 19.59 | 3.20 |
| *Cebus apella* | 20.19 | 5.18 | 15.52 | 6.08 | 18.36 | 6.35 | 23.09 | 8.97 |
| *Saimiri sciureus* | 22.82 | 6.15 | 14.36 | 3.84 | 9.14 | 8.07 | 19.20 | 3.71 |
| **Cercopithecidae** | | | | | | | | |
| *Colobus angolensis* | 5.62 | 4.47 | 12.24 | 4.15 | 13.86 | 5.33 | 21.55 | 4.25 |
| *Colobus polykomos* | 12.72 | 4.65 | 15.88 | 3.26 | 21.91 | 2.99 | 23.56 | 2.67 |
| *Procolobus verus* | - | - | 12.96 | 3.94 | 19.75 | 6.67 | 19.49 | 3.03 |
| *Macaca fascicularis* | 14.00 | 4.18 | 13.79 | 3.23 | 20.90 | 3.84 | 22.05 | 4.55 |
| *Macaca mulatta* | 18.05 | 4.58 | 19.61 | 2.87 | 25.04 | 4.80 | 27.73 | 3.69 |
| *Papio anubis* | 11.68 | 3.14 | 14.65 | 5.27 | 14.51 | 5.27 | 17.47 | 4.62 |
| *Papio cynocephalus* | 11.97 | 5.01 | 14.30 | 3.72 | 19.18 | 4.53 | 21.47 | 4.03 |
| **Hominidae** | | | | | | | | |
| *Gorilla beringei* | 29.13 | 7.04 | 36.04 | 4.65 | 48.61 | 12.55 | 47.89 | 5.86 |
| *Gorilla gorilla* | 29.38 | 5.85 | 35.83 | 4.89 | 39.27 | 3.23 | 47.57 | 3.63 |
| *Homo sapiens* | 15.59 | 5.73 | 21.84 | 6.69 | 32.58 | 4.79 | 35.80 | 5.60 |
| *Pan paniscus* | 15.66 | 4.50 | 23.11 | 3.71 | 28.43 | 4.58 | 31.49 | 6.54 |
| *Pan troglodytes* | 14.40 | 4.20 | 23.19 | 6.86 | 31.44 | 4.38 | 35.13 | 4.47 |
| *Pongo pygmaeus* | 23.50 | 5.84 | 29.05 | 5.12 | 41.11 | 6.06 | 41.07 | 3.24 |
| **Strepsirrhini** | | | | | | | | |
| *Eulemur mongoz* | - | - | 3.40 | 3.50 | - | - | 8.14 | 4.63 |
| *Lemur catta* | 21.89 | 3.34 | - | - | 3.19 | 1.38 | 4.35 | 3.15 |
| *Otolemur monteiri* | 14.01 | 4.08 | 5.88 | 2.55 | - | - | 5.76 | 3.98 |
| *Perodicticus potto* | 14.69 | 15.86 | 7.44 | 4.12 | 3.74 | 2.06 | 5.72 | 3.27 |

The fact that many adult specimens possess MLAs that cross the triangle of support anterior to the last molar has implications for understanding their masticatory systems. In these individuals, if bite force is produced using solely the most anterior MLA then distractive forces will be produced at the TMJ. It is possible that bite forces produced using only one adductor muscle are not high enough to cause damage to the

joint over time. It is also possible that this situation never occurs and that these individuals do not produce bite forces using only one muscle. To this end, data on muscle activation patterns are necessary to determine which muscles are used when biting on the most posterior molar. Electromyography (EMG) has been used on humans and a handful of nonhuman primates to show that jaw-muscle activity changes with the location of the bite point (Manns, Miralles, and Palazzi 1979; Pruim, de Jongh, and ten Bosch 1980; Hylander and Johnson 1985; Spencer 1998), but a systematic, ontogenetic, and cross-taxonomic evaluation of muscle activation patterns is necessary to understand how it influences the position of the resultant, at various bite points, both throughout ontogeny and in adulthood. In at least some of these species that are exceptions (*H. sapiens* and *C. apella*) the M3s are reduced in size and may not function in mastication. Therefore it may not matter that their molars are not positioned anterior to the resultant. Furthermore, the species that exhibit exceptions to the model may be employing behavioral modifications when feeding, such as preparing large of mechanically challenging foods pre-orally and only biting with their molars once food has been reduced. For example, capuchin monkeys are known to crack nuts with stones prior to ingestion (Boinski, Quatrone, Swartz 2001) and humans cook food in order to aid in its breakdown prior to mastication (Zink and Lieberman 2016).

Some of the greatest variability in *Resultant-Molar* was exhibited by the hominids as well as the papionins. Because *Resultant-Molar* is an absolute value, this increased variability may be due to the absolutely larger size of these taxa. It may also be related to the degree of sexual dimorphism in these species. For example, gorillas, orangutans, and papionins exhibit the largest variation in *Resultant-Molar* and also a large amount of

sexual dimorphism. This does not explain the reason for the variability observed within humans, however, and this issue should be explored in future research.

The present study found support for the hypothesis that the location of molar emergence is constrained to avoid TMJ distraction throughout ontogeny, but only if certain assumptions are made regarding the contribution of muscles to bite force. It appears that earlier in ontogeny (prior to M2 eruption) the masticatory system is safeguarded from distractive forces more so than later in ontogeny and in adulthood. Future research must focus on determining how PCSA changes throughout ontogeny and on charting muscle activation patters when biting on the last molar throughout ontogeny. Such data will provide a more complete picture of how the masticatory system accommodates a growing dentition while maintaining function.

CHAPTER 3

# FACTORS AFFECTING THE POSITION OF MOLAR EMERGENCE IN PRIMATES


## Abstract

A model for understanding the position of molar emergence among primates is critical to the study of how variation in molar-emergence age evolves and, ultimately, to unraveling the link between molar emergence schedules and life history. A previous analysis identified substantial variation in the position of molar emergence relative to the adductor muscle resultant. This chapter tested whether this variation is related to the size of the *buffer zone*, a safety factor that creates greater stability at the temporomandibular joints during biting. Specifically, this chapter investigated four factors that may contribute to ontogenetic and interspecific variation in the distance between the muscle resultant's intersection with the triangle of support and the position of molar emergence (i.e., the anterior section of the buffer zone): food mechanical properties, skull size, jaw gape, and the length of the next erupting molar. 3D coordinate data were collected from cross-sectional ontogenetic samples of primate skulls (n = 21 species; 1,258 specimens). These data were used to determine skull geometric mean and projected jaw gape. In addition, data on canine overlap and mesiodistal length of each molar were collected on the same specimens. General Linear Models (GMLs) were used to investigate ontogenetic variation in the distance from the distal-most molar to the resultant for each species and Phylogenetic Generalized Least-Squares (PGLS) models were used to investigate interspecific variation in the distance from that molar to the resultant. GLM and PGLS results indicate that more resistant foods, larger skulls, longer molars, and

longer jaws produce a larger buffer zone, but greater canine overlap produces a smaller buffer zone. These factors account for a large portion of both ontogenetic and interspecific variation in the distance between the distal-most molar and the resultant and reinforce the notion that the buffer zone is part of an important mechanism acting to modulate the position of molar emergence across primates.

## Introduction

Reconstructing the timing of molar emergence is a powerful tool for probing life history in the fossil record. The predictive power of molar-emergence ages is based on its strong correlation with a suite of life-history variables. The underlying process that leads to varying molar-emergence ages in primates remains elusive, however. One avenue for understanding the mechanism that produces variation in molar-emergence age is investigating the biomechanical constraints on the position of molar emergence. Research on the ontogeny of the masticatory system identified that the distance between the temporomandibular joint (TMJ) and the last molar to have emerged remains similar in humans and chimpanzees throughout ontogeny (Spencer and Schwartz 2008; Schwartz 2012), and increases only late in ontogeny in some papionins (Singleton 2015), suggesting that molars emerge at a constant position relative to the TMJ throughout growth. A more detailed analysis of the biomechanical constraints on the position of molar emergence revealed that (1) molars emerge significantly anterior to the adductor muscle resultant throughout all or most of ontogeny, depending on the method used to determine the position of the resultant, and that (2) the distance between the last molar and the resultant decreases throughout ontogeny in most taxa (Chapter 2).

The analysis in Chapter 2 was based on the Constrained Lever Model (CLM), a biomechanical model developed to understand variation in masticatory system morphology and the relative position of different tooth types (Greaves 1978, 1982, 1983). The CLM, as described by Greaves (1978, 1982, 1983, 1988), predicts that the posterior-most molar lies immediately anterior to the jaw adductor muscle resultant. Subsequent to the work of Greaves, several studies on adult primates found that the last molar's position is more anterior than predicted by the CLM ( Spencer 1999; Perry, Hartstone-Rose, and Logan 2011; Lucas 2012), a finding consistent with the results reported in Chapter 2 of this dissertation. Analyses of masticatory configuration in adult and subadult primates have indicated that substantial interspecific variation exists in the distance from the muscle resultant to the last molar (Spencer 1999; Chapter 2). Similarly, variation exists intraspecifically among molar emergence categories, particularly between individuals with emerged M2s and adults, on the one hand, and individuals at all earlier molar emergence categories (Chapter 2), on the other. The aim of this dissertation chapter is to determine what factor(s) contribute to this intra- and interspecific variation.

As described in Chapter 1, the triangle of support, bounded by the bite point and the working- and balancing-side temporomandibular joints (TMJs), must contain the muscle resultant in order to avoid distractive forces at the working-side TMJ (Greaves 1978, 1982, 1983, 1988). Spencer (1999) hypothesised that if the resultant moved freely within the triangle of support during the dynamic chewing process, then it would often come close to, or potentially drop outside of, its boundary. During force production, the resultant should therefore avoid the edges of the triangle of support (Spencer 1999). A *buffer zone*, first proposed by Greaves (1978), but refined by Spencer (1999), is

hypothesized to exists along the edges of the triangle where the resultant can migrate during submaximum force production (Fig. 15). The resultant should stay within the inner portion of the triangle of support, which Spencer (1999) termed the *sweet spot* (Fig. 15), during maximum force production because the resultant's position within the sweet spot produces the most stable loading scenario by avoiding the edges of the triangle of support.

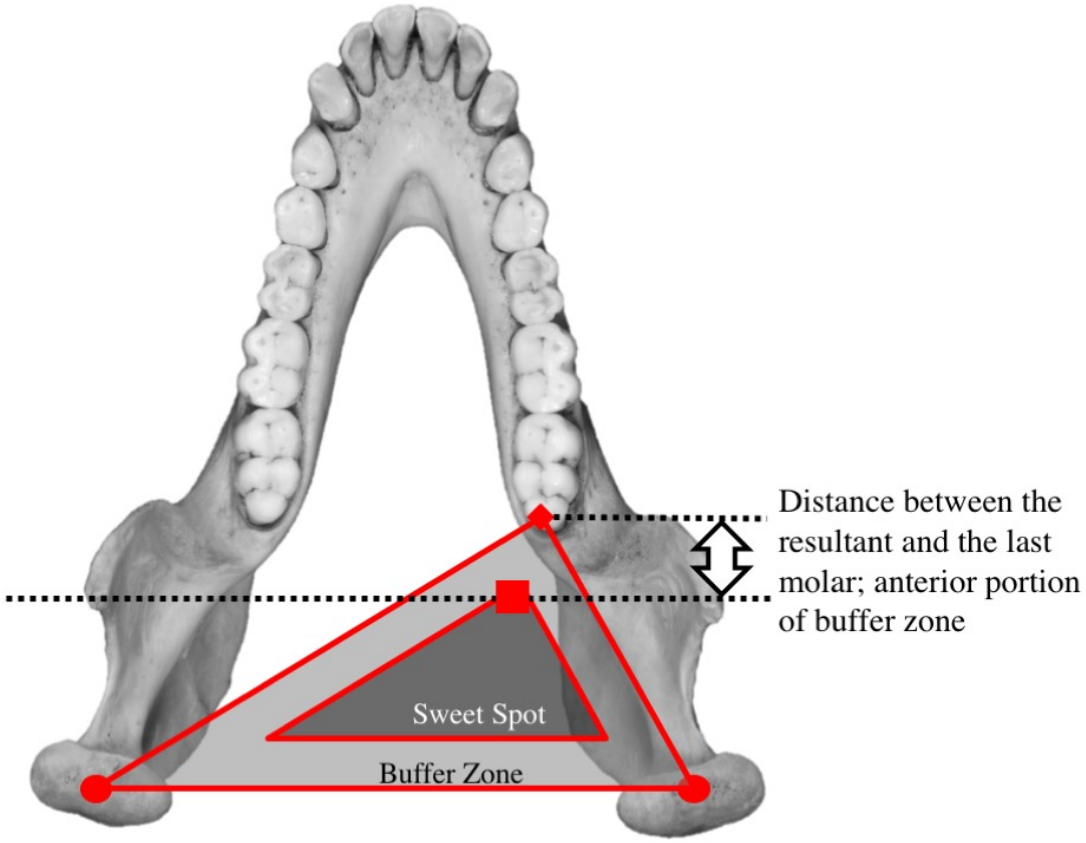


Figure 15. Occlusal view of the mandible showing the triangle of support with the buffer zone and the sweet spot, as described by Spencer (1999). The distance between the last molar (red diamond) and the muscle resultant (red square) represents the theoretical anterior portion of the buffer zone. See text for details.

In the CLM, the resultant's position is calculated based on the assumption of the simple loading condition of static isometric biting near centric occlusion. Further, the CLM assumes an anteroposteriorly fixed muscle resultant position based on maximum magnitude force vectors of each adductor muscle (i.e., maximum force production). During submaximum force production, however, the position of the muscle resultant can shift both anteriorly and posteriorly, depending on the relative contribution of each adductor muscle. Single muscles can produce forces of variable position (i.e., force vectors that vary in orientation and magnitude) through heterogeneous activity (Herring, Grimm, and Grimm 1979; Tonndorf, Sasaki, and Hannam 1989; Blanksma and van Eijden 1990; Blanksma, van Eijden, and Weijs 1992) and many combinations of muscle activity are adequate for the generation of a bite force with a given magnitude (Koolstra et al. 1988; van Eijden et al. 1988, 1990, 1991). Spencer (1999) noted that the resultant's position must change during different types of loading scenarios and thus masticatory systems should be configured to avoid distractive joint forces during behaviors other than isometric maximum bite force production. He proposed that selection may act to prevent TMJ distraction during both maximal and submaximal biting, creating a buffer zone for movement of the muscle resultant during submaximum force production. While the resultant should stay within the sweet spot during maximum bite force production, it can migrate into the buffer zone during periods of submaximum force production. The distance between the last molar and the muscle resultant represents the theoretical anterior portion of the buffer zone (Fig. 15). The purpose of this chapter is to determine what contributes to both intra- and interspecific variation in the distance between the last molar and the resultant (i.e., the anterior portion of the buffer zone).

## Hypothesis and Predictions

This research tests the hypothesis that the location of molar emergence is constrained to avoid TMJ distraction throughout ontogeny by determining if the location of emergence is influenced by factors related to the size of the buffer zone. Specifically, this chapter investigates four factors that may contribute to intra- and inter-specific variation in the distance between the muscle resultant's intersection with the triangle of support and the position of molar emergence: food mechanical properties, skull size, jaw gape, and the length of the next erupting molar.

Calculations based on the CLM of muscle force vector (and thus muscle resultant) position are performed with the mandible in a fully adducted position. Biting at more posterior points, especially on large items, prevents full adduction, however. In this case, the muscle force vectors intersect the triangle of support at different points than when the mandible is adducted and this can change the position at which the resultant intersects the triangle of support. With the mandible in abduction, the muscle line of action (MLA) of the anterior temporalis intersects the triangle of support at a more anterior location while the MLAs of the masseter and medial pterygoid muscles intersect the triangle of support at more posterior locations (Fig 16; Spencer 1999). Based on this observation, it has been proposed that selection may act to avoid TMJ distraction while biting on posterior bite points with large gapes (Spencer 1999; Perry, Hartstone-Rose, and Logan 2011). Therefore, species and individuals that possess larger gapes should have larger distances between the last molar and the resultant (i.e., larger buffer zones).

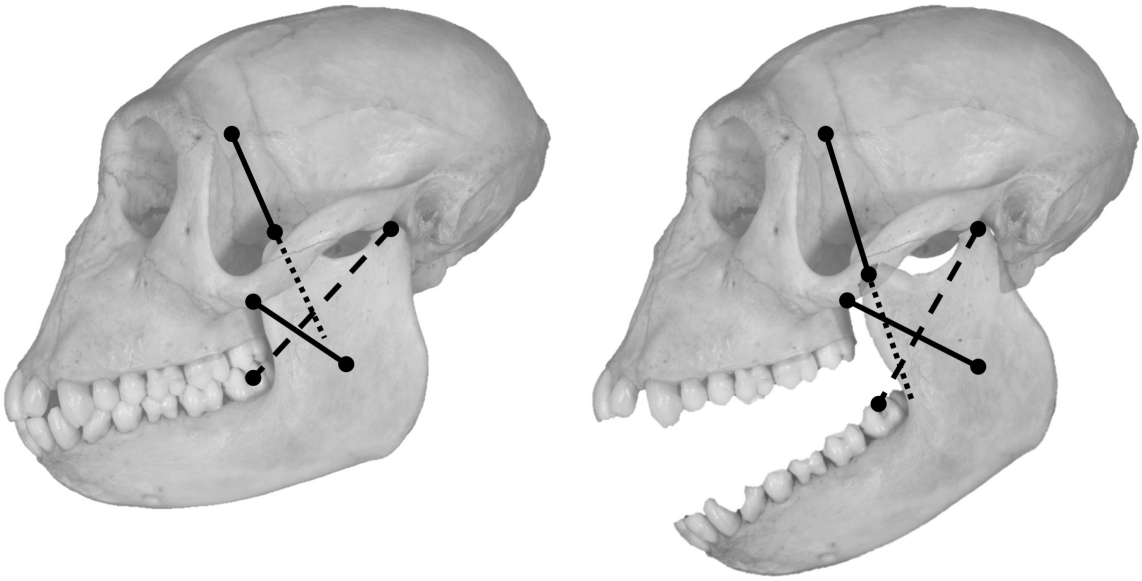

Figure 16. Effects on abducting the mandible on the position at which muscle lines of action cross the triangle of support. When the mandible is adducted (left) the anterior temporalis line of action crosses the triangle of support at a more posterior point than when the mandible is abducted (right). Conversely, the masseter line of action crosses the triangle of support at a more anterior point when the mandible is adducted (left) than when it is abducted (right).

Hard and tough foods require high-magnitude bite forces (Lucas 2004) and bite force magnitudes typically increase with decreasing distance to the muscle resultant (Spencer and Demes 1993; Lucas 2012). Food mechanical properties may, therefore, be related to the position of molar emergence relative to the resultant such that primates that feed on more mechanically challenging foods may possess shorter distances between the last molar and the resultant.

Overall skull size may explain variation in the distance between the last molar and the resultant. This distance may be longer in large individuals and shorter in small individuals simply as a function of variation in overall skull size.

The length of an erupting molar may also be an important factor in determining the distance between the last molar and the resultant. Molars vary in mesiodistal length

both intraspecifically (e.g., variation along the tooth row and among individuals) as well as among species. In papionins, for example, the M3 is the longest tooth, mesiodistally, while in humans the M3 tends to be the shortest of the three molars (Swindler 2002). Variation in length along the molar row is produced by varying activator-inhibitor signals during tooth formation (Kavanagh, Evans, and Jernvall 2007; Evans et al. 2016), while interspecific variation in molar length is related to overall size and diet (e.g., Kay 1975; Strait 1993; Lucas 2004). Individuals with mesiodistally longer molars may require more room to be available, anterior to the muscle resultant, before such a longer molar can emerge. These individuals may therefore possess longer distances between the resultant and the last molar. In other words, there should be a positive relationship between the distance between the resultant and the last molar and the mesiodistal length of the next molar to emerge.

## Material and Methods

### *Data Collection*

This research investigated four factors that may contribute to interspecific variation in the distance between the muscle resultant's intersection with the triangle of support and the position of molar emergence: jaw gape, food mechanical properties, skull size, and the mesiodistal length of the next molar to emerge. The landmark data collection methods and sample composition follow those described in Chapter 2. In addition to the landmark data collected to for the analysis in Chapter 2 (landmarks listed in Table 1: Chapter 2), several additional landmarks and data types were collected for the purpose of this study. Landmarks were collected to establish cranial breadth and length,

and facial breadth, height, and length (Table 9; Fig 17). These measurements were used to calculate *skull geometric mean (GM)* of each skull using the formula:

*Equation 21: Skull GM* $=$

$$\sqrt[5]{Cranial\ breadth + Cranial\ length + Facial\ breadth + Facial\ height + Facial\ length}$$

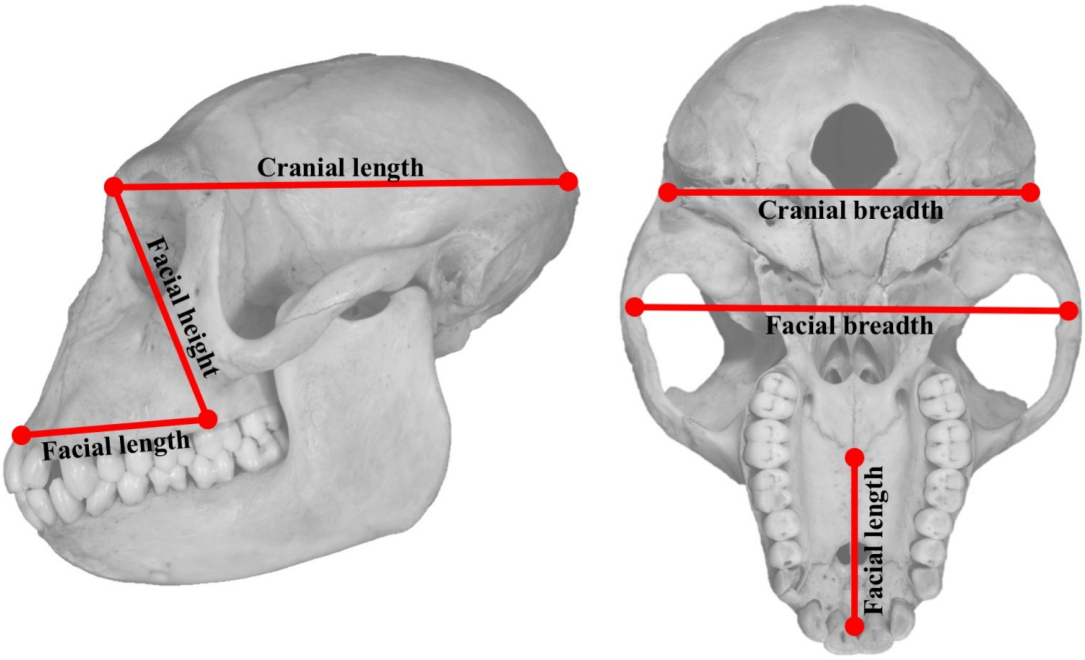


Figure 17. Measurements taken to calculate skull geometric mean.

Table 9. List of measurements taken on skulls to determine skull geometric mean.

| Name of measurement | Description of measurement |
|---|---|
| Cranial breadth | Left porion – right porion |
| Cranial length | Lambda – glabella |
| Facial breadth | Left inferior aspect of zygomaticotemporal suture – right inferior aspect of zygomaticotemporal suture |
| Facial height | Intersection of intermaxillary and maxillopalatine sutures – glabella |
| Facial length | Intersection of intermaxillary and maxillopalatine sutures – alveolare |

Hylander (2013) showed that jaw length, projected onto the mid-sagittal plane (which he called *projected jaw length*, a name that is also used here), and *canine overlap* together are excellent predictors of maximum jaw gape in anthropoid primates. These two variables were measured in the skeletal sample and used as a proxy for jaw gape. *Projected jaw length* was measured by determining the Euclidean distance between the center of the articular eminence and infradentale (i.e., a point between the two central mandibular incisors) along alveolar bone (the distance is *jaw length* in Fig. 18). Secondly, the Euclidean distance between landmarks at the centers of the right and left articular eminences was measured (*bicondylar breadth* in Fig. 18). Finally, *jaw length* and half of *bicondylar breadth* made up two sides of a right triangle (Fig. 18), *projected jaw length* was therefore determined using the equation:

*Equation 22:* $Projected\ jaw\ length = \sqrt{Jaw\ length^2 - (\frac{1}{2} Bicondylar\ breadth)^2}$

*Canine overlap* was measured directly from specimens using sliding calipers (Fig. 18). As described in Hylander (2013, 2017), the mandibular and maxillary dentition was placed in full occlusion and the calipers were positioned at the tips of the maxillary and mandibular canine. This distance was measured while the calipers were held parallel to the occlusal plane. *Canine overlap* was only measured in anthropoid primates. When canines are in full occlusion in strepsirrhine primates, the tip of the mandibular canine sits posterior to the maxillary canine and is obscured by the maxillary alveolar bone so a tip-to-tip measurement is impossible to take using sliding calipers.

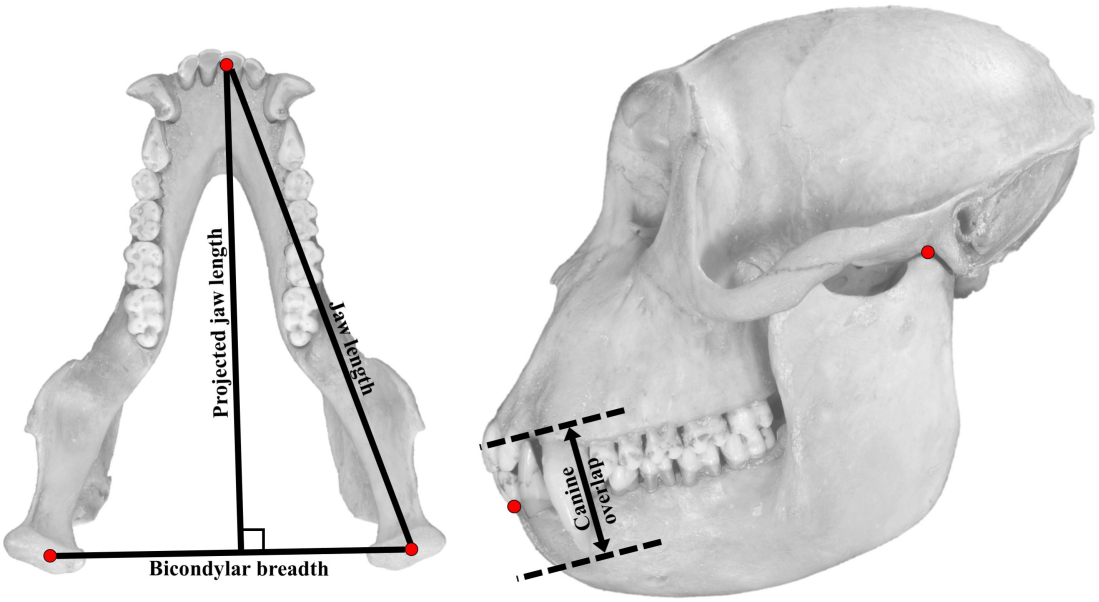


Figure 18. Measurements taken to calculate the variables *projected jaw length* and *canine overlap*. *Jaw length* is the Euclidean distance between the landmarks on the articular eminence (here shown on the mandibular condyle on the left and in lateral view on the right) and the point between the mandibular incisors (both landmarks marked by red circles). *Bicondylar breadth* is the distance between the left and right articular eminence (here also shown on the mandibular condyles). *Jaw length* is the hypotenuse of a right triangle with ½ *bicondylar breadth* and *projected jaw length* as the other sides. *Canine overlap* (right) was measured as the distance between the tips of the maxillary and mandibular canine when the teeth are in occlusion. The dashed lines indicate the position of the calipers, which were held parallel to the occlusal plane.

The mesiodistal length of all erupted mandibular M1s, M2s, and M3s were measured using sliding calipers. These data were used to determine the average mesiodistal length of each molar position in each species, a variable called *length of next molar* in this analysis. For the ontogenetic category where dp4 had emerged, the *length of next molar* was therefore the mean M1 mesiodistal length, and so forth. The "M3-emerged" category did not have a *length of next molar* associated with it because M3s are typically the last molars to erupt.

Data on food mechanical properties were collected from the literature. Toughness, *R* (in J $m^{-2}$), is the energy required to extend a unit area of a crack (Vincent 1992; Lucas et al. 2000). Young's modulus, *E* (in MPa), is the ratio of stress to strain throughout elastic deformation and defines an object's ability to resist elastic deformation ( Gordon 1978; Williams et al. 2005). Traditionally, in the absence of toughness and Young's modulus data, dietary categories (e.g., folivore, frugivore) and dietary composition (e.g., bark, leaves, fruit) are used as proxies of a species' dietary mechanical properties based on assumptions that leaves are tough and fruit is low in Young's modulus. Folivorous primates are therefore thought to have tough diets and frugivorous primates are thought to have diets that are not mechanically resistant (i.e., low in toughness and Young's modulus) (e.g., Ravosa 1996; Taylor 2006). A recent comparative study on the mechanical properties of primate diets indicates that such traditional dietary categories do not map onto the toughness and Young's modulus of primate foods (Coiner-Collier et al. 2016). These dietary categories fail to represent the variation in mechanical properties that exists within and between food items. Data on food mechanical properties are not available for all of the species included in this study. Despite this, and based on the results of the Coiner-Collier et al. (2016) study, it was important to use actual mechanical properties data to characterize the forces that primates produce when chewing food, rather than using dietary categories. The mechanical properties data used in this study are presented in Table 10. The variables collected, *MeanR* and *MeanE*, represent the average toughness and Young's modulus of the foods that these primates consume, respectively. Additionally, *MaxR* represents the toughest food in each species' diet. The majority of *Pongo pygmaeus* specimens included in this study are from the National Museum of

Natural History. The collection records of this institution list Borneo as the most common collection locality. Toughness and Young's modulus data are available for two subspecies of *Pongo pygmaeus*, *P. p. wurmbii* and *P. p. morio*. It is not possible to determine which subspecies is represented in the skeletal collection used in this study; the mechanical properties data were therefore averaged for the two subspecies.

Table 10. List of food mechanical properties from the literature used in this analysis.

| **Species** | **Mean*R*** | **Max*R*** | **Mean*E*** | **Source** |
|---|---|---|---|---|
| *Alouatta palliata* | 529.20 | 1419.48 | - | Coiner-Collier et al. (2016) |
| *Cebus apella* | 666.47 | 2308.60 | 91.87 | Coiner-Collier et al. (2016) |
| *Colobus angolensis* | 183.40 | 388.50 | - | Dunham et al. (2016) |
| *Gorilla beringei* | 1018.81 | 2869.07 | - | Coiner-Collier et al. (2016) |
| *Lemur catta* | 466.54 | 3148.42 | 681.03 | Coiner-Collier et al. (2016) |
| *Pan troglodytes* | 505.83 | 4223.00 | 1.03 | Coiner-Collier et al. (2016) |
| *Pongo pygmaeus* | 1108.2* | 5418.20* | 7.77** | Coiner-Collier et al. (2016) |

*Average of *P. p. morio* and *P. p. wurmbii* data

**Data for *P. p. wurmbii*

Two variables that were measured in Chapter 2 were also used in this study. Two methods were used to determine the position at which the muscle resultant crosses the triangle of support, which was then projected onto the occlusal plane and the distance between this point and the last molar measured. The first method involved averaging the positions of the three adductor MLAs. The resulting distance is called $Resultant_{Mean}$-*Molar.* The second method used the most anterior MLA to represent the position of the resultant. The variable produced by this method is called $Resultant_{Max}$-*Molar* (see Chapter 2 for details).

*Analytical Methods*

The analyses in this study are divided into two portions. The first set of analyses was aimed at determining the factors that contribute to ontogenetically-based *intraspecific* variation in the distance between the last molar and the resultant. The second set of analyses was used to determine the factors that contribute to *interspecific* variation in the distance between the last molar and the resultant.

Intraspecific Analyses

First, to determine what factors contribute to intraspecific variation in the distance between the last molar and the resultant, general linear models (GLMs) were used with the distance between the last molar and the resultant as the response variable (both $Resultant_{Mean}$-*Molar* and $Resultant_{Max}$-*Molar,* together referred as *Resultant-Molar,* were used as response variables in separate analyses) and *molar emergence category*, *projected jaw length*, *canine overlap*, and *skull GM* as predictor variables. Interaction terms were included among all predictor variables. If interactions were not significant, they were removed from the model. These analyses were performed on individual data and separate models were run for each species. The length of the next molar to emerge (i.e., the variable *length of next molar*) was not included in these models because these data are not available for each individual specimen (i.e., without possessing microCT scans of each specimen, the size of the forming molar in its crypt cannot be measured). Akaike's Information Criterion, with a correction for small sample size (AICc), was used to determine the best-fit model(s) and predictor variables(s) that explain intraspecific variation in *Resultant-Molar*. Models were selected based on their delta (Δ) AICc score,

which indicates the difference in AICc between the best model (i.e., the one with the lowest AICc) and other models. In addition to the model with the lowest AICc score, any models with delta AICc scores that were equal to or less than two ($\Delta$ AICc $\leq 2$) were also reported, as these are generally considered equally good as the model with the lowest AICc score (Burnham and Anderson 2002).

Interspecific Analyses

To determine what factors contribute to interspecific variation in the length of the distance between the last molar and the resultant (i.e., *Resultant-Molar*), Phylogenetic Generalized Least-Squares (PGLS) models were used, with *Resultant-Molar* as a continuous response variable, *projected jaw length*, *canine overlap*, *skull GM*, and *length of next molar* as continuous predictor variables. Interaction terms among the predictor variables were included in the model and removed if they were not significant. Separate models were performed for the response variables $Resultant_{Mean}$-*Molar* and $Resultant_{Max}$-*Molar*. A Type 1 model (i.e., least-squares) was used rather than a Type II model (e.g., reduced major axis) because the hypothesized relationships between *Resultant-Molar* and the predictor variables are causal (e.g., a larger *projected jaw length* and *skull GM* are expected to result in a longer *Resultant-Molar* distance*)* and therefore asymmetric, making Type I regression the appropriate method (Smith 2009). PGLS was used to determine which, if any, of these dependent variables explain a significant amount of interspecific variation in *Resultant-Molar*, while accounting for the influence of shared ancestry. The PGLS approach was taken here to remove potential statistical non-independence among the observations due to shared ancestry (Grafen 1989; Garland,

Theodore and Ives 2000; Freckleton, Harvey, and Pagel 2002; Nunn 2011). A maximum likelihood (ML) Pagel's λ (Pagel 1999; Freckleton, Harvey, and Pagel 2002) was estimated with the PGLS model, and was used to transform the variance-covariance matrix of the data and phylogentic tree according to the degree of phylogenetic signal. The power of using PGLS rather than Ordinary Least-Squares (OLS) regression is that in the former, the regression model is scaled according to how much phylogentic signal is present in the error of the model (Revell 2010). If the ML λ value is determined to be zero, for example, PGLS regression becomes statistically identical to OLS regression because the covariation due to shared ancestry is scaled by zero, fully removing its influence on the model. PGLS can therefore be used for all regression, because the degree to which phylogeny influences the data is accounted for. A phylogenetic tree for the analysis was downloaded from 10K Trees (Arnold, Matthews, and Nunn 2010). Separate analyses were performed on each molar emergence category. Analyses were performed on species means of all variables. Means included both males and females.

As in the intraspecific analyses, AICc was used to determine the best-fit model(s) and predictor variables(s) that explain interspecific variation in *Resultant-Molar* (Burnham and Anderson 2002). Models were selected based on their Δ AICc score, which represent the difference in AICc between the best model (i.e., the one with the lowest AICc) and each model. Models with Δ AICc $\leq$ 2 are considered equally good as the model with the lowest AICc score (Burnham and Anderson 2002).

A second set of the same interspecific analyses as above were performed on a subset of species. These included the seven species for which data on dietary toughness are available in the literature (Table 10). Data on dietary stiffness are only available for

four species included in this study, a sample size too small to be used in statistical analyses. Analyses with dietary stiffness as a response variable were therefore not performed, but data on dietary stiffness are reported for the four species (Table 10). Using data on the seven species for which dietary toughness data are available, PGLS models were evaluated with *Resultant-Molar* as the response variable and mean toughness (*MeanR)*, max toughness (*MaxR)*, *projected jaw length*, *canine overlap*, and *skull GM* as predictor variables. As above, separate models were performed for the response variables $Resultant_{Mean}$-*Molar* and $Resultant_{Max}$-*Molar*. Also, because the number of predictors was high and the number of species was low, separate models were performed with *MeanR* and *MaxR* as predictors. The majority of mechanical properties data reported in the literature are for adult diets and it is currently unknown for most species whether juvenile diets are mechanically similar to adult diets (but see Venkataraman et al. 2014; Chalk et al. 2016; Chalk-Wilayto et al. 2016 for mechanical properties data for juvenile primates). Therefore, for the purposes of this study, toughness data from the literature was used for adult specimens only (i.e., the M3 emerged category) and no analyses were performed with sub-adult skeletal data.

## Results

Summary data for all measurements can be found in SM 3.

*Intraspecific Models*

Results listing intraspecific GLMs using $Resultant_{Mean}$-*Molar* as the response variable are presented in Table 11 and those using $Resultant_{Max}$-*Molar* as the response variable are presented in Table 12. These tables list all models with a $\Delta AICc \leq 2$.

With $Resultant_{Mean}$-*Molar* as the response variable, all models, except for one *Lemur catta* model, were significant. There are taxonomic differences in how well the models explain variation in the distance between the last molar and the resultant. Among platyrrhines, the adjusted $R^2$ values ranged between 0.52 and 0.96 (Table 11). Similarly, among catarrhines, the adjusted $R^2$ values ranged between 0.81 and 0.92 (Table 11). The adjusted $R^2$ values were much lower among strepsirrhine models, where they ranged between 0.09 and 0.31.

With $Resultant_{Max}$-*Molar* as the response variable, all platyrrhine and catarrhine models were significant. Five out of the 10 strepsirrhine models were not significant, however. As above, there were taxonomic differences in how well the models explain variation in $Resultant_{Max}$-*Molar*. Among platyrrhines, the adjusted $R^2$ values ranged between 0.33 and 0.97 (Table 12) while among catarrhines, the adjusted $R^2$ values ranged between 0.69 and 0.97 (Table 12). As in the above set of analyses, the adjusted $R^2$ values for the significant strepsirrhine models were much lower, ranging from 0.11 and 0.29.

Overall, all predictor variables were included in at least some models. *Projected jaw length* was the most frequently included variable, included in 29 out of 34 models where $Resultant_{Mean}$-*Molar* was the response variable (Table 11) and in 30 out of 36 models where $Resultant_{Max}$-*Molar* was the response variable (Table 12). The slope for *projected jaw length* was almost always positive indicating a positive relationship with

Table 11. Results of intraspecific GLMs using *Resultant*$_{Mean}$*-Molar* as the response variable.

| Taxon | Molar emergence category | Projected jaw length | Canine overlap | Skull GM | AICc | Δ AICc | Model | |
|---|---|---|---|---|---|---|---|---|
| | | | | | | | Adj. $R^2$ | *p*-value |
| **Platyrrhini** | | | | | | | | |
| *Alouatta palliata* | + | 0.4 | -0.2 | | 117.1 | 0.00 | 0.96 | *** |
| *Ateles geoffroyi* | + | 0.3 | | 0.6 | 185.1 | 0.00 | 0.87 | *** |
| *Cebus apella* | | 0.1 | 0.6 | 0.2 | 293.2 | 0.00 | 0.52 | *** |
| *Saimiri sciureus* model 1 | + | 0.3 | -0.1 | | 141.2 | 0.00 | 0.56 | *** |
| *Saimiri sciureus* model 2 | + | | 0.1 | | 141.6 | 0.44 | 0.53 | *** |
| *Saimiri sciureus* model 3 | + | 0.3 | | | 142.3 | 1.11 | 0.55 | *** |
| *Saimiri sciureus* model 4 | + | | 0.0 | 0.3 | 142.4 | 1.18 | 0.54 | *** |
| *Saimiri sciureus* model 5 | + | | | 0.3 | 143.0 | 1.75 | 0.54 | *** |
| **Cercopithecidae** | | | | | | | | |
| *Colobus angolensis* | | 0.3 | 0.0 | | 168.2 | 0.00 | 0.87 | *** |
| *Colobus polykomos* model 1 | | 0.3 | 0.0 | | 111.2 | 0.00 | 0.90 | *** |
| *Colobus polykomos* model 2 | | 0.2 | -0.1 | 0.2 | 112.4 | 1.26 | 0.90 | *** |
| *Procolobus verus* model 1 | | 0.3 | 0.0 | | 80.9 | 0.00 | 0.81 | *** |
| *Procolobus verus* model 2 | + | 0.3 | 0.0 | | 82.6 | 1.77 | 0.82 | *** |
| *Macaca fascicularis* model 1 | | 0.3 | -0.1 | | 120.9 | 0.00 | 0.89 | *** |
| *Macaca fascicularis* model 2 | + | 0.3 | -0.1 | | 122.8 | 1.98 | 0.90 | *** |
| *Macaca mulatta* model 1 | + | 0.3 | -0.1 | | 420.7 | 0.00 | 0.89 | *** |
| *Macaca mulatta* model 2 | + | 0.3 | -0.1 | 0.1 | 422.5 | 1.81 | 0.89 | *** |
| *Papio anubis* | | 0.2 | -0.1 | | 181.8 | 0.00 | 0.92 | *** |
| *Papio cynocephalus* model 1 | | 0.2 | -0.1 | | 270.8 | 0.00 | 0.81 | *** |
| *Papio cynocephalus* model 2 | | | -0.1 | 0.4 | 271.1 | 0.23 | 0.81 | *** |
| *Papio cynocephalus* model 3 | | 0.1 | -0.1 | 0.2 | 272.2 | 1.38 | 0.81 | *** |
| *Papio cynocephalus* model 4 | + | 0.2 | -0.1 | | 272.5 | 1.69 | 0.81 | *** |
| **Hominidae** | | | | | | | | |
| *Gorilla beringei* | | 0.2 | 0.1 | | 401.3 | 0.00 | 0.84 | *** |
| *Gorilla gorilla* | | 0.3 | -0.1 | | 229.2 | 0.00 | 0.82 | *** |
| *Homo sapiens* [a] | + | 0.8 | -0.4 | 0.2 | 451.6 | 0.00 | 0.89 | *** |
| *Pan paniscus* | | 0.4 | -0.2 | | 182.0 | 0.00 | 0.88 | *** |
| *Pan troglodytes* | | 0.5 | 0.0 | -0.3 | 483.6 | 0.00 | 0.82 | *** |
| *Pongo pygmaeus* model 1 | + | 0.6 | 0.0 | -0.7 | 200.2 | 0.00 | 0.91 | *** |
| *Pongo pygmaeus* model 2 | | 0.6 | -0.2 | -0.5 | 201.0 | 0.80 | 0.90 | *** |
| **Strepsirrhini** | | | | | | | | |
| *Lemur catta* | | -0.1 | | | 112.0 | 0.00 | 0.00 | NS |
| *Eulemur mongoz* | | 0.3 | | | 70.9 | 0.00 | 0.31 | * |
| *Otolemur monteiri* | + | 0.5 | | | 171.9 | 0.00 | 0.22 | * |
| *Perodicticus potto* model 1 | + | | | | 184.0 | 0.00 | 0.20 | * |
| *Perodicticus potto* model 2 | | 0.2 | | | 185.9 | 1.92 | 0.09 | * |

+Categorical predictor variable (i.e., *molar emergence category*) included in the model

* p≤0.05, ** p≤0.01, *** p≤0.001

[a]Model includes interaction between *molar emergence category* and *projected jaw length*

Table 12. Results of intraspecific GLMs using *Resultant*$_{Max}$*-Molar* as the response variable.

| Taxon | Molar emergence category | Projected jaw length | Canine overlap | Skull GM | AICc | Δ AICc | Model | |
|---|---|---|---|---|---|---|---|---|
| | | | | | | | Adj. $R^2$ | *p*-value |
| **Platyrrhini** | | | | | | | | |
| *Alouatta palliata* model 1 | + | 0.56 | -0.11 | 0.30 | 150.4 | 0.00 | 0.97 | *** |
| *Alouatta palliata* model 2 | + | 0.67 | -0.01 | | 151.3 | 0.95 | 0.97 | *** |
| *Ateles geoffroyi* | + | 0.50 | | 0.85 | 217.3 | 0.00 | 0.88 | *** |
| *Cebus apella* | + | 0.50 | | 0.85 | 217.3 | 0.00 | 0.33 | *** |
| *Saimiri sciureus* model 1 | + | 0.48 | -0.08 | | 170.0 | 0.00 | 0.57 | *** |
| *Saimiri sciureus* model 2 | + | | 0.14 | | 171.7 | 1.76 | 0.53 | *** |
| **Cercopithecidae** | | | | | | | | |
| *Colobus angolensis* a | + | -0.05 | 0.11 | | 191.8 | 0.00 | 0.92 | *** |
| *Colobus polykomos* model 1 | | 0.36 | -0.04 | | 131.0 | 0.00 | 0.93 | *** |
| *Colobus polykomos* model 2 | | 0.24 | -0.08 | 0.30 | 131.6 | 0.59 | 0.92 | *** |
| *Procolobus verus* | + | 0.52 | -0.06 | | 94.0 | 0.00 | 0.81 | *** |
| *Macaca fascicularis* model 1 | + | 0.37 | -0.26 | | 163.8 | 0.00 | 0.86 | *** |
| *Macaca fascicularis* model 2 | | 0.36 | -0.20 | | 165.0 | 1.20 | 0.84 | *** |
| *Macaca fascicularis* model 3 | + | 0.27 | -0.29 | 0.24 | 165.4 | 1.65 | 0.86 | *** |
| *Macaca mulatta* model 1 | + | 0.42 | -0.12 | | 590.5 | 0.00 | 0.78 | *** |
| *Macaca mulatta* model 2 | + | 0.34 | -0.12 | 0.14 | 591.9 | 1.46 | 0.78 | *** |
| *Papio anubis* | | 0.31 | -0.20 | | 238.1 | 0.00 | 0.88 | *** |
| *Papio cynocephalus* b | | 0.50 | -0.03 | 0.64 | 295.3 | 0.00 | 0.86 | *** |
| **Hominidae** | | | | | | | | |
| *Gorilla beringei* | | 0.39 | 0.11 | | 507.5 | 0.00 | 0.74 | *** |
| *Gorilla gorilla* | | 0.40 | 0.04 | | 247.0 | 0.00 | 0.87 | *** |
| *Homo sapiens* model 1 | | 0.36 | -0.84 | 0.48 | 637.1 | 0.00 | 0.70 | *** |
| *Homo sapiens* model 2 | + | | -1.77 | 0.74 | 637.5 | 0.31 | 0.70 | *** |
| *Homo sapiens* model 3 | + | 0.23 | -1.50 | 0.50 | 638.1 | 0.91 | 0.71 | *** |
| *Homo sapiens* model 4 | | 0.67 | -0.40 | | 639.0 | 1.81 | 0.69 | *** |
| *Pan paniscus* | | 0.40 | -0.28 | | 194.1 | 0.00 | 0.87 | *** |
| *Pan troglodytes* | | 0.42 | -0.04 | | 492.6 | 0.00 | 0.87 | *** |
| *Pongo pygmaeus* | | 0.49 | -0.34 | | 175.9 | 0.00 | 0.97 | *** |
| **Strepsirrhini** | | | | | | | | |
| *Eulemur mongoz* model 1 | | 0.53 | | | 93.0 | 0.00 | 0.21 | * |
| *Eulemur mongoz* model 2 | + | 0.93 | | | 94.0 | 0.96 | 0.29 | * |
| *Lemur catta* model 1 | | -0.16 | | | 132.3 | 0.00 | 0.11 | * |
| *Lemur catta* model 2 | + | | | | 133.3 | 0.95 | 0.14 | NS |
| *Lemur catta* model 3 | | | | -0.23 | 133.9 | 1.62 | 0.05 | NS |
| *Otolemur monteiri* model 1 | + | 0.90 | | | 219.8 | 0.00 | 0.18 | * |
| *Otolemur monteiri* model 2 | + | | | 1.66 | 220.4 | 0.59 | 0.17 | * |
| *Otolemur monteiri* model 3 | | 0.22 | | | 221.7 | 1.94 | 0.06 | NS |
| *Perodicticus potto* model 1 | | 0.56 | | | 278.9 | 0.00 | 0.06 | NS |
| *Perodicticus potto* model 2 | | | | 0.95 | 279.0 | 0.14 | 0.06 | NS |

+Categorical predictor variable (i.e., *molar emergence category*) included in the model

* p≤0.05, ** p≤0.01, *** p≤0.001

[a]Model includes interaction between *molar emergence category* and *projected jaw length*

[b]Model includes interaction between *skull GM* and *projected jaw length*

both *Resultant$_{Mean}$-Molar* and *Resultant$_{Max}$-Molar*. Similarly, *canine overlap* was frequently included as a predictor variable, appearing in 26 out of 34 models where *Resultant$_{Mean}$-Molar* was the response variable (Table 11) and in 24 out of 36 models *overlap* was almost always negative indicating a negative relationship with both *Resultant$_{Mean}$-Molar* and *Resultant$_{Max}$-Molar*. *Molar emergence category* was included as a predictor in fewer models than the above two predictors; it was included in 16 out of the 34 models where *Resultant$_{Mean}$-Molar* was the response variable (Table 11) and in 18 out of the 36 models where *Resultant$_{Max}$-Molar* was the response variable (Table 12). Most of these were platyrrhine and macaque models. Similarly, *skull GM* was included in only 12 out of the 34 models where *Resultant$_{Mean}$-Molar* was the response variable (Table 11) and in 13 out of the 36 models where *Resultant$_{Max}$-Molar* was the response variable (Table 12). The slope for *skull GM* was almost always positive, with the exception of a few strepsirrhine and hominid models, indicating a positive relationship with both *Resultant$_{Mean}$-Molar* and *Resultant$_{Max}$-Molar*.

*Interspecific Models*

Results listing interspecific PGLS models using *Resultant$_{Mean}$-Molar* as the response variable are presented in Table 13 and those using *Resultant$_{Max}$-Molar* as the response variable are presented in Table 14. These tables list all models with a $\Delta$AICc $\leq$ 2.

With *Resultant$_{Mean}$-Molar* as the response variable, all models were significant and explained a large amount of variation in the distance between the last molar and the resultant ($R^2$ range: 0.79-0.95: Table 13). In the model looking at all species at the dp4-

emerged category, *skull GM* was included as a predictor variable with a positive slope, whereas in the models looking at all species at the M1-emerged category, *skull GM*, and *length of next molar* were included as predictor variables with positive slopes and *projected jaw length* was included as a predictor variable with a negative slope. In the next molar emergence category (i.e., M2-emerged), all predictor variables were included in at least one of the best-fit models. *Length of next molar* and *canine overlap* had negative slopes while *projected jaw length* and *skull GM* had positive slopes. In the final M3-emerged category, only *skull GM* was included as a predictor variable and it had a positive slope (Table 13).

Table 13. Results of interspecific PGLS models using $Resultant_{Mean}$-*Molar* as the response variable.

| Molar emergence category | Length of next molar | Projected jaw length | Canine overlap | Skull GM | AICc | Δ AICc | Model | | |
|---|---|---|---|---|---|---|---|---|---|
| | | | | | | | Adj. $R^2$ | *p*-value | ML lambda |
| dp4 emerged[a] | | | | 0.03 | -5.3 | 0.00 | 0.85 | *** | 0.00 |
| M1 emerged[a,b] | 0.39 | | | 0.02 | -14.9 | 0.00 | 0.93 | *** | 0.00 |
| M1 emerged[a,b] | 0.56 | -0.01 | | 0.02 | -13.8 | 1.13 | 0.94 | *** | 0.00 |
| M2 emerged | | 0.18 | -1.07 | 0.28 | 83.8 | 0.00 | 0.95 | *** | 0.00 |
| M2 emerged | | | -0.62 | 0.47 | 84.5 | 0.66 | 0.94 | *** | 0.00 |
| M2 emerged | | 0.33 | -1.12 | | 85.1 | 1.34 | 0.80 | *** | 1.00 |
| M2 emerged | -0.50 | 0.26 | -0.97 | 0.24 | 85.5 | 1.72 | 0.95 | *** | 0.00 |
| M3 emerged | NA | | | 0.33 | 88.7 | 0.00 | 0.79 | *** | 1.00 |

[a]Response variable log-transformed

[b]*Length of next molar* log-transformed

* $p \leq 0.05$

** $p \leq 0.01$

*** $p \leq 0.001$

Table 14. Results of interspecific PGLS models using *Resultant$_{Max}$-Molar* as the response variable.

| Molar emergence category | Length of next molar | Projected jaw length | Canine overlap | Skull GM | AICc | Δ AICc | Model | | |
|---|---|---|---|---|---|---|---|---|---|
| | | | | | | | Adj. $R^2$ | *p*-value | ML lambda |
| dp4 emerged [a] | | 0.02 | | | -2.6 | 0.00 | 0.81 | *** | 0.00 |
| M1 emerged [a,b] | 0.56 | | | 0.01 | -13.0 | 0.00 | 0.93 | *** | 0.00 |
| M1 emerged [a,b] | 0.99 | | | | -13.6 | 0.20 | 0.83 | *** | 0.94 |
| M2 emerged | | 0.55 | -1.68 | | 95.0 | 0.00 | 0.94 | *** | 0.00 |
| M2 emerged | | 0.41 | -1.41 | 0.17 | 96.9 | 1.96 | 0.94 | *** | 0.00 |
| M3 emerged | | | | 0.58 | 102.9 | 0.00 | 0.83 | *** | 0.99 |
| M3 emerged | NA | | -0.28 | 0.65 | 104.2 | 1.27 | 0.84 | *** | 1.00 |

[a]Response variable log-transformed

[b]*Length of next molar* log-transformed

* $p \leq 0.05$

** $p \leq 0.01$

*** $p \leq 0.001$

Similarly, with *Resultant$_{Max}$-Molar* as the response variable, all models were significant and also explained a large amount of variation in the distance between the last molar and the resultant ($R^2$ range: 0.81-0.94: Table 14). The dp4-emerged model included only one variable, *projected jaw length*, as a predictor and it had a positive slope. The M1-emerged models included both *length of next molar* and *skull GM* as predictor variables and both had positive slopes (Table 14). M2-emerged models included all predictor variables except *length of next molar*, and all slopes were positive except the negative slopes of *canine overlap*. M3-emerged models only included *canine overlap*, which had a negative slope, and *skull GM*, which had a positive slope, as predictor variables (Table 14).

Table 15. Results of interspecific PGLS models with either *Resultant$_{Mean}$-Molar* or *Resultant$_{Max}$-Molar* as response variables and including either *MeanR* or *MaxR* as predictor variables.

| | | | | | | | | Model | | |
|---|---|---|---|---|---|---|---|---|---|---|
| **Response Variable** | **Mean *R*** | **Max *R*** | **Projected jaw length** | **Canine overlap** | **Skull GM** | **AICc** | **Δ AICc** | **Adj. $R^2$** | ***p*-value** | **ML lambda** |
| Resultant$_{Mean}$-Molar model 1 | | NA | 0.26 | | | 40.20 | 0 | 0.88 | ** | 0.00 |
| Resultant$_{Mean}$-Molar model 2 | NA | 0.00 | 0.20 | | | 38.50 | 0 | 0.98 | ** | 0.00 |
| Resultant$_{Mean}$-Molar model 3 | | NA | | | 0.39 | 41.40 | 1.22 | 0.86 | ** | 0.00 |
| Resultant$_{Mean}$-Molar model 4 | NA | | 0.26 | | | 40.20 | 1.76 | 0.88 | ** | 0.00 |
| Resultant$_{Max}$-Molar model 1 | 0.02 | NA | 0.23 | | | 25.10 | 0 | 1.00 | *** | 0.00 |
| Resultant$_{Max}$-Molar model 2 | NA | | | | 0.52 | 44.00 | 0 | 0.68 | NS | 0.00 |
| Resultant$_{Max}$-Molar model 3 | NA | | 0.34 | | | 44.30 | 0.33 | 0.87 | ** | 0.00 |

* $p \leq 0.05$

** $p \leq 0.01$

*** $p \leq 0.001$

*MaxR* was included in one of the best-fit models predicting *Resultant$_{Mean}$-Molar* and it had a positive slope (Table 15). The best-fit models also included *projected jaw length* and *skull GM*, which also had positive slopes. Similarly, *MeanR* was included in one of the best-fit models predicting *Resultant$_{Max}$-Molar* and also had a positive slope (Table 15). The best-fit models predicting *Resultant$_{Max}$-Molar* also included *projected jaw length* and *skull GM* and these variables also had positive slopes. *Canine overlap* was not included as a predictor in any of the models. The adjusted $R^2$ values were high for both sets of models, explaining 86-98% of the variation in *Resultant$_{Mean}$-Molar* and 68-100% of the variation in *Resultant$_{Max}$-Molar* (Table 15).

## Discussion

This study examined factors that may contribute to variation in the distance from the last molar to the adductor muscle resultant. The analysis in Chapter 2 identified that there are differences in the position of molar emergence both intraspecifically (i.e., among molar emergence categories) and interspecifically. This variation may be related to a variety of factors including the size of the animal and its feeding behavior. This chapter tested the hypothesis that the position of molar emergence is influenced by factors related to the size of the buffer zone. Specifically, this chapter investigated whether food mechanical properties, skull size, jaw gape, and the length of the next molar to emerge contribute to intra- and interspecific variation in the distance between the muscle resultant's intersection with the triangle of support and the position of molar emergence.

Results indicated that among platyrrhines and catarrhines, *canine overlap* and *projected jaw length*, as well as *skull GM* and *molar emergence category* are important variables explaining intraspecific variation in the distance between the last molar and the resultant, although the latter two variables were included in fewer models than the former two. Among strepsirrhines, not all models significantly explained variation in the distance between the last molar and the resultant, but of the models that were significant, most included *projected jaw length* as a predictor variable. A high amount of interspecific variation in the distance between the last molar and the resultant is explained by various combinations of the predictor variables: *skull GM*, *canine overlap*, *projected jaw length*, *length of next molar*, and *MeanR* and *MaxR*. Depending on whether the response variable was $Resultant_{Mean}$-*Molar* or $Resultant_{Max}$-*Molar* and the molar-emergence category of the

analysis, some of the predictors appeared in more models than others, but no clear pattern was present.

The two predictors of gape, *canine overlap* and *projected jaw length*, were important factors in explaining variation in the distance between the resultant and the last molar. In both intra- and inter-specific models, *canine overlap* was included as a predictor variable less frequently than *projected jaw length*. In both types of models, increases in *projected jaw length* corresponded to increases in *Resultant-Molar*, while increases in *canine overlap* corresponded to decreases in *Resultant-Molar*. While the pattern found for *projected jaw length* fit the expectations of this chapter, the pattern found for *canine overlap* was opposite to what was expected. Both variables are thought to be proxies for jaw gape (Hylander 2013, 2017) and this chapter tested the expectation that as jaw gape increased, so should the distance between the last molar and the resultant, as a means to accommodate anterior migration of the resultant with a larger buffer zone. Gape is hypothesized to influence the size of the buffer zone because at least one of the adductor muscles crosses the triangle of support at a more anterior point when the jaws are abducted (Fig. 16). The size of the buffer zone should accommodate anterior migration of the resultant due to jaw abduction, which may occur when biting on large items, particularly at posterior bite points (Spencer 1999; Perry, Hartstone-Rose, and Logan 2011). The predictive relationship between *canine overlap* and gape was based on an interspecific analysis of adult anthropoid primates (Hylander 2013, 2017) and it is unknown whether *canine overlap* also predicts gape throughout ontogeny. One consideration is the dynamic nature of *canine overlap* throughout ontogeny. Deciduous canines are ultimately replaced by permanent canines and while permanent canines are

erupting, the degree of canine overlap changes. Furthermore, there is variation in the position of the canine in the emergence sequence both among anthropoid species and between the sexes (e.g., Smith 1994; Harvati 2000; Setchell and Wickings 2004). Similarly, the rates of canine growth and eruption differ both within (i.e., between the sexes) and among taxa (e.g., Schwartz, Reid, and Dean 2001; Leigh, Setchell, and Buchanan 2005). Therefore, the effect of canine overlap may be variable across ontogeny and the effect that this has on the relationship between canine overlap and gape is unknown.

In this chapter, maximum gape, itself estimated from *canine overlap* and *projected jaw length*, was used as a proxy for the maximum size of food items that primates ingest. This chapter therefore assumes that primates will ingest the largest possible food item permitted by their gape. Perry and Hartstone-Rose (2010) examined maximum ingested food size (which they called $V_b$) in strepsirrhines and found that this variable is positively related to mandible length, their proxy for gape, suggesting that strepsirrhines with larger gapes consume larger food items, especially if those food items are not mechanically resistant (Perry and Hartstone-Rose 2010). The analysis here, which showed that intraspecific variation in *Resultant-Molar* is explained by *projected jaw length* in all but one species of strepsirrhine, suggests that the relationship between gape and maximum ingested food size holds throughout ontogeny in strepsirrhines and influences the size of the buffer zone. It is unknown, however, whether primates place items that are large on their posterior molars or if these large items are first processed with the anterior dentition where bite force is lower but large items can be accommodated more easily. To determine this as well as $V_b$ for strepsirrhines throughout ontogeny, it

will be necessary to perform similar experiments on subadult strepsirrhines while noting the location of where food is placed along the tooth row.

Unfortunately, a similar analysis looking at the relationship between mandibular length and $V_b$ has not been performed on anthropoids primates, but there is reason to expect that these primates would not exhibit the same pattern. Perry and Hartstone-Rose (2010) found that the scaling relationship between $V_b$ and mandible length and $V_b$ and body mass was very similar, both in slope and explanatory power. In studies that included both strepsirrhines and anthropoid primates, it was determined that while $V_b$ increases with body mass in strepsirrhines, it decreases with body mass in anthropoids (Perry and Hartstone-Rose 2010; Perry et al. 2015). If the same relationship between mandible length and body mass holds for anthropoids as it does for strepsirrhines then it is expected that anthropoid primates with longer mandibles (i.e., larger gapes) should consume smaller food items than those with shorter mandibles (i.e., smaller gapes). Indeed, the analyses here indicated that one predictor of gape, *canine overlap*, was negatively related to the distance between the last molar and the resultant, both throughout ontogeny and interspecifically. On the other hand, the analysis here suggests that throughout ontogeny and interspecifically, there is a positive relationship between *projected jaw length* and the distance between the last molar and the resultant. More work is necessary to determine how the size of food items is related to gape and how these relate to the size of the buffer zone both intra- and interspecifically, but the results here suggest that *projected jaw length* and *canine overlap* have antagonistic effects on the size of the buffer zone.

Another factor that may be related to the size of food items that primates can ingest and the size of the buffer zone is the food's mechanical properties. Strepsirrhines have higher $V_b$ values for foods that are less mechanically resistant (i.e., do not require high bite forces to induce/propagate a fracture) and thus the largest food items are consumed by the largest strepsirrhines when eating fruit (Perry and Hartstone-Rose 2010; Perry et al. 2015). Anthropoids, on the other hand, exhibit no relationship between food mechanical properties and food size (Perry et al. 2015). Based on these results, it is expected that there should be an interaction between gape and food mechanical properties (i.e., as gape increases, food mechanical properties should decrease). This is opposite to the results of this study, however, as there was no significant interaction between either of the predictors of gape and food toughness. In fact, *projected jaw length*, *MeanR,* and *MaxR* are both positive predictors of *Resultant-Molar*. The positive relationship between food toughness and *Resultant-Molar* is contrary to what was expected in this chapter. The expectation was that primates that feed on tougher foods would possess shorter distances between the last molar and the resultant. Based on the results, it is possible that since tough food require repetitive mastication, a large buffer zone is more important to create a more stable loading environment during cyclical loading. The sample size for these analyses is very small, however, and consists of almost all anthropoids except for *L. catta*. Strepsirrhines consume some of the most resistant foods among primates (e.g., Yamashita 2002; Teaford et al. 2006; Quyet et al. 2007; Vogel et al. 2008; Yamashita et al. 2009, 2016; Venkataraman et al. 2014; Chalk-Wilayto et al. 2016; Coiner-Collier et al. 2016; Glowacka et al. 2017) and an analysis that includes more strepsirrhine species might be more revealing regarding these patterns.

The sample size was too low to perform any analyses of the Young's modulus data for the 4 species for which data are available (Table 10). The species that consume foods with higher Young's modulus (*C. apella* and *L. catta*) are much smaller-bodied than the species that consume foods with lower Young's modulus (*P. troglodytes* and *P. pygmaeus*) (Table 10). Despite this difference in size, the distance between the last molar and the resultant in these species is very similar (Chapter 2) suggesting that, similar to the results for food toughness, the size of the buffer zone is relatively greater in species that consume stiffer foods. Although there was little overlap in the species used in this study and those for which food mechanical properties data are available, based on the data that are available, the results of this chapter suggest that primates that feed on more resistant foods possess larger buffer zones. The reason for this is still unclear but it is possible that more resistant diets simply require greater safety mechanisms for the TMJs than less resistant diets.

Of the published food mechanical properties studies, many do not report how food is consumed (e.g., whether food is prepared extra-orally, what part of the dentition is used to prepare food prior to mastication, etc.). The assumption in this chapter is that primates are biting foods of given mechanical properties on their last molar. We know, however, that foods can be orally processed with the anterior dentition (i.e., incisors, canines) prior to mastication with the postcanine dentition and so the mechanical properties that are reported in most studies do not necessarily reflect the mechanical properties of the foods that are ultimately masticated by the molars (Ross, Iriarte-Diaz, and Nunn 2012; McGraw et al. 2016). Similarly, because there are no data for the species examined here on the mechanical properties of the diet throughout ontogeny, the

influence that food has on the size of the buffer zone throughout growth remains unexplored. The handful of studies that have looked at the mechanical differences between adult and juvenile diets report mixed results. Two studies report no significant differences between the mechanical properties of adult and juvenile diets of both *Sapajus libidinosus* and *Trachypithecus phayrei crepusculus* (Chalk et al. 2016; Chalk-Wilayto, Ossi-Lupo, and Raguet-Schofield 2016), while one study reports that infant and juvenile geladas eat foods that are less tough, on average, than adult foods (Venkataraman et al. 2014). The present study found supports for the idea that the position of molar emergence is influenced by factors related to the size of the buffer zone and provided new insight into the factors that contribute to the size of the buffer zone, both throughout ontogeny and interspecifically. More data are clearly needed on the mechanical properties of juvenile and adult diets and associated feeding behaviors for those foods. Similarly, the relationship between food size and gape requires further investigation, especially in anthropoid primates, before more can be said about its effects on the size of the buffer zone and the ontogeny of masticatory system configuration.

CHAPTER 4

# MOLAR-EMERGENCE AGE, MANDIBULAR ARCH GROWTH RATE, AND LIFE HISTORY IN PRIMATES


## Abstract

The strong relationship between age-at-M1-emergence and life history across primates provides a powerful means of reconstructing life history of fossil primates. However, the underlying process that leads to varying molar-emergence ages in primates remains elusive. Previous research has determined that the position of molar emergence is constrained by the biomechanics of mastication. To elucidate the mechanism by which variation in molar emergence schedules is achieved in primates, this study determined whether the biomechanics of the growing masticatory system constrain the timing of molar emergence by examining mandibular arch growth rates and durations. Data on mandibular arch length were collected on known-age skeletons of 5 primate species (*Homo sapiens, Pan troglodytes, Gorilla beringei, Macaca mulatta, and Papio cynocephalus*). Based on adult mandibular arch lengths and ages at molar emergence, predictions were generated for pairwise comparisons of mandibular arch length growth rates and durations for the five species. For each species, mandibular arch length growth curves were constructed and the age-at-growth-cessation was determined using segmented regression. These and the slopes of the first part of the regressions (i.e., growth rates) were compared between species. All predictions were supported by the results with the exception for the *P. troglodytes* and *G. beringei* comparison. The results suggest that molar-emergence ages are more similar between *P. troglodytes* and *G. beringei* than the current data suggest. To explore the relationship between life history

and molar-emergence age, Phylogenetic Generalized Least-Squares analysis was performed using life-history variables as predictors and mandibular arch growth rate and duration as response variables. Results indicate that life-history variables are significantly positively related to age-at-mandibular-arch-growth-cessation, but sample sizes were too small to detect a relationship with mandibular arch length growth rate. Overall, results suggest that molar emergence schedules result from the availability of space anterior to the muscle resultant, and the rate at which this space is made available. Comparisons of mandibular growth rates between species generally explain differences in the timing of molar emergence. This study provides a framework for understanding how variation in the timing of molar emergence evolves and suggests that life history is related to ages-at-molar-emergence through its influence on the duration of mandibular arch length growth.

## Introduction

A species' life history is the schedule of its allocation of energy to growth, maintenance, and reproduction and is best characterized a series of variables including gestation length, weaning age, age-at-first-reproduction, litter size, inter-birth interval, and lifespan, among others (Charnov 1993; Stearns 1992). The pace of dental development, especially the age at which the permanent first molar (M1) emerges into the oral cavity, is commonly used as a skeletal indicator of life history in fossil taxa (e.g., Kelley 1997; Kelley and Smith 2003; Nargolwalla et al. 2005; Kelley and Schwartz 2012), as age-at-M1-emergence is strongly correlated with life-history variables across primates (Smith 1989; Smith, Crummett, and Brandt 1994; Kelley and Schwartz 2010). Molar emergence should be completely integrated into the growth of the skull and part of

an integrated masticatory system (Smith 1989; Spencer and Schwartz 2008), but the exact mechanism underlying the relationship between age-at-M1-emergence and life history remains unknown. Two unanswered questions stand in the way of a more complete understanding of the timing of molar emergence in primates: (1) Why is age-at-M1-emergence so closely associated with fundamental aspects of a species' life history? and (2) What factors influence variation in age-at-M1-emergence among primates? This research attempts to answer these questions by exploring the relationships among life history, the timing of molar emergence, the biomechanical constraints on the position of molar emergence, and the rate and duration of jaw growth.

Previous research identified biomechanical constrains on the position of molar emergence in primates (Spencer and Schwartz 2008; Schwartz 2012; Singleton 2015; Chapter 2; Chapter 3). The masticatory system is configured to avoid distraction of the temporomandibular joint (TMJ) (i.e., when the mandibular condyle is pulled away from the articular eminence) during biting and chewing ( Greaves 1978; Spencer 1995, 1999). One key aspect of masticatory system configuration is the position of molars in the maxillary and mandibular arches: given the theoretical assumptions articulated in Chapter 2, the distal-most molar's position is constrained so that it is almost always anterior to the jaw adductor muscle resultant. Biting posterior to this point leads to TMJ distraction. This is the basis of the Constrained Lever Model (CLM) of chewing biomechanics (Greaves 1978, 1982; Spencer 1999). The study in Chapter 2 used the assumptions of the CLM to examine the position of molar emergence in relation to the position of the adductor muscle resultant and found that, across primates, molars emerge significantly anterior to the resultant throughout ontogeny. The analysis in Chapter 2 identified that

although molars emerge anterior to the resultant, there are intraspecific (i.e., among molar emergence categories) and interspecific differences in the position of molar emergence. Chapter 3 tested whether this intra- and interspecific variation is related to the size of the buffer zone, a safety factor that creates greater stability at the TMJs during biting. The results of the study in Chapter 3 indicated that more resistant foods, larger skulls, longer molars, and longer jaws produce a larger buffer zone, but greater canine overlap produces a smaller buffer zone. These factors account for a large portion of both ontogenetic and interspecific variation in the distance between the last molar and the resultant and suggest that the buffer zone is an important part of the mechanism acting to modulate the position of molar emergence in primates. Collectively, these studies have integrated biomechanical, comparative, and ontogenetic perspectives to the study of molar emergence in primates. This integrative approach has illuminated the mechanism that acts during ontogeny to constrain the *position* of molar emergence and can be used to further elucidate how variation in molar emergence *schedules* arises among primates. Under the assumption that the position of molar emergence is constrained by the biomechanics of the masticatory system, the research here investigates whether the rate and duration of growth of the mandibular arch determines the timing of molar emergence and, in turn, whether mandibular arch growth rate and duration are related to primate life history.

## Hypothesis and Model

This research tests the hypothesis that the timing of molar emergence is constrained to avoid TMJ distraction throughout ontogeny by determining if the rate at which space is made available in the jaw (anterior to the point at which the muscle

resultant intersects the triangle of support) and the duration of jaw growth determine the timing of molar emergence.

*Model*

Applying the CLM to molar emergence predicts that molars emerge anterior to the adductor muscle resultant. This prediction was confirmed (with some exceptions) by the study in Chapter 2, suggesting that the timing of molar emergence depends on the rate at which space is made available anterior to the resultant. All things being equal, a species with a mandibular arch[2] that grows at a faster rate should exhibit younger ages-at-molar-emergence than a species with a mandibular arch that grow at a slower rate. Species can be compared in this manner to determine if their rates of jaw growth explain differences in ages-at-molar-emergence. A complicating factor is that differences exist among species in the length of adult mandibular arches and in the duration of mandibular arch growth. Therefore, a species can grow its mandibular arch at a faster rate than another species but if its target mandibular arch length is greater, this species might attain later ages-at-molar-emergence. A model describing expectations of the relative timing of molar emergence in pairwise comparisons of a species with a shorter adult mandibular arch and one with a longer adult mandibular arch are described below and in Figure 19.

[2] The term mandibular arch here refers to the distance from the point between the two central mandibular incisors, along the buccal/labial aspect of the alveolar bone, to the resultant's intersection with the triangle of support, projected onto the occlusal plane (see Material and Methods section for details). Although this study refers to mandibular arches only, the model also applies to maxillary arches.

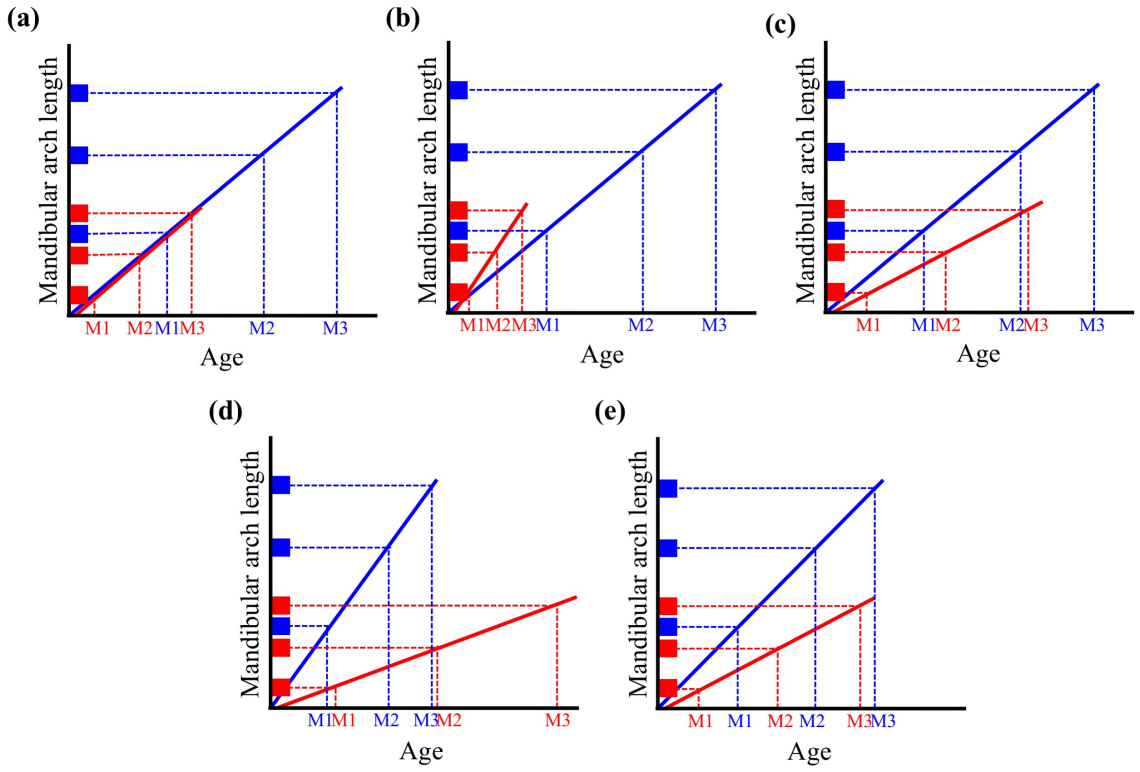


Figure 19. Schematic of mandibular arch length growth curves comparing taxa with longer and shorter adult mandibles. Boxes along y-axis indicate the mandibular arch length at which enough space has been vacated anterior to the muscle resultant for a molar to emerge. Relatively early molar emergence is attained either through a shorter mandibular arch that grows at the same (red line in a), faster (red line in b), or slower rate (red line in c), but for a shorter duration or through a longer mandibular arch that grows at a faster rate for a shorter duration (blue line in d). Relatively later molar emergence is attained either through a longer mandibular arch that grows at the same (blue line in a), faster (blue line in c), or slower rate (blue line in b), but for a longer duration or by a shorter mandibular arch that grows at a slower rate and for a longer duration (red line in d). Similar ages at molar emergence are attained through a longer mandibular arch that grows at a faster rate but for the same duration (blue line in e), through a shorter mandibular arch that grows at a slower rate and for the same duration (red line in e), or through similar mandibular arch lengths that grow at similar rates and for similar durations (not shown).

Earlier molar emergence occurs *either* in a shorter mandibular arch that grows at the same, faster, or slower rate, but for a shorter duration (Fig. 19a-c) *or* in a longer mandibular arch that grows at a faster rate and for a longer duration (Fig. 19d).

Later molar emergence occurs *either* in a longer mandibular arch that grows at the same, faster, or slower rate, and for a longer duration (Fig. 19a-c) *or* in a shorter mandible that grows at a slower rate and for a longer duration (Fig. 19d).

Similar ages at molar emergence occur in a longer mandibular arch that grows at a faster rate and for the same duration (Fig. 19e), in a shorter mandibular arch that grows at a slower rate and for the same duration (Fig. 19e), *or* in mandibular arches of similar length that grow at similar rates and for similar durations (in which case the trajectories in Fig. 19 would be identical).

An alternative way to compare species that differ in adult jaw lengths is by comparing relative jaw growth rates (i.e., the proportion of the adult value that has been reached by a given age). In this scenario, the following predictions can be made: earlier molar emergence occurs in a mandibular arch that grows at a relatively faster rate and for a shorter duration (Fig. 20); later molar emergence occurs in a mandibular arch that grows at a relatively slower rate and for a longer duration (Fig. 20); similar ages at molar emergence occur in mandibular arches that grow that grow at similar rates and for similar durations.

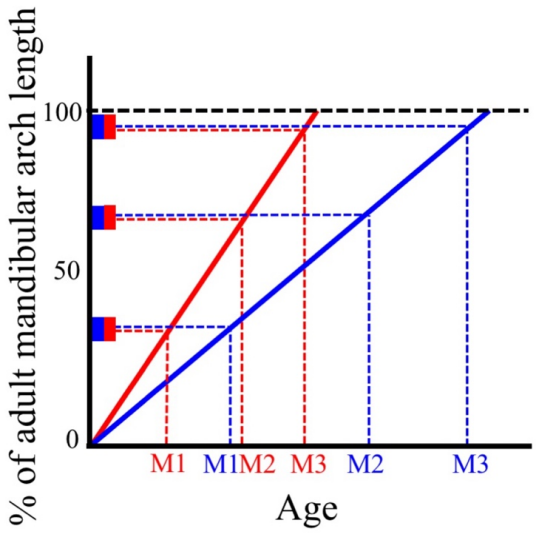


Figure 20. Schematic of mandibular arch length growth curves expressed as a percentage of adult mandibular arch length. Boxes along y-axis indicate the mandibular arch length at which enough space has been vacated anterior to the muscle resultant for a molar to emerge. Relatively early molar emergence occurs in a mandible that grows at a relatively faster rate and for a shorter duration (red line) while relatively late molar emergence occurs in a mandible that grows at a relatively slower rate and for a longer duration (blue line).

This model provides a mechanical and developmental context for explaining temporal and spatial variation in molar-emergence ages. As such, it predicts that the age at which a molar emerges results directly from the rate and duration of growth in the mandibular arch. In turn, mandibular arch growth rate and duration should be tightly integrated into the overall package of somatic and neural growth and should therefore be highly correlated to life history parameters that track overall growth and development. In addition to testing the above model, this research also investigates whether life-history variables are associated with mandibular arch growth rate and duration. Other factors that are related to life history, such as brain size, and body size, may also influence growth

schedules (Taylor 1965; Western 1979; Barrickman et al. 2008). The potential influence of these variables on mandibular arch growth is also considered.

## Material and Methods

### *Data Collection and Sample*

The landmark data collection methods follow those described in Chapter 2. In addition to the landmarks collected for that analysis (see landmarks listed in Table 1: Chapter 2), several other landmarks were collected along the labial/buccal aspect of the alveolar bone, distal to each tooth position (Table 16; Fig 21). The distances between the landmarks were summed and added to the distance between the last molar and the resultant to equal the variable *mandibular arch length* (i.e., the distance from the point between the two central mandibular incisors (infradentale) to the intersection of the resultant with the triangle of support, projected onto the occlusal plane, Fig. 22). Landmarks were obtained using a Microscribe G3X digitizer (Immersion Corp., San Jose, CA). Two variables that were measured in chapter 2 were also used here. Chapter 2 used two methods to determine the position at which the muscle resultant crosses the triangle of support, which was then projected onto the occlusal plane and the distance between this point and the last molar was measured. The first method involved averaging the positions of the three adductor muscles' lines of actions. The resulting distance was called $Resultant_{Mean}$-*Molar.* The second method used the most anterior muscle line of action to represent the position of the resultant. The variable produced by this method was called $Resultant_{Max}$-*Molar* (see chapter 2 for details). Both of these variables were used to represent the distance between the resultant and the last molar when calculating

mandibular arch length, yielding the variables *mandibular arch length*$_{mean}$ and *mandibular arch length*$_{max}$, respectively (together referred to as *mandibular arch length*).

Table 16. List of landmarks collected for study.

| Landmark # | Landmark description |
|---|---|
| 1 | Infradentale (midline point at apex of septum between central mandibular incisors) |
| 2 | Left distal to $I_1/i_1$ alveolar border |
| 3 | Left distal to $I_2/i_2$ alveolar border |
| 4 | Left distal to C/c alveolar border |
| 5 | Left distal to $P_3/dp_3$ alveolar border |
| 6 | Left distal to $P_4/dp_4$ alveolar border |
| 7 | Left distal to $M_1$ alveolar border |
| 8 | Left distal to $M_2$ alveolar border |
| 9 | Left distal to $M_3$ alveolar border |

Data were collected from cross-sectional ontogenetic samples of primate skulls representing 5 primate species (*Homo sapiens, Gorilla beringei, Pan troglodytes, Papio cynocephalus, and Macaca mulatta*; see SM 4 for sample specimen list**)**. The samples consisted of individuals with known ages at death. These non-human skeletal collections derive from long-term primatological field sites where individuals are observed on a regular basis and deceased individuals are skeletonized and curated for scientific study.

The modern human skeletal sample (n=94; SM 4A) was a combination of two skeletal collection. The majority of subadults were from the Atkinson Collection, a collection of human skulls from Mexico, India, Europe, Peru, Asia, and Australia/New Zealand amassed in the 1930s and housed at the Arthur A. Dugoni School of Dentistry at the University of the Pacific. These skulls were aged based on dental radiographs using standard dental ageing methods (Richards 2007). The Robert J. Terry Anatomical Skeletal Collection of modern human skeletons was also used in this study. This cadaveric collection is housed at the National Museum of Natural History and consists of

known-age individuals. Individuals with craniofacial malformations, missing teeth with bone resorption, or tooth agenesis were excluded for the purposes of this study.

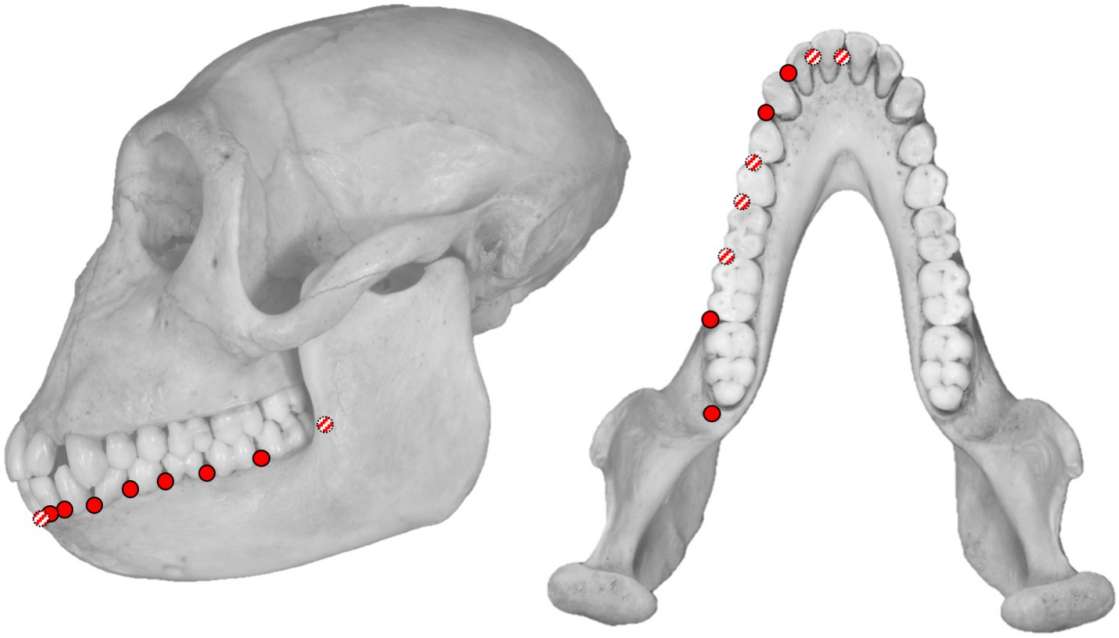

Figure 21. Landmarks collected for the purposes of this study. Landmarks were taken along the labial/buccal aspect of the alveolar bone, distal to each tooth position. Red dots indicate landmarks on visible bone surface whereas dashed red and white dots indicate landmarks that are obstructed in the specific view. Landmark definitions can be found in table 16.

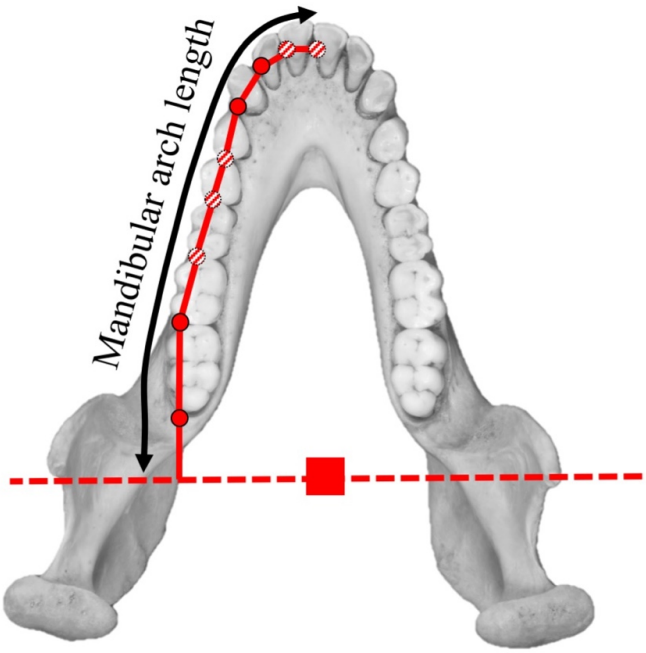


Figure 22. The variable *mandibular arch length* was calculated by summing the distances between landmarks. Landmarks as in Figure 21.

The mountain gorilla (*G. beringei*) sample (n=24; SM 4B) is a cross-sectional ontogenetic series of known-age wild mountain gorillas recovered from Volcanoes National Park, Rwanda. These mountain gorilla skeletons are part of a growing collection curated by the Mountain Gorilla Skeletal Project, in partnership with the Rwanda Development Board's Department of Tourism and Conservation, Dian Fossey Gorilla Fund International, Mountain Gorilla Veterinary Project, and other Rwandan and U.S. institutions (McFarlin et al. 2009, 2013). Age determination and attribution for the skeletons is described in further detail in McFarlin et al. (2013) and Galbany et al. (2016).

The chimpanzee sample (n=37; SM 4C) consisted of two skeletal populations. The first is of Taï chimpanzees (*P. troglodytes verus*) housed at the Max Planck Institute for Evolutionary Anthropology in Leipzig, Germany. Behavioral data have been collected

continuously on this community since 1989 and skeletal remains have been recovered since 1995 (Smith et al. 2010a). The second, smaller addition to the chimpanzee sample was that of western chimpanzees (*P. t. schweinfurthii*) from Gombe Stream National Park. Remains of deceased individuals have been collected, skeletonized, and curated at Gombe since the late 1970s (Jurmain 1997). While most of the skeletal collection from Gombe remains in Tanzania, some of the collection, including the individuals used in this study, is currently housed at the University of Minnesota, in the Evolutionary Anthropology Laboratory. Despite belonging to separate subspecies, the data from these two populations were combined to yield one chimpanzee sample in order to boost sample size.

The skeletal sample of yellow baboon (*P. cynocephalus*) individuals (n=18; SM 4D) is from a newly-established collection by the Amboseli Baboon Research Project (ABRP). The skeletal remains are from Amboseli National Park, Kenya, and represent individuals of known life history who were monitored in life by the ABRP (S. McFarlin, pers. comm.). The collection is curated at the National Museums of Kenya.

The final skeletal collection examined in this study was of rhesus macaques (*M. mulatta*) from the Cayo Santiago colony (n=104; SM 4E), established in 1938 and now part of the Caribbean Primate Research Center. Individuals here are provisioned and monitored on a daily basis. Deceased individuals are macerated and included in an extensive skeletal collection of known-age individuals. Details of the skeletal collection, including how it is amassed and curated can be found in Rothschild, Hong, and Turnquist (1999).

*Specific Predictions*

Based on the model described in the "Hypothesis and Model" section, specific predictions can be made for how mandibular growth rates and durations map onto molar-emergence ages. Table 17 lists reported molar-emergence ages in the literature for the species examined in this study. Based on these data and adult mandibular arch lengths data (Table 18; Table 22A), predictions were made for pairwise comparisons of mandibular arch length growth rate and growth duration (Table 22B).

Table 17. Molar-emergence ages reported in the literature for the species included in this study.

| Species | M1 emergence age (yrs) | M2 emergence age (yrs) | M3 emergence age (yrs) | Notes | Source |
|---|---|---|---|---|---|
| *P. troglodytes* | 2.7-3.8 | 5.6-7.3 | 9.0-13.1 | Mandibular gingival emergence for Kanyawara chimps | Machanda et al. 2015 |
| | | | 9.8-13.6 | Maxillary gingival emergence for Kanyawara chimps | Machanda et al. 2015 |
| | >3.8 | 6.4 | | Maxillary gingival emergence for Taï chimps | Smith et al. 2010 |
| *G. beringei* | 2.45- 3.16 | | Max 10.69 | Mandibular gingival emergence for Virunga gorillas | Vakiener et al. 2016 |
| *H. sapiens* | 6.15-6.4 | 10.52-12 | 19.8-20.5 | Gingival emergence mean ranges for males and females, and maxillary and mandibular molars | Smith et al. 1994 |
| *P. cynocephalus* | 1.58-2 | 3.75-3.92 | 6.17-7.08 | Gingival emergence mean ranges for males and females, and maxillary and mandibular molars | Smith et al. 1994 |
| *M. mulatta* | 1.32-1.49 | 3.15-3.36 | 5.4-6.43 | Gingival emergence mean ranges for males and females, and maxillary and mandibular molars | Smith et al. 1994 |

Table 18. Summary statistics for adult male and female *mandibular arch length*$_{mean}$ and *mandibular arch length*$_{max}$ values, and *t*-tests comparing sexes.

**A.** *Mandibular arch length*$_{mean}$

| Species | Adult male | | | Adult female | | | | | Adult average |
|---|---|---|---|---|---|---|---|---|---|
| | n | Mean (mm) | SD | n | Mean (mm) | SD | *t* | *p*-value | Mean (mm) |
| *G. beringei* | 23 | 154.68 | 9.83 | 34 | 126.85 | 10.44 | 10.23 | **0.00** | 140.77 |
| *H. sapiens* | 14 | 81.71 | 4.95 | 12 | 77.31 | 4.81 | 2.30 | 0.05 | 79.51 |
| *P. troglodytes* | 29 | 102.40 | 5.05 | 38 | 97.78 | 3.80 | 4.12 | **0.00** | 100.09 |
| *M. mulatta* | 28 | 77.58 | 4.76 | 30 | 68.26 | 4.12 | 7.95 | **0.00** | 72.92 |
| *P. cynocephalus* | 17 | 118.99 | 14.20 | 17 | 91.42 | 8.30 | 6.91 | **0.00** | 105.21 |

**B.** *Mandibular arch length*$_{max}$

| Species | Adult male | | | Adult female | | | | | Adult average |
|---|---|---|---|---|---|---|---|---|---|
| | n | Mean (mm) | SD | n | Mean (mm) | SD | *t* | *p*-value | Mean (mm) |
| *G. beringei* | 23 | 128.92 | 10.67 | 34 | 106.91 | 12.39 | 7.15 | **0.00** | 117.92 |
| *H. sapiens* | 14 | 71.82 | 7.62 | 12 | 69.39 | 5.53 | 0.94 | 0.36 | 70.61 |
| *P. troglodytes* | 29 | 93.38 | 5.51 | 38 | 89.27 | 3.63 | 3.48 | **0.00** | 91.33 |
| *M. mulatta* | 28 | 70.35 | 4.28 | 30 | 61.45 | 3.72 | 8.43 | **0.00** | 65.90 |
| *P. cynocephalus* | 17 | 110.10 | 14.22 | 17 | 82.74 | 7.27 | 7.06 | **0.00** | 96.42 |

Adult mandibular arch length data were calculated using the larger species samples, described in Chapter 2.

Significant results ($p \leq 0.05$) listen in bold.

Table 19. Predictions of mandibular arch growth rate and duration for the species in this study based on the model.

**A.** Comparisons of mandibular arch lengths and molar-emergence ages between species

| Species comparison | Mandibular arch length* | Molar emergence ages** |
|---|---|---|
| *G. beringei* vs. *H. sapiens* | > | < |
| *G. beringei* vs. *P. troglodytes* | > | < |
| *H. sapiens* vs. *P. troglodytes* | < | > |
| *H. sapiens* vs. *M. mulatta* | > | > |
| *P. troglodytes* vs. *M. mulatta* | > | > |
| *G. beringei* vs. *M. mulatta* | > | > |
| *P. cynocephalus* vs. *M. mulatta* | > | > |
| *P. cynocephalus* vs. *G. beringei* | < | < |
| *P. cynocephalus* vs. *P. troglodytes* | > | < |
| *P. cynocephalus* vs. *H. sapiens* | > | < |

**B.** Predictions based on model

| Species comparison | Absolute mandibular arch length | | Relative mandibular arch length | |
|---|---|---|---|---|
| | Growth Rate Prediction | Growth Duration Prediction | Growth Rate Prediction | Growth Duration Prediction |
| *G. beringei* vs. *H. sapiens* | > | < | > | < |
| *G. beringei* vs. *P. troglodytes* | <,=,> | < | > | < |
| *H. sapiens* vs. *P. troglodytes* | < | > | < | > |
| *H. sapiens* vs. *M. mulatta* | <,=,> | > | < | > |
| *P. troglodytes* vs. *M. mulatta* | <,=,> | > | < | > |
| *G. beringei* vs. *M. mulatta* | <,=,> | > | < | > |
| *P. cynocephalus* vs. *M. mulatta* | <,=,> | > | < | > |
| *P. cynocephalus* vs. *G. beringei* | <,=,> | < | > | < |
| *P. cynocephalus* vs. *P. troglodytes* | <,=,> | < | > | < |
| *P. cynocephalus* vs. *H. sapiens* | > | < | > | < |

*Comparisons based on adult average data in Table 17.

**Comparisons based on data in Table 18.

*Analytical Methods*

Two-sided *t*-tests were used to determine whether there are significant differences between adult male and female mandibular arch lengths. These tests were performed on a larger sample of adult individuals than the remainder of the analyses, regardless of whether age information was available or not (Table 18). It was determined that in all species except *H. sapiens*, there are significant sex differences in *mandibular arch length* (Table 18). Despite this, data for males and females were combined in the analyses below because data on sex attribution were not available for some of the subadult specimens and separating the sexes resulted in very small sample sizes for most of the species.

To determine whether the rate at which space is made available, anterior to the point at which the muscle resultant intersects the triangle of support, along with the duration of growth, determine the timing of molar emergence, pairwise comparisons of *mandibular arch length* growth trajectories were performed between taxa that differ in adult *mandibular arch length* and/or molar emergence timing. *Mandibular arch length growth rate* was determined using segmented (i.e., piecewise ) regressions, which described species-specific *mandibular arch length* growth curves (Neter, Wasserman, and Kutner 1985), with age as the independent variable and *mandibular arch length* (i.e., *mandibular arch length*$_{mean}$ and *mandibular arch length*$_{max}$) as the dependent variable. Segmented regressions were fit to the data using the *segmented* package (Muggeo 2008) in R (version 3.3.1). This package uses maximum likelihood to iteratively fit curves to the data and find breakpoints (Muggeo 2008). Growth data should be defined by two curves separated by one breakpoint; the first curve representing the growth phase and its positive slope representing growth rate, the breakpoint representing the age-at-growth-

cessation, and the second curve and its slope of zero representing the asymptotic phase (i.e., the adult phase). The segmented regression fit to the data was compared to an Ordinary Least-Squares (OLS) fit using Akaike's Information Criterion (AIC). If a segmented regression was a better fit to the data then it should possess lower AIC scores. Segmented regression is widely used to study growth and has been used to study growth rate and growth cessation in body mass in both captive and wild primates (Leigh 1994; Altmann and Alberts 2004) and the ontogeny of primate brain mass (McFarlin et al. 2013). Identified breakpoints were extracted as the variables *mandibular arch length growth cessation*$_{mean}$ and *mandibular arch length growth cessation*$_{max}$ (together referred to as *mandibular arch length growth cessation*) and were used to represent the endpoint of growth, and thus growth duration, for each species. After breakpoints were identified, data points from the growth phase of the curve were extracted. These data were then used in an OLS regression with age as the predictor variable and mandibular arch length as the response variable, and the resulting slopes (extracted as the variables *mandibular arch length growth rate*$_{mean}$ and *mandibular arch length growth rate*$_{max}$, together *mandibular arch length growth rate*) were compared between sets of taxa using an analysis of covariance (ANCOVA) to determine if the interaction between species and age is significantly different from zero; in other words, if the slopes of the two species are significantly different from each other. This was done to test the first set of predictions (Fig. 19 and Table 19B's "Absolute mandibular arch length: Growth rate predictions").

OLS regression was also performed with *relative mandibular arch length* as the response variable and age as the predictor variable. *Relative mandibular arch length*$_{mean}$ and *relative mandibular arch length*$_{max}$ (together, *relative mandibular arch length*) were

calculated for each specimen as the ratio of that specimen's *mandibular arch length* to the adult average for its species (adult means listed in Table 18). The resulting slopes were extracted as variables *relative mandibular arch length growth rate*$_{mean}$ and *relative mandibular arch length growth rate*$_{max}$ (together, *relative mandibular arch length growth rate*) and compared using ANCOVA to test the second set of predictions (Fig. 20 and Table 19B's "Relative mandibular arch length: Growth rate predictions").

The final set of analyses was aimed at determining if brain size, body size, and life-history variables have significant effects on *mandibular arch growth rate* and *mandibular arch growth cessation*, and thus on molar-emergence age in primates. *Brain size*, *body size*, and life history data (i.e., *age-at-first-reproduction* and *gestation length*) were collected from the literature (see Table 20). Wherever possible, the data collected were from the same populations as the skeletal collections included in this study (Table 20). Because this study considered *mandibular arch length growth rate* and *mandibular arch length growth cessation* for only five species, the number of predictor variables had to be reduced. Dimensionality reduction was performed through a phylogenetic Principal Components Analysis (PCA) (Revell 2009), implemented using the *phytools* package (Revell 2012) for R (version 3.3.1). Resulting principal components that explained at least 90% of the variance in the data were then used as predictor variables in several Phylogenetic Generalized Least-Squares (PGLS) analyses. Separate PGLS analyses were ran with (i) *mandibular arch length growth rate*$_{mean}$, (ii) *relative mandibular arch length growth rate*$_{mean}$, (iii) *mandibular arch length growth rate*$_{max}$, (iv) *relative mandibular arch length growth rate*$_{max}$, (v) *mandibular arch length growth cessation*$_{mean}$, and (vi) *mandibular arch length growth cessation*$_{max}$ as response variables and the principal

components as predictor variables. A phylogenetic tree for the analysis was downloaded from 10K Trees (Arnold, Matthews, and Nunn 2010). Data were $\log_{10}$-transformed if they did not meet the assumption of normality.

Table 20. Life-history data collected from the literature for the species included in this study.

| Species | BM (kg) | Source | BW (g) | Source | AFR (yrs) | Source | GL (days) | Source |
|---|---|---|---|---|---|---|---|---|
| *Gorilla beringei* | 95 | 1 | 457.3 | 1 | 9.5[ƒ] ** | 4 | 258[ƒ] | 2 |
| *Homo sapiens*[¶] | 54.4 | 1 | 1228 | 1 | 14.5 | 1 | 537 | 1 |
| *Pan troglodytes* | 31.3[§] | 2 | 380 | 1 | 13.6* | 5 | 225[§] | 2 |
| *Macaca mulatta* | 9.6[†] | 3 | 84.7 | 1 | 4.27[†] | 6 | 164.5 | 1 |
| *Papio cynocephalus* | 12.8[‡] | 2 | 164 | 1 | 5.82[‡] | 7 | 178[‡] | 2 |

Body mass (BM), brain weight (BW), ag at first reproduction (AFR), gestation length (GL), and inter-birth interval (IBI).

1: Kappeler and Pereira, (2003); 2: Bronikowski et al., (2011); 3: Turnquist and Kessler (1989); 4: Alberts et al., (2013); 5: Thompson (2013); 6: Blomquist (2009); 7: Charpentier et al., (2008).

*Data averaged for Gombe and Taï chimpanzees.

** AFR datum for mountain gorillas is the midpoint of the range provided in citation (9-10 yrs.)

*ƒ* Data for Karisoke mountain gorillas.

§ Data for Gombe chimpanzees.

† Data for Cayo Santiago rhesus macaques.

‡ Data for Amboseli baboons.

¶ Data for humans are means from several populations, as reported in 1.

## Results

### *Segmented Regression*

Segmented regression models all identified one breakpoint in each model, separating each mandibular arch length curve into a growth component and an adult component. The estimated breakpoint (i.e., *mandibular arch length growth cessation*$_{mean}$ and *mandibular arch length growth cessation*$_{max}$) values for each species are listed in Table 21 and are illustrated in Figures 23-27. With the exclusion of the *Papio cynocephalus* models (Table 21, Fig. 27), all breakpoint regression models had AIC values that were lower for the segmented regression models than in OLS regression models by at least a value of two, indicating that the breakpoint models fit the data better than OLS models (Table 21). In the segmented models, a large amount of variation in *mandibular arch length*$_{mean}$ was explained by *age* ($R^2$=0.58-0.90; Table 21A). Similarly, a large amount of variation in *mandibular arch length*$_{max}$ was explained by *age* ($R^2$=0.48-0.89; Table 21B).

### *Mandibular Arch Length Growth Rate*

Results of OLS regressions using growth data (i.e., individuals that were younger than the breakpoints identified in the above analysis) indicate that in all but the *P. cynocephalus* model slopes for *mandibular arch length*$_{mean}$ were positive (Table 22A). The 95% slope confidence intervals did not include zero, and the slopes were significantly different from zero (Table22A). In these significant models, *age* explained a large portion of the variation in *mandibular arch length*$_{mean}$ ($R^2$=0.75-0.89; Table 22A). Similarly, in all but the *P. cynocephalus* model, slopes for *relative mandibular arch*

*length*$_{mean}$ were positive, the 95% slope confidence intervals did not include zero, and the slopes were significantly different from zero. In these significant models, *age* explained a large portion of the variation in *relative mandibular arch length*$_{mean}$ ($R^2$=0.75-0.89; Table 22B). Slopes from the above analyses were extracted for future analysis and renamed as: *mandibular arch length growth rate*$_{mean}$ and *relative mandibular arch length growth rate*$_{mean}$.

Table 21. Segmented regression results.

**A**. *Mandibular arch length*$_{mean}$

| Species | $R^2$ | Breakpoint | St. Err | AIC (Breakpoint model) | AIC (OLS model) |
|---|---|---|---|---|---|
| *G. beringei* | 0.76 | 18.47 | 4.21 | 202.82 | 211.06 |
| *H. sapiens* | 0.75 | 21.98 | 1.04 | 553.15 | 586.87 |
| *P. troglodytes* | 0.88 | 12.54 | 0.92 | 231.19 | 277.66 |
| *M. mulatta* | 0.90 | 6.74 | 0.30 | 597.48 | 708.95 |
| *P. cynocephalus* | 0.58 | 7.48 | 6.05 | 161.22 | 161.35 |

**B**. *Mandibular arch length*$_{max}$

| Species | $R^2$ | Breakpoint | St. Err | AIC (Breakpoint model) | AIC (OLS model) |
|---|---|---|---|---|---|
| *G. beringei* | 0.77 | 18.58 | 3.58 | 194.11 | 201.39 |
| *H. sapiens* | 0.48 | 22.72 | 1.60 | 600.02 | 614.96 |
| *P. troglodytes* | 0.87 | 12.00 | 0.93 | 224.92 | 267.65 |
| *M. mulatta* | 0.89 | 6.75 | 0.30 | 585.28 | 697.40 |
| *P. cynocephalus* | 0.54 | 7.71 | 2.45 | 161.50 | 160.48 |

Breakpoint = *mandibular arch length growth cessation*

Slopes for *mandibular arch length*$_{max}$ were positive, the 95% slope confidence intervals did not include zero, and the slopes were significantly different from zero in all species (Table 22C). *Age* explained a large portion of the variation in *mandibular arch length*$_{max}$ ($R^2$=0.75-0.89; Table 22C). Similarly, slopes for *relative mandibular arch length*$_{max}$ were positive, the 95% slope confidence intervals did not include zero, and the

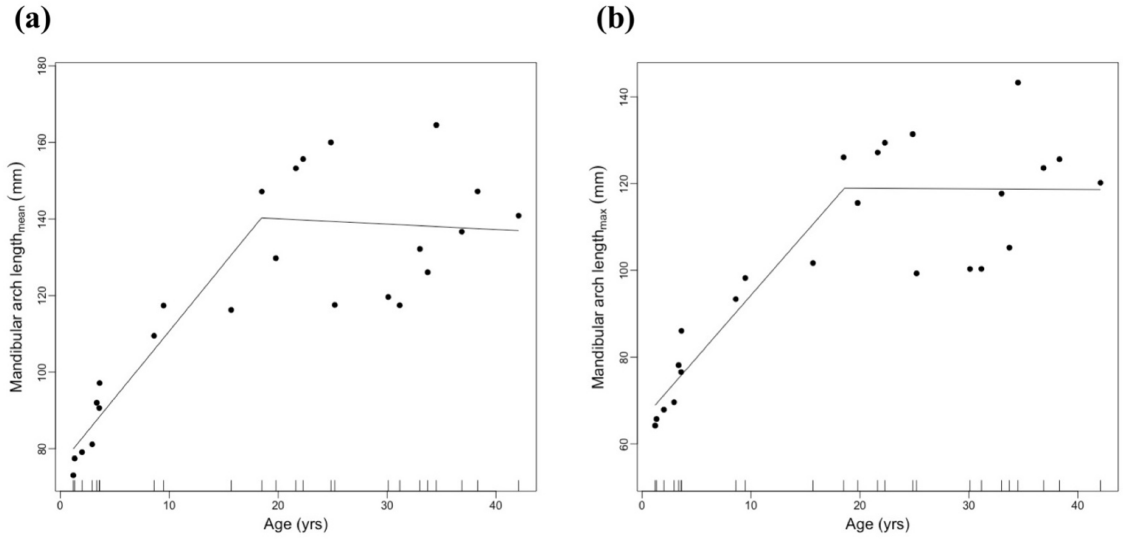


Figure 23. *Gorilla beringei* growth of *mandibular arch length*: *mandibular arch length*$_{mean}$ (a) and *mandibular arch length*$_{max}$ (b) plotted with the results of breakpoint analyses.

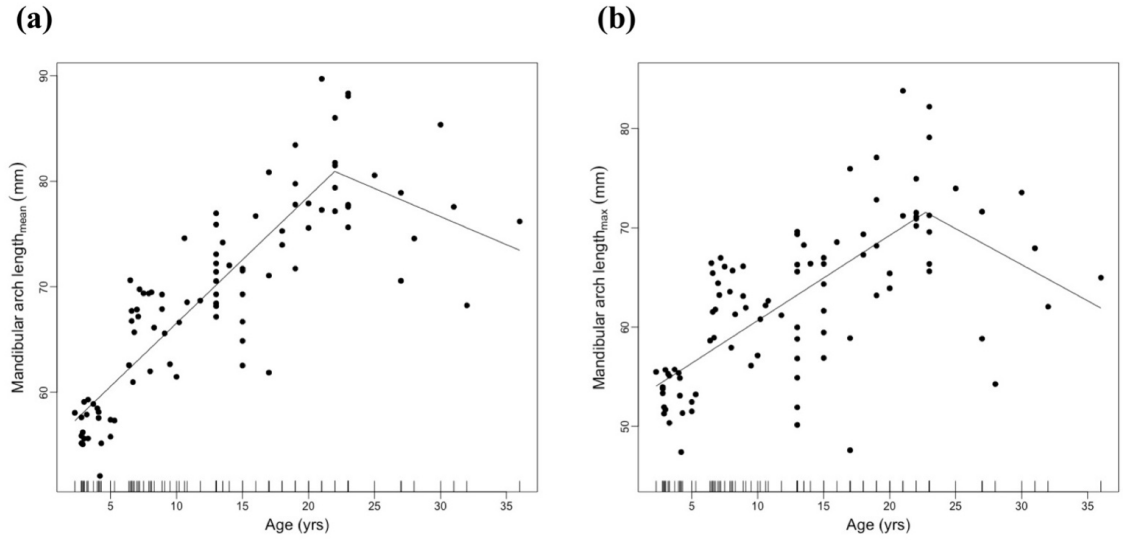


Figure 24. *Homo sapiens* growth of *mandibular arch length*: *mandibular arch length*$_{mean}$ (a) and *mandibular arch length*$_{max}$ (b) plotted with the results of breakpoint analyses.

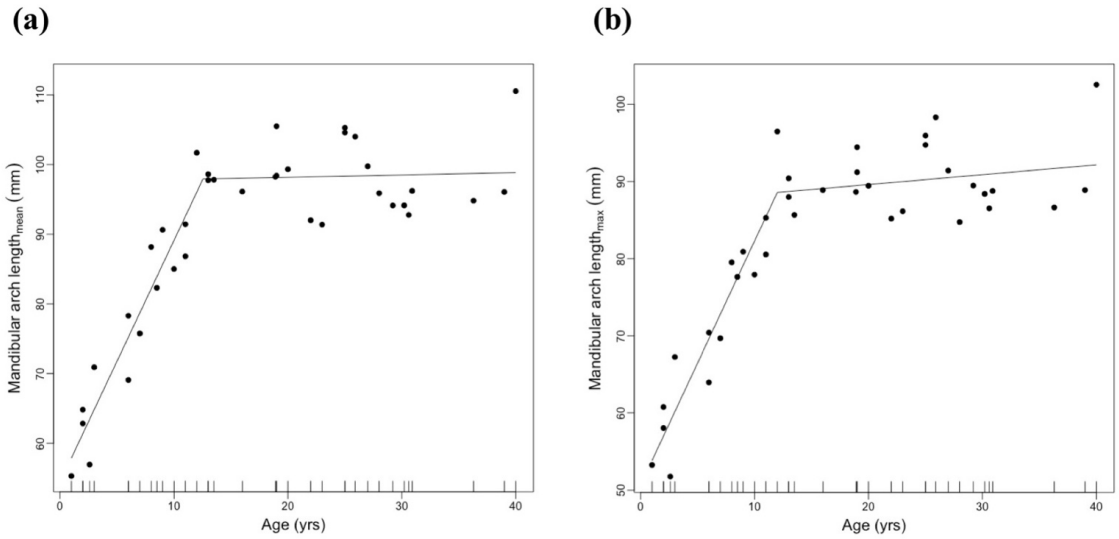


Figure 25. *Pan troglodytes* growth of *mandibular arch length*: *mandibular arch length*$_{mean}$ (a) and *mandibular arch length*$_{max}$ (b) plotted with the results of breakpoint analyses.

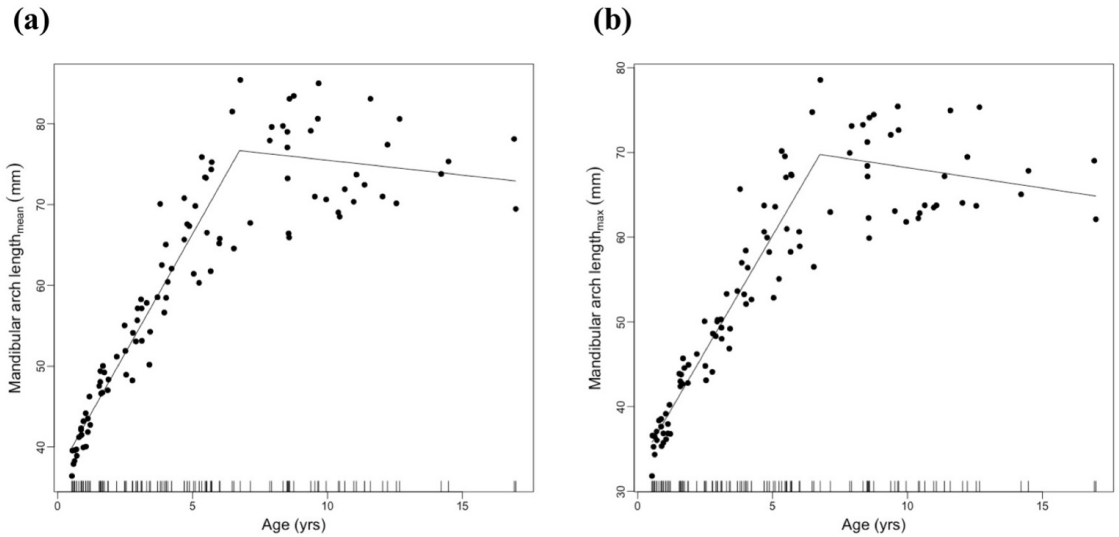


Figure 26. *Macaca mulatta* growth of *mandibular arch length*: *mandibular arch length*$_{mean}$ (a) and *mandibular arch length*$_{max}$ (b) plotted with the results of breakpoint analyses.

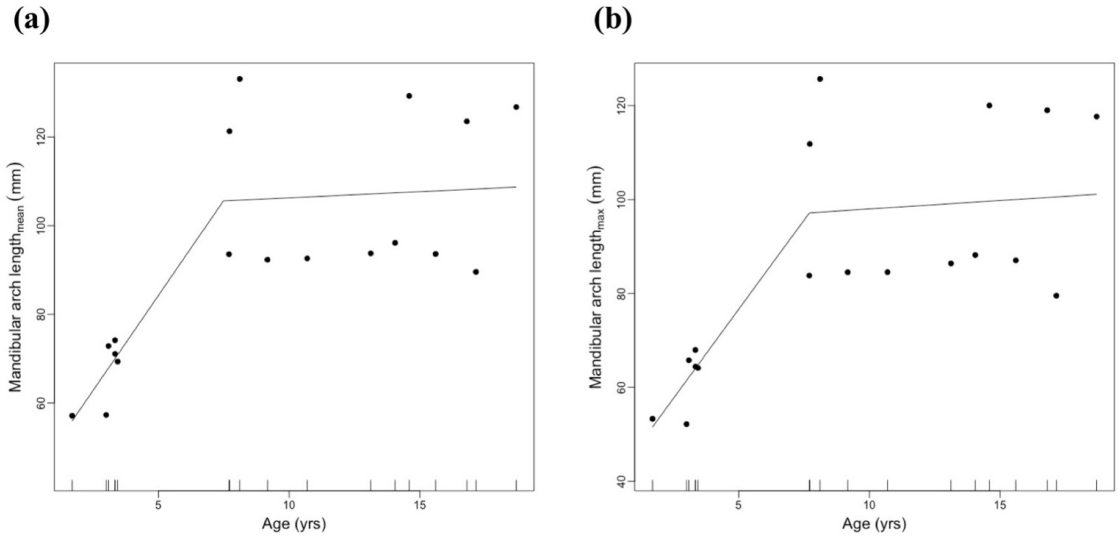


Figure 27. *Papio cynocephalus* growth of *mandibular arch length*: *mandibular arch length*$_{mean}$ (a) and *mandibular arch length*$_{max}$ (b) plotted with the results of breakpoint analyses.

slopes were significantly different from zero in all species (Table 22D). *Age* explained a large portion of the variation in *relative mandibular arch length*$_{max}$ ($R^2$=0.75-0.89; Table 22D). Slopes from the above analyses were extracted for future analysis and renamed as variables: *mandibular arch length growth rate*$_{max}$ and *relative mandibular arch length growth rate*$_{max}$.

Table 22. OLS regression results.

**A**. *Mandibular arch length*$_{mean}$

| Species | Slope | 95 % CI slope (lower bound) | 95 % CI slope (upper bound) | $R^2$ | *p*-value |
|---|---|---|---|---|---|
| *G. beringei* | 3.555 | 2.635 | 4.475 | 0.88 | **<0.000** |
| *H. sapiens* | 1.203 | 1.048 | 1.358 | 0.75 | **<0.000** |
| *P. troglodytes* | 3.470 | 2.722 | 4.218 | 0.88 | **<0.000** |
| *M. mulatta* | 5.916 | 5.407 | 6.424 | 0.89 | **<0.000** |
| *P. cynocephalus* | 8.592 | -2.807 | 19.991 | 0.40 | 0.105 |

**B**. *Relative mandibular arch length*$_{mean}$

| Species | Slope | 95 % CI slope (lower bound) | 95 % CI slope (upper bound) | $R^2$ | *p*-value |
|---|---|---|---|---|---|
| *G. beringei* | 0.025 | 0.019 | 0.032 | 0.88 | **<0.000** |
| *H. sapiens* | 0.015 | 0.013 | 0.017 | 0.75 | **<0.000** |
| *P. troglodytes* | 0.035 | 0.027 | 0.042 | 0.88 | **<0.000** |
| *M. mulatta* | 0.081 | 0.074 | 0.088 | 0.89 | **<0.000** |
| *P. cynocephalus* | 0.082 | -0.027 | 0.190 | 0.40 | 0.105 |

**C**. *Mandibular arch length*$_{max}$

| Species | Slope | 95 % CI slope (lower bound) | 95 % CI slope (upper bound) | $R^2$ | *p*-value |
|---|---|---|---|---|---|
| *G. beringei* | 3.051 | 2.315 | 3.787 | 0.90 | **<0.000** |
| *H. sapiens* | 0.858 | 0.659 | 1.057 | 0.48 | **<0.000** |
| *P. troglodytes* | 3.163 | 2.443 | 3.883 | 0.86 | **<0.000** |
| *M. mulatta* | 5.463 | 4.963 | 5.964 | 0.87 | **<0.000** |
| *P. cynocephalus* | 5.022 | 2.175 | 7.869 | 0.77 | **0.006** |

**D**. *Relative mandibular arch length*$_{max}$

| Species | Slope | 95 % CI slope (lower bound) | 95 % CI slope (upper bound) | $R^2$ | *p*-value |
|---|---|---|---|---|---|
| *G. beringei* | 0.026 | 0.020 | 0.032 | 0.90 | **<0.000** |
| *H. sapiens* | 0.012 | 0.009 | 0.015 | 0.48 | **<0.000** |
| *P. troglodytes* | 0.035 | 0.027 | 0.043 | 0.86 | **<0.000** |
| *M. mulatta* | 0.083 | 0.075 | 0.090 | 0.87 | **<0.000** |
| *P. cynocephalus* | 0.052 | 0.023 | 0.082 | 0.77 | **0.006** |

Significant results ($p \leq 0.05$) listen in bold.

*Growth Rate Comparisons*

ANCOVA results indicated that in both the *mandibular arch length growth rate$_{mean}$* and *relative mandibular arch length growth rate$_{mean}$* models, *G. beringei*, *P. troglodytes*, and *M. mulatta* had significantly steeper slopes (i.e., growth rates) than *H. sapiens* (Table 23A, B; Figs. 28, 29). The *mandibular arch length growth rate$_{mean}$* for *G. beringei* was not significantly different from that of the *P. troglodytes*, but the *relative mandibular arch length growth rate$_{mean}$* for *G. beringei* was significantly steeper, although just barely, than that for *P. troglodytes* (Table 23A, B; Figs. 28, 29). *Gorilla beringei* and *P. troglodytes* had significantly greater values for *mandibular arch length growth rate$_{mean}$* and *relative mandibular arch length growth rate$_{mean}$* than *M. mulatta* (Table 23A, B; Figs. 28, 29). *Mandibular arch length growth rate$_{mean}$* and *relative mandibular arch length growth rate$_{mean}$* values for *P. cynocephalus* were not compared to other species because the models were not significant (see above).

*Gorilla beringei*, *P. troglodytes*, *M. mulatta* and *P. cynocephalus* had significantly greater *mandibular arch length growth rate$_{max}$* and *relative mandibular arch length growth rate$_{max}$* values than *H. sapiens* (Table 23C, D; Figs. 30, 31). Neither the *mandibular arch length growth rate$_{max}$* nor the *relative mandibular arch length growth rate$_{max}$* values for *G. beringei* were significantly different from those for *P. troglodytes* (Table 23C, D; Figs. 30, 31). *Macaca mulatta* had a significantly greater *mandibular arch length growth rate$_{max}$* value than *G. beringei* and *P. troglodytes* while in *relative mandibular arch length growth rate$_{max}$*, *M. mulatta* had greater value than *G. beringei*, *P. troglodytes*, and *P. cynocephalus* (Table 23C, D; Figs. 30, 31).

Table 23. ANCOVA results comparing slopes between species.

**A.** Mandibular arch length$_{mean}$

| **Species comparison** | ***F*-value** | ***p*-value** |
|---|---|---|
| *G. beringei* vs. *H. sapiens* | 79.680 | **0.000** |
| *G. beringei* vs. *P. troglodytes* | 0.024 | 0.879 |
| *H. sapiens* vs. *P. troglodytes* | 50.390 | **0.000** |
| *H. sapiens* vs. *M. mulatta* | 285.760 | **0.000** |
| *P. troglodytes* vs. *M. mulatta* | 38.780 | **0.000** |
| *G. beringei* vs. *M. mulatta* | 38.670 | **0.000** |

**B**. Relative mandibular arch length$_{mean}$

| **Species comparison** | ***F*-value** | ***p*-value** |
|---|---|---|
| *G. beringei* vs. *H. sapiens* | 11.490 | **0.001** |
| *G. beringei* vs. *P. troglodytes* | 4.304 | **0.050** |
| *H. sapiens* vs. *P. troglodytes* | 25.338 | **0.000** |
| *H. sapiens* vs. *M. mulatta* | 328.510 | **0.000** |
| *P. troglodytes* vs. *M. mulatta* | 83.610 | **0.000** |
| *G. beringei* vs. *M. mulatta* | 154.700 | **0.000** |

**C**. Mandibular arch length$_{max}$

| **Species comparison** | ***F*-value** | ***p*-value** |
|---|---|---|
| *G. beringei* vs. *H. sapiens* | 50.540 | **0.000** |
| *G. beringei* vs. *P. troglodytes* | 0.056 | 0.815 |
| *H. sapiens* vs. *P. troglodytes* | 34.250 | **0.000** |
| *H. sapiens* vs. *M. mulatta* | 199.736 | **0.000** |
| *P. troglodytes* vs. *M. mulatta* | 35.840 | **0.000** |
| *G. beringei* vs. *M. mulatta* | 47.340 | 0.000 |
| *P. cynocephalus* vs. *M. mulatta* | 0.250 | 0.619 |
| *P. cynocephalus* vs. *G. beringei* | 2.317 | 0.150 |
| *P. cynocephalus* vs. *P. troglodytes* | 2.896 | 0.106 |
| *P. cynocephalus* vs. *H. sapiens* | 12.490 | **0.001** |

**D**. Relative mandibular arch length$_{max}$

| **Species comparison** | ***F*-value** | ***p*-value** |
|---|---|---|
| *G. beringei* vs. *H. sapiens* | 10.760 | **0.001** |
| *G. beringei* vs. *P. troglodytes* | 3.658 | 0.069 |
| *H. sapiens* vs. *P. troglodytes* | 16.989 | **0.000** |
| *H. sapiens* vs. *M. mulatta* | 225.221 | **0.000** |
| *P. troglodytes* vs. *M. mulatta* | 76.880 | **0.000** |
| *G. beringei* vs. *M. mulatta* | 140.150 | **0.000** |
| *P. cynocephalus* vs. *M. mulatta* | 5.652 | **0.020** |
| *P. cynocephalus* vs. *G. beringei* | 5.010 | **0.042** |
| *P. cynocephalus* vs. *P. troglodytes* | 2.201 | 0.155 |
| *P. cynocephalus* vs. *H. sapiens* | 5.874 | **0.018** |

Significant results ($p \leq 0.05$) listen in bold.

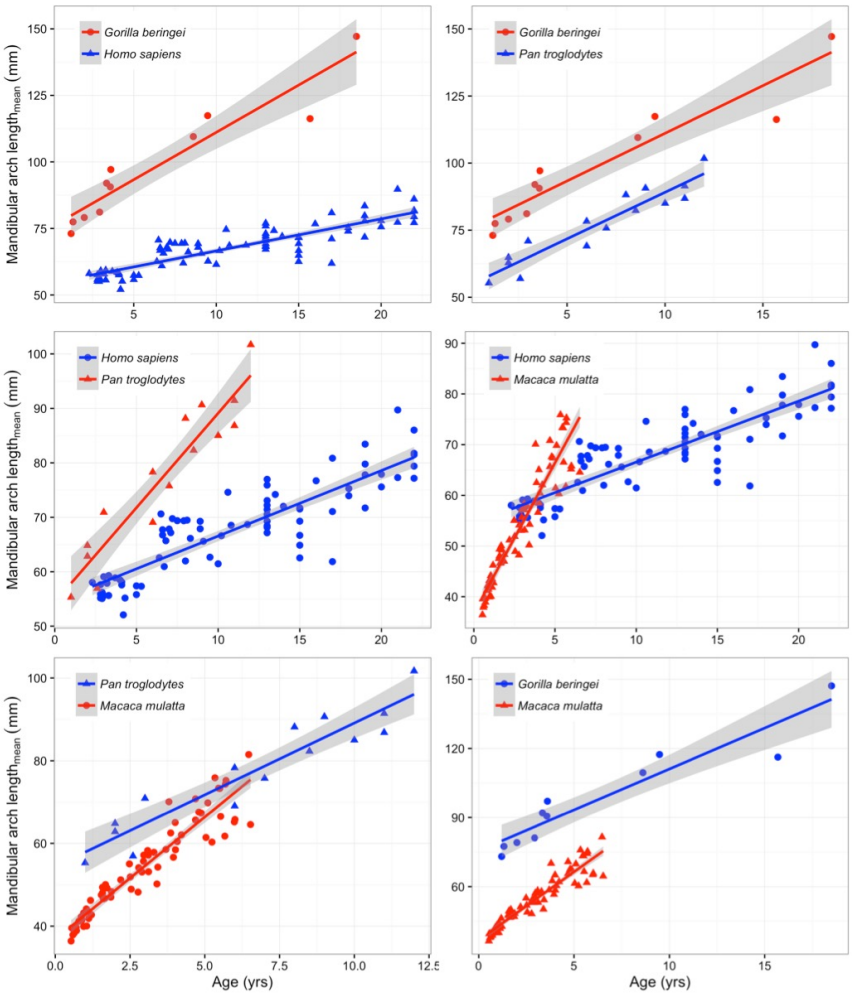


Figure 28. Pairwise comparisons of *mandibular arch length*$_{mean}$ growth rates.

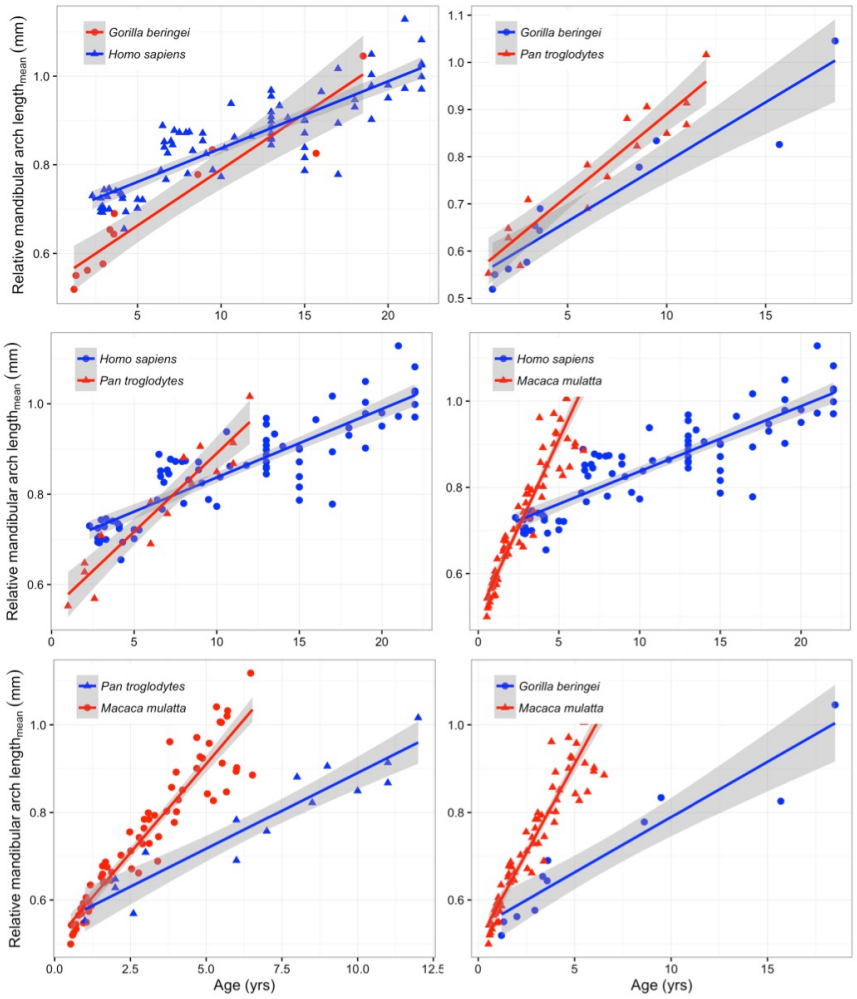


Figure 29. Pairwise comparisons of *relative mandibular arch length*$_{mean}$ growth rates.

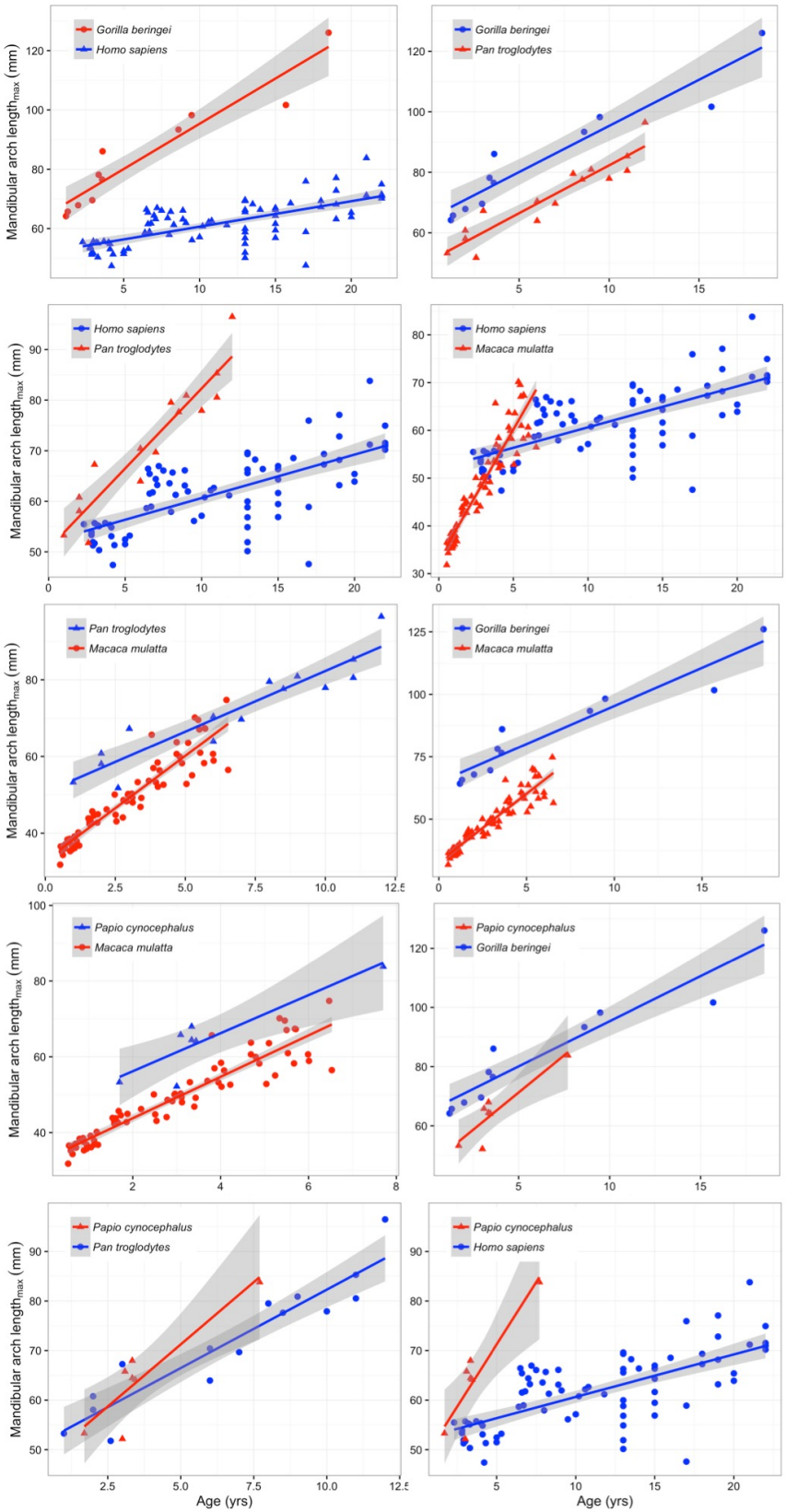


Figure 30. Pairwise comparisons of *mandibular arch length*$_{max}$ growth rates.

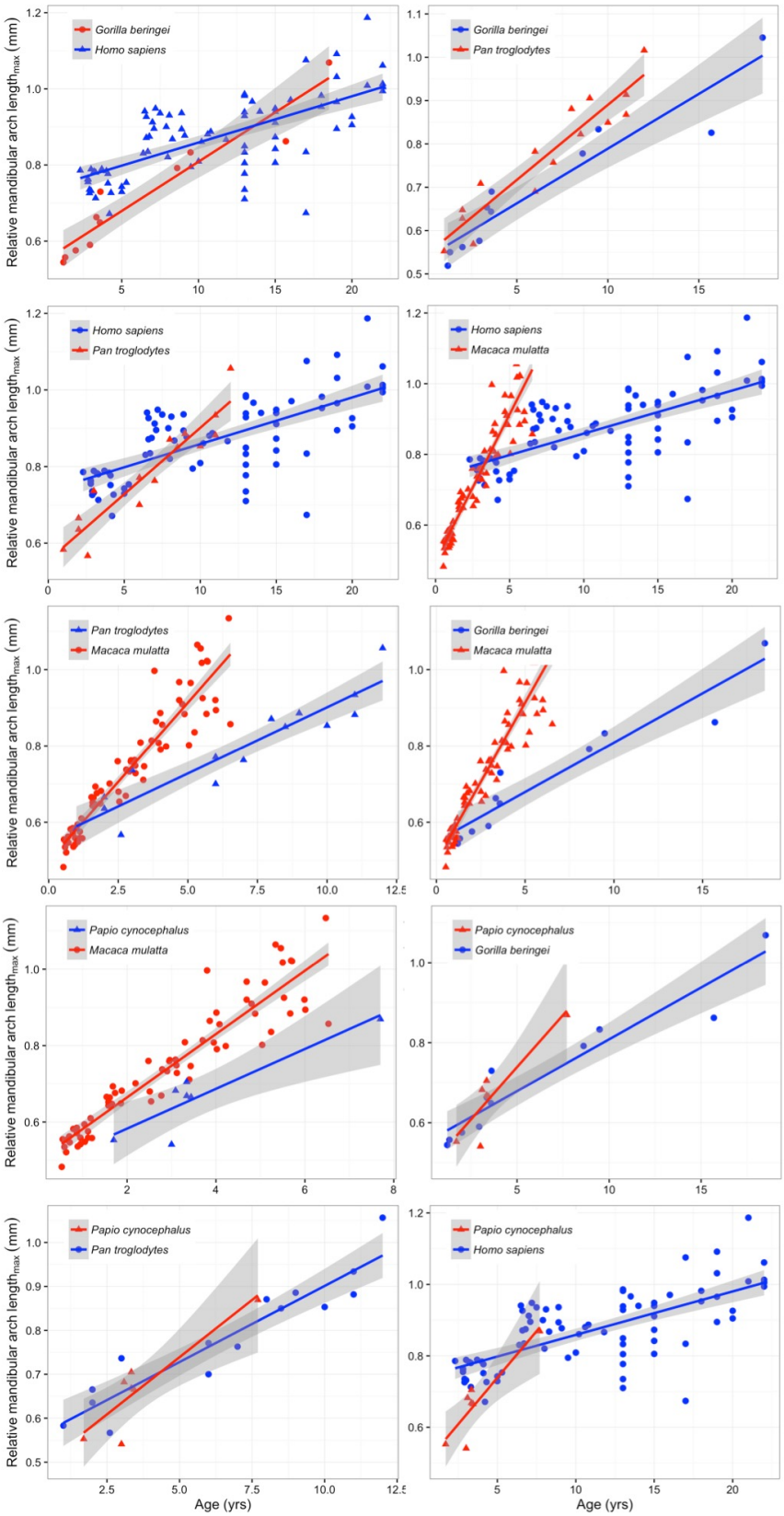


Figure 31. Pairwise comparisons of *relative mandibular arch length$_{max}$* growth rates.

*Phylogenetic PCA*

The phylogenetic PCA model yielded a lambda value of zero indicating that there was no phylogenetic signal in the error structure of the model (Table 24A), with the first component explaining 99.49% of variance in the data, and the remaining three components together explaining less than 0.5% of variance (Table 24B). Given the high amount of variance explained by *PC1*, this sole component was used as a variable in the analyses below to represent the cumulative effect of brain and body size, and life-history variables. Eigenvector loadings for *PC1* were all positive and all contributed substantially to the component, with *brain weight* and *gestation length* having the strongest contributions (Table 24C). Loadings for *PC1-4* are listed in Table 24C.

Table 24. Phylogenetic PCA results.

**A.** Lambda

| Lambda = 0.00 |
|---|

**B.** Variance explained

| | **PC1** | **PC2** | **PC3** | **PC4** |
|---|---|---|---|---|
| | 0.9949 | 0.0045 | 0.0006 | 0.0000 |

**C.** Eigenvector loadings

| **Variable** | **PC1** | **PC2** | **PC3** | **PC4** |
|---|---|---|---|---|
| Body mass | 0.4819 | -0.8699 | -0.1045 | -0.0008 |
| Brain weight | 1.0000 | -0.0046 | 0.0081 | 0.0001 |
| Age-at-first-reproduction | 0.7894 | -0.1612 | 0.5765 | -0.1360 |
| Gestation length | 0.9955 | 0.0639 | -0.0695 | -0.0008 |

*PGLS*

There was a negative relationship between *PC1* and *mandibular arch length growth rate*$_{mean}$, and between *PC1* and *mandibular arch length growth rate*$_{max}$ but the slopes were not significantly different from zero (Table 25; Fig. 32). *PC1* explained 45% of the variation in *mandibular arch length growth rate*$_{mean}$ and 41 % of the variation in *mandibular arch length growth rate*$_{max}$ (Table 25). The slopes for *relative mandibular arch length growth rate*$_{mean}$ and *relative mandibular arch length growth rate*$_{max}$ were also negative and the former was significantly different from zero (Table 25; Fig. 33). *PC1* explained 93% and 53% of the variation in *relative mandibular arch length growth rate*$_{mean}$ and *relative mandibular arch length growth rate*$_{max}$, respectively (Table 25). Unlike the growth rate data, data on age-at-growth-cessation (i.e., *mandibular arch length growth cessation*$_{mean}$ and *mandibular arch length growth cessation*$_{max}$) yielded significant positive relationships with *PC1*, and *PC1* explained 73% and 76% of the variation in *mandibular arch length growth cessation*$_{mean}$ and *mandibular arch length growth cessation*$_{max}$ respectively (Table 25; Fig. 34).

Table 25. PGLS results.

| **Response variable** | **ML lambda** | **Slope** | **$R^2$** | ***p*-value** |
|---|---|---|---|---|
| Mandibular arch length growth rate$_{mean}$ | 1.00 | -0.00293 | 0.45 | 0.132 |
| Mandibular arch length growth rate$_{max}$ | 1.00 | -0.00003 | 0.41 | 0.148 |
| Relative mandibular arch length growth rate$_{mean}$ | 1.00 | -0.00279 | 0.93 | **0.006** |
| Relative mandibular arch length growth rate$_{max}$ | 1.00 | -0.00003 | 0.53 | 0.144 |
| Mandibular arch length growth cessation$_{mean}$ | 0.00 | 0.01245 | 0.73 | **0.041** |
| Mandibular arch length growth cessation$_{max}$ | 0.00 | 0.01312 | 0.76 | **0.034** |

Significant results ($p \leq 0.05$) listen in bold.

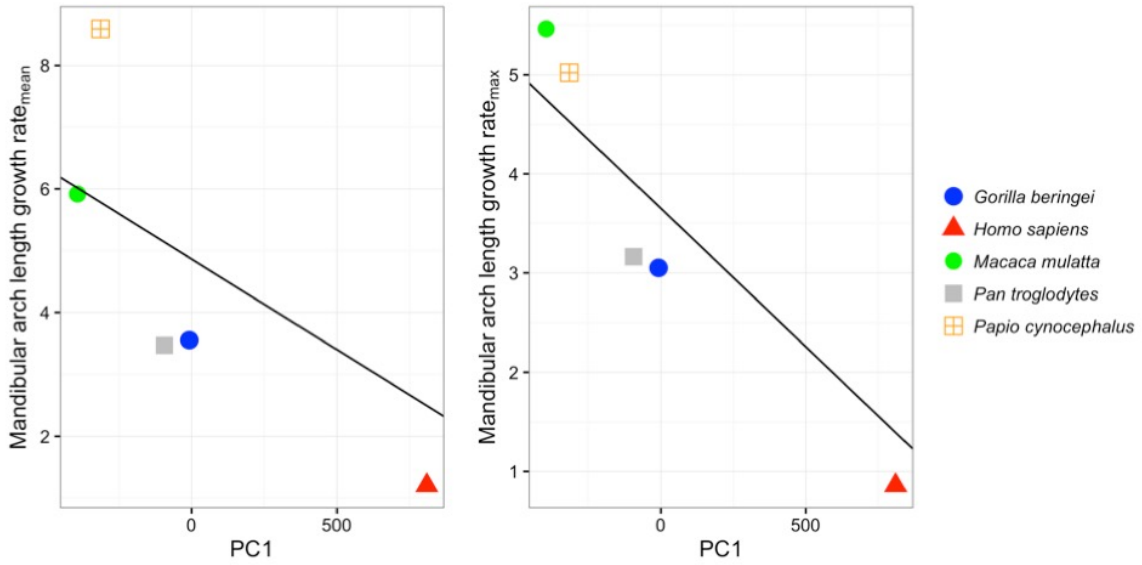


Figure 32. PGLS results for interspecific relationships between *mandibular arch length* and *PC1*. Results shown for the response variables: *mandibular arch length growth rate*$_{mean}$ (left) and *mandibular arch length growth rate*$_{max}$ (right), and the predictor variable *PC1*, a variable representing brain and body size as well as life-history variables.

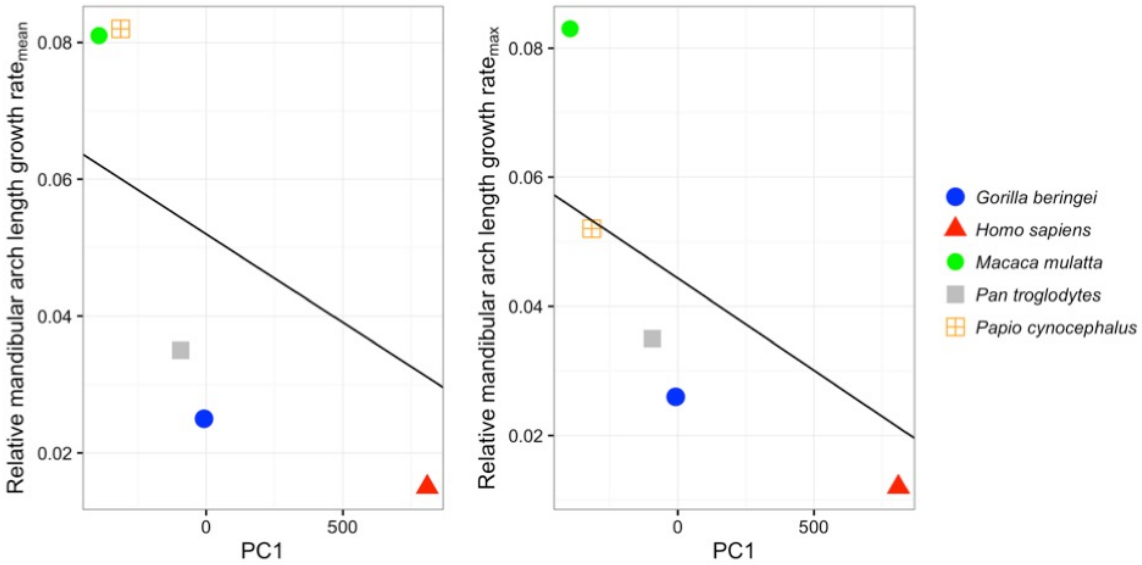


Figure 33. PGLS results for interspecific relationships between *mandibular arch length growth rate* and *PC1*. Results shown for the response variables: *relative mandibular arch length growth rate*$_{mean}$ (left) and *relative mandibular arch length growth rate*$_{max}$ (right), and the predictor variable *PC1*, a variable representing brain and body size as well as life-history variables.

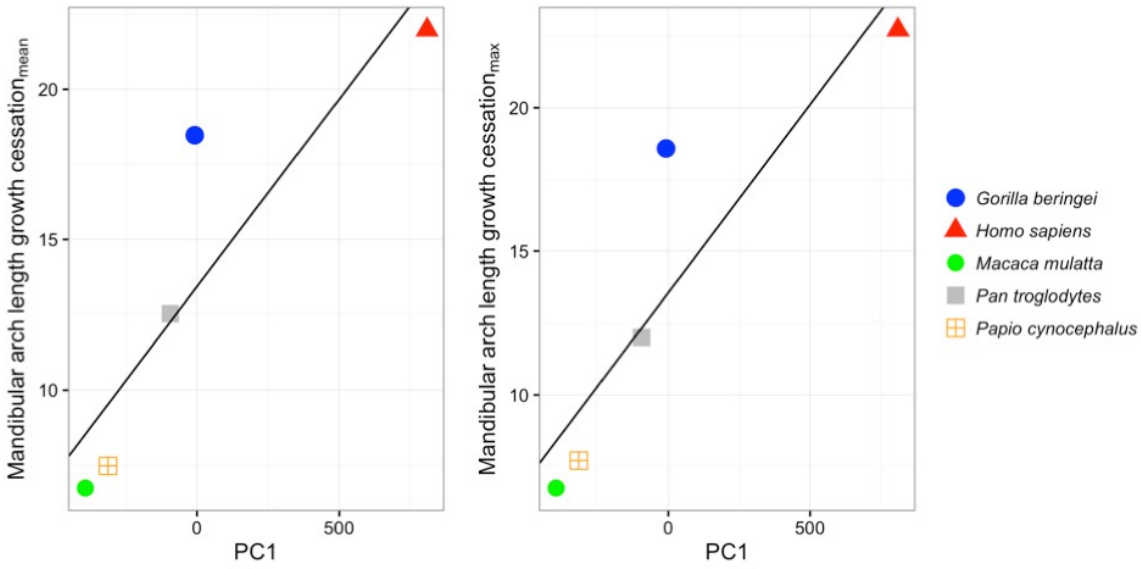


Figure 34. PGLS results for interspecific relationships between *mandibular arch length growth cessation* and *PC1*. Results shown for the response variables: *mandibular arch length growth cessation*$_{mean}$ (left) and *mandibular arch length growth cessation*$_{max}$ (right), and the predictor variable *PC1*, a variable representing brain and body size as well as life-history variables.

## Discussion

Reconstructing the timing of molar emergence is a powerful tool for probing life history in the fossil record. The predictive power of molar-emergence ages is based on strong correlations with certain key life-history variables (e.g., Smith 1989; Smith, Crummett, and Brandt 1994; Kelley and Schwartz 2010, 2012). However, the underlying process that leads to varying molar-emergence ages in primates remains elusive. To help unravel the mechanism by which variation in molar emergence schedules is achieved in primates, this study examined whether the biomechanics of the growing masticatory system constrain the timing of molar emergence. Based on the expectations of the CLM on the position of molar emergence, adult mandibular arch lengths, and ages at molar emergence, predictions were generated for the rate and duration of mandibular arch

length growth for the five taxa included in this study (Table 19). All predictions were supported by the results of the study with one notable exception (Table 26). The comparison between mountain gorillas and chimpanzees did not conform to the predictions of the model. Based on reported molar-emergence ages and adult mandibular arch lengths in these two species, it was predicted that the mountain gorilla mandibular arch would grow at the same, faster, or slower rate, but for a shorter duration than the chimpanzee mandibular arch and that on a relative scale, the mountain gorilla mandibular arch would grow at a faster rate and shorter duration than the chimpanzee mandibular arch (Table 19). Results indicate that the rate of absolute mandibular arch length growth in mountain gorillas is statistically indistinguishable from that of chimpanzees, which is consistent with the predictions, but that mountain gorillas grow their mandibular arches for longer durations than chimpanzees (Table 26), a finding that is inconsistent with the model. The results are more consistent with mountain gorillas either possessing similar or later ages at molar emergence than chimpanzees. The only study on mountain gorilla molar-emergence ages is a preliminary one and although the data are from sample of 56 individuals, only a handful of these individuals died at the critical points of molar emergence (Vakiener et al. 2016); thus, it is possible that mean molar-emergence ages for this population will change as more data become available. This idea is further supported by a recent radiographic study on molar development in the same Virunga mountain gorilla population, which found that this population is not accelerated in molar formation stages compared to chimpanzees (Kralick et al. 2017). Some of the most robust data on molar-emergence ages in great apes are from the Kanyawara chimpanzee population

Table 26. Evaluation of whether results conform to predictions.

**A.** *Mandibular arch length*$_{mean}$

| Species comparison | Slope comparison | Consistent with prediction? | Growth cessation comparison | Consistent with prediction? |
|---|---|---|---|---|
| *G. beringei* vs. *H. sapiens* | > | Yes | < | Yes |
| *G. beringei* vs. *P. troglodytes* | = | Yes | > | No |
| *H. sapiens* vs. *P. troglodytes* | < | Yes | > | Yes |
| *H. sapiens* vs. *M. mulatta* | < | Yes | > | Yes |
| *P. troglodytes* vs. *M. mulatta* | < | Yes | > | Yes |
| *G. beringei* vs. *M. mulatta* | < | Yes | > | Yes |

**B.** *Relative mandibular arch length*$_{mean}$

| Species comparison | Slope comparison | Consistent with prediction? | Growth cessation comparison | Consistent with prediction? |
|---|---|---|---|---|
| *G. beringei* vs. *H. sapiens* | > | Yes | < | Yes |
| *G. beringei* vs. *P. troglodytes* | < | No | > | No |
| *H. sapiens* vs. *P. troglodytes* | < | Yes | > | Yes |
| *H. sapiens* vs. *M. mulatta* | < | Yes | > | Yes |
| *P. troglodytes* vs. *M. mulatta* | < | Yes | > | Yes |
| *G. beringei* vs. *M. mulatta* | < | Yes | > | Yes |

**C**. *Mandibular arch length*$_{max}$

| Species comparison | Slope comparison | Consistent with prediction? | Growth cessation comparison | Consistent with prediction? |
|---|---|---|---|---|
| *G. beringei* vs. *H. sapiens* | > | Yes | < | Yes |
| *G. beringei* vs. *P. troglodytes* | = | Yes | > | No |
| *H. sapiens* vs. *P. troglodytes* | < | Yes | > | Yes |
| *H. sapiens* vs. *M. mulatta* | < | Yes | > | Yes |
| *P. troglodytes* vs. *M. mulatta* | < | Yes | > | Yes |
| *G. beringei* vs. *M. mulatta* | = | Yes | > | Yes |
| *P. cynocephalus* vs. *M. mulatta* | = | Yes | > | Yes |
| *P. cynocephalus* vs. *G. beringei* | = | Yes | < | Yes |
| *P. cynocephalus* vs. *P. troglodytes* | = | Yes | < | Yes |
| *P. cynocephalus* vs. *H. sapiens* | > | Yes | < | Yes |

**D.** *Relative mandibular arch length*$_{max}$

| Species comparison | Slope comparison | Consistent with prediction? | Growth cessation comparison | Consistent with prediction? |
|---|---|---|---|---|
| *G. beringei* vs. *H. sapiens* | > | Yes | < | Yes |
| *G. beringei* vs. *P. troglodytes* | = | No | > | No |
| *H. sapiens* vs. *P. troglodytes* | < | Yes | > | Yes |
| *H. sapiens* vs. *M. mulatta* | < | Yes | > | Yes |
| *P. troglodytes* vs. *M. mulatta* | < | Yes | > | Yes |
| *G. beringei* vs. *M. mulatta* | < | Yes | > | Yes |
| *P. cynocephalus* vs. *M. mulatta* | < | Yes | > | Yes |
| *P. cynocephalus* vs. *G. beringei* | > | Yes | < | Yes |
| *P. cynocephalus* vs. *P. troglodytes* | = | Yes | < | Yes |
| *P. cynocephalus* vs. *H. sapiens* | > | Yes | < | Yes |

(Smith et al. 2013; Machanda et al. 2015a). These mixed-longitudinal data were collected opportunistically by taking oral photographs of subadult known-age individuals and scoring them for the presence and absence of teeth. Such an approach should be undertaken to collect comparable data on Virunga mountain gorillas, which would yield larger sample sizes and thus more reliable ages at molar emergence for this population.

Molar-emergence ages for several of the other species in this study were acquired from a compendium on primate tooth emergence (Smith, Crummett, and Brandt 1994). Although the study provided some of the original sources used to compile the data, many of these sources are based on unknown sample sizes and are based on captive individuals. These data may not be problematic for the current study for several reasons, however. The skeletal data in the current study for *M. mulatta* are from the Cayo Santiago provisioned population, which may exhibit faster growth rates that are comparable to captive macaques. Further, as part of the resus macaque sample, Smith, Crummett, and Brandt (1994) included data from the Cayo Santiago population (Turnquist and Kessler 1990). Similarly, the reported data for *P. cynocephalus* from Smith, Crummett, and Brandt (1994) are from a wild population of this species, reported by (Phillips-Conroy and Jolly 1988).

Diet, a potentially influential factor on growth rates, was omitted from the analysis in this study. The ecological-risk-aversion hypothesis posits that populations experiencing high food competition should exhibit slow somatic growth rates to reduce the risk of death due to starvation (Janson and van Schaik 1993). Species feeding on high-quality resources (e.g., frugivores) should exhibit slow somatic growth and when the hypothesis is applied to molar emergence schedules, frugivores should exhibit later ages

at molar emergence than folivores. Despite some exceptions to the expectations of the ecological-risk-aversion hypothesis among primates (e.g., Godfrey et al. 2004; Bolter 2011; Borries et al. 2011), notably the mismatch between dental and somatic growth rates among indriids and lemurids (Godfrey et al. 2004), diet remains a potentially important factor influencing dental growth and emergence schedules. In the case of strepsirrhines, for example, the exceptionally fast dental development observed in indriids is timed to the availability of their highly folivorous diet (Eaglen 1985; Godfrey et al. 2004). The idea that the timing of dental development is tied to variation in the behavioral ontogeny of food processing has not been tested across primates (but see Dirks (2003) and Godfrey et al. (2004) for studies on the relationship between dental development and diet in a handful of primates). The ontogeny of food processing may be related to the material properties of food (e.g., Venkataraman et al. 2014) and/or to the amount of time required to learn the motor coordination and dexterity required to access adult foods (e.g., Chalk et al. 2016; Chalk-Wilayto et al. 2016). Such factors were not included in the present study as these types of data are not available for all five species included in this study. Further, due to the small sample size in this study, the number of predictor variables had to be kept to a minimum. It is possible that once aspects of diet, such as food availability and its nutritional content as well as mechanical properties, are included in the model, more variation in mandibular arch length growth rate and growth cessation would be explained, although the type of pattern that might emerge from this kind of analysis is unclear given the current sample. Once more skeletal collections of known-age individuals become available yielding larger sample sizes, diet should be taken into consideration as an influential variable.

Research on somatic growth rates in wild primates is in its infancy. While several studies have reported on growth rates in wild populations (Pusey et al. 2005; Zihlman, Bolter, and Boesch 2007; Breuer et al. 2009; Machanda et al. 2015b; Emery Thompson et al. 2016), methods tend to differ among these studies (e.g., skeletal growth, body mass growth, linear growth of body segments) making direct comparisons difficult. Although it would be valuable to determine how mandibular arch growth rates compare to overall somatic growth rates, such comparisons are not currently possible. Insight can be gained, however, by comparing data on ages at somatic growth cessation to the data on growth cessation from the current study.

Rhesus macaques from Cayo Santiago reach adult weight between the ages of six and seven years (Leigh and Bernstein 2006), which coincides with the age-at-mandibular-arch-length-growth-cessation estimated for this population here (~6.7 years; Table 21). Data on captive baboons, however, suggest that adult body mass is also reached at similar ages to Rhesus macaques (~6-7 years: Leigh 2006b; Leigh and Bernstein 2006). This is slightly younger than the ages at mandibular arch growth cessation identified by the present research (7.5-7.7; Table 21). This is not surprising, however, given that animals in captivity tend to exhibit accelerated development compared to wild conspecifics, a possible result of differences in food availability, maternal energetics, predators, and disease (e.g., Altmann and Alberts 1987; Phillips-Conroy and Jolly 1988; Stoinski et al. 2013). It is expected that yellow baboons living in the wild would exhibit slightly older ages at somatic growth cessation, perhaps similar to the ages at mandibular arch length growth cessation reported here.

Data on somatic growth are available for Kanyawara chimpanzees, which is a

different population than the two chimpanzee populations used in this study. These data indicate that in males, body lengths reach adult values at around age 10, but body area continues to grow until the ages of 15-17 (Machanda et al. 2015b). The present study identified ages at mandibular arch growth cessation of ~12 years for chimpanzees (Table 21), which falls between the body length and body area growth cessation ages identified for the Kanyawara chimpanzees and close to the ages reported for M3 emergence in the sample used for this study (Table 17). The age-at-mandibular-arch-growth-cessation identified for mountain gorillas (~18 years; Table 21), on the other hand, is much later than their age-at-M3-emergence (~10 years; Table 17). While this discrepancy in age may be due to the small sample size for this species, the growth cessation estimates are consistent with data on somatic growth rates for the same population. Although most Virunga mountain gorilla adult body proportions are variably reached between the ages of 11 and 16 years, head proportions are the last to reach adult values, especially in males where adult size is not reached until 16.7-18.1 years of age (Galbany et al. 2017). This late age at adult head proportion attainment may be related to the overall maturation of the masticatory system, including the attainment of secondary sexual characteristics, such as the late eruption of the permanent canines, the growth of the sagittal crest, which continues late into adulthood in gorillas (Balolia, Soligo, and Wood 2017), and related size increases of the masticatory muscles (Taylor 2003). In mountain gorillas, male dispersal occurs at around the same time as when adult size is reached (Harcourt 1978; Robbins 1995; Stoinski et al. 2009), and should coincide with these final stages of growth.

Adult sexual size dimorphism is achieved through ontogenetic shifts in growth

rate and/or duration (Shea 1986; Leigh, Shah, and Buchanan 2003). To boost sample sizes in this study, sexes were combined in all analyses, but doing so may have obstructed potential differences between the sexes that arise during ontogeny. Sexual dimorphism in *mandibular arch length* can be visualized in the more sexually dimorphic species in this study (*G. gorilla*: Fig 23; *P. cynocephalus*, Fig. 27) as two concentrations of data points in the adult phases of *mandibular arch length* curves, males with greater y-values and females with lower y-values. The males in these species may attain longer mandibular arches by having later ages at growth cessation and/or faster rates of mandibular arch growth than females. While it is possible that important information on sex-specific growth rates and ages at growth cessation are masked in this analysis, these data are being compared to data on molar emergence, which are also not sex-specific. The effect that sex-specific growth rates/cessations have on molar-emergence ages can only be evaluated when larger sample sizes and sex-specific data on molar-emergence ages become available.

The current research sought to determine the underlying cause for the close association between molar-emergence age and two key life-history variables that relate to reproductive scheduling. This was done in the context of the relationship between molar-emergence age and mandibular arch length growth rate and duration. Specifically, this analysis was aimed at determining if brain size, body size, and life history have significant effects on mandibular growth rate and duration, and thus on molar-emergence age in primates. These predictor variables were reduced to one variable using PCA. Interspecific analyses indicated that the principal component is significantly positively related to age-at-mandibular-arch-growth-cessation, but most relationships between the

component and growth rates, which were all negative, were not statistically significant.

The positive relationship between *PC1* and *mandibular arch length growth cessation* indicates that life history and body/brain size are related to the duration of mandibular arch length growth. This is perhaps not surprising given the fact that many life-history variables are strongly correlated with one another (Smith 1989) and that mandibular arch length growth cessation occurs at similar ages as M3 emergence and somatic growth rate cessation (discussed above) and M3 emergence is a skeletal marker of adulthood and thus the onset of reproduction ( Smith 1989; Smith and Tompkins 1995). Overall, these results suggest that mandibular arch growth is closely tied to the overall plan of growth and development, both of the skull as well as somatic growth in general, and molar emergence schedules reflect this close relationship (Smith 1989).

# CHAPTER 5

# DISCUSSION

## Summary of Findings

This dissertation explored molar emergence as part of a growing coordinated masticatory system to provide a biomechanical model that explained variation in the position and timing of molar emergence and yielded an understanding for the close association between molar-emergence age and life history among primates. Specifically, this dissertation tested the hypothesis that the location and timing of molar emergence is constrained to avoid TMJ distraction throughout ontogeny. This hypothesis was tested in Chapters 2-4 from three related perspectives that built upon one another.

Chapter 2 tested the spatial model of molar emergence based on the expectations of the Constrained Lever Model (CLM); it investigated whether molars emerge directly anterior to the point at which the muscle resultant intersects the triangle of support, as per the original formulation of the CLM by Greaves (1978), or significantly anterior to this point, which would be consistent with the finding that the last molar is positioned significantly anterior to the muscle resultant in adult primates (Spencer 1995, 1999; Perry, Hartstone-Rose, and Logan 2011). Overall, the study in Chapter 2 supported the hypothesis and found that molars emerge significantly anterior to the resultant; however, when the most anterior MLA was used to approximate the position of the resultant, the last molar was posterior to the MLA in later ontogenetic stages and adults of some taxa.

Chapter 3 was aimed at understanding what factors influence ontogenetic and interspecific variation in the position of molar emergence given different craniofacial

configurations, diets, and feeding behaviors that primates exhibit. It was determined that more resistant foods, larger skulls, longer molars, and longer jaws produce larger buffer zones, but greater canine overlap produces smaller buffer zones. These factors account for a large portion of both ontogenetic and interspecific variation in the distance between the distal-most molar and the resultant. These results suggest that the buffer zone is part of a mechanism modulating the position of molar emergence across primates to prevent TMJ distraction throughout ontogeny and in adulthood.

Chapter 4 looked at how shifting certain parameters in the model might produce variation in the timing of molar emergence. The chapter investigated whether the rate at which space is made available in the jaws, anterior to the resultant, and the duration of jaw growth determine the timing of molar emergence and whether these growth parameters are influenced by life-history variables. Comparisons of mandibular growth rates between species generally supported the hypothesis. The model proposed in the chapter explained differences in the timing of molar emergence between primate species. Furthermore, life-history variables were positively related to jaw growth duration, and suggested a positive relationship with mandibular arch length growth rate, suggesting that life-history variables are related to molar-emergence ages vis-à-vis their influence on jaw growth rate and duration.

Overall, this dissertation provides a mechanical and developmental model for explaining temporal and spatial variation in molar-emergence ages among primates and a framework for understanding how variation in the timing of molar emergence evolves among primates. The findings suggest that life history is related to ages at molar emergence through its influence on the duration and rate of mandibular arch length

growth in the overall context of masticatroy growth. Furthermore, this dissertation provides support for the integrated nature of craniofacial growth and has implications for the study of primate life history and masticatory morphology (discussed below).

## Life-History Reconstructions

Currently, life-history reconstructions based on molar-emergence ages rely on the discovery of fossil individuals that died at or near the age of M1 emergence (e.g., Kelley 1997; Kelley and Smith 2003; Smith et al. 2007b). Taphonomic bias towards preserving large bones (Behrensmeyer, Western, and Dechant Boaz 1979; Behrensmeyer 1981) means that subadult skeletal elements are less likely to be preserved in the fossil record. Consequently, juvenile fossilized remains tend to be more rare relative to adult remains reducing the chances of discovering individuals that died and became fossilized at or around the age of M1 emergence.

This dissertation offers a new way of reconstructing life history in the fossil record that does not rely on the discovery of individuals that died at the point of M1 emergence. Results indicate that there is a link between life history and age-at-mandibular-arch-length-growth-cessation as well as mandibular arch growth rate (Chapter 4). Based on the data in Chapter 4, faster life histories are linked with earlier ages-at-mandibular-arch-length-growth-cessation and faster mandibular arch growth rates. The sample size for the interspecific analyses in Chapter 4 was very small and not all of these relationships were statistically significant, but the link between life history and mandibular arch growth rate/cessation is intriguing and may offer a new method for determining the life histories for fossil primates.

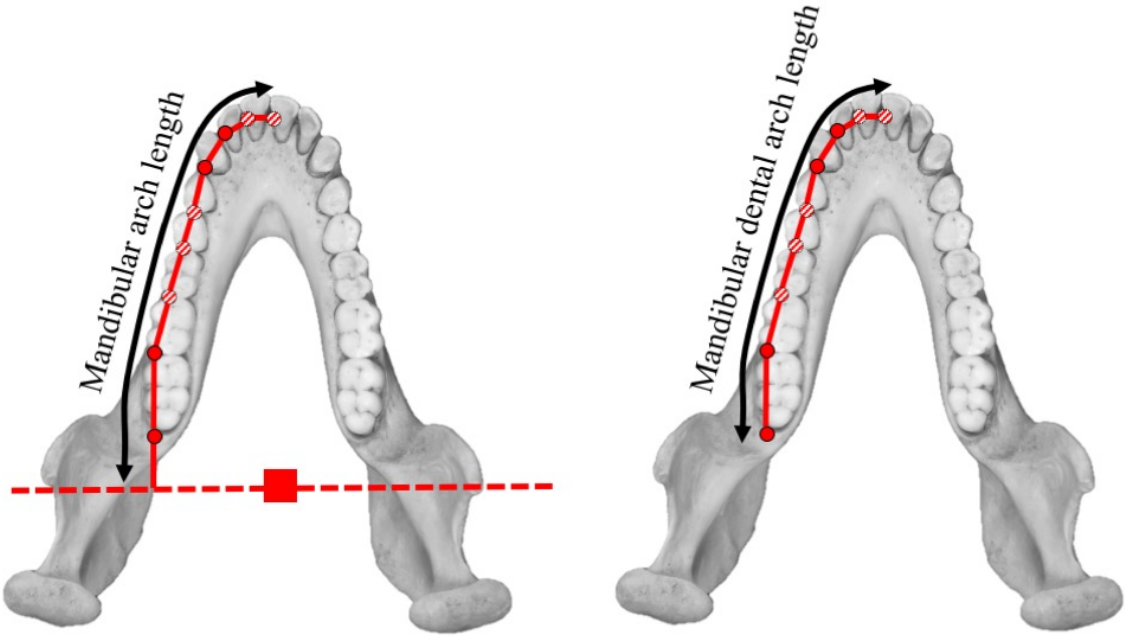


Figure 35. Variables *mandibular arch length* and *mandibular dental arch length*. Landmarks were taken along the labial/buccal aspect of the alveolar bone, distal to each tooth position. Red dots indicate landmarks on visible bone surface whereas dashed red and white dots indicate landmarks that are obstructed in the specific view. Red square indicates the position of the adductor muscle resultant as it intersects the triangle of support, projected onto the occlusal plane. *Mandibular arch length* (left), as measured in Chapter 4, describes the distance along the mandibular arch from the point between the two central mandibular incisors (infradentale) to the intersection of the resultant with the triangle of support, projected onto the occlusal plane (see Chapter 4 for description of calculation). *Mandibular dental arch length* (right) describes the distance along the mandibular arch from infradentale to the point distal to the last molar. This measurement is strongly correlated with mandibular arch length (Table 27) and its calculation does not require the presence of the entire skull.

A proxy for the variable *mandibular arch length*, which is necessary to measure for ontogenetic samples of fossil primates to use this method for reconstructing life history, can be easily measured using only mandibular or maxillary remains. The approach described in this dissertation of measuring *mandibular arch length* requires relatively complete skulls that preserve the attachment sites of the adductor muscles as well as the positions of all teeth. A preliminary analysis of the relationship between *mandibular arch length*, as defined in Chapter 4 (also shown in Fig. 35), and mandibular dental arch length (the distance along the mandibular arch from infradentale to the point distal to the last molar: Fig. 35) indicates that these two variables are highly correlated at all molar emergence categories (r = 0.96 - 0.98; Table 27). *Mandibular dental arch length* can therefore be used as a surrogate for *mandibular arch length* and the former's calculation does not require the presence of the entire skull, only the mandibular or maxillary dental arch. Alternatively, *mandibular arch length* can be predicted from *mandibular dental arch length,* given the high coefficients of determination in an ordinary least-squares (OLS) regression analysis between the two variables (Table 27; Fig. 36). By describing *mandibular arch length*/*mandibular dental arch length* growth rates and ages at growth cessation, a fossil taxon for which ontogenetic samples are relatively rich can be compared to modern primate mandibular growth rates to determine if the fossil taxon possessed a faster or slower life history profile than extant taxa. One particular case where such an approach could be informative is the life-history reconstruction of Neandertals. As described in the Chapter 1, the dental evidence for life history in this hominin species is conflicting, with some researchers reporting earlier ages at tooth formation and emergence than modern humans (Ramirez Rozzi and Bermudez de

Castro 2004; Smith et al. 2010), while others report late ages at molar emergence (Macchiarelli et al. 2006).

Another case where such an approach may be informative is the life-history reconstructions of australopith species. As discussed in Chapter 1, estimates of M1-emergence ages for *Australopithecus* and *Paranthropus*, based on enamel and dentine microstructure, has yielded a range of 2.7-3.9 years ( Dean et al. 1993; Kelley and Schwartz 2012). Although this range overlaps with the range of M1-emergence ages known for wild-shot apes (2.5-4.6 y: Kelley and Schwartz 2012; Smith et al. 2013; Machanda et al. 2015a), it falls at the lower end of the extant ape range suggesting that australopiths had an accelerated life history relative to the extant great apes, or alternatively, that there was selection for fast dental development in these taxa (Kelley and Schwartz 2012). Given the relatively larger brain sizes of australopiths compared to the extant great apes (Kimbel and Villmoare 2016), a faster life history would be surprising. Although rich ontogenetic series of australopith species do not exist, mandibular ontogenetic series are available for *A. afarensis* (Glowacka, Kimbel, and Johanson 2017) and *P. robustus* (Cofran 2014). Once the ages at death for the individuals in these samples are established, which can be performed using non-destructive X-ray synchrotron microtomography methods (e.g., Tafforeau et al. 2006; Smith et al. 2010; Le Cabec, Dean, and Begun 2017), their mandibular arch growth rates can be determined and compared to one another as well as to extant great apes and humans as an alternative means of determining the pace of life history.

Table 27. Results of OLS regressions and Pearson correlation coefficients (r) for the relationship between *mandibular dental arch length* and *mandibular arch length* for molar emergence categories.

**A**. *Mandibular arch length*$_{mean}$

| **Molar emergence category** | **slope** | **$R^2$** | **r** | ***p*-value** |
|---|---|---|---|---|
| dp4 emerged | 0.562 | 0.93 | 0.97 | **<0.001** |
| M1 emerged | 0.648 | 0.96 | 0.98 | **<0.001** |
| M2 emerged | 0.761 | 0.95 | 0.98 | **<0.001** |
| M3 emerged | 0.794 | 0.96 | 0.98 | **<0.001** |

**B**. *Mandibular arch length*$_{max}$

| **Molar emergence category** | **slope** | **$R^2$** | **r** | ***p*-value** |
|---|---|---|---|---|
| dp4 emerged | 0.627 | 0.92 | 0.96 | **<0.001** |
| M1 emerged | 0.741 | 0.96 | 0.98 | **<0.001** |
| M2 emerged | 0.855 | 0.92 | 0.96 | **<0.001** |
| M3 emerged | 0.902 | 0.93 | 0.96 | **<0.001** |

Relationship between (A) *mandibular dental arch length* (predictor variable) and *mandibular arch length*$_{mean}$ (response variable) and (B) *mandibular dental arch length* (predictor variable) and *mandibular arch length*$_{max}$ (response variable), for molar emergence categories.

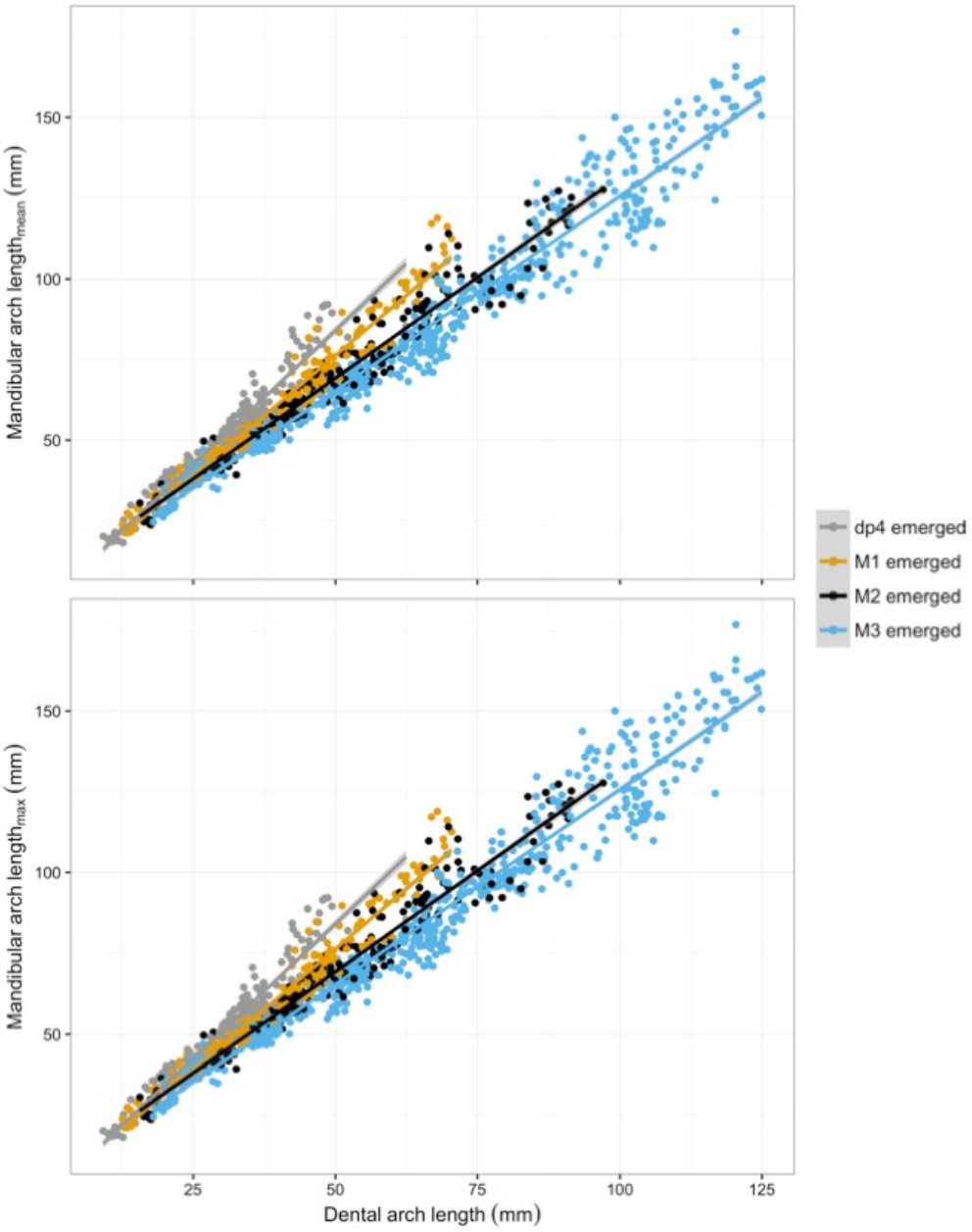


Figure 36. Relationship between *mandibular dental arch length* and *mandibular arch length$_{mean}$* and *mandibular dental arch length* and *mandibular arch length$_{max}$*, for molar emergence categories. The former is shown at the top and the latter at the bottom. OLS regression slopes as in Table 27.

Changes in Masticatory Morphology Throughout Ontogeny

Although it was determined that molars emerge significantly anterior to the resultant in primates, the exact distance between the distal-most molar and the resultant depended on taxonomic group as well as ontogenetic stage (Chapter 2). One novel finding of this dissertation is that the distance between the last molar and the resultant decreases as ontogeny progresses in most primates (Chapter 2). This phenomenon is also illustrated in Figure 36, where the slope between dental arch length and mandibular length is steeper at each progressive molar emergence category. This result can be interpreted in several ways.

Firstly, on a biomechanical basis, an increase in the distance between the distal-most molar and the resultant throughout ontogeny may be a result of the changing geometry of the masticatory system throughout ontogeny. Chapter 2 suggested that the angle between the tringle of support produced when biting on the last molar and the occlusal plane influences the point at which the resultant crosses the triangle of support. This angle is a result of two factors, the height of the TMJ above the occlusal plane and the distance between the last molar and the TMJ (Fig. 37). Larger angles and thus short distances between the distal-most molar and the TMJ are produced by increasing the height of the TMJ, decreasing the distance of the last molar to the TMJ, or both (Fig. 37 B, E). Conversely, small angles and long distances between the distal-most molar and the TMJ (i.e., the morphology found in subadult primates) are produced by decreasing the height of the TMJ, increasing the distance of the last molar to the TMJ, or both (Fig. 37 C, D, F). The height of the TMJ increases throughout growth (e.g., Ravosa and Ross 1994; Taylor 2002, 2003) and the last molar is positioned closer to the resultant with

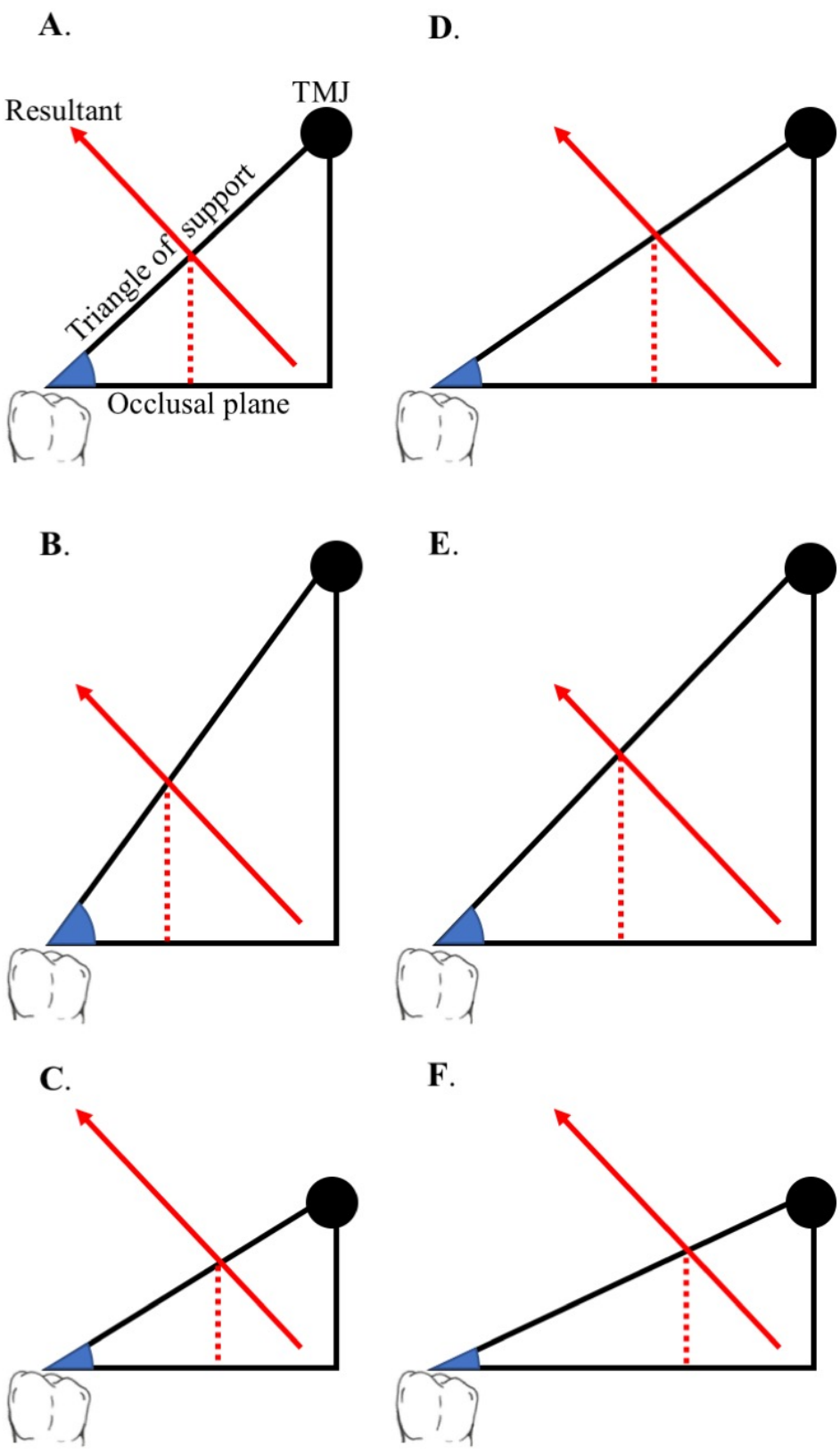
A.
TMJ
Resultant
Triangle of support
Occlusal plane
D.
B.
E.
C.
F.

Figure 37. Effects of changing TMJ height above the occlusal plane and the distance of the distal-most molar to the TMJ on (1) the angle (blue) between the occlusal plane and the triangle of support and (2) the point at which the resultant intersects the triangle of support, projected onto the occlusal plane (red dashed line). The following comparisons are relative to the morphology in **A**. Raising the TMJ (**B**) results in a larger angle and brings the resultant's intersection with the triangle of support closer to the distal-most molar, lowering the TMJ (**C**) reduces the angle and brings the resultant's intersection with the triangle of support further from the distal-most molar. Moving the distal-most molar anteriorly (**D**) reduces the angle and brings the resultant's intersection with the triangle of support further from the distal-most molar. Moving the distal-most molar anteriorly and raising the TMJ (**E**) maintains the angle and maintains the resultant's intersection with the triangle of support. Moving the distal-most molar anteriorly and lowering the TMJ (**F**) reduces the angle and brings the resultant's intersection with the triangle of support further from the distal-most molar.

increasing age (Chapter 2), thus the angle between the triangle of support and the occlusal plane increases throughout growth (Fig 37; Chapter 2) explaining the phenomenon of decreasing distance from the last molar to the resultant as primates mature.

The decreasing distance between the distal-most molar and the resultant throughout ontogeny may also be a result of the fact that the number of molars that are yet to erupt decrease throughout ontogeny (i.e., at the dp4 emerged category, there are three molars yet to erupt, while at the M2 emerged category there is only one molar remaining). Among cercopithecoids, there is little or no temporal overlap in the completion of crown formation of the M1 and the initiation of the M2, nor between completion of the M2 and the initiation of the M3 (e.g., Swindler and Gavin 1962; Swindler 1985; Swindler and Meekins 1991; Dirks et al. 2002; Dirks and Bowman 2007). Apes and strepsirrhines, on the other hand, exhibit temporal overlap in molar formation, (Anemone, Watts, and Swindler 1991; Beynon, Dean, and Reid 1991a; Dirks 1998; Schwartz et al. 2005; Godfrey et al. 2006; Dirks and Bowman 2007). If the number of

forming molars distal to the distal-most emerged molar influences the distance between that molar and the resultant then this pattern should only be present in cercopithecoids and not in apes or strepsirrhines, however, the results here indicate that the distance between the last molar and the resultant increases throughout ontogeny in both cercopithecoids and apes, but not in strepsirrhines (Chapter 2). Furthermore, Boughner and Dean (2004) found that that spatial availability in the jaws does not constrain molar development in both cercopithecoids and apes (discussed in Chapter 1).

A further possible reason for the decreasing distance between the distal-most molar and the resultant throughout ontogeny is related to the acquisition of adult masticatory function. While some primate studies report little evidence of differences in diet between adults and subadults (Watts 1985; Stone 2006; Nowell and Fletcher 2008), many field-based studies suggest at least some age-driven changes in dietary composition, pre-oral processing behavior, feeding or processing time (e.g., Post, Hausfater, and McCuskey 1980; Boinski and Fragaszy 1989; Corp and Byrne 2002; Gunst et al. 2010; Venkataraman et al. 2014; O'Mara 2015; Chalk et al. 2016; Chalk-Wilayto et al. 2016). The masticatory system undergoes substantial shape changes throughout ontogeny. Growth differs across jaw muscles (Cachel 1984; Dickson, Fitton, and Kupczik 2017) and muscle mechanical advantage increases throughout ontogeny (Dechow and Carlson 1990; Glowacka and Schwartz 2017), suggesting that subadults and adults may engage in disparate jaw muscle recruitment patterns (Herring 1985), and that subadults produce lower bite forces during feeding (Thompson, Biknevicius, and German 2003; La Croix et al. 2011; Edmonds and Glowacka 2014). As a result, subadults are likely to be at a disadvantage especially when feeding on tough, hard, or large food

items and subadult primates may require a larger buffer zone to safeguard their TMJs when developing the skills and morphology necessary to feed on an adult diet. In particular, it may be critical for subadults to have larger buffer zones as an extra safety mechanism in order to safeguard their TMJ while they are learning how to extract and process the foods necessary to fuel their growth. This hypothesis is difficult to test, however, and would require studies of how chewing kinematics and muscle activation patterns change during ontogeny in primates. Available data on the ontogeny of the mammalian chewing system suggest that subadults chew foods at slower rates, possibly due to the changes that occur to muscle activation patterns and muscle's lines of action throughout ontogeny and suggest that ontogenetic changes in feeding behavior reflect a learning process accompanied by feedback relationships to anatomical development of the masticatory system (Herring 1985).

## Hominin Masticatory Ontogeny and Morphology

In addition to providing a model that tests similarities/differences in life history among fossil and extant primate species, the CLM and the results of this dissertation can also shed light on the evolution and function of unusual hominin craniofacial anatomy.

### *Neandertals*

Neandertal masticatory morphology differs markedly from that of modern humans, with Neandertals exhibiting striking midfacial projection and humans exhibiting short orthognathic faces that are situated inferior to the anterior cranial fossa, Neandertals having a more posterior zygomatic root, and a retromolar space between the last molar

and the root of the mandibular ramus (Brace 1962; Smith 1983; Rak 1986; Trinkaus 1987; Lieberman, McBratney, and Krovitz 2002). In Neanderthals, mandibular ontogeny proceeds mainly in the forward and downward direction, with anterior displacement of the molar region of the alveolar process, whereas in humans, growth is characterized by a strong vertical component of facial ontogenetic shape change, with increasing height of the ramus and projection of the chin (Bastir, O'Higgins, and Rosas 2007). These differences in adult masticatory morphology therefore arise early in ontogeny and are maintained throughout growth (e.g., Ponce de León and Zollikofer 2001; Krovitz 2003; Bastir, O'Higgins, and Rosas 2007; Williams and Cofran 2016). The masticatory configuration of Neandertals is also unique among primates and it would appear that adaptations for efficient bite forces across the dental arcade can explain some of the unique features of Neandertal craniofacial morphology (Spencer and Demes 1993).

In their biomechanical analysis of the masticatory system, Spencer and Demes (1993) reported that the masticatory configuration of Neandertals is consistent with an adaptation for high/repetitive bite forces at the anterior dentition without compromising bite forces at the posterior dentition. This is achieved through an anterior migration of the dental arch coupled with an anterior migration of the adductor resultant, resulting in increased mechanical advantage at all bite points as well as adductor muscles (Spencer and Demes 1993). This configuration differs from that of extant primate taxa that have adaptations for efficient bite forces at the anterior dentition. For example, among platyrrhines, *Cebus apella* has more anteriorly positioned masseter and temporalis muscles, which increase mechanical advantage at the incisors and canines, as it consumes very tough food items with its anterior dentition, but compromises bite forces on the M3s,

which are reduced in size (Wright 2005). It is the combination of an anteriorly migrated dental arch, coupled with an anterior resultant that produces the midfacial projection typical of Neandertal faces (Spencer and Demes 1993).

The retromolar gap, another unique feature of Neandertals, may be the outcome of facial projection in relation to a fixed ramus position, selection for a large buffer zone, or both. The results of Chapter 2 indicate that species that violated the model as adults (i.e., those that possessed distal-most molars that are posterior to the resultant) are also the species with some of the most obtuse angles between the occlusal plane and the triangle of support (Chapter 2: Table 10). This angle is a function of both TMJ height and the position of the last molar relative to the TMJ (discussed above in Changes in Masticatory Morphology Throughout Ontogeny section**)**. Neandertal TMJs are positioned absolutely closer to the occlusal plane than it other hominoids, including humans (Rak, Ginzburg, and Geffen 2002), but the more anterior position of the last molar would produce a more acute angle between the triangle of support and the occlusal plane, and thus a longer distance between the resultant and the last molar. Chapter 3 defined this distance as the anterior portion of the buffer zone and indicated that a large buffer zone may be a result of processing more resistant foods, which is consistent with the hypothesis of extensive oral processing and high bite force production with the anterior dentition (Smith 1983; Rak 1986; Trinkaus 1983; Demes 1987) as well as the posterior dentition (Spencer and Demes 1993) in Neandertals.

*Australopiths*

Researchers have long used the gross morphology of the masticatory system to make inferences about dietary adaptations of fossil taxa (e.g., Robinson 1954, 1963; Bock and von Wahlert 1965). Microwear and isotopic analyses have made dietary reconstructions more contentious as results using different methods often do not yield the same dietary signal (e.g., Ungar, Grine, and Teaford 2008; Cerling et al. 2011; Ungar and Sponheimer 2011). One persistent mystery has been the dietary reconstruction of *Paranthropus boisei*, which possessed an overall masticatory morphology that suggests a hard-object eating adaptation with large and anteriorly placed attachment sites for the muscles of mastication, large, flat, and thickly enameled premolars and molars, and a deep and wide mandible with a tall ramus (Tobias 1967; Rak 1983), yet its microwear signature is that of a tough-food consumer, (e.g., Ungar, Grine, and Teaford 2008). A recent analysis of the biomechanics of *P. boisei* mastication found that despite the fact that the masticatory morphology of the species (a combination of distally positioned molar teeth with an anteriorly positioned masseter) suggested that TMJ distraction should be an important constraint on this species' masticatory system, the TMJ did not experience distractive forces when biting on M2 even when the working and balancing side adductor muscles were used equally to produce maximum bite force (Smith et al. 2015). This surprising finding suggests that despite molars being positioned close to the resultant, and thus the buffer zone being very small, *P. boisei* could produce very high bite forces without producing distraction at the TMJ, which the authors interpreted as an adaptation to a hard-food diet (Smith et al. 2015). This is unlike other hominins that have been examined thus far (*A. africanus* and *A. sediba*), which exhibit distractive forces at

the TMJ when biting on molars with working and balancing side adductor muscles activated equally (Ledogar et al. 2016b). The *P. boisei* result also suggests that the premolars and molars of *P. boisei*, at least the P3 and M2, are positioned within Region I, defined by the CLM. This finding is surprising in the context of the expectations of the CLM, and unusual among primates. In studies of bite force and CLM region distributions in extant anthropoids, it was found that molars, and often premolars are positioned within Region II ( Spencer 1999; Lucas 2012). That the M2 is positioned within Region I may only be possible due to the species' very widely spaced TMJs (Tobias 1967; Picq 1990), which would act to increase the size of Region I and thus decrease the size of Region II (Spencer 1995). Widely spaced TMJs are not a specialization of *P. boisei,* however, as they are found among all australopiths (Kimbel et al. 2014), therefore this feature alone cannot explain the unusual distribution of Region I in *P. boisei*.

The interpretation that *P. boisei* was feeding on a hard diet is somewhat inconsistent with the results of this dissertation, which found that the size of the buffer zone is positively related to dietary toughness, and a positive relationship is also suggested with Young's modulus (Chapter 3). With a very high TMJ and anteriorly positioned and inclined masseter muscles, it is expected that the muscle resultant would cross the triangle of support at an anterior location and thus produce a small buffer zone between the resultant and the distal-most tooth. Based on the current understanding of primate masticatory morphology, the morphology of P. *boisei* is unique among primates.

Ledogar et al. (2016b) applied the CLM to the MH1 *A. sediba* specimen to test whether this species possessed adaptations for high bite force production. These authors found that the MH1 cranium experienced tensile forces at the TMJ when biting on the

M2 with equal force using the working and balancing size adductor muscles, indicating that that the balancing side muscle force had to be reduced when biting on this molar in order to keep the resultant inside the triangle of support. MH1 is a subadult, with erupted M2s but unerupted M3s and growth simulations indicate that significant size and shape changes would take place between its ontogenetic stage and adulthood (Kimbel and Rak 2017). In this vein, the results of this dissertation suggest that the distance between the last erupted molar and the resultant decrease throughout ontogeny, with the smallest distance occurring in adulthood. This has implications for understanding the masticatory biomechanics of the MH1 specimen. The results of this dissertation indicate that as an adult, the M3 would be positioned closer to the resultant then in a subadult. The conclusions of Ledogard et al. (2016b) that *A. sediba* was not adapted to produce high bite forces on its molars are therefore strengthened by the results of this dissertation and indicate that when biting on M3, *A. sediba* would be required to reduce balancing side force to an even greater degree than previously thought, causing a further reduction in bite force.

*Modern Humans*

Modern human masticatory morphology is unique among primates; humans exhibit small and short maxillae (Fleagle, Gilbert, and Baden 2010), orthognathic faces (Lieberman, McBratney, and Krovitz 2002), and small postcanine dentition and masticatory muscles (e.g., Robinson 1954; Rak 1983; Demes and Creel 1988). This study, as have others (Spencer and Demes 1993; Spencer 1999), found that the modern human masticatory system is capable of producing efficient bite forces due to the

proximity of the molars to the TMJ; however, this proximity also puts humans at risk of distractive forces at the TMJ (Ledogar et al. 2016a). In fact, in this study humans (adult humans, specifically) were one of the few species that violated the CLM. It is therefore unlikely that a reduction of the human masticatory system was a byproduct of selection for increased bite forces at the molars (but see evidence for selection for increased bite forces at the anterior dentition in Inuit populations in Spencer and Demes 1993) (Ledogar et al. 2016a). However, the model tested here suggests that selection for shorter faces (Lieberman, McBratney, and Krovitz 2002) and a prolonged growth schedule (Schultz 1960b) in the lineage leading to modern humans would have had the concomitant effect of delaying molar emergence.

## Study of Masticatory Morphology and Future Research

### *A Cautionary Note on Using Models*

To understand systematically how masticatory configuration is coordinated throughout ontogeny to avoid TMJ distraction, a mathematical model was used that treats the jaw as if it were a Class III lever (Gysi 1921; Greaves 1978; Smith 1978; Spencer 1995). This model of feeding mechanics is crucial to the study of the ontogeny and evolution of masticatory system function, but it is important to note that, it is a simplification of a complex system and is therefore incomplete to some extent. A fundamental assumption of the hypothesis tested in this dissertation is that the masticatory system grows and functions in accordance with the CLM. While the simplifications of models may obscure the finer details of any mechanical structure, they are necessary in order to answer simple questions that would otherwise go unanswered

due to complex interactions within the system. While the dissertation found support for the hypothesis that the position and timing of molar emergence is constrained by the biomechanics of mastication, there were some exceptions to this finding, particularly among adults. In the future, it will be critical to evaluate the these 'exceptions' in order to gain further insight into the system, which may aid in refining the model. To this end, future studies of the feeding behavior of wild and captive primates, including studies on how chewing kinematics and muscle activation patterns change during ontogeny may provide insight into how subadults and adults may differ in how they use their masticatory systems.

*Evolution of the Masticatory System*

Understanding the proximate and ultimate factors that produce changes in skull morphology is important for reconstructing the lifeways of fossil taxa. Throughout human evolution, for example, large brains and bipedal locomotion have reshaped the neurocranium and the base of the skull (Bastir et al. 2010; Lieberman 2011; Kimbel et al. 2014), while the ability to cook and use tools to prepare food have caused a drastic reduction in the modern human facial skeletons and teeth (Organ et al. 2011; Zink and Lieberman 2016). Understanding the causes of these morphological changes and the sequence of their evolution allows for the formulation of evolutionary scenarios. The morphology of the masticatory system is a compromise among many interrelated factors, including behavior, diet, ontogeny, and phylogeny (Fig. 38) and studying these factors both independently as well as holistically across a wide range of taxa can provide a more nuanced understanding of the selective forces that have shaped the primate skull.

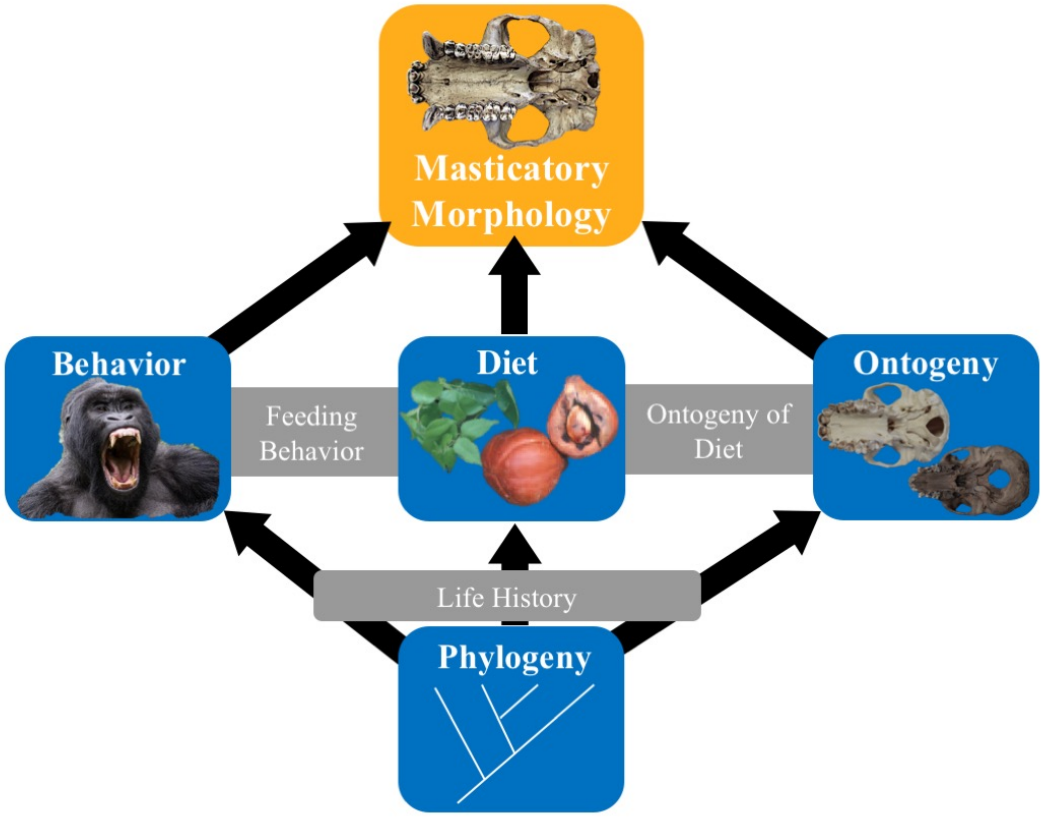


Figure 38. Schematic representing the complex relationship among the factors that contribute to adult masticatory morphology. See text for details.

Diet, and the material properties of food items specifically, are a primary factor that shape masticatory morphology, although the details of how differences in diet affect different species remains unknown, largely due to the complex interactions among factors that produce adult masticatory morphology (e.g., feeding behavior, food mechanical and geometric properties, and loading regimes: Ross et al. 2012). The muscles of mastication must be able to generate enough forces so that mastication can occur and the jaws must be able to withstand the forces produced by these muscles (e.g., Daegling and Hylander

2000; Taylor and Vinyard 2013). Similarly, the chewing surfaces of teeth must be designed to help break down food in an efficient way (Kay 1975; Sheine and Kay 1977). Not trivial are the changes that occur to the chewing surfaces as teeth wear with use. An important feature of teeth is that they should stay functional even as their shapes change with wear as teeth interact with food particles as well as with one another (Janis and Fortelius 1988; Ungar and M'Kirera 2003; King et al. 2005; Glowacka et al. 2016; Pampush et al. 2016).

Behavior also influences the masticatory system. For example, social organization is related to canine size sexual dimorphism in primates such that large, sexually dimorphic canines occur in species where competition for females is high (Plavcan and van Schaik 1992; Plavcan, van Schaik, and Kappeler 1995). Large canines influence the shape of the jaws through their large roots (Plavcan and Daegling 2006; Glowacka, Kimbel, and Johanson 2017), and cause repositioning of the masticatory muscles due to the demand for larger gapes (Hylander 2013). Feeding behavior, at the interface between diet and behavior, is important in producing morphological changes. Primates that perform oral preparation of food with their anterior dentition, for example, exhibit adaptations for this behavior in the masticatory system (e.g., Wright 2005). Feeding behavior is expected to change during ontogeny, as animals begin to consume adult foods (Chalk 2011). The masticatory system changes drastically throughout ontogeny. The eruption of new teeth and the demands of a more adult diet produce growth-related shape changes to the system (Krogman 1930, 1931a, 1931b; Schultz 1960a, 1962; Enlow 1964, 1966; Enlow and Bang 1965; Corner and Richtsmeier 1991, 1992, 1993; Richtsmeier et al. 1993; Humphrey, Dean, and Stringer 1999). Because diet is such an important factor

in producing adult morphology, it is critical to assess how growth-related shifts in the types of food or the frequency of their consumption affect the ontogeny of the masticatory system in primates that vary in masticatory morphology, diet, and growth schedules (e.g., Venkataraman et al. 2014).

All of the above factors are influenced by phylogeny. Behavior, diet, and ontogenetic patterns can be similar in two species simply due to shared ancestry as opposed to independent instances of adaptation (Harvey, Martin, and Clutton-Brock 1987; Harvey and Pagel 1991). Life history is strongly influenced by phylogeny (Kamilar and Cooper 2013). Life history, in turn, affects some of the factors that contribute to adult masticatory morphology, such as the timing of permanent molar and emergence, described in this dissertation, and permanent canine emergence, both of which have consequences for jaw growth (Smith 1989; Schwartz and Dean 2001; Glowacka, Kimbel, and Johanson 2017; Chapter 4).

Much current research focuses on how diet influences adult masticatory form (e.g., Ravosa 2000; Taylor 2006; Vogel et al. 2008, 2014; Strait et al. 2012; Ross and Iriarte-Diaz 2014; Scott et al. 2014; Ravosa et al. 2015), but as discussed above, diet is just one of the many interrelated factors that contribute to adult masticatory morphology. While diet and feeding behavior are key in producing adult masticatory morphology, it is shifts in the rate and timing of growth processes, which are influenced by life history, that ultimately produce evolutionary changes to masticatory morphology (Gould 1977; Alberch et al. 1979; Ravosa and Ross 1994; Leigh, Shah, and Buchanan 2003; Mitteroecker, Gunz, and Bookstein 2005; Leigh 2006a). This dissertation offers one component of the larger group of factors that contribute to masticatory form and function

across primates. By relating the biomechanics of mastication to the position and timing of molar emergence, this dissertation has provided the mechanism that acts during ontogeny to produce variation in molar-emergence ages across primates. Knowing this mechanism not only allows paleoanthropologists to confidently use molar-emergence ages to reconstruct life history in the fossil record, but also offers a biomechanical perspective for understanding craniofacial growth and how it contributes to the diversity of skull form across primates. Future studies should take a holistic approach to understanding the evolution of masticatory diversity by looking at masticatory morphology across a taxonomically wide variety of primate species that vary in life history, diet, and behavior. Relating data on chewing behavior to the mechanical properties of food, the morphology of their masticatory system, both in juvenile and adult primates, including the shape of teeth and a measure of chewing performance will yield a powerful model for understanding the evolution of the chewing system. These types of data will help paleoanthropologists use teeth and masticatory morphology to make more informed dietary and ecological reconstructions of extinct primate species and will ultimately guide a deeper understanding of the forces that have shaped primate skull evolution.

REFERENCES

Ackermann, RR. 2005. “Ontogenetic Integration of the Hominoid Face.” *Journal of Human Evolution* 48 (2): 175–97.

Alberch, P, SJ Gould, GF Oster, and DB Wake. 1979. “Size and Shape in Ontogeny and Phylogeny.” *Paleobiology* 5: 296–317.

Alemseged, Z, F Spoor, WH Kimbel, R Bobe, D Geraads, D Reed, and JG Wynn. 2006. “A Juvenile Early Hominin Skeleton from Dikika, Ethiopia.” *Nature* 443 (7109): 296–301.

Altmann, J, and SC Alberts. 1987. “Body Mass and Growth Rates in a Wild Primate Population.” *Oecologia* 72 (1): 15–20.

———. 2003. “Intraspecific Variability in Fertility and Offspring Survival in a Non-Human Primate: Behavioral Control of Ecological and Social Sources.” In *Offspring: Human Fertility Behavior in a Biodemographic Perspective*, edited by KW Wachter and RA Bulatao, 140–69. Washington, DC: National Academy Press.

———. 2004. “Growth Rates in a Wild Primate Population: Ecological Influences and Maternal Effects.” *Behavioral Ecology and Sociobiology* 57 (5): 490–501.

Anemone, RL, ES Watts, and DR Swindler. 1991. “Dental Development of Known-Age Chimpanzees, *Pan troglodytes* (Primates, Pongidae).” *American Journal of Physical Anthropology* 86: 229–41.

Antón, SC. 1993. “Internal Masticatory Muscle Architecture in the Japanese Macaque and its Influence on Bony Morphology.” *American Journal of Physical Anthropology* 36 (S16): 50.

———. 1996. “Tendon-Associated Bone Features of the Masticatory System in Neandertals.” *Journal of Human Evolution* 31: 391–408.

———. 2000. “Macaque Pterygoid Muscles: Internal Architecture, Fiber Length, and Cross-Sectional Area.” *International Journal of Primatology* 21 (1): 131–56.

Arnold, C, LJ Matthews, and CL Nunn. 2010. “The 10kTrees Website: A New Online

Resource for Primate Phylogeny." *Evolutionary Anthropology* 19 (3). Wiley Subscription Services, Inc., A Wiley Company: 114–18.

Austin, C, TM Smith, A Bradman, K Hinde, R Joannes-Boyau, D Bishop, DJ Hare, P Doble, B Eskenazi, and M Arora. 2013. "Barium Distributions in Teeth Reveal Early-Life Dietary Transitions in Primates." *Nature* 498 (7453): 216–19.

Balolia, KL, C Soligo, and B Wood. 2017. "Sagittal Crest Formation in Great Apes and Gibbons." *Journal of Anatomy* 230 (6): 820–32.

Barrickman, NL, ML Bastian, K Isler, and CP van Schaik. 2008. "Life History Costs and Benefits of Encephalization: A Comparative Test Using Data from Long-Term Studies of Primates in the Wild." *Journal of Human Evolution* 54 (5): 568–90.

Bastir, M, A Rosas, C Stringer, JM Cuétara, R Kruszynski, GW Weber, CF Ross, and MJ Ravosa. 2010. "Effects of Brain and Facial Size on Basicranial Form in Human and Primate Evolution." *Journal of Human Evolution* 58 (5): 424–31.

Bastir, M, P O'Higgins, and A Rosas. 2007. "Facial Ontogeny in Neanderthals and Modern Humans." *Proceedings of the Royal Society B: Biological Sciences* 274 (1614): 1125–32.

Behrensmeyer, AK. 1981. "Vertebrate Paleoecology in a Recent East African Ecosystem." In *Communities of the Past*, edited by J Gray, AJ Boucot, and WBN Berry, 591–615. Strasbourg: Hutchinson Ross Publishing Co.

Behrensmeyer, AK, D Western, and DE Dechant Boaz. 1979. "New Perspectives in Vertebrate Paleoecology from a Recent Bone Assemblage." *Paleobiology* 5: 12–21.

Berger, LR, DJ de Ruiter, SE Churchill, P Schmid, KJ Carlson, PHGM Dirks, and JM Kibii. 2010. "*Australopithecus sediba*: A New Species of *Homo*-like Australopith from South Africa." *Science* 328 (5975): 195–204.

Berger, LR, J Hawks, DJ de Ruiter, SE Churchill, P Schmid, LK Delezene, TL Kivell, et al. 2015. "*Homo naledi*, a New Species of the Genus *Homo* from the Dinaledi Chamber, South Africa." Edited by Johannes Krause and Nicholas J Conard. *eLife* 4: e09560.

Beynon, AD, and MC Dean. 1988. “Distinct Dental Development Patterns in Early Fossil Hominids.” *Nature* 335: 509–14.

Beynon, AD, MC Dean, and DJ Reid. 1991a. “Histological Study on the Chronology of the Developing Dentition in *Gorilla* and *Orangutan*.” *American Journal of Physical Anthropology* 86 (2): 189–203.

———. 1991b. “On Thick and Thin Enamel in Hominoids.” *American Journal of Physical Anthropology* 86 (2): 295–309.

Blanksma, NG, and TMGJ van Eijden. 1990. “Electromyographic Heterogeneity in the Human Temporalis Muscle.” *Journal of Dental Research* 69: 1686–90.

Blanksma, NG, TMGJ van Eijden, and WA Weijs. 1992. “Electromyographic Heterogeneity in the Human Masseter Muscle.” *Journal of Dental Research* 71: 47–52.

Blurton Jones, N, K Hawkes, and JF O’Connell. 1999. “Some Current Ideas about the Evolution of the Human Life History.” In *Comparative Primate Socioecology*, edited by PC Lee, 140–66. London: Cambridge University Press.

Bock, WJ, and G von Wahlert. 1965. “Adaptation and the Form-Function Complex.” *Evolution* 19 (3). Society for the Study of Evolution: 269–99.

Bogin, B. 1999. *Patterns of Human Growth*. 2nd ed. Cambridge: Cambridge University Press.

Boinski, S, RP Quatrone, H Swartz. 2001. "Substrate and tool use by brown capuchins in Suriname: ecological contexts and cognitive bases." *American Anthropologist* 102:741–761.

Boinski, S, and DM Fragaszy. 1989. “The Ontogeny of Foraging in Squirrel Monkeys, *Saimiri oerstedi*.” *Animal Behaviour* 37: 415–28.

Bolter, DR. 2011. “A Comparative Study of Growth Patterns in Crested Langurs and Vervet Monkeys.” *Anatomy Research International* 2011 (January): 12.

Borries, C, A Lu, K Ossi-Lupo, E Larney, and A Koenig. 2011. “Primate Life Histories and Dietary Adaptations: A Comparison of Asian Colobines and Macaques.” *American Journal of Physical Anthropology* 144 (2): 286–99.

Boughner, JC, and MC Dean. 2004. “Does Space in the Jaw Influence the Timing of Molar Crown Initiation? A Model Using Baboons (*Papio anubis*) and Great Apes (*Pan troglodytes, Pan paniscus*).” *Journal of Human Evolution* 46 (3): 255–77.

Boyde, A. 1963. “Estimation of Age at Death of Young Human Skeletal Remains from Incremental Lines in the Dental Enamel.” In *Third International Meeting in Forensic Immunology, Medicine, Pathology, and Toxicology*, 16–24. London.

———. 1964. “The Structure and Development of Mammalian Enamel. PhD Dissertation, University of London.” University of London.

———. 1990. “Developmental Interpretation of Dental Microstructure.” In *Primate Life History and Evolution*, edited by CJ De Rousseau, 229–67. New York: Wiley-Liss.

Brace, CL. 1962. “Refocusing on the Neanderthal Problem.” *American Anthropologist* 64 (4): 729–41.

Bradley, RE. 1961. “The Relationship between Eruption, Calcification, and Crowding of Certain Mandibular Teeth.” *The Angle Orthodontist* 41: 230–36.

Bramble, DM. 1978. “Origin of the Mammalian Feeding Complex: Models and Mechanisms.” *Paleobiology* 4 (3): 271–301.

Breuer, T, M Breuer-Ndoundou Hockemba, C Olejniczak, RJ Parnell, and EJ Stokes. 2009. “Physical Maturation, Life-History Classes and Age Estimates of Free-Ranging Western Gorillas-Insights from Mbeli Bai, Republic of Condo.” *American Journal of Physical Anthropology* 71: 106–19.

Bromage, TG, and MC Dean. 1985. “Re-Evaluation of the Age at Death of Immature Fossil Hominids.” *Nature* 317: 525–27.

Brown, F, J Harris, R Leakey, and A Walker. 1985. “Early Homo Erectus Skeleton from West Lake Turkana, Kenya.” *Nature* 316: 788–92.

Burnham, KP, and D Anderson. 2002. *Model Selection and Multi-Model Inference*. New York: Springer.

Cachel, S. 1984. "Growth and Allometry in Primate Masticatory Muscles." *Archives of Oral Biology* 29 (4): 287–93.

Cameron, EZ. 1998. "Is Suckling Behaviour a Useful Predictor of Milk Intake? A Review." *Animal Behaviour* 56: 521–32.

Cerling, TE, E Mbua, FM Kirera, F Kyalo Manthi, FE Grine, MG Leakey, M Sponheimer, and KT Uno. 2011. "Diet of *Paranthropus boisei* in the Early Pleistocene of East Africa." *Proceedings of the National Academy of Sciences of the United States of America* 108 (23): 9337–41.

Chalk, J. 2011. "The Effects of Feeding Strategies and Food Mechanics on the Ontogeny of Masticatory Function in the *Cebus libidinosus* Cranium." PhD Dissertation, The George Washington University.

Chalk, J, BW Wright, PW Lucas, KD Schuhmacher, ER Vogel, D Fragaszy, E Visalberghi, P Izar, and BG Richmond. 2016. "Age-Related Variation in the Mechanical Properties of Foods Processed by *Sapajus libidinosus*." *American Journal of Physical Anthropology* 159 (2): 199–209.

Chalk-Wilayto, J, K Ossi-Lupo, and M Raguet-Schofield. 2016. "Growing up Tough: Comparing the Effects of Food Toughness on Juvenile Feeding in *Sapajus libidinosus* and *Trachypithecus phayrei crepusculus*." *Journal of Human Evolution* 98: 76–89.

Charnov, EL. 1993. *Life History Invariants: Some Explorations of Symmetry in Evolutionary Ecology*. Oxford: Oxford University Press.

Charnov, EL, and D Berrigan. 1993. "Why Do Female Primates Have Such Long Lifespans and so Few Babies? Or Life in the Slow Lane." *Evolutionary Anthropology* 1 (6): 191–94.

Cobb, SN, and P O'Higgins. 2004. "Hominins Do Not Share a Common Postnatal Facial Ontogenetic Shape Trajectory." *Journal of Experimental Zoology* 302 (3): 302–21.

Cofran, Z. 2014. “Mandibular Development in *Australopithecus robustus*.” *American Journal of Physical Anthropology* 154 (3): 436–46.

Coiner-Collier, S, RS. Scott, J Chalk-Wilayto, SM Cheyne, P Constantino, NJ Dominy, AA Elgart, et al. 2016. “Primate Dietary Ecology in the Context of Food Mechanical Properties.” *Journal of Human Evolution* 98: 103–18.

Conroy, GC, and MW Vannier. 1991. “Dental Development in South African Australopithecines. Part II: Dental Stage Assessment.” *American Journal of Physical Anthropology* 86 (2): 137–56.

Corner, BD, and JT Richtsmeier. 1991. “Morphometric Analysis of Craniofacial Growth in *Cebus apella*.” *American Journal of Physical Anthropology* 84: 323–42.

———. 1992. “Cranial Growth in the Squirrel Monkey (*SamirisSciureus*): A Quantitative Analysis Using Three Dimensional Coordinate Data.” *American Journal of Physical Anthropology* 87: 67–81.

———. 1993. “Cranial Growth and Dimorphism in *Ateles geoffroyi*.” *American Journal of Physical Anthropology* 92: 371–94.

Corp, N, and R Byrne. 2002. “The Ontogeny of Manual Skill in Wild Chimpanzees: Evidence from Feeding on the Fruit of *Saba florida*.” *Behaviour* 139 (1): 137–68.

Daegling, DJ. 2004. “Relationship of Strain Magnitude to Morphological Variation in the Primate Skull.” *American Journal of Physical Anthropology* 124 (4): 346–52.

———. 2010. “Understanding Skull Function from a Mechanobiological Perspective.” In *A Companion to Biological Anthropology*, edited by CS Larsen, 501–15. Oxford: Wiley-Blackwell.

Daegling, DJ, and FE Grine. 1991. “Compact Bone Distribution and Biomechanics of Early Hominid Mandibles.” *American Journal of Physical Anthropology* 86 (3): 321–39.

Daegling, DJ, and WL Hylander. 2000. “Experimental Observation, Theoretical Models, and Biomechanical Inference in the Study of Mandibular Form.” *American Journal of Physical Anthropology* 112 (4): 541–51.

Dean, MC. 1987. “Growth Layers and Incremental Markings in Hard Tissues; a Review of the Literature and Some Preliminary Observations about Enamel Structure in *Paranthropus boisei*.” *Journal of Human Evolution* 16: 157–72.

———. “Tooth Microstructure Tracks the Pace of Human Life-History Evolution.” *Proceedings of the Royal Society B: Biological Sciences* 273 (1603): 2799–2808.

Dean, MC, and AD Beynon. 1991a. “Histological Reconstruction of Crown Formation Times and Initial Root Formation Times in a Modern Human Child.” *American Journal of Physical Anthropology* 86 (2): 215–28.

———. 1991b. “Tooth Crown Heights, Tooth Wear, Sexual Dimorphism and Jaw Growth in Hominoids.” *Zeitschrift Fur Morphologie Und Anthropologie* 78: 425–40.

Dean, MC, AD Beynon, JF Thackeray, and GA Macho. 1993. “Histological Reconstruction of Dental Development and Age at Death of a Juvenile *Paranthropus robustus* Specimen, SK 63, from Swartkrans, South Africa.” *American Journal of Physical Anthropology* 91 (4). Wiley Subscription Services, Inc., A Wiley Company: 401–19.

Dean, MC, MG Leakey, DJ Reid, F Schrenk, GT Schwartz, C Stringer, and A Walker. 2001. “Growth Processes in Teeth Distinguish Modern Humans from *Homo erectus* and Earlier Hominins.” *Nature* 414 (6864): 628–31.

Dechow, PC, and DS Carlson. 1990. “Occlusal Force and Craniofacial Biomechanics during Growth in Rhesus Monkeys.” *American Journal of Physical Anthropology* 83 (2): 219–37.

Demes, B. 1987. “Another Look at an Old Face: Biomechanics of the Neandertal Facial Skeleton Reconsidered.” *Journal of Human Evolution* 16: 297–303.

Demes, B, and N Creel. 1988. “Bite Force, Diet, and Cranial Morphology of Fossil Hominids.” *Journal of Human Evolution* 17 (7): 657–70.

Dickson, E, LC Fitton, and K Kupczik. 2017. “Scaling Relationships within Architectural Properties of the Jaw Adductormusculature in *Macaca fascicularis*.” *American Journal of Physical Anthropology* 162 (S64): 162.

Dirks, PHGM, LR Berger, EM Roberts, JD Kramers, J Hawks, PS Randolph-Quinney, M Elliott, et al. 2015. "Geological and Taphonomic Context for the New Hominin Species *Homo Naledi* from the Dinaledi Chamber, South Africa." *eLife* 4: e09561.

Dirks, W. 1998. "Histological Reconstruction of Dental Development and Age at Death in a Juvenile Gibbon (*Hylobates Lar*)." *Journal of Human Evolution* 35 (4–5): 411–25.

Dirks, W. 2003. "Effect of Diet on Dental Development in Four Species of Catarrhine Primates." *American Journal of Primatology* 61 (1): 29–40.

Dirks, W, and JE Bowman. 2007. "Life History Theory and Dental Development in Four Species of Catarrhine Primates." *Journal of Human Evolution* 53 (3): 309–20.

Dirks, W, DJ Reid, CJ Jolly, JE Phillips-Conroy, and FL Brett. 2002. "Out of the Mouths of Baboons: Stress, Life History, and Dental Development in the Awash National Park Hybrid Zone, Ethiopia." *American Journal of Physical Anthropology* 118: 239–52.

du Brul, EL. 1976. "Early Hominid Feeding Mechanisms." *American Journal of Physical Anthropology* 47: 305–20.

Duterloo, HS, and DH Enlow. 1970. "A Comparative Study of Cranial Growth in *Homo* and *Macaca*." *American Journal of Anatomy* 127: 357–68.

Eaglen, RH. 1985. "Behavioral Correlates of Tooth Eruption in Madagascar Lemurs." *American Journal of Physical Anthropology* 66 (3): 307–15.

Edmonds, HM, and H Glowacka. 2014. "The Ontogeny of Bite Force: A Test of the Constrained Lever Model." *American Journal of Physical Anthropology* 153 (S58): 112.

Emery TM, MN Muller, K Sabbi, ZP Machanda, E Otali, and RW Wrangham. 2016. "Faster Reproductive Rates Trade off against Offspring Growth in Wild Chimpanzees." *Proceedings of the National Academy of Sciences of the United States of America* 113 (28): 7780–85.

Enlow, DH. 1964. "A Study of the Postnatal Growth of the Human Mandible." *American*

*Journal of Orthodontics* 50: 25–50.

———. 1966. “A Comparative Study of Facial Growth in *Homo* and *Macaca*.” *American Journal of Physical Anthropology* 24 (3): 293–308.

Enlow, DH, and MG Hans. 1996. *Essentials of Facial Growth*. Philadelphia: WB Saunders Company.

Enlow, DH, and RE Moyers. 1971. “Growth and Architecture of the Face.” *The Journal of the American Dental Association* 82: 763–74.

Enlow, DH, and S Bang. 1965. “Growth and Remodeling of the Human Maxilla.” *American Journal of Orthodontics* 51: 446–64.

Enlow, DH, Moyers RE, Hunter WS, and JA Jr McNamara. 1969. “A Procedure for the Analysis of Intrinsic Facial Form and Growth.” *American Journal of Orthodontics* 56: 6–23.

Evans, AR, ES Daly, KK Catlett, KS Paul, SJ King, MM Skinner, HP Nesse, et al. 2016. “A Simple Rule Governs the Evolution and Development of Hominin Tooth Size.” *Nature* 530 (7591): 477–80.

Fleagle, JG, CC Gilbert, and AL Baden. 2010. “Primate Cranial Diversity.” *American Journal of Physical Anthropology* 142 (4): 565–78.

Freckleton, RP, PH Harvey, and M Pagel. 2002. “Phylogenetic Analysis and Comparative Data: A Test and Review of Evidence.” *The American Naturalist* 160 (6): 712–26.

Galbany, J, D Abavandimwe, M Vakiener, W Eckardt, A Mudakikwa, F Ndagijimana, TS Stoinski, and SC McFarlin. 2017. “Body Growth and Life History in Wild Mountain Gorillas (*Gorilla Beringei Beringei*) from Volcanoes National Park, Rwanda.” *American Journal of Physical Anthropology*. doi:10.1002/ajpa.23232.

Galbany, J, O Imanizabayo, A Romero, V Vecellio, H Glowacka, MR Cranfield, TG Bromage, A Mudakikwa, TS Stoinski, and SC McFarlin. 2016. “Tooth Wear and Feeding Ecology in Mountain Gorillas from Volcanoes National Park, Rwanda.” *American Journal of Physical Anthropology* 159 (3): 457–65.

Galdikas, BMF, and JW Wood. 1990. “Birth Spacing Patterns in Humans and Apes.” *American Journal of Physical Anthropology* 83 (2):185–91.

Garland , T Jr, and AR Ives. 2000. “Using the Past to Predict the Present: Confidence Intervals for Regression Equations in Phylogenetic Comparative Methods.” *The American Naturalist* 155 (3): 346–64.

Glowacka, H, and GT Schwartz. 2017. “The Ontogeny of Masticatory Efficiency and Implications for Hominin Canine Reduction.” *American Journal of Physical Anthropology* 162 (S64): 195–96.

Glowacka, H, SC McFarlin, ER Vogel, TS Stoinski, F Ndagijimana, D Tuyisingize, A Mudakikwa, and GT Schwartz. 2017. “Toughness of the Virunga Mountain Gorilla (*Gorilla beringei beringei*) Diet across an Altitudinal Gradient.” *American Journal of Primatology*. doi: 10.1002/ajp.22661.

Glowacka, H, SC McFarlin, KK Catlett, A Mudakikwa, TG Bromage, MR Cranfield, TS Stoinski, and GT Schwartz. 2016. “Age-Related Changes in Molar Topography and Shearing Crest Length in a Wild Population of Mountain Gorillas from Volcanoes National Park, Rwanda.” *American Journal of Physical Anthropology* 160 (1): 3–15.

Glowacka, H, WH Kimbel, and DC Johanson. 2017. “Aspects of Mandibular Ontogeny in *Australopithecus afarensis*.” In *Human Paleontology and Prehistory: Contributions in Honor of Yoel Rak*, edited by A Marom and E Hovers, 127–44. Cham: Springer International Publishing.

Godfrey, LR, KE Samonds, WL Jungers, and MR Sutherland. 2001. “Teeth, Brains, and Primate Life Histories.” *American Journal of Physical Anthropology* 114 (3): 192–214.

Godfrey, LR, KE Samonds, WL Jungers, and MR Sutherland. 2003. “Dental Development and Primate Life Histories.” In *Primate Life Histories and Socioecology*, edited by PM Kappeler and ME Perreira, 177–203. Chicago: The University of Chicago Press.

Godfrey, LR, GT Schwartz, KE Samonds, WL Jungers, and KK Catlett. 2006. “The Secrets of Lemur Teeth.” *Evolutionary Anthropology* 15 (4): 142–54.

Godfrey, LR, KE Samonds, WL Jungers, MR Sutherland, and MT Irwin. 2004.

"Ontogenetic Correlates of Diet in Malagasy Lemurs." *American Journal of Physical Anthropology* 123 (3): 250–76.

Gordon, JE. 1978. "Structures, or Why Don't Things Fall Down." Princeton: Princeton University Press.

Gould, SJ. 1977. *Ontogeny and Phylogeny*. Cambridge: Harvard University Press.

Grafen, A. 1989. "The Phylogenetic Regression." *Philosophical Transactions of the Royal Society of London. Series B, Biological Sciences* 326 (1233): 119–57.

Greaves, WS. 1978. "The Jaw Lever System in Ungulates: A New Model." *Journal of Zoology* 184: 271–85.

———. 1983. "A Functional Analysis of Carnassial Biting." *Biological Journal of the Linnean Society* 20 (4): 353–63.

———. 1982. "A Mechanical Limitation on the Position of the Jaw Muscles of Mammals: The One-Third Rule." *Journal of Mammalogy* 63 (2): 261–66.

———. 1988. "The Maximum Average Bite Force for a given Jaw Length." *Journal of Zoology* 214 (2): 295–306.

———. 1991. "The Orientation of the Force of the Jaw Muscles and the Length of the Mandible in Mammals." *Zoological Journal of the Linnean Society* 102 (4): 367–74.

———. 2000. "Location of the Vector of Jaw Muscle Force in Mammals." *Journal of Morphology* 243 (3): 293–99.

Gunst, N, J-B Leca, S Boinski, and D Fragaszy. 2010. "The Ontogeny of Handling Hard-to-Process Food in Wild Brown Capuchins (*Cebus apella apella*): Evidence from Foraging on the Fruit of *Maximiliana maripa*." *American Journal of Primatology* 72 (11): 960–73.

Gysi, S. 1921. "Studies on the Leverage Problem of the Mandible." *Dental Digest* 27 (74): 144.

Harcourt, AH. 1978. “Strategies of Emigration and Transfer by Primates, with Particular Reference to Gorillas.” *Zeitschrift Für Tierpsychologie* 48 (4): 401–20.

Harris, TR, CA Chapman, and SL Monfort. 2010. “Small Folivorous Primate Groups Exhibit Behavioral and Physiological Effects of Food Scarcity.” *Behavioral Ecology* 21: 46–56.

Harvati, K. 2000. “Dental Eruption Sequence among Colobine Primates.” *American Journal of Physical Anthropology* 112 (1): 69–85.

Harvey, PH, and M Pagel. 1991. “The Comparative Method for Studying Adaptation.” *The Comparative Method in Evolutionary Biology*, 1–34.

Harvey, PH, and TH Clutton-Brock. 1985. “Life History Variation in Primates.” *Evolution* 39 (3): 559–81.

Harvey, PH, RD Martin, and TH Clutton-Brock. 1987. “Life Histories in Comparative Perspective.” In *Primate Societies*, edited by BB Smuts, DL Cheney, RM Seyfarth, RW Wrangam, and TT Struhsaker, 181–96. Chicago: University of Chicago Press.

Hawkes, K. 2006. “Slow Life Histories and Human Evolution.” In *The Evolution of Human Life History*, 95–126. Santa Fe: School of American Research Press.

Hawkes, K, JF O’Connell, NG Blurton Jones, H Alvarez, and EL Charnov. 1998. “Grandmothering, Menopause, and the Evolution of Human Life Histories.” *Proceedings of the National Academy of Sciences of the United States of America* 95 (February): 1336–39.

Hawks, J, M Elliott, P Schmid, SE Churchill, DJ de Ruiter, EM Roberts, H Hilbert-Wolf, et al. 2017. “New Fossil Remains of *Homo naledi* from the Lesedi Chamber, South Africa.” *eLife* 6: e24232.

Hens, SM. 2005. “Ontogeny of Craniofacial Sexual Dimorphism in the Orangutan (*Pongo pygmaeus*). I: Face and Palate.” *American Journal of Primatology* 65 (2): 149–66.

Herring, SW. 1985. “The Ontogeny of Mammalian Mastication.” *American Zoologist* 25 (2): 339–50.

Herring, SW, AF Grimm, and BR Grimm. 1979. “Functional Heterogeneity in a Multipinnate Muscle.” *American Journal of Anatomy* 154 (4): 563–75.

Humphrey, LT. 2010. “Weaning Behaviour in Human Evolution.” *Seminars in Cell and Developmental Biology* 21: 453–61.

Humphrey, LT, MC Dean, and CB Stringer. 1999. “Morphological Variation in Great Ape and Modern Human Mandibles.” *Journal of Anatomy* 195 (November): 491–513.

Hylander, WL. 1985a. “Mandibular Function and Biomechanical Stress and Scaling.” *Integrative and Comparative Biology* 25 (2): 315–30.

———. 1985b. “Mandibular Function and Temporomandibular Joint Loading.” In *Developmental Aspects of Temporomandibular Joint Disorders. Monograph 16, Craniofacial Growth Series, Center for Human Growth and Development*, edited by DS Carlson, JA McNamara, and KA Ribbens, 19–35. Ann Arbor: University of Michigan.

———. 2013. “Functional Links between Canine Height and Jaw Gape in Catarrhines with Special Reference to Early Hominins.” *American Journal of Physical Anthropology* 150: 247–59.

———. 2017. “Canine Height and Jaw Gape in Catarrhines with Reference to Canine Reduction in Early Hominins.” In *Human Paleontology and Prehistory*, edited by A Marom and E Hovers, 71–93. New York: Springer.

Hylander, WL, and KR Johnson. 1985. “Temporalis and Masseter Muscle Function during Incision in Macaques and Humans.” *International Journal of Primatology* 6 (3): 289–322.

Hylander, WL, CE Wall, CJ Vinyard, C Ross, MR Ravosa, SH Williams, and KR Johnson. 2005. “Temporalis Function in Anthropoids and Strepsirrhines: An EMG Study.” *American Journal of Physical Anthropology* 128 (1): 35–56.

Hylander, WL, CJ Vinyard, CE Wall, SH Williams, and KR Johnson. 2011. “Functional and Evolutionary Significance of the Recruitment and Firing Patterns of the Jaw Adductors during Chewing in Verreaux’s Sifaka (*Propithecus verreauxi*).” *American Journal of Physical Anthropology* 145 (4): 531–47.

Janis, CM, and M Fortelius. 1988. “On the Means Whereby Mammals Achieve Increased Functional Durability of Their Dentitions, with Special Reference to Limiting Factors.” *Biological Reviews* 63: 197–230.

Janson, C, and C van Schaik. 1993. “Ecological Risk Aversion in Juvenile Primates: Slow and Steady Wins the Race.” In *Juvenile Primates: Life History, Development and Behavior*, edited by ME Pereira and LA Fairbanks, 57–76. New York: Oxford University Press.

Johnson, SE. 2003. “Life History and the Competitive Environment: Trajectories of Growth, Maturation, and Reproductive Output among Chacma Baboons.” *American Journal of Physical Anthropology* 120: 83–98.

Jurmain, R. 1997. “Skeletal Evidence of Trauma in African Apes, with Special Reference to the Gombe Chimpanzees.” *Primates* 38 (1): 1–14.

Kamilar, JM, and N Cooper. 2013. “Phylogenetic Signal in Primate Behaviour, Ecology and Life History.” *Philosophical Transactions of the Royal Society B: Biological Sciences* 368 (1618).

Kavanagh, KD, AR Evans, and J Jernvall. 2007. “Predicting Evolutionary Patterns of Mammalian Teeth from Development.” *Nature* 449 (7161): 427–32.

Kay, RF. 1975. “The Functional Adaptations of Primate Molar Teeth.” *American Journal of Physical Anthropology* 43 (2): 195–216.

Kelley, J. 1997. “Paleobiological and Phylogenetic Significance of Life History in Miocene Hominoids.” In *Function, Phylogeny, and Fossils: Miocene Hominoid Evolution and Adaptations*, edited by DR Begun, CV Ward, and MD Rose, 173–208. New York: Plenum.

———. 2002. “Life History Evolution in Miocene and Extant Apes.” In *Human Evolution Through Developmental Change*, edited by N Minugh-Purvis and KJ McNamara, 223–48. Baltimore: Johns Hopkins University Press.

Kelley, J, and GT Schwartz. 2010. “Dental Development and Life History in Living African and Asian Apes.” *Proceedings of the National Academy of Sciences of the United States of America* 107 (3): 1035–40.

———. 2012. “Life-History Inference in the Early Hominins *Australopithecus* and *Paranthropus*.” *International Journal of Primatology* 33 (6): 1332–63.

Kelley, J, and TM Smith. 2003. “Age at First Molar Emergence in Early Miocene *Afropithecus turkanensis* and Life-History Evolution in the Hominoidea.” *Journal of Human Evolution* 44 (3): 307–29.

Kennedy, GE. 2005. “From the Ape’s Dilemma to the Weanling’s Dilemma: Early Weaning and Its Evolutionary Context.” *Journal of Human Evolution* 48: 123–45.

Kiliaridis, S. 1995. “Masticatory Muscle Influence on Craniofacial Growth.” *Acta Odontologica Scandinavica* 53 (3). Informa Scandinavian: 196–202.

Kimbel, WH, and B Villmoare. 2016. “From *Australopithecus* to *Homo*: The Transition That Wasn’t.” *Philosophical Transactions of the Royal Society B: Biological Sciences* 371 (1698).

Kimbel, WH, and Y Rak. 2017. “*Australopithecus Sediba* and the Emergence of *Homo*: Questionable Evidence from the Cranium of the Juvenile Holotype MH 1.” *Journal of Human Evolution* 107: 94–106.

Kimbel, WH, G Suwa, B Asfaw, Y Rak, and TD White. 2014. “*Ardipithecus ramidus* and the Evolution of the Human Cranial Base.” *Proceedings of the National Academy of Sciences* 111 (3): 948–53.

King, SJ, SJ Arrigo-Nelson, ST Pochron, GM Semprebon, LR Godfrey, PC Wright, and J Jernvall. 2005. “Dental Senescence in a Long-Lived Primate Links Infant Survival to Rainfall.” *Proceedings of the National Academy of Sciences of the United States of America* 102 (46): 16579–83.

Klingenberg, CP, K Mebus, and J-C Auffray. 2003. “Developmental Integration in a Complex Morphological Structure: How Distinct Are the Modules in the Mouse Mandible?” *Evolution and Development* 5 (5). Blackwell Science Inc: 522–31.

Koenig, A. 2000. “Competitive Regimes in Forest-Dwelling Hanuman Langur Females (*Semnopithecus entellus*).” *Behavioral Ecology and Sociobiology* 48: 93–109.

Koenig, A, C Borries, MK Chalise, and P Winker. 1997. “Ecology, Nutrition, and Timing

of Reproductive Events in an Asian Primate, the Hanuman Langur (*Presbytis entellus*)." *Journal of Zoology* 243: 215–35.

Koolstra, JH, TMGJ van Eijden, WA Weijs, and M Naeije. 1988. "A Three-Dimensional Mathematical Model of the Human Masticatory System Predicting Maximum Possible Bite-Forces." *Journal of Biomechanics* 21: 563–76.

Koyabu, DB, and H Endo. 2009. "Craniofacial Variation and Dietary Adaptations of African Colobines." *Journal of Human Evolution* 56 (6): 525–36.

Kralick, AE, M L Burgess, H Glowacka, K Arbenz-Smith, K McGrath, CB Ruff, K Chong Chan, et al. 2017. "A Radiographic Study of Permanent Molar Development in Wild Virunga Mountain Gorillas of Known Chronological Age from Rwanda." *American Journal of Physical Anthropology* 163 (1): 129–47.

Krogman, WM. 1930. "Studies in Growth Changes in the Skull and Face of Anthropoids. I. The Eruption of the Teeth in Anthropoids and Old World Apes." *American Journal of Anatomy* 46 (2): 303–13.

———. 1931a. "Studes in Growth Changes in the Skull and Face of Anthropoids III. Growth Changes in the Skull and Face of the Gorilla." *American Journal of Anatomy* 47 (1): 89–115.

———. 1931b. "Studies in Growth Changes in the Skull and Face of Anthropoids. IV. Growth Changes in the Skull and Face of the Chimpanzee." *American Journal of Anatomy* 47 (2): 325–42.

Krovitz, GE. 2003. "Shape and Growth Differences between Neandertals and Modern." In *Patterns of Growth and Development in the Genus* Homo, edited by JL Thompson, GE Krovitz, and AJ Nelson, 320–42. New York: Cambridge University Press.

La Croix, S, ML Zelditch, JA Shivik, BL Lundrigan, and KE Holekamp. 2011. "Ontogeny of Feeding Performance and Biomechanics in Coyotes." *Journal of Zoology* 285 (4): 301–15.

Le Cabec, A, MC Dean, and DR Begun. 2017. "Dental Development and Age at Death of the Holotype of *Anapithecus hernyaki* (RUD 9) Using Synchrotron Virtual Histology." *Journal of Human Evolution* 108: 161–75.

Ledogar, JA, AL Smith, S Benazzi, GW Weber, MA Spencer, KB Carlson, KP McNulty, PC Dechow, IR Grosse, and CF Ross. 2016b. "Mechanical Evidence That *Australopithecus sediba* Was Limited in Its Ability to Eat Hard Foods." *Nature Communications* 7: 10596.

Ledogar, JA, PC Dechow, Q Wang, PH Gharpure, AD Gordon, KL Baab, AL Smith, et al. 2016a. "Human Feeding Biomechanics: Performance, Variation, and Functional Constraints." *PeerJ* 4: e2242.

Lee, PC. 1996. "The Meanings of Weaning: Growth, Lactation, and Life History." *Evolutionary Anthropology* 5 (3): 87–98.

Lee-Thorp, JA, NJ van der Merwe, and CK Brain. 1994. "Diet of *Australopithecus robustus* at Swartkrans from Stable Carbon Isotopic Analysis." *Journal of Human Evolution* 27: 361–72.

Leigh, SR. 1994. "Ontogenetic Correlates of Diet in Anthropoid Primates." *American Journal of Physical Anthropology* 94 (4): 499–522.

———. 2004. "Brain Growth, Life History, and Cognition in Primate and Human Evolution." *American Journal of Primatology* 62 (3): 139–64.

———. 2006a. "Cranial Ontogeny of Papio Baboons (*Papio hamadryas*)." *American Journal of Physical Anthropology* 130 (1): 71–84.

———. 2006b. "Growth and Development." In *The Baboon in Biomedical Research*, edited by JL VandeBerg, S Williams-Blangero, and S Tardiff, 57–88. New York: Kluwer Academic Press.

Leigh, SR, and RM Bernstein. 2006. "Ontogeny, Life History, and Maternal Investment in Baboons." In *Reproduction and Fitness in Baboons: Behavioral, Ecological, and Life History Perspectives*, edited by L Swedell and SR Leigh, 225–55. Boston, MA: Springer US.

Leigh, SR, JM Setchell, and LS Buchanan. 2005. "Ontogenetic Bases of Canine Dimorphism in Anthropoid Primates." *American Journal of Physical Anthropology* 127 (3): 296–311.

Leigh, SR, NF Shah, and LS Buchanan. 2003. "Ontogeny and Phylogeny in Papionin Primates." *Journal of Human Evolution* 45 (4): 285–316.

Lieberman, DE. 2011. *The Evolution of the Human Head*. London: The Belknap Press of Harvard University Press.

Lieberman, DE, BM McBratney, and G Krovitz. 2002. "The Evolution and Development of Cranial Form in *Homo sapiens*." *Proceedings of the National Academy of Sciences of the United States of America* 99: 1134–39.

Lieberman, DE, GE Krovitz, FW Yates, M Devlin, and M St Claire. 2004. "Effects of Food Processing on Masticatory Strain and Craniofacial Growth in a Retrognathic Face." *Journal of Human Evolution* 46 (6): 655–77.

Liversidge, H. 2003. "Variation in Modern Human Dental Development." In *Patterns of Growth in the Genus* Homo, edited by JL Thompson, GE Krovitz, and JN Andrew, 73–113. Cambridge: Cambridge University Press.

Lucas, L. 2012. "Variation in Dental Morphology and Bite Force Along the Tooth Row in Anthropoids." PhD Dissertation, Arizona State University.

Lucas, PW. 2004. *Dental Functional Morphology*. Cambridge: Cambridge University Press.

Lucas, PW, IM Turner, NJ Dominy, and N Yamashita. 2000. "Mechanical Defences to Herbivory." *Annals of Botany* 86 (5): 913–20.

Macchiarelli, R, L Bondioli, A Debénath, A Mazurier, J-F Tournepiche, W Birch, and MC Dean. 2006. "How Neanderthal Molar Teeth Grew." *Nature* 444 (7120): 748–51.

Machanda, Z, NF Brazeau, AB Bernard, RM Donovan, AM Papakyrikos, R Wrangham, and TM Smith. 2015a. "Dental Eruption in East African Wild Chimpanzees." *Journal of Human Evolution* 82: 137–44.

Machanda, Z, NF Brazeau, E Castillo, E Otarola-Castillo, H Ponzer, ME Thompson, M Muller, and R Wrangham. 2015b. "Musculoskeletal Growth Patterns in Wild Chimpanzees (*Pan troglodytes*)." *American Journal of Physical Anthropology* 156:

210.

Madrigal, L, and M Meléndez-Obando. 2008. “Grandmothers’ Longevity Negatively Affects Daughters’ Fertility.” *American Journal of Physical Anthropology* 136 (2): 223–29.

Manns, A, R Miralles, and C Palazzi. 1979. “EMG, Bite Force, and Elongation of the Masseter Muscle under Isometric Voluntary Contractions and Variations of Vertical Dimension.” *The Journal of Prosthetic Dentistry* 42 (6): 674–82.

Martin, RD. 1983. *Human Brain Evolution in an Ecological Context*. American Museum of Natural History.

Martinez-Maza, C, A Rosas, and M Nieto-Díaz. 2013. “Postnatal Changes in the Growth Dynamics of the Human Face Revealed from Bone Modelling Patterns.” *Journal of Anatomy* 223 (3): 228–41.

Masi, S. 2007. “Seasonal Influence of Foraging Strategies, Activity and Energy Budgets of Western Lowland Gorillas (*Gorilla gorilla gorilla*) in Bai-Hokou, Central African Republic.” PhD Dissertation, University of Roma.

McCarthy, RC. 2004. “Constraints and Primate Craniofacial Growth and Form.” PhD Dissertation, George Washington University.

McFarlin, SC, SK Barks, MW Tocheri, JS Massey, AB Eriksen, KA Fawcett, TS Stoinksi, et al. 2013. “Early Brain Growth Cessation in Wild Virunga Mountain Gorillas (*Gorilla beringei beringei*).” *American Journal of Primatology* 75 (5): 450–63.

McFarlin, SC, TG Bromage, AA Lilly, MR Cranfield, SP Nawrocki, A Eriksen, D Hunt, A Ndacyayisenga, C Kanimba Misago, and A Mudakikwa. 2009. “Recovery and Preservation of a Mountain Gorilla Skeletal Resource in Rwanda.” *American Journal of Physical Anthropology* 148 (S48): 187–88.

McGraw, WS, and DJ Daegling. 2012. “Primate Feeding and Foraging: Integrating Studies of Behavior and Morphology.” *Annual Review of Anthropology* 41 (1): 203–19.

McGraw, WS, A van Casteren, E Kane, E Geissler, B Burrows, and DJ Daegling. 2016. "Feeding and Oral Processing Behaviors of Two Colobine Monkeys in Tai Forest, Ivory Coast." *Journal of Human Evolution* 98: 90–102.

Mitteroecker, P, P Gunz, and FL Bookstein. 2005. "Heterochrony and Geometric Morphometrics: A Comparison of Cranial Growth in *Pan paniscus* versus *Pan troglodytes*." *Evolution and Development* 7 (3): 244–58.

Moss, ML. 1997a. "The Functional Matrix Hypothesis Revisited. 1. The Role of Mechanotransduction." *American Journal of Orthodontics and Dentofacial Orthopedics* 112 (1): 8–11.

———. 1997b. "The Functional Matrix Hypothesis Revisited. 2. The Role of an Osseous Connected Cellular Network." *American Journal of Orthodontics and Dentofacial Orthopedics* 112 (2): 221–26.

———. 1997c. "The Functional Matrix Hypothesis Revisited. 3. The Genomic Thesis." *American Journal of Orthodontics and Dentofacial Orthopedics* 112 (3): 338–42.

———. 1997d. "The Functional Matrix Hypothesis Revisited. 4. The Epigenetic Antithesis and the Resolving Synthesis." *American Journal of Orthodontics and Dentofacial Orthopedics* 112 (4): 410–17.

Moss, ML, and L Salentijn. 1969a. "The Primary Role of Functional Matrices in Facial Growth." *American Journal of Orthodontics* 55 (6): 566–77.

———. 1969b. "The Capsular Matrix." *American Journal of Orthodontics* 56 (5): 474–90.

Moss, ML, and RW Young. 1960. "A Functional Approach to Craniology." *American Journal of Physical Anthropology* 18: 281–92.

Muggeo, VMR. 2008. "Segmented: An R Package to Fit Regression Models with Broken-Line Relationships." *R News* 8 (1): 20–25.

Nargolwalla, MC, DR Begun, MC Dean, DJ Reid, and L Kordos. 2005. "Dental Development and Life History in *Anapithecus hernyaki*." *Journal of Human Evolution* 49 (1): 99–121.

Neter, J, W Wasserman, and M Kutner. 1985. *Applied Linear Statistical Models*. Homewood, IL: Irwin Press.

Nowell, A, and A Fletcher. 2008. "The Development of Feeding Behaviour in Wild Western Lowland Gorillas (*Gorilla gorilla gorilla*)." *Behaviour* 145 (2): 171–93.

Nunn, CL. 2011. *The Comparative Approach in Evolutionary Anthropology and Biology*. Chicago: University of Chicago Press.

O'Mara, M T. 2015. "Ecological Risk Aversion and Juvenile Ring-Tailed Lemur Feeding and Foraging." *Folia Primatologica* 86 (1–2): 96–105.

Organ, C, CL Nunn, Z Machanda, and RW Wrangham. 2011. "Phylogenetic Rate Shifts in Feeding Time during the Evolution of *Homo*." *Proceedings of the National Academy of Sciences of the United States of America* 108 (35): 14555–59.

Osborn, JW. 1978. "Morphogenetic Gradients: Fields versus Clones." In *Development, Function and Evolution of Teeth*, edited by PM Butler and KA Joysey, 171–201. London: Academic Press.

Pagel, M. 1999. "Inferring the Historical Patterns of Biological Evolution." *Nature* 401 (6756): 877–84.

Pampush, JD, JP Spradley, PE Morse, AR Harrington, KL Allen, DM Boyer, and RF Kay. 2016. "Wear and Its Effects on Dental Topography Measures in Howling Monkeys (*Alouatta palliata*)." *American Journal of Physical Anthropology* 161 (4): 705–21.

Peccei, JS. 2001. "A Critique of the Grandmother Hypotheses: Old and New." *American Journal of Human Biology* 13 (4): 434–52.

Perry, JMG, and A Hartstone-Rose. 2010. "Maximum Ingested Food Size in Captive Strepsirrhine Primates: Scaling and the Effects of Diet." *American Journal of Physical Anthropology* 142 (4): 625–35.

Perry, JMG, A Hartstone-Rose, and RL Logan. 2011. "The Jaw Adductor Resultant and Estimated Bite Force in Primates." *Anatomy Research International* 2011: 929848.

Perry, JMG, ML Bastian, E St Clair, and A Hartstone-Rose. 2015. “Maximum Ingested Food Size in Captive Anthropoids.” *American Journal of Physical Anthropology* 158 (1): 92–104.

Phillips-Conroy, JE, and C J Jolly. 1988. “Dental Eruption Schedules of Wild and Captive Baboons.” *American Journal of Primatology* 15 (1): 17–29.

Picq, PG. 1990. *L’articulation temporo-mandibulaire des Hominidés*. Paris: Centre national de la recherche scientifique.

Plavcan, JM, and CP van Schaik. 1992. “Intrasexual Competition and Canine Dimorphism in Anthropoid Primates.” *American Journal of Physical Anthropology* 87 (4): 461–77.

Plavcan, JM, and DJ Daegling. 2006. “Interspecific and Intraspecific Relationships between Tooth Size and Jaw Size in Primates.” *Journal of Human Evolution* 51 (2): 171–84.

Plavcan, JM, CP van Schaik, and PM Kappeler. 1995. “Competition, Coalitions and Canine Size in Primates.” *Journal of Human Evolution* 28 (3): 245–76.

Ponce de León, MS, and CP Zollikofer. 2001. “Neanderthal Cranial Ontogeny and Its Implications for Late Hominid Diversity.” *Nature* 412 (6846): 534–38.

Post, DG, G Hausfater, and SA McCuskey. 1980. “Feeding Behavior of Yellow Baboons (*Papio cynocephalus*): Relationship to Age, Gender and Dominance Rank.” *Folia Primatologica* 34 (3–4): 170–95.

Pruim, GJ, HJ de Jongh, and JJ ten Bosch. 1980. “Forces Acting on the Mandible during Bilateral Static Bite at Different Bite Force Levels.” *Journal of Biomechanics* 13 (9): 755–63.

Pucciarelli, HM, V Dressino, and MH Niveiro. 1990. “Changes in Skull Components of the Squirrel Monkey Evoked by Growth and Nutrition: An Experimental Study.” *American Journal of Physical Anthropology* 81 (4): 535–43.

Pusey, AE, GW Oehlert, JM Williams, and J Goodall. 2005. “Influence of Ecological and Social Factors on Body Mass of Wild Chimpanzees.” *International Journal of*

*Primatology* 26 (1): 3–31.

Quyet, LK, AD Nguyen, VA Tai, BW Wright, and HH Covert. 2007. "Diet of the Tonkin Snub-Nosed Monkey (*Rhinopithecus avunculus*) in the Khau Ca Area, Ha Giang Province, Northeastern Vietnam." *Vietnamese Journal of Primatology* 1 (1): 75–83.

R Core Team. 2013. "R. A Language and Environment for Statistical Computing." Vienna, Austria: R Foundation for Statistical Computing.

Rak, Y. 1983. *The Australopithecine Face*. New York: Academic Press.

———. "The Neanderthal: A New Look at an Old Face." *Journal of Human Evolution* 15 (3): 151–64.

Rak, Y, A Ginzburg, and E Geffen. 2002. "Does *Homo neanderthalensis* Play a Role in Modern Human Ancestry? The Mandibular Evidence." *American Journal of Physical Anthropology* 119 (3): 199–204.

Rak, Y, and WL Hylander. 2008. "What Else Is the Tall Mandibular Ramus of the Robust Australopiths Good For?" In *Primate Craniofacial Function and Biology*, edited by CJ Vinyard, MJ Ravosa, and CE Wall. New York: Springer.

Rak, Y, WH Kimbel, and E Hovers. 1994. "A Neandertal Infant from Amud Cave, Israel." *Journal of Human Evolution* 26 (4): 313–24.

Ramirez Rozzi, FV, and JM Bermudez de Castro. 2004. "Surprisingly Rapid Growth in Neanderthals." *Nature* 428 (6986): 936–39.

Ravosa, MJ. 1996. "Jaw Morphology and Function in Living and Fossil Old World Monkeys." *International Journal of Primatology* 17 (6): 909–32.

———. "Size and Scaling in the Mandible of Living and Extinct Apes." *Folia Primatologica* 71: 305–22.

Ravosa, MJ, and CF Ross. 1994. "Craniodental Allometry and Heterochrony in Two Howler Monkeys: *Alouatta seniculus* and *A. palliata*." *American Journal of Primatology* 33 (4): 277–99.

Ravosa, MJ, CJ Vinyard, M Gagnon, and SA Islam. 2000. “Evolution of Anthropoid Jaw Loading and Kinematic Patterns.” *American Journal of Physical Anthropology* 112 (4): 493–516.

Ravosa, MJ, JE Scott, KR McAbee, AJ Veit, and AL Fling. 2015. “Chewed out: An Experimental Link between Food Material Properties and Repetitive Loading of the Masticatory Apparatus in Mammals.” *PeerJ* 3: e1345.

Revell, LJ. 2009. “Size-Correction and Principal Components for Interspecific Comparative Studies.” *Evolution* 63 (12): 3258–68.

———. 2010. “Phylogenetic Signal and Linear Regression on Species Data.” *Methods in Ecology and Evolution* 1 (4): 319–29.

———. 2012. “Phytools: An R Package for Phylogenetic Comparative Biology (and Other Things).” *Methods in Ecology and Evolution* 3 (2): 217–23.

Richards, GD. 2007. “Basicranial Ontogeny and Evolution in Homo Sapiens.” PhD Dissertation, University of California, Berkley.

Richtsmeier, JT, BD Corner, HM Grausz, JM Cheverud, and SE Danahey. 1993. “The Role of Postnatal Growth Pattern in the Production of Facial Morphology.” *Systematic Biology* 42 (3): 307–30.

Robbins, MM. 1995. “A Demographic Analysis of Male Life History and Social Structure of Mountain Gorillas.” *Behaviour* 132 (1/2): 21–47.

———. 2008. “Feeding Competition and Agonistic Relationships among Bwindi *Gorilla beringei*.” *International Journal of Primatology* 29: 999–1018.

Robinson, C, J Kirkham, SJ Brookes, WA Bonnass, and RC Shore. 1995. “The Chemistry of Enamel Development.” *International Journal of Developmental Biology* 39: 145–52.

Robinson, JT. 1954. “Prehominid Dentition and Hominid Evolution.” *Evolution* 8: 324–34.

———. 1963. “Adaptive Radiation in the Australopithecines and the Origin of Man.” In *African Ecology and Human Evolution*, edited by FC Howell and F Bourliere, 385–416. Chicago: Aldine de Gruyter.

Robson, SL, and B Wood. 2008. “Hominin Life History: Reconstruction and Evolution.” *Journal of Anatomy* 212 (4): 394–425.

Robson, SL, CP van Schaik, and K Hawkes. 2006. “The Derived Features of Human Life History.” In *The Evolution of Human Life History*, edited by K Hawkes and RL Paine, 17–44. Santa Fe: School of American Research Press.

Rogers, ME, K Abernethy, M Bermejo, C Cipolletta, D Doran, K McFarland, T Nishihara, M Remis, and CEG Tutin. 2004. “Western Gorilla Diet: A Synthesis from Six Sites.” *American Journal of Primatology* 64: 173–92.

Ross, CF, and J Iriarte-Diaz. 2014. “What Does Feeding System Morphology Tell Us about Feeding?” *Evolutionary Anthropology* 23 (3): 105–120.

Ross, CF, J Iriarte-Diaz, and CL Nunn. 2012. “Innovative Approaches to the Relationship between Diet and Mandibular Morphology in Primates.” *International Journal of Primatology* 33 (3): 632–60.

Ross, CF, R Dharia, SW Herring, WL Hylander, Z-J Liu, KL Rafferty, MJ Ravosa, and SH Williams. 2007. “Modulation of Mandibular Loading and Bite Force in Mammals during Mastication.” *The Journal of Experimental Biology* 210 (6): 1046–63.

Rothschild, BM, N Hong, and JE Turnquist. 1999. “Skeletal Survey of Cayo Santiago Rhesus Macaques: Osteoarthritis and Articular Plate Excrescences.” *Seminars in Arthritis and Rheumatism* 29 (2): 100–111.

Sacher, GA. 1959. “Reationship of Lifespan to Brain Weight and Body Weight in Mammals.” In *Foundation Colloquia on Aging Volume 5: The Lifespan of Animals*, edited by GEW Wolstenholme and M O’Connor, 115–33. London: Churchill.

———. 1975. “Maturity and Longevity in Relation to Cranial Capacity in Hominid Evolution.” In *Primate Functional Morphology and Evolution*, edited by RH Tuttle, 417–41. The Hague: Mouton.

Sacher, GA, and EF Staffeldt. 1974. “Relation of Gestation Time to Brain Weight for Placental Mammals: Implications for the Theory of Vertebrate Growth.” *The American Naturalist* 108 (963): 593–615.

Sardi, ML, and FV Ramirez Rozzi. 2005. “A Cross-Sectional Study of Human Craniofacial Growth.” *Annals of Human Biology* 32 (2): 390–96.

Scheuer, JL, and SM Black. 2000. *Developmental Juvenile Osteology*. London: Academic Press.

Schultz, AH. 1924. “Growth Studies on Primates Bearing upon Man’s Evolution.” *American Journal of Physical Anthropology* 7 (2): 149–64.

———. 1935. “Eruption and Decay of the Permanent Teeth in Primates.” *American Journal of Physical Anthropology* 19 (4): 489–581.

———. 1960a. “Age Changes and Variability in the Skulls and Teeth of the Central American Monkeys *Alouatta*, *Cebus*, and *Ateles*.” *Proceedings of the Zoological Society of London* 133 (3): 337–90.

———. 1960b. “Age Changes in Primates and Their Modification in Man.” In *Human Growth*, edited by JM Tanner, 1–20. Oxford: Pergamon Press.

———. 1962. “Metric Age Changes and Sex Differences in Primate Skulls.” *Zeitschrift Für Morphologie Und Anthropologie* 52 (3): 239–55.

Schwartz, GT. 2012. “Growth, Development, and Life History throughout the Evolution of *Homo*.” *Current Anthropology* 53 (Suppl. 6): S395–408.

Schwartz, GT, and C Dean. 2001. “Ontogeny of Canine Dimorphism in Extant Hominoids.” *American Journal of Physical Anthropology* 115 (3): 269–83.

Schwartz, GT, DJ Reid, and MC Dean. 2001. “Developmental Aspects of Sexual Dimorphism in Hominoid Canines.” *International Journal of Primatology* 22 (5): 837–60.

Schwartz, GT, DJ Reid, MC Dean, and AL Zihlman. 2006. “A Faithful Record of

Stressful Life Events Recorded in the Dental Developmental Record of a Juvenile Gorilla." *International Journal of Primatology* 27 (4): 1201–19.

Schwartz, GT, KE Samonds, LR Godfrey, WL Jungers, and EL Simons. 2002. "Dental Microstructure and Life History in Subfossil Malagasy Lemurs." *Proceedings of the National Academy of Sciences of the United States of America* 99 (9): 6124–29.

Schwartz, GT, P Mahoney, LR Godfrey, FP Cuozzo, WL Jungers, and GFN Randria. 2005. "Dental Development in *Megaladapis edwardsi* (Primates, Lemuriformes): Implications for Understanding Life History Variation in Subfossil Lemurs." *Journal of Human Evolution* 49 (6): 702–21.

Scott, JE, KR McAbee, MM Eastman, and MJ Ravosa. 2014. "Experimental Perspective on Fallback Foods and Dietary Adaptations in Early Hominins." *Biology Letters* 10: 20130789.

Scott, RS, PS Ungar, TS Bergstrom, CA Brown, FE Grine, MF Teaford, and AWalker. 2005. "Dental Microwear Texture Analysis Shows within-Species Diet Variability in Fossil Hominins." *Nature* 436 (7051): 693–95.

Setchell, JM, and EJ Wickings. 2004. "Sequences and Timing of Dental Eruption in Semi-Free-Ranging Mandrills (*Mandrillus sphinx*)." *Folia Primatologica* 75 (3): 121–32.

Shea, BT. 1986. "Ontogenetic Approaches to Sexual Dimorphism in Anthropoids." *Human Evolution* 1 (2): 97–110.

Sheine, WS, and RF Kay. 1977. "An Analysis of Chewed Food Particle Size and Its Relationship to Molar Structure in the Primates *Cheirogaleus medius* and *Galago senegalensis* and the Insectivoran *Tupaia glis*." *American Journal of Physical Anthropology* 47: 15–20.

Singleton, M. 2015. "Functional Geometric Morphometric Analysis of Masticatory System Ontogeny in Papionin Primates." *The Anatomical Record* 298: 48–63.

Smith, AL, S Benazzi, JA Ledogar, K Tamvada, LC Pryor Smith, GW Weber, MA Spencer, et al. 2015. "The Feeding Biomechanics and Dietary Ecology of *Paranthropus Boisei*." *The Anatomical Record* 298 (1): 145–67.

Smith, BH. 1989. “Dental Development as a Measure of Life History in Primates.” *Evolution* 43 (3): 683–88.

———. 1991. “Dental Development and the Evolution of Life History in Hominidae.” *American Journal of Physical Anthropology* 86 (2): 157–74.

———. 1992. “Life History and the Evolution of Human Maturation.” *Evolutionary Anthropology* 1: 134–42.

———. 1994. “Sequence of Emergence of the Permanent Teeth in *Macaca*, *Pan*, *Homo*, and *Australopithecus*: Its Evolutionary Significance.” *American Journal of Physical Anthropology* 6: 61–76.

Smith, BH, TL Crummett, and KL Brandt. 1994. “Ages of Eruption of Primate Teeth: A Compendium for Aging Individuals and Comparing Life Histories.” *Yearbook of Physical Anthropology* 37: 177–231.

Smith, BH, and RL Tompkins. 1995. “Toward a Life History of the Hominidae.” *Annual Review of Anthropology* 25: 257–79.

Smith, FH. 1983. “Behavioral Interpretation of Changes in Craniofacial Morphology Across the Archaic/Modern *Homo sapiens* Transition.” In *The Mousterian Legacy: Human Biocultural Change in the Upper Pleistocene*, edited by E Trinkaus, 141–63.

Smith, RJ. 1978. “Mandibular Biomechanics and Temporomandibular Joint Function in Primates.” *American Journal of Physical Anthropology* 49 (3): 341–450.

Smith, RJ. 2009. “Use and Misuse of the Reduced Major Axis for Line-Fitting.” *American Journal of Physical Anthropology* 140 (3): 476–86.

Smith, TM. 2013. “Teeth and Human Life-History Evolution.” *Annual Review of Anthropology* 42 (1): 191–208.

———. 2016. “Dental Development in Living and Fossil Orangutans.” *Journal of Human Evolution* 94: 92–105.

Smith, TM, BH Smith, DJ Reid, H Siedel, L Vigilant, J-J Hublin, and C Boesch. 2010a.

"Dental Development of the Taï Forest Chimpanzees Revisited." *Journal of Human Evolution* 58 (5): 363–73.

Smith, TM, DJ Reid, MC Dean, AJ Olejniczak, RJ Ferrell, and LB Martin. 2007a. "New Perspectives on Chimpanzee and Human Molar Crown Development." In *Dental Perspectives on Human Evolution*, edited by SE Bailey and J-J Hublin, 177–92. Dordrecht: Springer.

Smith, TM, P Tafforeau, DJ Reid, R Grün, S Eggins, M Boutakiout, and J-J Hublin. 2007b. "Earliest Evidence of Modern Human Life History in North African Early *Homo sapiens*." *Proceedings of the National Academy of Sciences of the United States of America* 104 (15): 6128–33.

Smith, TM, P Tafforeau, DJ Reid, J Pouech, V Lazzari, JP Zermeno, D Guatelli-Steinberg, et al. 2010b. "Dental Evidence for Ontogenetic Differences between Modern Humans and Neanderthals." *Proceedings of the National Academy of Sciences of the United States of America* 107 (49): 20923–28.

Smith, TM, Z Machanda, AB Bernard, RM Donovan, AM Papakyrikos, MN Muller, and R Wrangham. 2013. "First Molar Eruption, Weaning, and Life History in Living Wild Chimpanzees." *Proceedings of the National Academy of Sciences of the United States of America* 110 (8): 2787–91.

Snaith, TV, and CA Chapman. 2007. "Primate Group Size and Interpreting Socioecological Models: Do Folivores Really Play by Different Rules?" *Evolutionary Anthropology* 16: 94–106.

Spencer, MA. 1995. "Masticatory System Configuration and Diet in Anthropoid Primates." PhD Dissertation, State University of New York at Stony Brook.

———. 1998. "Force Production in the Primate Masticatory System: Electromyographic Tests of Biomechanical Hypotheses." *Journal of Human Evolution* 34 (1): 25–54.

———. 1999. "Constraints on Masticatory System Evolution in Anthropoid Primates." *American Journal of Physical Anthropology* 108 (4): 483–506.

Spencer, MA, and B Demes. 1993. “Biomechanical Analysis of Masticatory System Configuration in Neandertals and Inuits.” *American Journal of Physical Anthropology* 91 (1): 1–20.

Spencer, MA, and GT Schwartz. 2008. “The Ontogeny of Masticatory System Configuration in Humans and Its Influence on the Timing of Molar Eruption.” *American Journal of Physical Anthropology* Suppl. 46: 199.

Sponheimer, M, BH Passey, DJ de Ruiter, D Guatelli-Steinberg, TE Cerling, and JA Lee-Thorp. 2006. “Isotopic Evidence for Dietary Variability in the Early Hominin *Paranthropus robustus*.” *Science* 314 (5801): 980–82.

Stearns, SC. 1992. *The Evolution of Life Histories*. New York: Oxford University Press.

Stoinski, TS, B Perdue, T Breuer, and MP Hoff. 2013. “Variability in the Developmental Life History of the Genus *Gorilla*.” *American Journal of Physical Anthropology* 152 (2): 165–72.

Stoinski, TS, V Vecellio, T Ngaboyamahina, F Ndagijimana, S Rosenbaum, and KA Fawcett. 2009. “Proximate Factors Influencing Dispersal Decisions in Male Mountain Gorillas, *Gorilla beringei beringei*.” *Animal Behaviour* 77 (5): 1155–64.

Stone, AI. 2006. “Foraging Ontogeny Is Not Linked to Delayed Maturation in Squirrel Monkeys (*Saimiri sciureus*).” *Ethology* 112 (2): 105–15.

Strait, SG. 1993. “Differences in Occlusal Morphology and Molar Size in Frugivores and Faunivores.” *Journal of Human Evolution* 25 (6): 471–84.

Strait, DS, GW Weber, P Constantino, PW Lucas, BG Richmond, MA Spencer, PC Dechow, et al. 2012. “Microwear, Mechanics and the Feeding Adaptations of *Australopithecus africanus*.” *Journal of Human Evolution* 62 (1): 165–68.

Strait, DS, GW Weber, S Neubauer, J Chalk, BG Richmond, PW Lucas, MA Spencer, et al. 2009. “The Feeding Biomechanics and Dietary Ecology of *Australopithecus africanus*.” *Proceedings of the National Academy of Sciences of the United States of America* 106 (7): 2124–29.

Strand Vioarsdóttir, U, and S Cobb. 2004. “Inter- and Intra-Specific Variation in the

Ontogeny of the Hominoid Facial Skeleton: Testing Assumptions of Ontogenetic Variability." *Annals of Anatomy* 186: 423–28.

Swindler, DR. 1985. "Nonhuman Primate Dental Development and Its Relationship to Human Dental Development." In *Nonhuman Primate Models for Human Growth and Development*, edited by E Watts, 67–94. New York: Alan R Liss.

———. *Primate Dentition: An Introduction to the Teeth of Non-Human Primates*. Cambridge: Cambridge University Press.

Swindler, DR, and D Meekins. 1991. "Dental Development of the Permanent Mandibular Teeth in the Baboon, *Papio cynocephalus*." *American Journal of Human Biology* 3: 571–80.

Swindler, DR, and JA Gavin. 1962. "Calcification of the Mandibular Molars in Rhesus Monkeys." *Archives of Oral Biology* 7: 727–34.

Tafforeau, P, R Boistel, E Boller, A Bravin, M Brunet, Y Chaimanee, P Cloetens, et al. 2006. "Applications of X-Ray Synchrotron Microtomography for Non-Destructive 3D Studies of Paleontological Specimens." *Applied Physics A: Materials Science and Processing* 83 (2): 195–202.

Taylor, AB. 2002. "Masticatory Form and Function in the African Apes." *American Journal of Physical Anthropology* 117 (2): 133–56.

———. 2003. "Ontogeny and Function of the Masticatory Complex in *Gorilla*: Functional, Evolutionary, and Taxonomic Implications." In *Gorilla Biology: A Multidisciplinary Perspective*, edited by AB Taylor and ML Goldsmith, 132–93. Cambridge: Cambridge University Press.

———. 2006. "Diet and Mandibular Morphology in African Apes." *International Journal of Primatology* 27 (1): 181–201.

Taylor, AB, and CJ Vinyard. 2013. "The Relationships among Jaw-Muscle Fiber Architecture, Jaw Morphology, and Feeding Behavior in Extant Apes and Modern Humans." *American Journal of Physical Anthropology* 151: 120–34.

Taylor, SCS. 1965. "A Relation between Mature Weight and Time Taken to Mature in

Mammals." *Animal Production* 7 (2): 203–20.

Teaford, MF, PW Lucas, PS Ungar, and KE Glander. 2006. "Mechanical Defenses in Leaves Eaten by Costa Rican Howling Monkeys (*Alouatta palliata*)." *American Journal of Physical Anthropology* 129 (1): 99–104.

Thompson, EN, AR Biknevicius, and RZ German. 2003. "Ontogeny of Feeding Function in the Gray Short-Tailed Opossum *Monodelphis domestica*: Empirical Support for the Constrained Model of Jaw Biomechanics." *Journal of Experimental Biology* 206 (5): 923–932.

Tobias, PV. 1967. "The Cranium and Maxillary Dentition of *Australopithecus* (*Zinjanthropus*) *boisei*." In *Olduvai Gorge, Vol. 2*. Cambridge: Cambridge University Press.

Tompkins, RL. 1996. "Human Population Variability in Relative Dental Development." *American Journal of Physical Anthropology* 99: 79–102.

Tonndorf, ML, K Sasaki, and AG Hannam. 1989. "Single-Wire Recording of Regional Activity in the Human Masseter Muscle." *Brain Research Bulletin* 23 (1–2): 155–59.

Trinkaus, E. 1983. *The Shanidar Neandertals*. New York: Academic Press.

———. 1987. "The Neandertal Face: Evolutionary and Functional Perspectives on a Recent Hominid Face." *Journal of Human Evolution* 16 (5): 429–43.

Turnquist, JE, and MJ Kessler. 1990. "Dental Eruption in Free-Ranging *Macaca mulatta* on Cayo Santiago." *American Journal of Physical Anthropology* 81: 309.

Ungar, PS, and F M'Kirera. 2003. "A Solution to the Worn Tooth Conundrum in Primate Functional Anatomy." *Proceedings of the National Academy of Sciences of the United States of America* 100 (7): 3874–77.

Ungar, PS, and M Sponheimer. 2011. "The Diets of Early Hominins." *Science* 334 (6053): 190–93.

Ungar, PS, FE Grine, and MF Teaford. 2008. “Dental Microwear and Diet of the Plio-Pleistocene Hominin *Paranthropus boisei*.” *PLoS ONE* 3 (4): e2044.

Vakiener, M, MR Cranfield, TS Stoinski, K Arbenz-Smith, DJ Reid, TG Bromage, A Mudakikwa, and SC McFarlin. 2016. “Dental Emergence in a Naturally Accumulated Skeletal Collection of Virunga Mountain Gorllas (*Gorilla beringei beringei*) from Rwanda. Poster Presented at the Annual Meeting of the International Primatological Society, Chicago, IL.” In .

van Eijden, TMGJ. 1990. “Jaw Muscle Activity in Relation to the Direction and Point of Application of Bite Force.” *Journal of Dental Research* 69: 901–5.

van Eijden, TMGJ. 1991. “Three-Dimensional Analyses of Human Bite-Force Magnitude and Moment.” *Archives of Oral Biology* 36 (7): 535–39.

van Eijden, TMGJ, JH Koolstra, P Brugman, and WA Weijs. 1988. “A Feedback Method to Determine the Three Dimensional Bite Force Capabilities of the Human Masticatory System.” *Journal of Dental Research* 67: 450–54.

Venkataraman, VV, H Glowacka, J Fritz, M Clauss, C Seyum, N Nguyen, and PJ Fashing. 2014. “Effects of Dietary Fracture Toughness and Dental Wear on Chewing Efficiency in Geladas (*Theropithecus gelada*).” *American Journal of Physical Anthropology* 155 (1): 17–32.

Vincent, JFV. 1992. *Biomechanics: Materials, a Practical Approach*. New York: Oxford University Press.

Vogel, ER, A Zulfa, M Hardus, SA Wich, NJ Dominy, and AB Taylor. 2014. “Food Mechanical Properties, Feeding Ecology, and the Mandibular Morphology of Wild Orangutans.” *Journal of Human Evolution* 75 (October): 110–24.

Vogel, ER, JT van Woerden, PW Lucas, SS Utami Atmoko, CP van Schaik, and NJ Dominy. 2008. “Functional Ecology and Evolution of Hominoid Molar Enamel Thickness: *Pan troglodytes schweinfurthii* and *Pongo pygmaeus wurmbii*.” *Journal of Human Evolution* 55 (1): 60–74.

Walker, A. 1976. “A 3-Dimensional Analysis of the Mechanics of Mastication.” *American Journal of Physical Anthropology* 44: 213.

Watts, DP. 1985. “Observations on the Ontogeny of Feeding Behavior in Mountain Gorillas (*Gorilla gorilla beringei*).” *American Journal of Primatology* 10: 1–10.

———. 1984. “Composition and Variability of Mountain Gorilla Diets in the Central Virungas.” *American Journal of Primatology* 7: 323–256.

Western, D. 1979. “Size, Life History and Ecology in Mammals.” *African Journal of Ecology* 17 (4): 185–204.

Williams, FL, and Z Cofran. 2016. “Postnatal Craniofacial Ontogeny in Neandertals and Modern Humans.” *American Journal of Physical Anthropology* 159 (3): 394–409.

Williams, SH, BW Wright, VD Truong, CR Daubert, and CJ Vinyard. 2005. “Mechanical Properties of Foods Used in Experimental Studies of Primate Masticatory Function.” *American Journal of Primatology* 67: 329–46.

Williams, SH, CE Wall, CJ Vinyard, and WL Hylander. 2002. “A Biomechanical Analysis of Skull Form in Gum-Harvesting Galagids.” *Folia Primatologica* 73 (4): 197–209.

Wood, B. 1996. “Hominid Palaeobiology: Have Studies of Comparative Development Come of Age?” *American Journal of Physical Anthropology* 99: 9–15.

Wood, B, and DE Lieberman. 2001. “Craniodental Variation in *Paranthropus boisei*: A Developmental and Functional Perspective.” *American Journal of Physical Anthropology* 116 (1): 13–25.

Wood, JW. 1990. “Fertility in Anthropological Populations.” *Annual Review of Anthropology* 19: 211–42.

Wright, BW. 2005. “Craniodental Biomechanics and Dietary Toughness in the Genus *Cebus*.” *Journal of Human Evolution* 48 (5): 473–92.

Yamashita, N. 2002. “Diets of Two Lemur Species in Different Microhabitats in Beza Mahafaly Special Reserve, Madagascar.” *International Journal of Primatology* 23 (5): 1025–51.

Yamashita, N, CJ Vinyard, and CL Tan. 2009. “Food Mechanical Properties in Three Sympatric Species of *Hapalemur* in Ranomafana National Park, Madagascar.” *American Journal of Physical Anthropology* 139 (3): 368–81.

Yamashita, N, FP Cuozzo, ML Sauther, E Fitzgerald, A Riemenschneider, and PS Ungar. 2016. “Mechanical Food Properties and Dental Topography Differentiate Three Populations of *Lemur catta* in Southwest Madagascar.” *Journal of Human Evolution* 98: 66–75.

Zihlman, AL, DR Bolter, and C Boesch. 2004. “Wild Chimpanzee Dentition and Its Implications for Assessing Life History in Immature Hominin Fossils.” *Proceedings of the National Academy of Sciences of the United States of America* 101 (29): 10541–43.

———. 2007. “Skeletal and Dental Growth and Development in Chimpanzees of the Taï National Park, Côte D’Ivoire.” *Journal of Zoology* 273 (1): 63–73.

Zink, KD, and DE Lieberman. 2016. “Impact of Meat and Lower Palaeolithic Food Processing Techniques on Chewing in Humans.” *Nature* 531 (7595): 500–503.

# APPENDIX A

## SUPPLEMENTARY TABLES FOR CHAPTER 2 (SM1 TO SM2)

SM 1. Results of *t*-tests comparing $Resultant_{Mean}$-*Molar* to zero.

| Taxon | Molar emergence category | Mean | Min. | Max. | *t*-statistic | df | *p*-value (two-sided) | *p*-value (one-sided) |
|---|---|---|---|---|---|---|---|---|
| **Platyrrhini** | | | | | | | | |
| *Alouatta palliata* | dp4 | 15.48 | 12.27 | 18.54 | 23.19 | 9 | *** | *** |
| | M1 | 15.01 | 12.50 | 18.16 | 27.33 | 9 | *** | *** |
| | M2 | 13.54 | 11.00 | 15.25 | 28.87 | 9 | *** | *** |
| | M3 | 9.34 | 4.28 | 14.19 | 14.67 | 19 | *** | *** |
| *Ateles geoffroyi* | dp4 | 17.73 | 16.00 | 19.54 | 42.80 | 6 | *** | *** |
| | M1 | 17.68 | 15.00 | 19.88 | 36.84 | 9 | *** | *** |
| | M2 | 15.78 | 13.41 | 20.73 | 21.55 | 9 | *** | *** |
| | M3 | 15.94 | 14.02 | 18.41 | 51.74 | 19 | *** | *** |
| *Cebus apella* | dp4 | 16.95 | 13.08 | 29.80 | 10.06 | 9 | ** | ** |
| | M1 | 14.14 | 10.50 | 26.89 | 9.55 | 9 | ** | ** |
| | M2 | 12.30 | 6.71 | 17.97 | 8.23 | - | - | - |
| | M3 | 19.83 | -5.70 | 44.23 | 8.62 | 29 | *** | *** |
| *Saimiri sciureus* | dp4 | 9.09 | 7.71 | 10.09 | 18.21 | - | - | - |
| | M1 | 8.36 | 7.54 | 9.46 | 31.81 | 8 | *** | *** |
| | M2 | 8.61 | 6.31 | 11.56 | 15.95 | 9 | *** | *** |
| | M3 | 7.94 | 6.44 | 11.19 | 34.59 | 18 | *** | *** |
| **Cercopithecidae** | | | | | | | | |
| *Colobus angolensis* | dp4 | 16.15 | 10.53 | 19.85 | 16.87 | 9 | *** | *** |
| | M1 | 17.57 | 15.31 | 19.29 | 31.94 | 8 | *** | *** |
| | M2 | 17.40 | 13.97 | 20.00 | 32.94 | 9 | *** | *** |
| | M3 | 18.05 | 12.75 | 22.90 | 36.09 | 18 | *** | *** |
| *Colobus polykomos* | dp4 | 15.22 | 14.84 | 15.81 | 51.49 | - | - | - |
| | M1 | 15.12 | 13.82 | 17.16 | 22.98 | - | - | - |
| | M2 | 16.40 | 13.62 | 19.00 | 24.58 | 7 | *** | *** |
| | M3 | 15.24 | 11.55 | 18.82 | 37.24 | 19 | *** | *** |
| *Procolobus verus* | M1 | 15.21 | 12.90 | 17.56 | 19.52 | - | - | - |
| | M2 | 12.69 | 10.67 | 15.02 | 22.00 | 6 | ** | *** |
| | M3 | 12.05 | 10.20 | 15.00 | 34.41 | 18 | *** | *** |
| *Macaca fascicularis* | dp4 | 14.67 | 11.10 | 19.59 | 19.87 | 9 | *** | *** |
| | M1 | 15.87 | 11.26 | 18.92 | 24.76 | 9 | *** | *** |
| | M2 | 17.22 | 14.08 | 20.01 | 23.63 | 7 | *** | *** |
| | M3 | 15.20 | 11.36 | 20.76 | 19.70 | 15 | *** | *** |
| *Macaca mulatta* | dp4 | 15.90 | 11.81 | 21.34 | 37.51 | 27 | *** | *** |
| | M1 | 17.61 | 13.37 | 22.76 | 37.35 | 32 | *** | *** |
| | M2 | 19.06 | 13.11 | 26.10 | 30.89 | 30 | *** | *** |
| | M3 | 16.60 | 11.42 | 21.28 | 44.64 | 57 | *** | *** |
| *Papio anubis* | dp4 | 26.46 | 20.28 | 32.02 | 22.66 | 9 | *** | *** |
| | M1 | 28.89 | 20.36 | 38.51 | 17.46 | 9 | *** | *** |
| | M2 | 32.91 | 23.45 | 44.20 | 15.05 | 9 | *** | *** |
| | M3 | 37.71 | 26.18 | 50.27 | 32.19 | 27 | *** | *** |

| | | | | | | | | |
|---|---|---|---|---|---|---|---|---|
| | dp4 | 21.67 | 15.37 | 24.56 | 27.63 | 11 | *** | *** |
| *Papio cynocephalus* | M1 | 26.17 | 21.22 | 36.56 | 15.72 | 9 | *** | *** |
| | M2 | 27.47 | 19.38 | 38.77 | 20.21 | 16 | *** | *** |
| | M3 | 27.49 | 16.02 | 38.14 | 25.98 | 33 | *** | *** |
| **Hominidae** | | | | | | | | |
| | dp4 | 36.47 | 30.82 | 43.86 | 33.35 | 15 | *** | *** |
| *Gorilla beringei* | M1 | 36.17 | 30.70 | 50.93 | 20.93 | 13 | *** | *** |
| | M2 | 32.37 | 24.62 | 39.57 | 19.64 | 8 | *** | *** |
| | M3 | 27.59 | 0.43 | 56.28 | 18.66 | 56 | *** | *** |
| | dp4 | 35.04 | 22.06 | 43.69 | 11.66 | 6 | * | * |
| *Gorilla gorilla* | M1 | 37.34 | 28.63 | 46.46 | 22.14 | 9 | *** | *** |
| | M2 | 29.96 | 22.93 | 38.09 | 12.24 | - | - | - |
| | M3 | 22.60 | 7.69 | 44.57 | 11.54 | 28 | *** | *** |
| | dp4 | 22.49 | 18.31 | 26.40 | 62.82 | 24 | *** | *** |
| *Homo sapiens* | M1 | 21.06 | 16.95 | 28.28 | 35.01 | 21 | *** | *** |
| | M2 | 16.13 | 10.11 | 21.13 | 30.89 | 30 | *** | *** |
| | M3 | 11.38 | -1.73 | 17.27 | 19.54 | 49 | *** | *** |
| | dp4 | 20.23 | 16.28 | 23.10 | 33.06 | 9 | *** | *** |
| *Pan paniscus* | M1 | 18.93 | 13.82 | 25.69 | 18.96 | 9 | *** | *** |
| | M2 | 17.10 | 13.64 | 22.69 | 24.71 | 11 | *** | *** |
| | M3 | 14.53 | 6.44 | 20.24 | 20.44 | 20 | *** | *** |
| | dp4 | 25.46 | 19.72 | 35.18 | 28.21 | 15 | *** | *** |
| *Pan troglodytes* | M1 | 25.02 | 17.95 | 38.08 | 27.32 | 20 | *** | *** |
| | M2 | 23.60 | 17.89 | 31.75 | 28.47 | 20 | *** | *** |
| | M3 | 19.26 | 10.61 | 29.16 | 44.54 | 68 | *** | *** |
| | dp4 | 22.29 | 16.20 | 26.70 | 20.17 | 8 | *** | *** |
| *Pongo pygmaeus* | M1 | 26.47 | 20.54 | 36.76 | 15.37 | 10 | *** | *** |
| | M2 | 19.70 | 12.26 | 30.44 | 11.40 | 11 | *** | *** |
| | M3 | 16.00 | 3.96 | 38.68 | 7.89 | 18 | *** | *** |
| **Strepsirrhini** | | | | | | | | |
| *Eulemur mongoz* | M1 | 17.98 | 17.01 | 18.95 | 18.54 | - | - | - |
| | M3 | 15.47 | 11.86 | 19.25 | 22.52 | 12 | *** | *** |
| | dp4 | 11.95 | 7.70 | 15.74 | 5.12 | - | - | - |
| *Lemur catta* | M2 | 19.19 | 14.03 | 22.86 | 11.15 | - | - | - |
| | M3 | 16.28 | 12.92 | 20.47 | 26.10 | 17 | *** | *** |
| | dp4 | 6.82 | 5.49 | 8.06 | 9.18 | - | - | - |
| *Otolemur monteiri* | M1 | 14.27 | 12.75 | 15.07 | 18.76 | - | - | - |
| | M3 | 13.24 | 5.55 | 20.29 | 23.46 | 30 | *** | *** |
| | dp4 | 10.10 | 9.25 | 10.95 | 11.86 | - | - | - |
| *Perodicticus potto* | M1 | 11.23 | 5.84 | 13.90 | 12.16 | 7 | ** | ** |
| | M2 | 13.20 | 10.10 | 16.86 | 18.40 | 7 | *** | *** |
| | M3 | 11.91 | 4.90 | 18.69 | 16.01 | 19 | *** | *** |

* $p<0.000189$, ** $p<0.00001$, *** $p<0.000001$

SM 2. Results of *t*-tests comparing $Resultant_{Max}$-*Molar* to zero.

| Taxon | Molar emergence category | Mean | Min. | Max. | *t*-statistic | df | *p*-value (two-sided) | *p*-value (one-sided) |
|---|---|---|---|---|---|---|---|---|
| **Platyrrhini** | | | | | | | | |
| *Alouatta palliata* | dp4 | 10.36 | 8.77 | 11.58 | 31.40 | 9 | *** | *** |
| | M1 | 7.27 | 4.83 | 8.82 | 19.65 | 9 | *** | *** |
| | M2 | 5.88 | 2.07 | 9.32 | 7.53 | 9 | * | * |
| | M3 | -1.89 | -9.83 | 3.36 | -3.02 | 19 | NS | NS |
| *Ateles geoffroyi* | dp4 | 15.75 | 12.61 | 17.71 | 22.71 | 6 | *** | *** |
| | M1 | 15.37 | 12.36 | 19.24 | 22.83 | 9 | *** | *** |
| | M2 | 13.40 | 10.87 | 20.25 | 14.44 | 9 | *** | *** |
| | M3 | 9.74 | 7.43 | 13.94 | 24.97 | 19 | *** | *** |
| *Cebus apella* | dp4 | 11.81 | 7.11 | 25.44 | 7.19 | 9 | * | * |
| | M1 | 10.52 | 5.95 | 24.57 | 6.27 | 9 | * | * |
| | M2 | 7.98 | 4.05 | 14.53 | 5.35 | - | - | - |
| | M3 | 8.06 | -56.94 | 36.86 | 2.85 | 29 | NS | NS |
| *Saimiri sciureus* | dp4 | 5.67 | 4.09 | 6.93 | 8.48 | - | - | - |
| | M1 | 6.36 | 5.28 | 7.94 | 19.86 | 8 | *** | *** |
| | M2 | 7.23 | 4.48 | 11.35 | 8.93 | 9 | ** | ** |
| | M3 | 5.18 | 3.98 | 7.51 | 27.00 | 18 | *** | *** |
| **Cercopithecidae** | | | | | | | | |
| *Colobus angolensis* | dp4 | 14.34 | 7.45 | 19.49 | 12.58 | 9 | ** | *** |
| | M1 | 13.80 | 11.60 | 16.40 | 29.09 | 8 | ** | *** |
| | M2 | 13.28 | 10.26 | 16.75 | 21.51 | 9 | *** | *** |
| | M3 | 10.99 | 5.55 | 17.19 | 18.20 | 18 | *** | *** |
| *Colobus polykomos* | dp4 | 12.12 | 10.20 | 13.19 | 12.60 | - | - | - |
| | M1 | 11.34 | 10.02 | 13.05 | 22.83 | - | - | - |
| | M2 | 9.03 | 5.60 | 11.32 | 12.41 | 7 | ** | ** |
| | M3 | 8.64 | 6.25 | 12.13 | 21.82 | 19 | *** | *** |
| *Procolobus verus* | M1 | 12.13 | 10.28 | 14.02 | 23.10 | - | - | - |
| | M2 | 9.38 | 5.61 | 11.98 | 12.17 | 6 | * | ** |
| | M3 | 8.93 | 6.47 | 11.31 | 27.45 | 18 | *** | *** |
| *Macaca fascicularis* | dp4 | 11.31 | 8.89 | 13.58 | 23.86 | 9 | *** | *** |
| | M1 | 12.47 | 8.22 | 14.93 | 20.47 | 9 | *** | *** |
| | M2 | 11.85 | 6.35 | 14.83 | 12.05 | 7 | ** | ** |
| | M3 | 10.13 | 6.06 | 16.33 | 12.36 | 15 | *** | *** |
| *Macaca mulatta* | dp4 | 10.77 | -7.09 | 14.39 | 14.92 | 27 | *** | *** |
| | M1 | 12.57 | 7.10 | 17.69 | 29.43 | 32 | *** | *** |
| | M2 | 12.33 | 6.11 | 19.15 | 19.06 | 30 | *** | *** |
| | M3 | 9.58 | 5.76 | 14.82 | 30.98 | 57 | *** | *** |
| *Papio anubis* | dp4 | 21.72 | 17.30 | 25.67 | 24.79 | 9 | *** | *** |
| | M1 | 22.20 | 17.19 | 28.52 | 18.69 | 9 | *** | *** |
| | M2 | 25.30 | 12.97 | 35.99 | 11.78 | 9 | ** | *** |
| | M3 | 27.36 | 16.53 | 38.43 | 22.56 | 27 | *** | *** |

| | | | | | | | | |
|---|---|---|---|---|---|---|---|---|
| | dp4 | 17.54 | 12.94 | 21.89 | 28.36 | 11 | *** | *** |
| *Papio* | M1 | 20.71 | 15.80 | 30.90 | 13.21 | 9 | *** | *** |
| *cynocephalus* | M2 | 20.41 | 12.26 | 31.20 | 17.19 | 16 | *** | *** |
| | M3 | 18.70 | 8.56 | 33.65 | 17.94 | 33 | *** | *** |
| **Hominidae** | | | | | | | | |
| | dp4 | 24.45 | 19.04 | 33.04 | 27.55 | 15 | *** | *** |
| *Gorilla beringei* | M1 | 21.91 | 14.94 | 32.05 | 17.20 | 13 | *** | *** |
| | M2 | 13.66 | 7.45 | 21.70 | 8.70 | 8 | * | * |
| | M3 | 5.30 | -49.63 | 27.47 | 3.27 | 56 | NS | NS |
| | dp4 | 23.88 | 14.99 | 29.48 | 13.65 | 6 | * | ** |
| *Gorilla gorilla* | M1 | 23.69 | 17.89 | 28.86 | 21.30 | 9 | *** | *** |
| | M2 | 14.51 | 6.88 | 27.76 | 4.08 | - | - | - |
| | M3 | 3.70 | -14.85 | 21.08 | 2.58 | 28 | NS | NS |
| | dp4 | 18.90 | 13.65 | 25.30 | 36.80 | 24 | *** | *** |
| *Homo sapiens* | M1 | 16.58 | 11.12 | 21.00 | 30.21 | 21 | *** | *** |
| | M2 | 7.76 | -4.03 | 15.18 | 7.89 | 30 | *** | *** |
| | M3 | 1.07 | -41.79 | 12.80 | 0.86 | 49 | NS | NS |
| | dp4 | 17.45 | 12.75 | 20.74 | 25.30 | 9 | *** | *** |
| *Pan paniscus* | M1 | 14.62 | 11.17 | 19.29 | 20.51 | 9 | *** | *** |
| | M2 | 13.07 | 11.06 | 17.25 | 24.37 | 11 | *** | *** |
| | M3 | 9.72 | 1.77 | 17.38 | 11.95 | 20 | *** | *** |
| | dp4 | 21.42 | 14.55 | 31.16 | 23.36 | 15 | *** | *** |
| *Pan troglodytes* | M1 | 19.66 | 13.16 | 37.25 | 18.25 | 20 | *** | *** |
| | M2 | 15.66 | 11.57 | 22.25 | 26.28 | 20 | *** | *** |
| | M3 | 10.53 | -2.01 | 17.09 | 25.13 | 68 | *** | *** |
| | dp4 | 15.74 | 11.65 | 20.00 | 16.70 | 8 | *** | *** |
| *Pongo pygmaeus* | M1 | 17.07 | 11.22 | 24.61 | 13.31 | 10 | *** | *** |
| | M2 | 7.37 | -3.73 | 22.02 | 3.55 | 11 | NS | NS |
| | M3 | 1.69 | -13.36 | 13.92 | 1.00 | 18 | NS | NS |
| **Strepsirrhini** | | | | | | | | |
| *Eulemur mongoz* | M1 | 13.92 | 9.63 | 18.22 | 3.24 | - | - | - |
| | M3 | 11.57 | 7.47 | 18.36 | 11.11 | 12 | *** | *** |
| | dp4 | 7.30 | 2.59 | 12.48 | 2.55 | - | - | - |
| *Lemur catta* | M2 | 17.04 | 10.93 | 21.94 | 8.48 | - | - | - |
| | M3 | 14.07 | 10.06 | 20.05 | 19.34 | 17 | *** | *** |
| | dp4 | 2.98 | 1.00 | 5.49 | 2.25 | - | - | - |
| *Otolemur monteiri* | M1 | 12.38 | 10.54 | 13.45 | 13.35 | - | - | - |
| | M3 | 9.47 | -3.86 | 17.24 | 10.90 | 30 | *** | *** |
| | dp4 | 7.31 | 5.25 | 9.38 | 3.54 | - | - | - |
| *Perodicticus* | M1 | 9.04 | 0.32 | 12.68 | 6.49 | 7 | NS | * |
| *potto* | M2 | 11.88 | 9.39 | 16.36 | 14.36 | 7 | ** | *** |
| | M3 | 5.69 | -37.39 | 14.76 | 2.21 | 19 | NS | NS |

* $p<0.000189$, ** $p<0.00001$, *** $p<0.000001$, NS: not significant

# APPENDIX B

## SUPPLEMENTAL TABLES FOR CHAPTER 3 (SM 3)

SM3. Summary statistics for skull variables used in GLM and PGLS models.

| Taxon | Emerg. stage | 1 | SD | 2 | SD | 3 | SD | 4 | SD | 5 | SD | 6 | SD |
|---|---|---|---|---|---|---|---|---|---|---|---|---|---|
| **Platyrrhini** | | | | | | | | | | | | | |
| *A. palliata* | dp4 | 10.29 | 1.52 | 15.41 | 2.34 | 31.61 | 1.69 | 41.36 | 3.09 | 3.06 | 0.93 | 7.55 | 0.42 |
| | M1 | 12.33 | 0.97 | 20.07 | 2.11 | 36.23 | 1.22 | 49.97 | 2.81 | 3.65 | 0.53 | 8.34 | 0.49 |
| | M2 | 15.36 | 1.63 | 23.02 | 2.42 | 39.57 | 2.13 | 59.31 | 2.32 | 3.50 | 0.53 | 8.26 | 0.41 |
| | M3 | 19.76 | 2.12 | 30.99 | 3.92 | 47.04 | 3.23 | 72.53 | 5.74 | 9.73 | 3.39 | NA | NA |
| *A. geoffroyi* | dp4 | 5.34 | 2.37 | 7.32 | 3.74 | 33.81 | 1.74 | 35.97 | 3.19 | 3.17 | 0.76 | 5.47 | 0.24 |
| | M1 | 6.75 | 2.36 | 9.07 | 3.24 | 38.34 | 1.46 | 44.02 | 2.24 | 3.32 | 0.85 | 5.41 | 0.39 |
| | M2 | 7.90 | 2.97 | 10.27 | 3.93 | 40.45 | 1.50 | 48.83 | 2.50 | 4.08 | 1.09 | 4.98 | 0.29 |
| | M3 | 14.09 | 1.05 | 20.29 | 1.90 | 45.25 | 1.20 | 61.74 | 1.55 | 10.18 | 2.99 | NA | NA |
| *C. apella* | dp4 | 8.65 | 1.08 | 13.78 | 1.75 | 40.31 | 12.46 | 38.73 | 2.23 | 5.20 | 1.19 | 5.09 | 0.24 |
| | M1 | 7.81 | 1.48 | 11.43 | 2.42 | 37.09 | 8.82 | 37.73 | 5.26 | 5.61 | 0.88 | 4.66 | 0.26 |
| | M2 | 9.60 | 2.22 | 13.92 | 3.19 | 40.52 | 7.49 | 40.71 | 12.68 | 6.38 | 2.10 | 3.66 | 0.29 |
| | M3 | 15.46 | 5.94 | 27.23 | 17.62 | 52.38 | 14.38 | 42.53 | 13.85 | 10.11 | 3.35 | NA | NA |
| *S. sciureus* | dp4 | 5.22 | 0.72 | 8.63 | 0.85 | 21.12 | 1.09 | 21.79 | 1.08 | 1.77 | 0.58 | 3.18 | 0.20 |
| | M1 | 5.09 | 0.57 | 7.08 | 1.00 | 21.73 | 0.41 | 23.51 | 0.86 | 2.12 | 0.48 | 2.92 | 0.22 |
| | M2 | 3.48 | 2.19 | 4.86 | 3.14 | 22.77 | 1.22 | 24.90 | 1.30 | 2.21 | 0.65 | 2.37 | 0.17 |
| | M3 | 6.70 | 0.73 | 9.45 | 1.11 | 25.38 | 0.96 | 29.84 | 1.74 | 5.73 | 2.69 | NA | NA |
| **Cercopithecidae** | | | | | | | | | | | | | |
| *C. angolensis* | dp4 | 5.18 | 1.94 | 7.00 | 2.89 | 34.52 | 1.71 | 35.57 | 2.42 | 3.57 | 1.11 | 6.91 | 0.42 |
| | M1 | 9.21 | 2.45 | 12.98 | 3.60 | 39.98 | 2.27 | 47.14 | 4.12 | 3.97 | 0.62 | 7.35 | 0.40 |
| | M2 | 11.83 | 2.92 | 15.95 | 4.08 | 45.59 | 1.37 | 57.84 | 3.67 | 5.04 | 2.59 | 8.76 | 0.55 |
| | M3 | 15.56 | 1.46 | 22.62 | 1.77 | 51.82 | 2.06 | 70.86 | 5.14 | 15.36 | 5.60 | NA | NA |
| *C. polykomos* | dp4 | 8.02 | 0.85 | 11.13 | 2.14 | 35.39 | 1.39 | 39.37 | 2.72 | 3.70 | 0.80 | 7.36 | 0.48 |
| | M1 | 9.80 | 1.68 | 13.59 | 2.08 | 39.77 | 2.08 | 46.39 | 4.16 | 3.82 | 1.25 | 7.86 | 0.54 |
| | M2 | 13.47 | 1.25 | 20.84 | 2.76 | 46.54 | 2.30 | 61.53 | 3.98 | 5.66 | 4.00 | 9.39 | 0.80 |

| | | | | | | | | | | | | | |
|---|---|---|---|---|---|---|---|---|---|---|---|---|---|
| | M3 | 17.35 | 1.47 | 23.94 | 1.83 | 52.43 | 2.77 | 74.91 | 4.03 | 15.09 | 5.87 | NA | NA |
| *P. verus* | M1 | 8.71 | 2.03 | 11.79 | 3.05 | 36.02 | 2.55 | 39.47 | 5.26 | 2.54 | 0.52 | 5.89 | 0.36 |
| | M2 | 10.17 | 0.85 | 13.48 | 1.67 | 38.19 | 1.16 | 43.64 | 2.01 | 4.32 | 2.46 | 6.86 | 0.50 |
| | M3 | 12.33 | 1.27 | 15.46 | 1.46 | 43.59 | 2.03 | 52.28 | 2.80 | 10.54 | 6.31 | NA | NA |
| *M. fascicularis* | dp4 | 8.21 | 1.68 | 11.57 | 2.48 | 35.92 | 2.28 | 38.57 | 3.83 | 3.46 | 0.51 | 6.66 | 0.57 |
| | M1 | 9.98 | 1.06 | 13.37 | 1.82 | 40.22 | 1.34 | 48.35 | 3.43 | 3.11 | 0.61 | 7.47 | 0.54 |
| | M2 | 13.15 | 1.44 | 18.52 | 1.77 | 45.26 | 3.36 | 60.62 | 4.96 | 6.96 | 4.16 | 8.61 | 0.78 |
| | M3 | 14.27 | 1.16 | 19.34 | 1.93 | 49.36 | 4.04 | 66.77 | 7.16 | 13.27 | 7.36 | NA | NA |
| *M. mulatta* | dp4 | 10.65 | 1.99 | 15.78 | 4.61 | 41.35 | 2.12 | 43.51 | 3.55 | 3.63 | 0.82 | 7.46 | 0.35 |
| | M1 | 12.93 | 1.90 | 17.96 | 2.48 | 46.78 | 2.76 | 54.15 | 5.38 | 3.41 | 0.90 | 8.57 | 0.42 |
| | M2 | 16.34 | 1.83 | 23.06 | 2.55 | 54.15 | 3.51 | 68.80 | 6.00 | 8.06 | 4.52 | 10.76 | 0.91 |
| | M3 | 17.88 | 2.02 | 24.89 | 2.49 | 59.40 | 4.35 | 78.44 | 6.83 | 13.24 | 7.85 | NA | NA |
| *P. anubis* | dp4 | 12.59 | 1.91 | 17.33 | 3.25 | 56.74 | 2.33 | 64.28 | 4.10 | 5.96 | 1.51 | 11.48 | 0.84 |
| | M1 | 14.97 | 2.96 | 21.65 | 5.36 | 63.32 | 4.55 | 81.18 | 10.05 | 5.11 | 1.35 | 13.48 | 1.02 |
| | M2 | 17.12 | 3.12 | 24.73 | 5.31 | 72.10 | 6.79 | 102.88 | 12.57 | 14.41 | 10.94 | 16.84 | 1.54 |
| | M3 | 24.43 | 2.41 | 34.79 | 4.17 | 90.15 | 8.56 | 139.32 | 16.82 | 28.83 | 17.09 | NA | NA |
| *P. cynocephalus* | dp4 | 10.65 | 3.38 | 14.78 | 4.79 | 50.83 | 3.37 | 58.22 | 6.35 | 4.86 | 1.44 | 9.74 | 0.92 |
| | M1 | 14.39 | 2.48 | 19.85 | 3.55 | 58.12 | 2.88 | 74.26 | 7.91 | 5.11 | 0.80 | 11.36 | 1.23 |
| | M2 | 17.94 | 2.50 | 25.00 | 3.71 | 65.08 | 5.69 | 88.81 | 12.35 | 8.45 | 4.14 | 14.79 | 1.67 |
| | M3 | 21.04 | 3.51 | 29.83 | 4.08 | 75.71 | 8.56 | 112.81 | 19.56 | 21.87 | 13.97 | NA | NA |
| **Hominidae** | | | | | | | | | | | | | |
| *G. beringei* | dp4 | 21.37 | 3.32 | 33.39 | 5.71 | 74.61 | 4.25 | 89.08 | 7.17 | 8.97 | 2.45 | 16.36 | 0.91 |
| | M1 | 26.39 | 2.85 | 40.65 | 5.19 | 85.91 | 5.99 | 107.14 | 9.39 | 11.10 | 2.41 | 18.04 | 1.13 |
| | M2 | 32.52 | 3.96 | 51.23 | 5.22 | 100.19 | 3.89 | 135.46 | 10.71 | 12.82 | 2.61 | 18.05 | 1.61 |
| | M3 | 40.56 | 6.51 | 62.85 | 12.19 | 119.25 | 11.50 | 162.05 | 18.47 | 16.37 | 9.52 | NA | NA |
| *G. gorilla* | dp4 | 20.49 | 3.45 | 31.65 | 6.75 | 74.19 | 8.58 | 85.54 | 13.87 | 9.24 | 3.76 | 15.51 | 0.91 |

| | | | | | | | | | | | | | |
|---|---|---|---|---|---|---|---|---|---|---|---|---|---|
| | M1 | 29.71 | 2.99 | 43.36 | 4.62 | 90.51 | 5.62 | 115.15 | 10.14 | 10.69 | 1.26 | 16.98 | 1.13 |
| | M2 | 35.89 | 6.43 | 51.33 | 9.81 | 102.18 | 8.16 | 133.74 | 10.47 | 10.22 | 0.80 | 16.86 | 1.24 |
| | M3 | 40.58 | 5.16 | 59.48 | 8.31 | 116.99 | 11.38 | 154.38 | 17.32 | 18.90 | 8.31 | NA | NA |
| | dp4 | 19.36 | 3.90 | 22.96 | 4.93 | 69.60 | 3.13 | 61.74 | 3.70 | 2.48 | 0.78 | 11.35 | 0.67 |
| *H. sapiens* | M1 | 25.12 | 3.48 | 29.61 | 4.54 | 78.70 | 3.78 | 75.09 | 5.47 | 2.15 | 0.68 | 11.10 | 0.96 |
| | M2 | 30.82 | 2.91 | 39.19 | 5.74 | 85.72 | 4.23 | 84.86 | 5.92 | 3.36 | 0.53 | 11.26 | 1.18 |
| | M3 | 33.96 | 3.33 | 44.28 | 8.40 | 91.25 | 3.98 | 93.02 | 5.35 | 2.90 | 0.98 | NA | NA |
| | dp4 | 14.88 | 2.43 | 17.67 | 2.84 | 56.37 | 3.05 | 55.65 | 3.34 | 5.33 | 0.88 | 9.82 | 0.65 |
| *P. paniscus* | M1 | 18.11 | 2.46 | 22.41 | 2.99 | 63.33 | 2.73 | 66.33 | 6.03 | 5.27 | 1.01 | 10.11 | 0.53 |
| | M2 | 24.25 | 2.43 | 28.28 | 2.86 | 72.34 | 3.13 | 83.19 | 5.43 | 6.78 | 3.19 | 9.12 | 0.60 |
| | M3 | 28.33 | 3.60 | 33.13 | 4.25 | 81.23 | 2.44 | 96.41 | 4.93 | 9.42 | 2.59 | NA | NA |
| | dp4 | 15.31 | 2.37 | 19.35 | 3.18 | 60.95 | 2.89 | 64.20 | 4.63 | 6.23 | 1.68 | 11.37 | 0.70 |
| *P. troglodytes* | M1 | 22.17 | 5.07 | 27.54 | 6.18 | 71.97 | 3.34 | 82.35 | 6.50 | 8.32 | 1.32 | 11.48 | 0.75 |
| | M2 | 28.43 | 3.11 | 36.37 | 4.18 | 83.84 | 6.02 | 103.44 | 8.20 | 9.03 | 3.69 | 10.75 | 0.88 |
| | M3 | 31.98 | 3.61 | 40.71 | 3.69 | 90.93 | 4.18 | 115.86 | 6.33 | 14.46 | 6.51 | NA | NA |
| | dp4 | 19.61 | 2.60 | 26.16 | 4.34 | 62.91 | 4.39 | 70.23 | 6.52 | 5.66 | 1.60 | 13.56 | 0.88 |
| *P. pygmaeus* | M1 | 26.66 | 3.21 | 36.05 | 5.17 | 74.70 | 4.66 | 93.49 | 10.80 | 8.33 | 2.03 | 14.21 | 1.00 |
| | M2 | 35.34 | 4.33 | 47.68 | 4.55 | 86.82 | 4.04 | 119.07 | 9.26 | 10.31 | 2.22 | 14.12 | 1.18 |
| | M3 | 44.01 | 6.79 | 58.31 | 9.69 | 100.35 | 10.92 | 139.62 | 16.95 | 18.34 | 9.42 | NA | NA |
| **Strepsirrhini** | | | | | | | | | | | | | |
| | dp4 | 6.57 | 0.85 | 11.22 | 1.49 | 21.68 | 1.91 | 29.92 | 3.09 | NA | NA | 5.30 | 0.38 |
| *L. catta* | M2 | 4.50 | 1.33 | 6.64 | 2.18 | 30.02 | 1.29 | 47.85 | 2.98 | NA | NA | 5.47 | 0.28 |
| | M3 | 5.14 | 2.07 | 7.34 | 2.98 | 32.46 | 1.67 | 51.25 | 2.16 | NA | NA | NA | NA |
| | M1 | 4.53 | 3.51 | 8.59 | 8.21 | 27.09 | 0.15 | 40.18 | 2.17 | NA | NA | 5.28 | 0.25 |
| *E. mongoz* | M3 | 6.65 | 2.42 | 10.55 | 4.73 | 30.87 | 1.01 | 50.33 | 3.47 | NA | NA | NA | NA |
| *O. monteiri* | dp4 | 6.05 | 1.62 | 9.89 | 2.54 | 16.82 | 0.23 | 23.08 | 0.57 | NA | NA | 4.34 | 0.21 |

| | | | | | | | | | | | | | |
|---|---|---|---|---|---|---|---|---|---|---|---|---|---|
| | M1 | 4.79 | 1.44 | 6.68 | 1.47 | 24.00 | 0.78 | 32.60 | 2.63 | NA | NA | 4.10 | 0.19 |
| | M3 | 7.17 | 2.59 | 10.93 | 4.91 | 28.41 | 1.26 | 42.84 | 2.35 | NA | NA | NA | NA |
| *P. potto* | dp4 | 4.94 | 2.29 | 7.73 | 4.01 | 18.45 | 2.19 | 23.53 | 5.02 | NA | NA | 3.73 | 0.27 |
| | M1 | 4.91 | 1.91 | 7.10 | 3.28 | 20.73 | 1.48 | 26.97 | 2.57 | NA | NA | 3.87 | 0.34 |
| | M2 | 2.99 | 1.47 | 4.32 | 2.17 | 22.37 | 1.01 | 29.98 | 2.39 | NA | NA | 3.33 | 0.33 |
| | M3 | 6.53 | 2.90 | 12.75 | 11.58 | 26.03 | 1.10 | 35.93 | 2.33 | NA | NA | NA | NA |

1. *Resultant$_{Mean}$-Molar*
2. *Resultant$_{Max}$-Molar*
3. *Skull GM*
4. *Projected jaw length*
5. *Canine overlap*
6. *Length of next molar*

# APPENDIX C

## SUPPLEMENTAL TABLES FOR CHAPTER 4 (SM 4)

SM 4. Specimen list for five species included in the study.

**A.** Specimen list for *Homo sapiens*

| Species | Age (yrs) | Specimen # | Sex | Molar emergence category | Mand. arch length$_{mean}$ | Mand. arch length$_{max}$ |
|---|---|---|---|---|---|---|
| *H. sapiens* | 2.3 | AC A73 | - | dp4 | 58.04 | 55.48 |
| *H. sapiens* | 2.8 | AC 64 | - | dp4 | 57.62 | 53.79 |
| *H. sapiens* | 2.8 | AC A69 | - | dp4 | 55.17 | 53.94 |
| *H. sapiens* | 2.8 | AC A75 | - | dp4 | 55.88 | 53.33 |
| *H. sapiens* | 2.9 | AC A67 | - | dp4 | 55.07 | 51.27 |
| *H. sapiens* | 2.9 | AC A76 | - | dp4 | 56.20 | 51.92 |
| *H. sapiens* | 3.0 | AC D41 | - | dp4 | 59.09 | 55.69 |
| *H. sapiens* | 3.0 | AC D51 | - | dp4 | 55.61 | 51.68 |
| *H. sapiens* | 3.2 | AC A206 | - | dp4 | 57.89 | 55.28 |
| *H. sapiens* | 3.3 | AC A68 | - | dp4 | 55.62 | 50.34 |
| *H. sapiens* | 3.3 | AC D38 | - | dp4 | 59.29 | 55.08 |
| *H. sapiens* | 3.7 | AC A65 | - | dp4 | 58.88 | 55.72 |
| *H. sapiens* | 4.0 | AC D42 | - | dp4 | 58.48 | 55.37 |
| *H. sapiens* | 4.1 | AC A62 | - | dp4 | 57.56 | 53.08 |
| *H. sapiens* | 4.1 | AC D39 | - | dp4 | 58.12 | 54.85 |
| *H. sapiens* | 4.2 | AC D47 | - | dp4 | 52.07 | 47.40 |
| *H. sapiens* | 4.3 | AC D270 | - | dp4 | 55.16 | 51.32 |
| *H. sapiens* | 5.0 | AC A105 | - | dp4 | 55.79 | 52.45 |
| *H. sapiens* | 5.0 | AC A131 | - | dp4 | 57.39 | 51.50 |
| *H. sapiens* | 5.3 | AC A140 | - | dp4 | 57.31 | 53.21 |
| *H. sapiens* | 6.4 | AC D299 | - | M1 | 62.57 | 58.64 |
| *H. sapiens* | 6.5 | AC A145 | - | M1 | 70.62 | 66.44 |
| *H. sapiens* | 6.6 | AC A144 | - | M1 | 66.75 | 61.53 |
| *H. sapiens* | 6.6 | AC D263 | - | M1 | 67.72 | 65.42 |
| *H. sapiens* | 6.7 | AC D53 | - | M1 | 60.96 | 58.93 |
| *H. sapiens* | 6.8 | AC A147 | - | M1 | 65.69 | 61.77 |
| *H. sapiens* | 7.0 | AC A101 | - | M1 | 67.84 | 64.41 |
| *H. sapiens* | 7.1 | AC A181 | - | M1 | 67.18 | 63.23 |
| *H. sapiens* | 7.2 | AC A116 | - | M1 | 69.75 | 66.96 |
| *H. sapiens* | 7.5 | AC A115 | - | M1 | 69.38 | 66.08 |
| *H. sapiens* | 7.9 | AC A193 | - | M1 | 69.37 | 63.56 |
| *H. sapiens* | 8.0 | AC A55 | - | M1 | 61.98 | 57.93 |
| *H. sapiens* | 8.1 | AC 102 | - | M1 | 69.48 | 65.69 |
| *H. sapiens* | 8.3 | AC A183 | - | M1 | 66.13 | 61.28 |
| *H. sapiens* | 8.9 | AC A151 | - | M1 | 69.27 | 66.11 |
| *H. sapiens* | 8.9 | AC A191 | - | M1 | 67.89 | 63.12 |
| *H. sapiens* | 9.1 | AC A153 | - | M1 | 65.59 | 61.95 |
| *H. sapiens* | 9.5 | AC D294 | - | M1 | 62.67 | 56.12 |
| *H. sapiens* | 10.0 | AC D43 | - | M2 | 61.46 | 57.14 |
| *H. sapiens* | 10.2 | AC A152 | - | M1 | 66.62 | 60.79 |
| *H. sapiens* | 10.6 | AC A157 | - | M1 | 74.59 | 62.18 |
| *H. sapiens* | 10.8 | AC A158 | - | M1 | 68.53 | 62.64 |
| *H. sapiens* | 11.8 | AC C196 | - | M2 | 68.69 | 61.19 |
| *H. sapiens* | 13.0 | AC A228 | - | M2 | 68.16 | 54.88 |
| *H. sapiens* | 13.0 | AC B195 | - | M2 | 75.91 | 69.62 |
| *H. sapiens* | 13.0 | AC B219 | - | M2 | 69.29 | 50.14 |
| *H. sapiens* | 13.0 | AC B220 | - | M2 | 73.08 | 59.97 |
| *H. sapiens* | 13.0 | AC B221 | - | M2 | 72.21 | 66.28 |
| *H. sapiens* | 13.0 | AC B65 | - | M2 | 71.41 | 58.81 |

| | | | | | | |
|---|---|---|---|---|---|---|
| *H. sapiens* | 13.0 | AC B66 | - | M2 | 70.53 | 65.58 |
| *H. sapiens* | 13.0 | AC C112 | - | M2 | 68.43 | 51.91 |
| *H. sapiens* | 13.0 | AC C134 | - | M2 | 67.16 | 56.84 |
| *H. sapiens* | 13.0 | AC C152 | - | M2 | 76.97 | 69.34 |
| *H. sapiens* | 13.5 | AC A215 | - | M2 | 74.19 | 68.25 |
| *H. sapiens* | 14.0 | NMNH 1363 | F | M3 | 72.02 | 66.38 |
| *H. sapiens* | 15.0 | AC 194 | - | M2 | 71.52 | 66.35 |
| *H. sapiens* | 15.0 | AC A192 | - | M2 | 71.72 | 66.97 |
| *H. sapiens* | 15.0 | AC D268 | - | M2 | 69.29 | 64.32 |
| *H. sapiens* | 15.0 | AC D275 | - | M2 | 64.87 | 59.46 |
| *H. sapiens* | 15.0 | AC D297 | - | M2 | 62.54 | 56.88 |
| *H. sapiens* | 15.0 | AC D56 | - | M2 | 66.69 | 61.64 |
| *H. sapiens* | 16.0 | NMNH 822 | F | M2 | 76.71 | 68.54 |
| *H. sapiens* | 17.0 | NMNH 306 | F | M2 | 61.86 | 47.58 |
| *H. sapiens* | 17.0 | NMNH 329 | M | M2 | 71.06 | 58.88 |
| *H. sapiens* | 17.0 | NMNH 562 | F | M3 | 80.85 | 75.94 |
| *H. sapiens* | 18.0 | AC D223 | - | M2 | 73.96 | 67.27 |
| *H. sapiens* | 18.0 | NMNH 800R | F | M2 | 75.29 | 69.34 |
| *H. sapiens* | 19.0 | NMNH 567 | F | M2 | 71.72 | 63.19 |
| *H. sapiens* | 19.0 | NMNH 129 | M | M3 | 83.43 | 77.08 |
| *H. sapiens* | 19.0 | NMNH 1434R | F | M3 | 77.80 | 68.17 |
| *H. sapiens* | 19.0 | NMNH 760 | M | M3 | 79.77 | 72.82 |
| *H. sapiens* | 20.0 | NMNH 1183 | M | M2 | 75.58 | 65.40 |
| *H. sapiens* | 20.0 | NMNH 210 | M | M3 | 77.90 | 63.90 |
| *H. sapiens* | 21.0 | NMNH 1187 | M | M3 | 89.71 | 83.80 |
| *H. sapiens* | 21.0 | NMNH 970 | F | M3 | 77.29 | 71.21 |
| *H. sapiens* | 22.0 | NMNH 1503 | M | M3 | 79.39 | 71.12 |
| *H. sapiens* | 22.0 | NMNH 39 | F | M3 | 81.76 | 70.92 |
| *H. sapiens* | 22.0 | NMNH 477 | M | M3 | 86.01 | 71.53 |
| *H. sapiens* | 22.0 | NMNH 594 | M | M3 | 77.17 | 70.20 |
| *H. sapiens* | 22.0 | NMNH 723 | F | M3 | 81.49 | 74.94 |
| *H. sapiens* | 23.0 | NMNH 1507 | F | M2 | 77.71 | 71.25 |
| *H. sapiens* | 23.0 | NMNH 1544 | F | M2 | 75.64 | 65.61 |
| *H. sapiens* | 23.0 | NMNH 1539 | M | M3 | 88.34 | 82.19 |
| *H. sapiens* | 23.0 | NMNH 850 | M | M3 | 88.07 | 79.10 |
| *H. sapiens* | 23.0 | NMNH 859 | M | M3 | 77.77 | 66.35 |
| *H. sapiens* | 23.0 | NMNH 886 | F | M3 | 77.57 | 69.58 |
| *H. sapiens* | 25.0 | NMNH 1206 | F | M3 | 80.56 | 73.96 |
| *H. sapiens* | 27.0 | NMNH 49R | M | M3 | 78.91 | 71.63 |
| *H. sapiens* | 27.0 | NMNH 880 | F | M3 | 70.56 | 58.83 |
| *H. sapiens* | 28.0 | NMNH 645 | M | M3 | 74.57 | 54.25 |
| *H. sapiens* | 30.0 | NMNH 235 | M | M3 | 85.36 | 73.56 |
| *H. sapiens* | 31.0 | NMNH 125 | M | M3 | 77.58 | 67.93 |
| *H. sapiens* | 32.0 | NMNH 815 | F | M3 | 68.23 | 62.05 |
| *H. sapiens* | 36.0 | NMNH 920 | F | M3 | 76.20 | 64.97 |
| **N=94** | | | | | | |

**B.** Specimen list for *Gorilla beringei*

| **Species** | **Age (yrs)** | **Specimen #** | **Sex** | **Molar emergence category** | **Mand. arch length$_{mean}$** | **Mand. arch length$_{max}$** |
|---|---|---|---|---|---|---|
| *G. beringei* | 1.2 | GP 012 | M | dp4 | 73.06 | 64.20 |
| *G. beringei* | 1.3 | GP 171 | M | dp4 | 77.46 | 65.72 |

| | | | | | | |
|---|---|---|---|---|---|---|
| *G. beringei* | 2.0 | GP 182 | M | dp4 | 79.11 | 67.88 |
| *G. beringei* | 2.9 | GP 151 | M | dp4 | 81.14 | 69.60 |
| *G. beringei* | 3.4 | GP 169 | M | M1 | 92.00 | 78.16 |
| *G. beringei* | 3.6 | GP 183 | F | M1 | 90.61 | 76.54 |
| *G. beringei* | 3.6 | GP 165 | F | M1 | 97.12 | 86.06 |
| *G. beringei* | 8.6 | GP 147 | F | M2 | 109.50 | 93.37 |
| *G. beringei* | 9.5 | GP 196 | F | M2 | 117.38 | 98.23 |
| *G. beringei* | 15.7 | GP 167 | F | M3 | 116.25 | 101.67 |
| *G. beringei* | 18.5 | GP 161 | M | M3 | 147.16 | 126.05 |
| *G. beringei* | 19.8 | GP 148 | F | M3 | 129.73 | 115.54 |
| *G. beringei* | 21.6 | GP 176 | M | M3 | 153.22 | 127.17 |
| *G. beringei* | 22.3 | GP 069 | M | M3 | 155.65 | 129.40 |
| *G. beringei* | 24.8 | GP 150 | M | M3 | 159.98 | 131.38 |
| *G. beringei* | 25.2 | GP 020 | F | M3 | 117.55 | 99.29 |
| *G. beringei* | 30.1 | GP 153 | F | M3 | 119.61 | 100.31 |
| *G. beringei* | 31.2 | GP 149 | F | M3 | 117.45 | 100.33 |
| *G. beringei* | 33.0 | GP 127 | M | M3 | 132.16 | 117.71 |
| *G. beringei* | 33.7 | GP 143 | F | M3 | 126.07 | 105.22 |
| *G. beringei* | 34.5 | GP 065 | M | M3 | 164.52 | 143.27 |
| *G. beringei* | 36.9 | GP 117 | F | M3 | 136.69 | 123.60 |
| *G. beringei* | 38.3 | GP 131 | F | M3 | 147.20 | 125.61 |
| *G. beringei* | 42.1 | GP 134 | F | M3 | 140.88 | 120.19 |
| **N=24** | | | | | | |

**C.** Specimen list for *Pan troglodytes*

| **Species** | **Age (yrs)** | **Specimen #** | **Sex** | **Molar emergence category** | **Mand. arch length$_{mean}$** | **Mand. arch length$_{max}$** |
|---|---|---|---|---|---|---|
| *P. t. verus* | 1.0 | MPI 06 55 | F | dp4 | 55.30 | 53.26 |
| *P. t. verus* | 2.0 | MPI 06 15 | M | dp4 | 64.81 | 60.77 |
| *P. t. verus* | 2.0 | MPI 06 45 | M | dp4 | 62.83 | 58.05 |
| *P. t. schweinfurthii* | 2.6 | UM PT | M | dp4 | 56.94 | 51.77 |
| *P. t. verus* | 3.0 | MPI 06 37 | - | M1 | 70.92 | 67.26 |
| *P. t. verus* | 6.0 | MPI 06 10 | M | M1 | 78.30 | 70.42 |
| *P. t. verus* | 6.0 | MPI 06 57 | M | M1 | 69.07 | 63.96 |
| *P. t. verus* | 7.0 | MPI 06 64 | M | M1 | 75.77 | 69.69 |
| *P. t. verus* | 8.0 | MPI 06 46 | M | M2 | 88.16 | 79.52 |
| *P. t. schweinfurthii* | 8.5 | UM FT | M | M2 | 82.30 | 77.64 |
| *P. t. verus* | 9.0 | MPI 06 29 | F | M2 | 90.64 | 80.90 |
| *P. t. verus* | 10.0 | MPI 08 64 | F | M2 | 85.01 | 77.93 |
| *P. t. verus* | 11.0 | MPI 06 15 | F | M2 | 91.44 | 85.29 |
| *P. t. verus* | 11.0 | MPI 06 50 | F | M2 | 86.83 | 80.54 |
| *P. t. verus* | 12.0 | MPI 06 31 | F | M3 | 101.69 | 96.47 |
| *P. t. schweinfurthii* | 13.0 | UM MM | M | M3 | 98.62 | 90.41 |
| *P. t. verus* | 13.0 | MPI 06 18 | M | M3 | 97.76 | 88.00 |
| *P. t. schweinfurthii* | 13.5 | UM MCD | M | M3 | 97.83 | 85.67 |
| *P. t. verus* | 16.0 | MPI 06 14 | F | M3 | 96.13 | 88.90 |
| *P. t. schweinfurthii* | 18.9 | UM GK | F | M3 | 98.24 | 88.65 |
| *P. t. verus* | 19.0 | MPI 06 17 | F | M3 | 98.40 | 91.21 |
| *P. t. verus* | 19.0 | MPI 06 65 | M | M3 | 105.50 | 94.44 |
| *P. t. verus* | 20.0 | MPI 06 40 | M | M3 | 99.34 | 89.45 |
| *P. t. verus* | 22.0 | MPI 06 52 | F | M3 | 92.01 | 85.20 |
| *P. t. verus* | 23.0 | MPI 06 39 | F | M3 | 91.39 | 86.15 |

| | | | | | | |
|---|---|---|---|---|---|---|
| *P. t. verus* | 25.0 | MPI 06 19 | F | M3 | 104.59 | 94.73 |
| *P. t. verus* | 25.0 | MPI 15 04 | M | M3 | 105.28 | 95.95 |
| *P. t. schweinfurthii* | 25.9 | UM CH | M | M3 | 104.00 | 98.31 |
| *P. t. verus* | 27.0 | MPI 06 47 | F | M3 | 99.75 | 91.42 |
| *P. t. verus* | 28.0 | MPI 06 09 | F | M3 | 95.90 | 84.76 |
| *P. t. schweinfurthii* | 29.2 | UM PL | F | M3 | 94.14 | 89.48 |
| *P. t. schweinfurthii* | 30.2 | UM MB | F | M3 | 94.15 | 88.40 |
| *P. t. schweinfurthii* | 30.6 | UM PS | F | M3 | 92.78 | 86.53 |
| *P. t. schweinfurthii* | 30.9 | UM MF | F | M3 | 96.22 | 88.78 |
| *P. t. schweinfurthii* | 36.3 | UM ML | F | M3 | 94.82 | 86.64 |
| *P. t. verus* | 39.0 | MPI 06 25 | F | M3 | 96.07 | 88.89 |
| *P. t. verus* | 40.0 | MPI 06 48 | M | M3 | 110.54 | 102.54 |
| **N=37** | | | | | | |

**D.** Specimen list for *Papio cynocephalus*

| **Species** | **Age (yrs)** | **Specimen #** | **Sex** | **Molar emergence category** | **Mand. arch length$_{mean}$** | **Mand. arch length$_{max}$** |
|---|---|---|---|---|---|---|
| *P. cynocephalus* | 1.7 | OM 8713 | M | dp4 | 57.13 | 53.30 |
| *P. cynocephalus* | 3.0 | OM 9017 | F | dp4 | 57.30 | 52.18 |
| *P. cynocephalus* | 3.1 | OM 8588 | F | M1 | 72.86 | 65.79 |
| *P. cynocephalus* | 3.3 | OM 8585 | F | M1 | 71.10 | 64.44 |
| *P. cynocephalus* | 3.3 | OM 8590 | F | M1 | 74.17 | 67.97 |
| *P. cynocephalus* | 3.4 | OM 8589 | F | M1 | 69.36 | 64.13 |
| *P. cynocephalus* | 7.7 | OM 8598 | F | M2 | 93.54 | 83.81 |
| *P. cynocephalus* | 7.7 | OM 8591 | M | M3 | 121.30 | 111.83 |
| *P. cynocephalus* | 8.1 | OM 8599 | M | M3 | 133.08 | 125.68 |
| *P. cynocephalus* | 9.2 | OM 8594 | F | M3 | 92.30 | 84.51 |
| *P. cynocephalus* | 10.7 | OM 8597 | F | M3 | 92.60 | 84.54 |
| *P. cynocephalus* | 13.1 | OM 8504 | F | M3 | 93.74 | 86.40 |
| *P. cynocephalus* | 14.1 | OM 8592 | F | M3 | 96.10 | 88.18 |
| *P. cynocephalus* | 14.6 | OM 8582 | M | M3 | 129.26 | 120.02 |
| *P. cynocephalus* | 15.6 | OM 8711 | F | M3 | 93.60 | 87.03 |
| *P. cynocephalus* | 16.8 | OM 8595 | M | M3 | 123.51 | 119.01 |
| *P. cynocephalus* | 17.2 | OM 8600 | F | M3 | 89.57 | 79.52 |
| *P. cynocephalus* | 18.7 | OM 8596 | M | M3 | 126.74 | 117.67 |
| **N=18** | | | | | | |

**E.** Specimen list for *Macaca mulatta*

| **Species** | **Age (yrs)** | **Specimen #** | **Sex** | **Molar emergence category** | **Mand. arch length$_{mean}$** | **Mand. arch length$_{max}$** |
|---|---|---|---|---|---|---|
| *M. mulatta* | 0.5 | CPRCMUS-00484 | F | dp4 | 36.42 | 31.80 |
| *M. mulatta* | 0.6 | CPRCMUS-00449 | F | dp4 | 39.55 | 36.57 |
| *M. mulatta* | 0.6 | CPRCMUS-00474 | F | dp4 | 37.90 | 35.25 |
| *M. mulatta* | 0.6 | CPRCMUS-00461 | F | dp4 | 39.59 | 36.45 |
| *M. mulatta* | 0.6 | CPRCMUS-00516 | F | dp4 | 38.28 | 34.33 |
| *M. mulatta* | 0.7 | CPRCMUS-00527 | F | dp4 | 39.70 | 37.05 |
| *M. mulatta* | 0.7 | CPRCMUS-00491 | M | dp4 | 38.92 | 36.03 |
| *M. mulatta* | 0.8 | CPRCMUS-00475 | M | dp4 | 41.21 | 38.34 |
| *M. mulatta* | 0.9 | CPRCMUS-00011 | F | dp4 | 42.31 | 37.63 |
| *M. mulatta* | 0.9 | CPRCMUS-00473 | M | dp4 | 42.12 | 38.53 |

| | | | | | | |
|---|---|---|---|---|---|---|
| *M. mulatta* | 0.9 | CPRCMUS-00340 | M | dp4 | 41.48 | 35.32 |
| *M. mulatta* | 1.0 | CPRCMUS-00464 | M | dp4 | 43.18 | 36.83 |
| *M. mulatta* | 1.0 | CPRCMUS-00477 | F | dp4 | 39.94 | 35.71 |
| *M. mulatta* | 1.0 | CPRCMUS-00549 | M | dp4 | 44.16 | 39.14 |
| *M. mulatta* | 1.1 | CPRCMUS-00479 | M | dp4 | 40.05 | 36.13 |
| *M. mulatta* | 1.1 | CPRCMUS-00339 | M | dp4 | 43.51 | 37.94 |
| *M. mulatta* | 1.1 | CPRCMUS-00481 | F | dp4 | 41.85 | 36.82 |
| *M. mulatta* | 1.2 | CPRCMUS-00104 | M | dp4 | 46.23 | 40.19 |
| *M. mulatta* | 1.2 | CPRCMUS-00366 | F | dp4 | 42.73 | 36.77 |
| *M. mulatta* | 1.5 | CPRCMUS-00148 | M | M1 | 47.54 | 43.86 |
| *M. mulatta* | 1.6 | CPRCMUS-00072 | F | M1 | 48.05 | 42.97 |
| *M. mulatta* | 1.6 | CPRCMUS-00140 | F | M1 | 49.40 | 42.37 |
| *M. mulatta* | 1.6 | CPRCMUS-00052 | F | M1 | 46.62 | 43.77 |
| *M. mulatta* | 1.7 | CPRCMUS-00084 | F | M1 | 46.73 | 42.66 |
| *M. mulatta* | 1.7 | CPRCMUS-00096 | F | M1 | 50.04 | 45.69 |
| *M. mulatta* | 1.7 | CPRCMUS-00592 | M | M1 | 49.23 | 44.55 |
| *M. mulatta* | 1.9 | CPRCMUS-00311 | F | M1 | 47.00 | 42.76 |
| *M. mulatta* | 1.9 | CPRCMUS-03018 | M | M1 | 48.35 | 44.94 |
| *M. mulatta* | 2.2 | CPRCMUS-00116 | M | M1 | 51.19 | 46.21 |
| *M. mulatta* | 2.5 | CPRCMUS-00676 | M | M1 | 55.04 | 50.07 |
| *M. mulatta* | 2.5 | CPRCMUS-00054 | F | M1 | 51.89 | 44.80 |
| *M. mulatta* | 2.5 | CPRCMUS-00794 | M | M1 | 48.93 | 43.09 |
| *M. mulatta* | 2.8 | CPRCMUS-00079 | F | M1 | 48.23 | 44.09 |
| *M. mulatta* | 2.8 | CPRCMUS-00178 | F | M1 | 54.13 | 48.62 |
| *M. mulatta* | 2.9 | CPRCMUS-00059 | M | M1 | 53.08 | 48.31 |
| *M. mulatta* | 3.0 | CPRCMUS-00190 | M | M1 | 55.68 | 50.03 |
| *M. mulatta* | 3.0 | CPRCMUS-00831 | M | M1 | 57.16 | 50.22 |
| *M. mulatta* | 3.1 | CPRCMUS-00088 | F | M1 | 58.27 | 50.29 |
| *M. mulatta* | 3.1 | CPRCMUS-00427 | M | M2 | 57.15 | 49.32 |
| *M. mulatta* | 3.1 | CPRCMUS-00346 | F | M1 | 53.15 | 48.00 |
| *M. mulatta* | 3.3 | CPRCMUS-00350 | F | M2 | 57.84 | 53.30 |
| *M. mulatta* | 3.4 | CPRCMUS-00352 | F | M1 | 50.20 | 46.85 |
| *M. mulatta* | 3.4 | CPRCMUS-00349 | F | M1 | 54.26 | 49.19 |
| *M. mulatta* | 3.7 | CPRCMUS-00600 | M | M1 | 58.53 | 53.63 |
| *M. mulatta* | 3.8 | CPRCMUS-00118 | M | M2 | 70.09 | 65.68 |
| *M. mulatta* | 3.9 | CPRCMUS-00254 | M | M2 | 62.51 | 56.98 |
| *M. mulatta* | 4.0 | CPRCMUS-00160 | F | M2 | 56.64 | 53.25 |
| *M. mulatta* | 4.0 | CPRCMUS-00333 | M | M2 | 65.04 | 58.41 |
| *M. mulatta* | 4.0 | CPRCMUS-00062 | F | M2 | 58.45 | 52.11 |
| *M. mulatta* | 4.1 | CPRCMUS-00353 | F | M2 | 60.43 | 56.38 |
| *M. mulatta* | 4.2 | CPRCMUS-00130 | F | M2 | 62.06 | 52.64 |
| *M. mulatta* | 4.7 | CPRCMUS-00150 | M | M2 | 70.80 | 63.74 |
| *M. mulatta* | 4.7 | CPRCMUS-00314 | M | M2 | 65.66 | 60.64 |
| *M. mulatta* | 4.8 | CPRCMUS-00324 | M | M2 | 67.59 | 59.94 |
| *M. mulatta* | 4.9 | CPRCMUS-00068 | M | M2 | 67.35 | 58.23 |
| *M. mulatta* | 5.0 | CPRCMUS-00404 | F | M2 | 61.43 | 52.84 |
| *M. mulatta* | 5.1 | CPRCMUS-00258 | M | M2 | 69.83 | 63.59 |
| *M. mulatta* | 5.2 | CPRCMUS-00397 | F | M2 | 60.31 | 55.07 |
| *M. mulatta* | 5.3 | CPRCMUS-00044 | M | M3 | 75.89 | 70.17 |
| *M. mulatta* | 5.5 | CPRCMUS-00371 | M | M3 | 73.37 | 69.55 |
| *M. mulatta* | 5.5 | CPRCMUS-00131 | M | M2 | 73.31 | 67.07 |
| *M. mulatta* | 5.5 | CPRCMUS-00120 | F | M3 | 66.53 | 60.98 |
| *M. mulatta* | 5.7 | CPRCMUS-00145 | F | M3 | 61.75 | 58.25 |
| *M. mulatta* | 5.7 | CPRCMUS-00154 | M | M2 | 74.35 | 67.40 |

| | | | | | | |
|---|---|---|---|---|---|---|
| *M. mulatta* | 5.7 | CPRCMUS-00321 | M | M3 | 75.25 | 67.29 |
| *M. mulatta* | 6.0 | CPRCMUS-00259 | F | M2 | 65.18 | 60.64 |
| *M. mulatta* | 6.0 | CPRCMUS-00391 | F | M3 | 65.77 | 58.91 |
| *M. mulatta* | 6.5 | CPRCMUS-00060 | M | M3 | 81.50 | 74.76 |
| *M. mulatta* | 6.5 | CPRCMUS-00032 | F | M2 | 64.55 | 56.48 |
| *M. mulatta* | 6.8 | CPRCMUS-00394 | M | M3 | 85.42 | 78.56 |
| *M. mulatta* | 7.1 | CPRCMUS-00040 | F | M3 | 67.74 | 62.97 |
| *M. mulatta* | 7.9 | CPRCMUS-00031 | M | M3 | 77.92 | 69.94 |
| *M. mulatta* | 7.9 | CPRCMUS-00163 | M | M3 | 79.60 | 73.12 |
| *M. mulatta* | 8.4 | CPRCMUS-00361 | M | M3 | 79.72 | 73.27 |
| *M. mulatta* | 8.5 | CPRCMUS-00379 | M | M3 | 77.07 | 68.41 |
| *M. mulatta* | 8.5 | CPRCMUS-00380 | M | M3 | 79.00 | 71.23 |
| *M. mulatta* | 8.5 | CPRCMUS-00478 | F | M3 | 73.25 | 67.17 |
| *M. mulatta* | 8.6 | CPRCMUS-00051 | F | M3 | 66.43 | 62.27 |
| *M. mulatta* | 8.6 | CPRCMUS-00047 | F | M3 | 65.92 | 59.88 |
| *M. mulatta* | 8.6 | CPRCMUS-00323 | M | M3 | 83.09 | 74.11 |
| *M. mulatta* | 8.8 | CPRCMUS-00320 | M | M3 | 83.45 | 74.46 |
| *M. mulatta* | 9.4 | CPRCMUS-00337 | M | M3 | 79.13 | 72.08 |
| *M. mulatta* | 9.5 | CPRCMUS-00406 | F | M3 | 70.99 | 63.09 |
| *M. mulatta* | 9.6 | CPRCMUS-00381 | M | M3 | 80.62 | 75.42 |
| *M. mulatta* | 9.7 | CPRCMUS-00360 | M | M3 | 85.00 | 72.64 |
| *M. mulatta* | 10.0 | CPRCMUS-00038 | F | M3 | 70.64 | 61.81 |
| *M. mulatta* | 10.4 | CPRCMUS-00374 | F | M3 | 69.03 | 62.24 |
| *M. mulatta* | 10.5 | CPRCMUS-00383 | F | M3 | 68.51 | 62.85 |
| *M. mulatta* | 10.6 | CPRCMUS-00637 | F | M3 | 71.91 | 63.76 |
| *M. mulatta* | 11.0 | CPRCMUS-00596 | F | M3 | 70.36 | 63.50 |
| *M. mulatta* | 11.1 | CPRCMUS-00597 | F | M3 | 73.71 | 63.76 |
| *M. mulatta* | 11.4 | CPRCMUS-00598 | F | M3 | 72.45 | 67.18 |
| *M. mulatta* | 11.6 | CPRCMUS-00382 | M | M3 | 83.09 | 74.95 |
| *M. mulatta* | 12.0 | CPRCMUS-00440 | F | M3 | 71.00 | 64.05 |
| *M. mulatta* | 12.2 | CPRCMUS-00300 | M | M3 | 77.41 | 69.47 |
| *M. mulatta* | 12.6 | CPRCMUS-00326 | F | M3 | 70.16 | 63.70 |
| *M. mulatta* | 12.7 | CPRCMUS-00156 | M | M3 | 80.60 | 75.34 |
| *M. mulatta* | 14.2 | CPRCMUS-00672 | F | M3 | 73.80 | 65.06 |
| *M. mulatta* | 14.5 | CPRCMUS-00364 | M | M3 | 75.34 | 67.84 |
| *M. mulatta* | 16.9 | CPRCMUS-00620 | F | M3 | 78.12 | 69.02 |
| *M. mulatta* | 17.0 | CPRCMUS-00617 | F | M3 | 69.47 | 62.12 |
| **N=104** | | | | | | |